Expression and function of GDNF family ligands and their receptors by human immune cells

Dissertation
zur Erlangung des
Doktorgrades der Naturwissenschaften
(Dr. rer. nat.)
der Fakultät für Biologie
der Ludwig-Maximilians-Universität München

vorgelegt von
Vivian Vargas-Leal
Venezuela

München, Dezember 2003

Hiermit erkläre ich, dass ich die vorliegende Dissertation selbständig und ohne unerlaubte Hilfe habe.
Ich habe weder anderweitig versucht, eine Dissertation oder Teile einer Dissertation einzureichen beziehungsweise einer Prüfungskommission vorzulegen, noch eine Doktorprüfung durchzuführen.

München, Dezember 2003

Dissertation eingereicht: 18. Dezember 2003

Tag der mündlichen Prüfung: 2. April 2004

Erstgutachter: Prof. Dr. Elisabeth Weiß
Zweitgutachter: Prof. Dr. Georg Dechant

Acknowledgments

This work has been performed under the support of the "Fundación Gran Mariscal de Ayacucho" from the government of Venezuela, which provided me with a fellowship for four years. I am extremely grateful to the Foundation for making my dreams possible.

Thanks are due to the max-Planck Institute of Neurobiology, Martinsried, where I performed all of my investigation. I am indebted to Prof. Dr. Hartmut Wekerle, head of the department of Neuroimmunology , and prof. Dr. Reinhard Hohlfeld, head of the Institute of Clinical Neuroimmunology – LMU.

I would like to thank my family, specially my mother, for their unconditional support and help in each moment of my life, whenever and wherever they had been. Without them I could have not finished these studies.

I whish to thank:

- Prof. Dr. Edgar Meinl for his experimental advice and supervision, stimulating discussions and for directing my thesis over many years.
- Prof. Dr. Leonardo Mateu (from Instituto Venezolano de Investigaciones Científicas), who even from a great distance has always helped me in any difficulty, giving his wise advice and great understanding.
- Prof. Dr. Georg Dechant for his discussion and suggestions for my work.
- Prof. Frau Dr. Elisabeth Weiß for supporting this thesis at the Ludwig-Maximilian Universität of Munich.
- Many thanks for the help received from my colleagues from the department of Neuroimmunology, in particular: Martina Sölch, Dr. Tobias Derfuß, Dr. Roxana Bruno and Dr. Alexander Flügel.
- Also many thanks to my closest friends: Dr. Marta Labeur, Dr. Seiko Kataoka, Ms. Ute Sukop, Dr. Eva Vonasek.
- Finally very special thanks to Dr. Enrico Marchetti for having supported me in all my difficulties.

And of course, many thanks to God and his Angels: they have been always around me.

1 INDEX

2 SUMMARY

Expression of GDNF-Family ligands and their receptors by immune cells

GDNF (Glial cell line-Derived Neurotrophic Factor) and NTN (Neurturin) are two of the four members of the GDNF family ligands (GFLs) and are potent survival and developmental factors for the kidney as well as the peripheral and central neurons. Persephin (PSP), a third family member, behaves only as survival factor for central neurons.

GDNF and NTN signaling is mediated by a two-component receptor containing a ligand specific binding component, GFRα-1 (higher GDNF affinity) and GFRα-2 (higher NTN affinity) respectively, and the common signal transducing component, RET. PSP signals only through the binding to GFRα-4 and RET.

The aim of this study was to investigate possible mutual interactions between the nervous and immune system mediated by GFLs and their receptors.

While GDNF, the prototype of its family, was not expressed by any of the studied human immune cells, the related molecule NTN, was found to be expressed by T and B cells and monocytes as seen by RT-PCR, Western blot and immunocytochemistry. Additionally, PSP was found in peripheral blood mononuclear cells (PBMCs) by RT-PCR.

The RET gene, expressed in all the studied immune cells, contains 21 exons and encodes a tyrosine kinase receptor. Multiple splice variants of this gene have been described. Various cell subsets were found to express distinct *RET* 3' or 5'-isoforms. In T and B cells, the expression of the 3'-end *RET* isoforms, where $CD4^+$ and $CD8^+$-T lymphocytes show different expressions patterns, was regulated by cell activation.

At the 5'-end however, a new isoform that lacks exon 5, resulted in a partial deletion of the receptor's extracellular part. The latter was detected only in $CD8^+$-T cells (non-activated and activated cells) and in non-activated B cells. Interestingly, monocytes expressed full length *RET* mRNA indicating their responsiveness to GFLs.

Immune cells also expressed the GDNF and NTN binding components: named GFRα-1 and GFRα-2. Whereas the GFRα-1 receptor was mostly detected on monocytes, GFRα-2 was abundantly expressed on both, monocytes and lymphocytes. Several GFRα-2 isoforms

were detected in various cell types, the most abundant, which lack exons 2 and 3, was observed in T cells and monocytes. The predicted protein therefore loses its N-terminal cysteine-rich domain and one of the N-glycosylation sites, a region not critical for the binding of NTN and interaction with RET.

Several experiments were performed to find out the functional effects NTN or GDNF might have on immune cells. The expression of the activation markers, HLA-DR, CD38, CD40, CD69, and CD86 was not modulated neither was the proliferation nor production of IL-4 and IFN-γ. However, TNF-α was found to be regulated by both NTN and GDNF: when GDNF or NTN was added to PBMCs five or six days after activation by LPS+IFN-γ or by ConA, a reduced amount of TNF-α was observed after 24 hours. Data from diverse experiments suggested that the decrease in TNF-α was due to an increased uptake or consumption rather than a reduced production.

In summary, this study shows that all subsets of human immune cells express the ligand NTN, up-regulated after cell activation, and probably PSP mRNA, as well as the receptor GFRα-1 and predominantly GFRα-2 with protein upregulation seen upon cellular activation; that multiple isoforms of the signaling component RET were constitutively expressed and then regulated by cellular activation. Whether the transmembrane receptor levels differ upon activation remains unclear and as well as NTN and GDNF modulating the uptake and/or consumption of TNF-α. These findings suggest that immune cells communicate with each other and with the nervous system via GFLs.

ZUSAMMENFASSUNG

GDNF (*glial cell line-derived neurotrophic factor*) und NTN (Neurturin), die zwei zuerst beschriebenen Liganden der GDNF-Familie, fungieren als Überlebens- und Entwicklungsfaktoren für definierte Populationen von zentralen und peripheren Neuronen. GDNF ist darüber hinaus für die Nierenentwicklung erforderlich. Für die Vermittlung ihrer biologischen Wirkung benutzten GDNF und NTN einen Rezeptor, der aus zwei Ketten besteht: Die Signal-transduzierende Komponente *RET* wird sowohl von GDNF als auch von NTN benutzt. *RET* wird von 21 Exonen kodiert und kommt in multiplen Spleiß-Varianten vor. Für die Liganden-Spezifität ist eine zweite Rezeptorkomponente verantwortlich, ein Mitglied der GFR-Familie. GFRα-1 bindet präferentiell GDNF, während GFRα-2 NTN stärker als GDNF bindet.

Ziel dieser Arbeit war es, mögliche wechselseitige Interaktionen zwischen dem Nerven- und Immunsystem durch die GDNF-Familie zu untersuchen. Zu diesem Zweck wurde zunächst die Expression von GDNF, NTN und ihrer Rezeptoren in gereinigten Immunzell-Subtypen untersucht. Dabei zeigte sich, dass der Prototyp dieser Liganden-Familie, GDNF, von keiner der untersuchten Immunzellen exprimiert wurde. Hingegen wurde das verwandte NTN von T-Zellen, B-Zellen und Monozyten exprimiert wie mit RT-PCR, Western Blot und Immunzytochemie gesehen wurde. Transkripte für das zu NTN und GDNF verwandte Persephin (PSP) wurden in Monozyten und mononukleären Zellen des peripheren Blutes gefunden. Der Transmembran-Rezeptor RET wurde von allen untersuchten Immunzell-Subtypen exprimiert. B-Zellen und T-Zellen exprimierten unterschiedliche Isoformen von *RET*, sowohl im extrazellulären Liganden-bindenden als auch im intrazellulären Signal-transduzierenden Teil. Die Expression der Isoformen von RET wurde zudem in T-Zellen und B-Zellen noch stark durch Aktivierung reguliert. In $CD8^+$-T-Zellen wurde auch eine bislang noch nicht beschriebene Spleiß-Variante am 5` Ende beobachtet. Im Gegensatz zu T-Zellen und B-Zellen exprimierten Monozyten nur die volle Länge von *RET*.

Auch die Liganden-bindenden Ketten GFRα-1 und GFRα-2 wurden von Immunzellen exprimiert wie mit RT-PCR und FACS gesehen wurde. GFRα-2 war deutlich abundanter

als GFRα-1. Von GFRα-2 wurden verschiedene Isoformen in Immunzellen gefunden. In der in T-Zellen und B-Zellen am stärksten exprimierten Isoform ist Exon 2 und 3 nicht enthalten. Dem resultierenden Protein fehlen die N-terminale Cystein-reiche Domäne und eine N-Glykosylierungsstelle, eine Region, die allerdings für die Bindung von NTN und die Interaktion mit RET entbehrlich ist.

Mögliche Effekte von GDNF und NTN auf Immunzellen wurden untersucht. Dabei zeigte sich, dass GDNF und NTN an der Regulation von TNF-α beteiligt sind. Wenn GDNF oder NTN nach 5 oder 6 Tagen zu LPS+IFN-γ stimulierten Blutzellen oder zu ConA aktivierten T-Zellen gegeben wurde, dann war nach weiteren 24 h der TNF-α-Gehalt im Überstand reduziert. Weitere Experimente wiesen daraufhin, dass diese Reduktion des TNF-α-Gehalts auf eine verstärkte Aufnahme oder Verbrauch zurückzuführen ist. Proliferation, Expression von Aktivierungsmarkern (HLA-DR, CD38, CD40, CD69, CD86) oder Produktion von IFN-γ und IL-4 wurden durch GDNF und NTN nicht beeinflusst.

Zusammenfassend zeigt diese Arbeit, dass Immunzellen den neurotrophen Faktor NTN produzieren und Rezeptoren für GDNF und NTN besitzen. Multiple Isoformen der Signal-transduzierenden Kette *RET* wurden exprimiert und durch Aktivierung reguliert. NTN und GDNF regulierten in aktivierten T-Zellen und Monozyten die Aufnahme oder den Verbrauch von TNF-α. Diese Befunde weisen daraufhin, dass Immunzellen miteinander und auch mit dem Nervensystem mit Hilfe der GDNF-Familie interagieren können.

3 INTRODUCTION

3.1. GDNF FAMILY LIGANDS

3.1.1. General description of GFLs

Glial cell line-Derived Neurotrophic Factor (GDNF) is the first member of a growing family of proteins named ***"GDNF family ligands (GFLs)"*** or ***"GDNF family of neurotrophic factors"***. The family consists of GDNF (Lin et al., 1993), Neurturin (NTN) (Kotzbauer et al., 1996), Artemin (ART) (Baloh et al., 1998; Masure et al., 1998), and Persephin (PSP) (Mildbrandt et al., 1998) all of which are basic secretory proteins, biologically active as homodimers. GFLs are structurally distant members of the transforming growth factor-β superfamily (TGF-β) (Unsicker, 1996) due to seven-conserved cysteine residues (Cys) located in the same relative spacing in the mature protein. Both of the aforementioned groups (TGF-β and GFLs) belong to the "cysteine knot growth factor superfamily" (McDonald and Hendrickson, 1993).

GFLs are produced in the form of a precursor, namely *prepro*GFL. The signal sequence is cleaved upon secretion, and activation of the proGFL probably occurs by proteolytic cleavage. They seem to bind heparan-sulphate side chains of extracellular-matrix proteoglycans, which might restrict their diffusion and raise their local concentration (Hamilton et al., 2001).

The gene regulation of GFLs, the mechanisms of secretion and the activation of GFL precursors are not yet well understood. The specific proteases that cleave GFL precursors have not been identified. Interestingly, recent evidence indicates that secreted pro-neurotrophins are biologically active (pro-NGF) (Lee et al., 2001).

The amino acid sequence homology between members of the GFLs is between 40 and 50% (NTN to GDNF: 43%, PSP to GDNF: 50%, PSP to NTN: 40%), and less than 20% with other members of the TGF-β superfamily (Saarma, 2000).

Similarities between GFLs functions can be summarized as follows: GDNF, NTN and ART exert important roles for the survival of mesencephalic dopaminergic (DA) neurons and spinal cord motor neurons (MN), as well as for peripheral sympathetic, neural crest- and placode-derived sensory and enteric neurons. However, PSP supports only the survival of central neurons but not of peripheral neurons.

The RET, GDNF and GFRα-1 knock-out mice showed similar phenotype, consisting in renal agenesis and colon aganglionosis, demonstrating their importance for the development of the kidney and the enteric nervous system (ENS) (Schuchart et al., 1994, Pichel et al. 1996, Enomoto et al. 1998).

3.1.2. GDNF-Family Ligand receptor complex

Each ligand (GDNF, NTN, ART and PSP) requires the presence of two receptors on the target cell to induce the activation of intracellular signaling pathways (Airaksinen and Saarma, 2002).

1) **GFRα -1/4 surface receptors** (GDNF family receptors α-1/4) are the ligand-binding components; they are small proteins anchored by a glycosyl-phosphatidylinositol (GPI)-link to the outer plasma membrane.
2) **RET, the transmembrane tyrosine kinase receptor,** signals through the autophosphorylation of its multiple intracellular tyrosine (Tyr) residues, which are also potential docking sites for adaptor proteins.

The following signaling model was proposed: first, a homodimeric member of the GDNF family binds to the corresponding surface receptor GFRα-(1 to 4), allowing the subsequent interaction of the GFL/GFRα-1 to 4 complex with two molecules of RET, inducing its homodimerization, autophosphorylation and further activation of signaling pathways to the nucleus (Treanor et al., 1995; Trupp et al., 1996). This process occurs in lipid raft domains within the membrane (Saarma, 2001).

All ligands share the same transmembrane receptor RET; however, each ligand binds a preferred GFRα surface receptor: GDNF signals preferentially via the GFRα-1 receptor; NTN via GFRα-2; ART through GFRα-3 and PSP through GFRα-4. However, cross talk between the different ligands and receptors has also been described *in vitro* (Sanicola et al., 1997) and *in vivo* (Baloh et al., 1997; Sanicola et al., 1997; Trupp et al., 1998). For instance, GDNF binds with high affinity to GFRα-1 and with low affinity to either GFRα-2 or GFRα-3 (Airaksinen et al., 1999). Although GFRα-3 does not bind GDNF directly, it is able to interact with GDNF only in the presence of RET (Baloh et al., 1997). NTN and

ART may cross-talk weakly with GFRα-1, while PSP, on the other hand, has only been reported binding to GFRα-4 (Masure et al. 2000), see Figure 1.

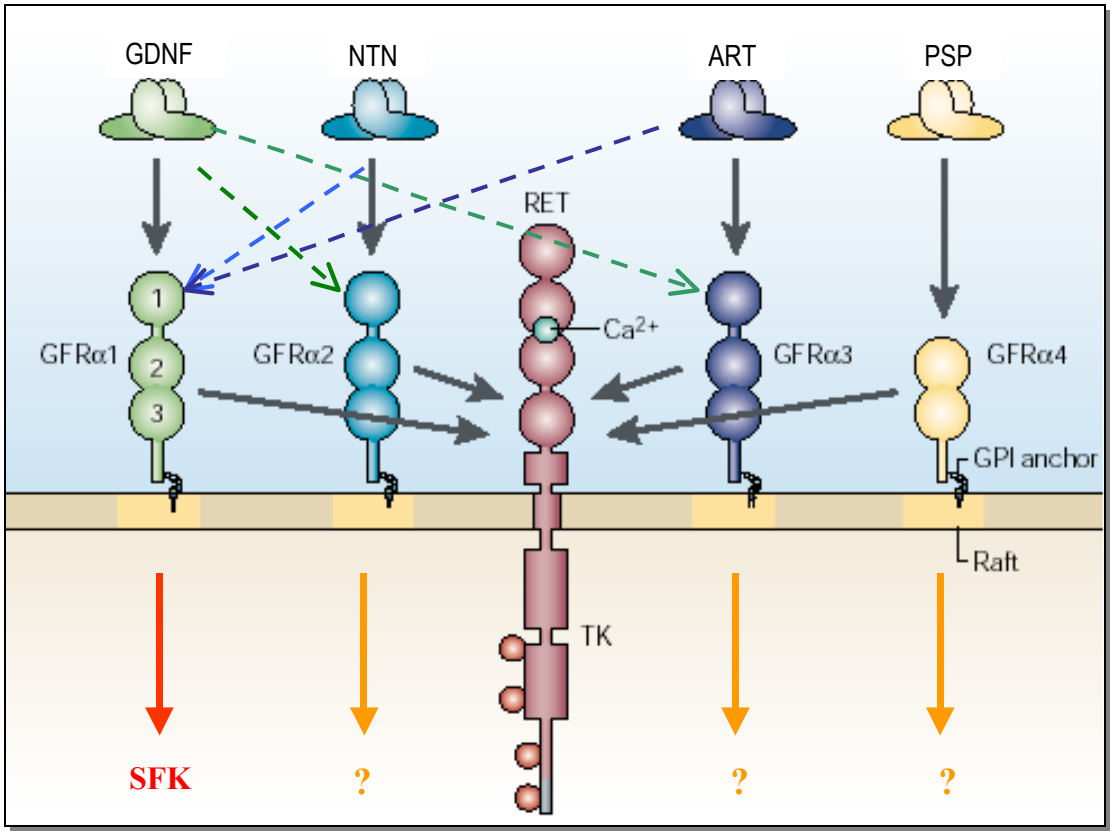

Figure 1: GDNF family ligands and receptors interactions. RET can bind to all the GFRα receptors (indicated by black arrows) and each GFRα receptor has a preferred ligand. The latter is only the case in the absence of RET, whereas in its presence the GFRαs can interact with 2 or 3 GDNF family ligands (dashed arrows). GFRα proteins are attached to the plasma membrane by a GPI anchor located in raft membranes. Four Tyr residues present on the intracellular part of RET serve as docking sites for adaptor proteins (red circles). Yellow arrows represent possible independent signaling pathways, which can signal in the absence of RET. Only one alternative pathway, triggered by the phosphorylation of the Src family kinase (SFK), has been described after the binding of GDNF to GFRα-1 (from Airaksinen and Saarma, 2002).

Although RET alone does not bind directly any of the GFLs, it is capable of modifying the interactions between the ligands and their GFRα receptors. Thus, in the absence of RET, each receptor binds only to a single ligand, whereas in the presence of RET, the GFRα receptors become more promiscuous and can interact with 2 or 3 different GFLs. Ca^{2+} ions

bind to one of the four extracellular cadherin-like domains (CLD) of RET and are required for RET activation by GFLs.

A RET independent signaling pathway has been described for GDNF once bound to GFRα-1 in a lipid raft. In this case, kinases of the Src family are activated and signal to the nucleus.

3.2. Interactions between the CNS, PNS and the immune system

Until recently, the central nervous system (CNS) and immune system (IS) were thought to operate independently of each other. Recent data have changed this view. Various paradigms about the dynamic inter-relationships of both systems have arisen from studies examining the events initiated by stressors (Maier et al., 1994) that activate neural circuits in the brain, leading to activation of brain-outflow pathways to the periphery, such as the hypothalamic-pituitary-adrenal axis and sympathetic nervous system. In turn, the hormones and transmitters released bind to receptors expressed by immune cells, altering immune functions (Maier and Watkins, 1998). This activity is bi-directional. Products of activated immune cells feed back to the brain to alter neural activity.

Neurotrophins (NTs), named nerve growth factor (NGF), brain-derived neurotrophic factor (BDNF), neurotrophin-3 (NT-3), and neurotrophin-4/5 (NT-4/5), are proteins that were shown to have different effects on the nervous system, such as enhancement of neuronal survival, development and maintenance of CNS and PNS, regulation of neurotransmitter release, dendritic growth, neuronal regeneration and survival in response to injury and degeneration (Levi-Montalcini, 1987; Sendtner et al., 1992; Thoenen, 1995; Lewin and Barde, 1996; Sawai et al., 1996; Barde, 1997; Semkova and Krieglstein, 1999).

Additionally, expression of NTs by immune cells has been also reported: NGF and its receptor TrkA are expressed in activated $CD4^+$-T cell clones (Ehrhard et al., 1993b; Santambrogio et al., 1994); NGF is expressed by B cells (Torcia et al., 1996), macrophages and microglia (Elkabes et al., 1996; Heese et al., 1998), mast cells (Leon et al., 1998), eosinophils (Solomon et al., 1998), and basophiles (Burgi et al., 1996). mRNA of neurotrophins is expressed in spleen and thymus (Laurenzi et al., 1994) and in inflamed tissues. In our laboratory, it was demonstrated that activated T cells, B cells, and

monocytes produce BDNF *in vitro* and in inflammatory brain lesions (Kerschensteiner et al., 1999). Human hematopoietic cells (Chevalier et al., 1994) and stimulated PBMCs express Trk receptors (Ehrhard et al., 1993a; Ehrhard et al., 1994; Besser and Wank, 1999). NTs are able to modulate certain functions of the IS: NGF increases lymphocyte proliferation rate (Thorpe and Perez Polo, 1987) and differentiation of immune cells (Matsuda et al., 1988; Otten et al., 1989), stimulates immunoglobulin (Ig) production, and induces mast cell degranulation (Mazurek et al., 1986). Both NT-3 and BDNF induce proliferation and phagocytic activity of microglia (Elkabes et al., 1996). Myelin reactive T cells secrete effector molecules that mediate tissue destruction, but also produce neurotrophic factors, providing support to aid neuronal survival (Kerschensteiner et al., 1999; Moalem et al., 1999; Hohlfeld et al., 2000). The ability of neuroantigen-reactive T cells to infiltrate the CNS might be used to deliver molecules that augment a recovery response to degenerative, malignant or traumatic processes (Rapalino et al., 1998; Becher, 2000). Autoimmune T cells express NGF, BDNF, NT-3, and NT-4/5 when reactivated by their specific antigen in the injured CNS, suggesting a neuroprotective effect on the autoimmune damaged tissue (Schwartz et al., 1999; Hohlfeld et al., 2000; Moalem et al., 2000; Stadelmann et al., 2002; Kerschensteiner et al., 2003).

Besides the beneficial effects of NTs secreted from both systems, they have also been implicated in sickness and pain (Snider and McMahon, 1998; Benett, 1999; Shu and Mendell, 1999; Watkins and Maier, 1999). Hyperalgesia or exaggerated pain is triggered by pro-inflammatory cytokines released by activated macrophages, stimulating peripheral nerves that signal to the brain through the neighboring paraganglia, in which microglia and astrocytes release neuroexcitatory substances creating exaggerated pain responses.

Since most NTs exert functions in both systems, establishing neuro-immune communications, it is possible that also GFLs could have similar effects. However, few and contradictory reports have been published concerning the expression and/or functions of GFLs and their receptors in human immune and hematopoietic cells.

A putative role of RET in the regulation of hematopoietic cells has been suggested by the presence of RET in lympho-hematopoietic tissues of mice and rats, including fetal liver, thymus, spleen and lymph nodes (Avantaggiato et al., 1994; Tsuzuki et al., 1995), as well as in two human leukemia cell lines (Takahashi et al., 1985; Tahira et al., 1990; Takahashi

et al., 1991). Subsequently, *RET* expression was shown in some myelomonocytic, B cell and T cell leukemia/lymphoma cell lines (Gattei et al., 1997; Nakayama et al., 1999).
In contrast, transcripts of GFRα-1, GFRα-2 and GFRα-3 neither are found in THP-1 and HL-60 leukemia cells expressing *RET* nor in normal human peripheral blood cells (Nakayama et al., 1999).
Bone marrow (BM) hemopoietic cells express only *RET*, whereas BM stromal cells express GFRα-1, GFRα-2 and GDNF. It was speculated that GFRα on the surface of BM stromal cells function like soluble GFRα, and thus, the interaction between BM hemopoietic cells and stromal cells may induce the formation of a functional GDNF/RET complex involved in maturation of myelomonocytic cells in the BM microenvironment (Nakayama et al., 1999).
Despite these preliminary indications, expression of RET in human lympho-hematopoietic cells has not been investigated in detail so far.
The aim of this study was to investigate possible interactions between the nervous system and the immune system mediated by members of the GFLs, as well as their receptors: RET GFRα-1 and GFRα-2.

3.3. GDNF

3.3.1. Description and characteristics

GDNF was purified and characterized by Lin (Lin et al., 1993) from the supernatant of a rat glial cell line (B49) as a potent growth factor as well as survival factor for embryonic substantia nigra DA neurons (which degenerate in Parkinson's disease).
GDNF is processed and secreted as a mature protein of 134 amino acids that contains two *N*-linked glycosylation sites. It is a homodimer (disulfide-linked dimer) with a molecular mass of ~32 to 45 kDa, and under reducing conditions of ~18 to 22 kDa. Subsequently, it was found that GDNF was also a potent survival factor for spinal motoneurons (Henderson et al., 1994), and for sympathetic neurons.
However, the main function of GDNF is related to development, migration and survival of neural crest cells, which migrate to the kidney and to the enteric nervous system (ENS).

3.3.2. The GDNF gene

The human GDNF gene contains three exons and two introns. The second exon encodes the first 143 bp of the coding sequences that translates the *prepro*-region of the protein. The 3'-end region of this exon possesses an alternative splice site, resulting in an internal deletion of 78 bp. At the protein level, this deletion results in a loss of 26 amino acids in the *prepro*-region, leading to two identical isoforms (Woodbury et al., 1998). The third exon contains the majority of the coding sequences, the remainder of the *prepro*-region and all the amino acids found in the mature polypeptide.

The GDNF gene is highly regulated; its promoter region contains putative *cis*-elements that may account for the complex spatiotemporal pattern of expression and for rapid up-regulation by environmental stimuli.

3.3.3. GDNF knock-out mice

The importance of GDNF was revealed by GDNF knockout mice ($GDNF^{-/-}$), which displayed defects in the developing kidneys and lacked the ENS due to failed migration of neural crest cells (Moore et al., 1996; Pichel et al., 1996; Sanchez et al., 1996). These mice showed complete renal agenesis owing to lack of induction of the uretheric bud, an early step in kidney development. These mice die shortly after birth due to renal failure, and do not have enteric neurons, causing pyloric stenosis and dilation of duodenum.

In the nervous system, the total number of DA neurons is normal. Only a small deficit in sensory, sympathetic and motoneurons has been detected.

The phenotype of $GDNF^{-/-}$ mice is similar to both, $RET^{-/-}$ and $GFR\alpha\text{-}1^{-/-}$ mice, suggesting that they act upon similar signaling pathways.

3.3.4. Signaling

RET-dependent signaling of GDNF: GDNF induces different signaling pathways when acting through the GFRα-1/RET receptor complex (Trupp et al., 1999; Pezeshki et al., 2001); some of these pathways include PLCγ/AKT, RAS-MAPK-ERK (inducing phosphorylation of CREB), and JNK (Jun N-terminal kinase) (Airaksinen et al., 1999).

RET-independent signaling of GDNF via GFRα molecules: The GFRα-1 surface receptor located in lipid rafts together with an unknown transmembrane protein recruits

and activates Src-type kinases upon GDNF binding to GRFα receptor. Src kinases, in turn, phosphorylate PLCγ, leading to the production of IP_3 and release of intracellular Ca^{2+}.
In the absence of RET, GFRα-1 failed to activate AKT and RAS-MEK-ERK cascade, but activated a Src-like kinase that allowed ERK-independent phosphorylation of CREB (Pezeshki et al., 2001). Depending on the cell type, ligand-induced clustering of GPI-anchored proteins may activate different signaling pathways. GDNF induced Fos activation in cells expressing GFRα-1 but lacking RET (Trupp et al., 1998).

3.3.5. Expression and physiological functions

GDNF exhibits an extensive and complex spatiotemporal pattern of expression.
GDNF is essential as a differentiation, migration and growth factor in developing kidneys and the enteric nervous system (Sanchez et al., 1996).
Developmental and neonatal GDNF mRNA expression has been found at several sites in rat (Scharr et al., 1993) and in mouse CNS (Suter-Crazzolara and Unsicker, 1994): e.g. cerebral cortex, hippocampus, thalamus, striatum, cerebellum, olfactory bulb, superior cervical ganglia, dorsal root ganglia (DRG) and spinal cord. GDNF, NTN and their receptors were found in rat glial cultures (type-1 and type-2 astrocytes), and in glial precursors (Franke et al., 1998). TPA-treatment increased their levels (Remy et al., 2001), and following exposure to glutamate agonists, GDNF was a strong survival factor for astrocytes (Ho et al., 1995).
Low GDNF expression is maintained throughout life, particularly in the brain (Stromberg et al., 1993). In human adult CNS, a widespread distribution of GDNF protein was demonstrated (Kawamoto et al., 2000) in neuronal somas, dendrites and axons. It was also found in astrocytes (Moretto et al., 1996) and in microglia of the neocortex and white matter, hippocampus, basal forebrain, basal ganglia, hypothalamus, thalamus, mesencephalon (including SN), pons, medulla oblongata, cerebellum and spinal cord.
In the periphery, the expression of GDNF is widespread in many organs (Trupp et al., 1995): e.g. kidneys, skin, stomach, lungs, bone, heart, liver, spleen, blood (Suter-Crazzolara and Unsicker, 1994), peripheral nerves (Schwann cells), skeletal muscle (Springer et al., 1995) and reproductive tract: ovary but not in testis (Widenfalk et al., 2000).

GDNF in the CNS promoted the survival, induced differentiation and increased the high-affinity DA uptake of SN **dopaminergic neurons** *in vitro* (Lin et al., 1993) and *in vivo* (Hudson et al., 1995). Retrograde axonal transport of GDNF from the DA terminal region to the SN demonstrated its trophic effects on DA neurons in the adult brain (Tomac et al., 1995). GDNF also exerted a trophic effect on **noradrenergic neurons** (Arenas et al, 1995), and prevented neuronal degeneration when applied prior to the neurotoxic insult (6-OHDA) (Lapchak et al., 1997a). Similar effect was seen in **cholinergic neurons** located in the septo-hippocampal pathway, important for locomotor activity (Lapchak et al., 1997b).

GDNF may act in a paracrine-like fashion for the regulation of somatotrophic cell growth and in other cell functions, since its expression was found in the **anterior pituitary-cell types**: gonadotrophs, corticotrophs and the somatotrophs (Urbano et al., 2000).

GDNF enhanced the development and differentiation of Purkinje cells **(cerebellar neurons)**, which are the principal output cells of the cerebellum (Mount et al., 1995).

Approximately 50% of spinal cord motoneurons (MN) degenerate and die at a time when they are establishing synaptic connections with their target muscles. The survival of developing MN depends on the access to trophic molecules (such as BDNF or NGF). During this period, GDNF has a dose-dependent effect on the survival of MN cultures from embryonic (day 14) rat (Henderson et al., 1994) or embryonic (day 5) chick spinal cords (Oppenheim et al., 1995; Houenou et al., 1996). GDNF is 75 fold more potent than other NTs in supporting survival of **motoneurons**.

An age-dependent response to GDNF of **peripheral sensory neurons**, such as sympathetic, parasympathetic, cutaneous sensory and enteroceptive neurons has been reported (Buj-Bello et al., 1995). DRG neurons and MN are able to retrogradely transport radiolabelled GDNF (Matheson et al., 1997) from the periphery to the spinal cord. Additionally, during the post-natal life, GDNF has a more potent trophic effect than NGF on sensory neurons from the DRG (Snider and Wright, 1996; Molliver et al., 1997).

GDNF is present within the axons and in surrounding Schwann cells of **peripheral nerves** (Scharr et al., 1993), which highly express the full length and the truncated GDNF mRNA (Springer et al., 1995).

At **neuromuscular junctions**, transgenic over-expression of GDNF led to an increase in the number of motor axons innervating muscle fibers at the time when axons are being eliminated (Nguyen et al., 1998). Subcutaneous GDNF injections during the post-natal life

increased the number of axons converging at neuromuscular junctions (Keller-Peck et al., 2001). Over-expression of GDNF in skeletal muscle produced hyper-innervation of neuromuscular junctions with abnormal motor endplates (Zwick et al., 2001). Probably, one role of GDNF in post-natal MN is to promote terminal axon branching and synapse formation.

Elevated expression of the truncated GDNF isoform was found in normal human **skeletal muscle** (Springer et al., 1995). GDNF mRNA in muscle may not be entirely muscle-derived, but rather derived from peripheral nerve segments sheathed by proliferating Schwann cells infiltrating the fascicles.

GDNF could promote MN survival acting as a target-derived neurotrophic factor (Suzuki et al., 1998a) through retrograde transport to the motoneurons (Yan et al., 1995).

GDNF in **lympho-hematopoietic system** probably plays a role in terminal (Gattei et al., 1997) or intermediate differentiation (Nakayama et al., 1999) of myelomonocytic cell maturation in the BM microenvironment. BM stromal cells expressed GDNF, as well as GFRα-1 and GFRα-2; thus the interaction between hematopoietic cells expressing RET and stromal cells may form a functional GDNF/GFRα-1 complex. The involvement of GDNF in the regulation of normal and neoplastic monocytic cells was also supported by the developmental relationships between glial cells and the monocyte/macrophage system, and by the high expression of these factors in non-neural tissues, including hematopoietic organs such as liver and spleen (Treanor et al., 1995; Trupp et al., 1995).

GDNF in **embryogenic kidney** is localized in the metanephric mesenchyme at early stages, and is repressed in the induced mesenchyme when epithelial conversion occurs (Hellmich et al., 1996). GDNF stimulated branching morphogenesis in the kidney and induced ectopic uretheric buds from the nephric duct (Sainio et al., 1997).

GDNF may function as a paracrine morphogen secreted by cells of mesenchymal and neuroectodermal origin to modulate epithelial cell functions, such as migration during development and post-natal life in kidneys (Sainio et al., 1997) and in the ENS (Pichel et al., 1996; Sanchez et al., 1996). *In vitro,* GDNF promotes migration of human corneal epithelial cells, which express the receptors GFRα-1 and RET, indicating that GDNF is a chemoattractant factor for **epithelial cells** (You et al., 2001).

GDNF possess the ability to regulate spermatogonia renewal and differentiation during male **spermatogenesis** (Meng et al., 2000).

3.3.6. Regulation of GDNF expression

Signaling through multiple secondary messenger systems could regulate synthesis and release of GDNF in neuroblastoma and glioma cell lines (Verity et al., 1999). In glial cells, fibroblast growth factor (FGF) family members (-1,-2,-9) stimulated GDNF release as a consequence of re-entry into the cell cycle; pro-inflammatory cytokines: TNF-α, TNF-β, IL-1β and LPS also elevated GDNF expression. In contrast, in neuroblastoma cells, the same cytokines and LPS repressed GDNF release. TNF-α and IL-1β exerted inhibitory effects at the level of protein synthesis, post-translation modifications, or release of GDNF. Several stimuli could elevate GDNF release from neuroblastoma cells without changing mRNA levels, such as direct application of cAMP, activators of adenyl cyclase, inhibitors of phosphodiesterase activity, and prostaglandins (PGA_2, PGE_2 and PGI_2) that elevated intracellular cAMP levels, suggesting a regulated secretion of GDNF protein. A requirement for regulated release is the pre-existence of intracellular stores. GDNF has been also found in chromaffin granules (Krieglstein et al., 1998).

3.3.7. GDNF during pathological conditions

Parkinson's disease is characterized by degeneration of SN dopaminergic neurons in the midbrain that innervate the caudate nucleus and the putamen, forming the nigro-striatal dopaminergic system (Adams and Victor, 1993). Therefore, GDNF that could potentially prevent this degeneration and increase the functional activity of the remaining DA neurons, is of clinical interest and has been tested in several animal models (Gash et al., 1995; Kearns and Gash, 1995; Sauer et al., 1995; Tomac et al., 1995; Cass, 1996; Gash et al., 1996; Schultz et al., 1996; Lapchak et al., 1997; Date et al., 1998; Lapchak et al., 1998a; Lapchak et al., 1998b; Rosenblad et al., 2000). Due to these successful results, a multicenter clinical study of Parkinson's disease started in 1996, consisting of either GDNF or placebo intraventricular administration for one whole year. At the end, some patients entered the open-labeled phase, receiving GDNF therapy monthly. However, three years later, clinicopathological findings of a GDNF-treated patient, who died after seven months of treatment, were published, indicating that intraventricular GDNF treatment neither improved clinical Parkinsonism nor reduced dopaminergic degeneration. The conclusion was that the intracerebroventricular route of GDNF delivery might be

suboptimal in humans, suggesting the need for other delivery techniques for GDNF administration (Kordower et al., 1999).

Shaker mutant rats, an animal model for spinocerebellar ataxias **(cerebellar disease)** with degeneration of cerebellar Purkinje cells were treated with GDNF, which caused a delay in the degeneration of many but not all Purkinje cells (Tolbert et al., 2001), while only supporting the survival of spatially related Purkinje cells. Degenerated cells after treatment were not responsive to GDNF due to lack of GFR-α receptors (Burazin and Gundlach, 1999). Increased amounts of GDNF were also detected in the cerebellum of patients with multiple system atrophy compared to control patients (Kawamoto et al., 2000).

Epileptogenesis can be studied in animal models, such as the one caused by injection of kainic acid (Martin et al., 1995) or kindling-evoked recurring seizures (Kokaia et al., 1999). After induction of seizures, an increase in mRNA expression of GDNF, NTN and its receptors was observed in different regions of the brain. Thus, GDNF and NTN may modulate seizure susceptibility.

GDNF exhibited potent neuroprotective effects against **brain infarction** induced by middle cerebral artery occlusion and then reperfusion (Wang et al., 1997), and gave protection against the subsequent edema (Abe and Hayashi, 1997a; Abe et al., 1997b). GDNF protected against delayed neuronal dead induced in the hippocampus by transient forebrain ischemia (Miyazaki et al., 1999), which was related to transient increases of hippocampal GDNF, GFRα-1 and RET, as well as cortical GFRα-2 mRNA levels (Kokaia et al., 1999; Arvidsson et al., 2001).

Glioblastoma and gliosarcoma expressed GDNF and GFRα-1 protein at concentrations up to five times higher compared to normal tissue. GDNF could act as an autocrine or paracrine factor for gliomas *in vivo*, suggesting an involvement of GDNF for their growth and differentiation (Wiesenhofer et al., 2000).

GDNF can rescue neonatal rat facial MN from axotomy-induced cell death and atrophy. 90% of facial MN degenerate after **peripheral nerve axotomy**; however, all MN survived and exhibited normal soma morphology after GDNF treatment. Therefore, GDNF can be a physiological and pharmacological trophic factor for spinal MN (Henderson et al., 1994).

After sciatic nerve lesions in adult animals, GDNF mRNA levels increased in Schwann cells and in denervated muscles. Thus, GDNF produced by muscle could act as a target-

derived neurotrophic factor for MN (Springer et al., 1995; Trupp et al., 1995), which took up and retrogradely transported GDNF from a terminal field on muscles.

After axotomy, Schwann cells proliferated in the distal stump of a transected peripheral nerve; this coincided with the up-regulation of the GDNF-full length mRNA and *RET* mRNA observed distal to the nerve site injury, and on the satellite cells of the affected DRG (Hammarberg et al., 1996; Bär et al., 1998). If a significant amount of GDNF protein is synthesized in injured nerves after trauma and becomes available to primary sensory, sympathetic and MN, it could have important survival and regenerative effects on these groups of peripheral neurons (Ramer et al., 2000). The rapid appearance of cytokines in injured nerve tissue suggests that TNF-α and IL1-β may in part regulate injury-induced glial GDNF synthesis/release.

Locally administered GDNF prevented 50% of cell death in adult mice after **avulsion-induced cell death**, and induced hypertrophy of surviving MN (Li et al., 1995).

In **peripheral neuropathies**, GDNF can be transported retrogradely in a receptor-mediated fashion: spinal MN express GDNF receptors, thus, skeletal muscle-derived GDNF exerts a trophic function on these neurons, which had been disconnected from their target muscle after nerve-fiber lesion. GDNF might enhance axonal sprouting, contributing to re-innervation (Lie and Weis, 1998).

GDNF, GFRα-1 and *RET* mRNAs were examined in sural nerve biopsies from normal controls and from various peripheral neuropathies (vasculitis, ischemic, acute and chronic inflammatory demyelinating neuropathies, and others). GDNF and GFRα-1 mRNA levels were elevated to variable extents in the diseased nerves compared to controls, but independent of the type of disease. GDNF mRNA was related neither to axonal or demyelinating pathology, nor to the presence of inflammatory cells. In contrast, an increase in GFRα-1 mRNA expression was correlated with the extent of axonal pathology, and was also proportional to the nerve invasion by T cells and macrophages. The proportional relationship between GFRα-1 levels and the extent of inflammatory cell invasion could indicate that these cells may express GFRα-1 mRNA (Yamamoto et al., 1998). RET mRNA expression was not detected in normal or diseased nerves.

Biopsies from normal human skeletal muscle and from **muscular diseases**, such as polymyositis (PM, an inflammatory autoimmune muscle disease) and Duchenne muscular dystrophy (DMD, a genetic muscle disease) were studied (Suzuki et al., 1998b). In both diseases, muscle fibers undergo massive necrosis with focal lyses of the plasma membrane; satellite cells surrounding necrotic fibers are activated and differentiated into myogenic cells. Finally, regenerating post-mitotic myoblasts fuse to multinucleated myotubes, similar to immature muscle fibers. GDNF was present in the periphery of normal myofibers and was up-regulated only in regenerating muscle fibers in both diseases.
Muscle contusion also induced up-regulation of GDNF and GFRα-1 mRNAs in Schwann cells of intramuscular nerves in damaged muscle fibers (Kami et al., 1999).

Neurogenic atrophy of skeletal muscles is caused by peripheral neuropathy or by degeneration of MN (i.e.: **Amyotrophic Lateral Sclerosis**: ALS). In ALS, denervation is incomplete combined with different stages of atrophy, being partially compensated by collateral reinervation and muscle fiber hypertrophy, all of them present at the same time.
In muscle biopsies from patients with **motor neuropathy**, the full-length GDNF mRNA was increased, but four weeks after denervation, both isoforms showed similar expression.
Muscle biopsies taken from ALS patients showed that both GDNF isoforms were elevated in all post-mortem spinal cords of end-stage disease patients. High levels of GDNF were found in muscles with high number of partially atrophic, recently denervated fibers, indicating an increased demand of GDNF from MN, probably related to excessive collateral nerve sprouting. In contrast, a down-regulation in the muscular expression of GDNF mRNA was found in end-stages of ALS, due to a reduction in the number of muscle fibers, and replacement of them by connective tissue (Corse et al., 1995; Grundstrom et al., 1999). Increased levels of GDNF protein were found in 12 out of 15 ALS-cerebrospinal fluid samples compared to controls.
Taken together, the increased expression of GDNF mRNA in muscle of ALS indicates that the capacity to synthesize GDNF is enhanced in ALS (Grundstrom et al., 2000).

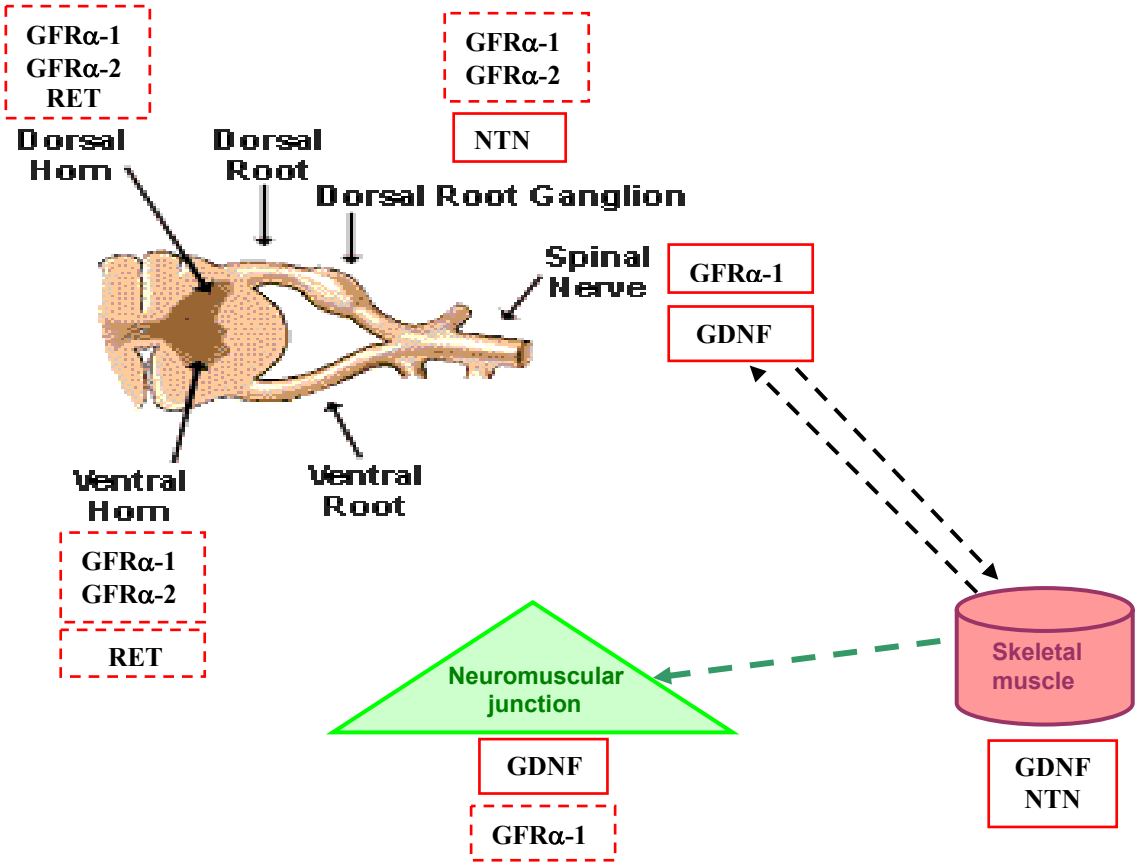

Figure 2: Expression of GDNF, NTN, RET, GFRα-1 and GFRα–2 in the neuromuscular system. The scheme shows the spinal cord, the dorsal root ganglia (DRG) and ventral root ganglia (VRG), peripheral nerves, neuromuscular junction and muscles. Skeletal muscles express GDNF and NTN, both can be retrogradely transported to the ventral horn of the spinal cord (motoneurons) where the receptors RET, GFRα-1 and GFRα-2 are expressed and bind GFLs. Schwann cells ensheathing the axons of peripheral nerves also express GDNF.

The relation between perineural **invasion of tumor cells** and expression of GDNF, GFRα-1 and RET was investigated in patients with bile duct carcinoma (Iwahashi et al., 2002). High expression levels of GDNF were found in normal epithelial cells of the bile duct, whereas GFRα-1 and RET proteins were undetectable in the same cells. In peripheral nerve tissues surrounding the bile duct, strong expression of GFRα-1 and moderate expression of RET and GDNF was observed. In specimens of bile duct carcinoma, expression of GDNF was down-regulated during its development. GDNF in tumor cells, as well as GFRα-1 and RET expression in peripheral nerves may play a role in perineural invasion of bile duct carcinoma through chemoattraction among these molecules.

3.4. NEURTURIN

3.4.1. Description and characteristics

Neurturin (NTN) was discovered due to the fact that conditioned medium of Chinese hamster ovary cells could support the long-term survival of sympathetic neurons from the superior cervical ganglion (SCG). This survival factor was purified and a novel protein, with a molecular weight of 25 kDa and similar structural characteristics of GDNF was described (Kotzbauer et al., 1996). The *prepro*-NTN contains 195 amino acids and the mature peptide 100 amino acids. Its sequence shares 42% similarity with the mature GDNF, containing the seven-conserved Cys residues spaced similarly as other member of the TGF-β superfamily.

The mRNA sequence for *prepro*-NTN is encoded by two exons containing 594 base pairs. The intron begins at position 169. The coding sequence for the mature protein is located in exon 2, between nucleotides 286 and 591 (Heuckeroth et al., 1997).

NTN is a trophic factor that promotes the survival of numerous neuronal populations including peripheral parasympathetic, nodose and DRG sensory neurons, as well as central midbrain DA neurons.

3.4.2. NTN knock-out mice

$NTN^{-/-}$ mice are viable and fertile but have defects in the ENS, including reduced myenteric plexus innervations and reduced gastrointestinal motility. The phenotype shows periorbital abnormalities, with eyelid droopiness, crusting drainage around the eye, and reduced tear production, resulting from defects in the lachrymal gland parasympathetic innervation, which also affects the submandibular salivary gland. Parasympathetic neurons have a reduced size and diminished fiber density, indicating that NTN is a trophic factor for them. GFRα-2-expressing cells in the trigeminal ganglia, DRG, cilliary ganglion and submandibular salivary gland are also depleted (Heuckeroth et al., 1999).

3.4.3. Signaling

Like other members of the GFLs, NTN signals through the RET tyrosine kinase and also requires a GPI-linked surface receptor, GFRα-2. Binding of NTN induces autophosphorylation of RET and subsequent activation of different signaling pathways

(Airaksinen et al., 1999), such as MAPK pathway, which is activated in sensory cervical ganglia neurons, as well as the PI_3-K pathway (Creedon et al., 1997).

NTN also activated RET through the binding to GFRα-1 in fibroblasts transfected with GFRα-1 but not with GFRα-2 (Baloh et al., 1997). However, a similar RET-activation was not observed when neurons were transfected with GFRα-2 (Buj-Bello et al., 1997). In addition, cell-free studies failed to show specific binding of NTN to GFRα-1, even at NTN concentrations that should activate RET. These results indicated that the RET-independent action of GFRα-1 was highly selective for GDNF, but not for NTN (Pezeshki et al., 2001).

NTN and GFRα-2 expression patterns are in some cases complementary, but not in others, suggesting multiple modi operandi in relation to RET and GFRα-1. For example, NTN co-localized with RET and GFRα-1, but not with GFRα-2 in uretheric buds of developing kidney.

However, the similarity of potency and efficacy of NTN and GDNF on DA neurons was difficult to explain with the low expression of GFRα-2 on these neurons. Probably, NTN signals via low levels of GFRα-2 on the surface of DA neurons, or NTN might signal *in vivo* through GFRα-1. Alternatively, GFRα-2 expressed by cells in the vicinity of nigral DA neurons may be presented to nigral dopaminergic neurons either by cell-cell contact or by diffusion of soluble GFRα-2.

3.4.4. Expression and physiological functions

NTN expression is developmentally regulated in the nigrostriatal system, exhibiting potent actions on the survival and function of midbrain **DA neurons**, with efficiencies similar to GDNF, being sequentially expressed in mature nigral DA neurons (Horger et al., 1998).

NTN mRNA expression was found in mouse CNS in the postnatal cerebral cortex, striatum, brain stem, pineal gland and in the developing pituitary gland.

Low levels of NTN mRNA are expressed in **astrocytes** (Franke et al., 1998; Remy et al., 2001).

During development, NTN is expressed in the **smooth muscle** layer of the intestines, in smooth muscle of the urether, and in bronchiole. In salivary glands NTN showed an epithelial expression, whereas GFRα-2 is located in the surrounding tissue.

NTN and GFRα-2 are also found in developing sensory organs, in Sertoli cells and in the epithelium of the oviduct, whereas germ cells express only GFRα-2.

In neonatal animals, NTN mRNA is strongly detected in **blood**, the heart, the brain, seminiferous tubules of the testis, in the uterus, but less in the ovaries (Widenfalk et al., 2000). However, in adult tissues NTN expression is stronger in heart and less in blood, brain or ovaries (Creedon et al., 1997).

In adult rats, NTN is expressed in smooth muscle of penile blood vessels, corpus cavernosum, and in several intrapelvic organs, whereas GFRα-2 and RET mRNA are expressed in the penile neurons of the pelvic ganglia. NTN acted as a target-derived survival factor for penile erection-inducing postganglionic neurons, being specific transported from the axon terminals to neuronal soma (Laurikainen et al., 2000).

NTN is a trophic factor for **parasympathetic and postmitotic enteric neurons**. To form the ENS, neural crest cells migrate from the vagal and sacral regions of the spinal cord to the gastrointestinal tissue. While migrating, these cells undergo many rounds of proliferation to produce enough neurons and glial cells to populate the ENS. Post-mitotic neurons extend axonal processes to create a network of cells that regulate motility, sensation and mucosal secretion in the gut. $GDNF^{-/-}$ mice have intestinal aganglionosis, as a result of insufficient proliferation of ENS precursor cells. $NTN^{-/-}$ mice have a reduction in the ENS-nerve fibers and abnormal gastrointestinal motility, with minimal reduction in the enteric neuron number; thus, NTN is important as a trophic factor rather than migration factor for postmitotic myenteric neurons.

3.4.5. Regulation of expression of NTN

GDNF signaling via the RET/GFRα-1 complex is required early for proliferation and migration of the neuronal precursors of the parasympathetic cranial ganglia: submandibular, sphenopalatine and otic. NTN exerts its effects subsequently during development and is important for the maintenance of these neurons. This switch in ligand dependency during development was partly governed by the altered expression of GFRα, as demonstrated by the predominant expression of GFRα-2 in parasympathetic neurons after ganglia formation (Enomoto et al., 2000). Synthesis of NTN was maintained throughout the cell death period. In contrast to stable levels of NTN and GFRα-2, the down-regulation of GDNF and GFRα-1 suggested a novel mechanism by which multiple

neurotrophic factors and their receptors contribute to neural differentiation and survival (Hashino et al., 2001). NTN also regulated heat sensitivity in a subpopulation of unmyelinated nociceptors.

3.4.6. NTN under pathological conditions

GFLs signaling exert a **neuroprotective role after brain insults** as shown after the administration of recombinant GFLs to the brain in animal models. GDNF, NTN and ART could reduce death of DA neurons following lesions of the nigrostriatal pathway (Tseng et al., 1998; Bjorklund et al., 2000; Rosenblad et al., 2000). *In vivo*, a single administration of NTN led to a threefold increase in nigral cells survival after intrastriatal injection of 6-OHDA (Horger et al., 1998).

Seizure activity regulated gene expression for NTN, similarly to GDNF; therefore NTN could also modulate **seizure susceptibility** (Kokaia et al., 1999).

NTN was expressed in **human neuroblastoma cell lines**, but its function is not yet known (Hishiki et al., 1998).

3.5. PERSEPHIN

3.5.1. Description and characteristics

Persephin (PSP) was identified as a new member of the GDNF family ligands using degenerate PCR and homology cloning. PSP showed 40–50% amino acid homology to GDNF and NTN (Mildbrandt et al., 1998). The human PSP gene contains 468 nucleotides coding the prepro-protein of 156 residues; the mature protein is encoded by 96 amino acids. The PSP gene contains one intron that begins at position 153. RT-PCR revealed a short and a long isoform, which were identical except for the 88 bp intron sequence continued in the longer version. Similar to NTN, PSP contains a long C-G rich region (Jaszai et al., 1998).

Analysis of various tissues showed that PSP mRNA was inefficiently spliced, since spliced and unspliced mRNA species were found at equal levels. The relative abundance of the unspliced mRNA suggested that the regulation of PSP mRNA processing may be an important means of regulating the production of PSP protein in some tissues.

3.5.2. PSP knock-out mice

$PSP^{-/-}$ mice showed normal development and behavior. No abnormalities were seen in the intestinal tract, ENS, kidney, liver, gonads, heart or skeletal muscle. Several tests for red/white blood cells, chemistry dysfunction, and chemical panel were performed on blood collected from adult mice of $^{+/+}$, $^{+/-}$, and $^{-/-}$ PSP genotypes; however, no significant differences between groups were observed. These findings suggested that PSP is not a survival or growth factor for CNS or peripheral tissues. The only abnormality found was hypersensitivity to focal cerebral ischemia or stroke (Tomac et al., 2002).

3.5.3. Signaling

PSP can bind only to the surface receptor GFRα-4, and then to RET receptor located on the lipid rafts (Airaksinen et al., 1999; Lindahl et al., 2001; Airaksinen and Saarma, 2002).

3.5.4. Expression and physiological functions

PSP mRNA was detected in the SNC in the cortex, hippocampus, striatum, mesencephalon, and cerebellum. In peripheral tissues it was found in heart, kidney, liver, skin, skeletal muscles, DRG, spinal cord, and MN (Jaszai et al., 1998). However, higher levels were found in embryonic than in adult tissues.

PSP, like GDNF and NTN, promoted the survival of midbrain DA neurons in culture. It also promoted uretheric bud branching during developing stage. On the contrary, PSP had no survival-promoting effect on any peripheral neuron, including SCG, sensory neurons in DRG, and enteric neurons (Mildbrandt et al., 1998).

3.5.5. PSP under pathological conditions

PSP prevented degeneration of *dopaminergic neurons after toxic stimulus in vivo*, and supported the survival of MN *in vitro* and *in vivo* after sciatic **nerve axotomy**. In spinal cord motoneuron cultures, high doses of PSP enhanced glutamate transport inhibitor (Ho et al., 2000). Exogenous and endogenous PSP were critical components of neuroprotection mechanisms against **ischemic brain injury** induced via glutamate excitotoxicity/dysfunction (Tomac et al., 2002).

3.6. RET Tyrosine kinase receptor

3.6.1. Description and characteristics

RET was originally identified as an oncogene activated by DNA rearrangement (Takahashi et al., 1985), (RE-arranged during Transfection). The product of the *Ret proto-oncogene* is a cell surface and transmembrane receptor with an intracellular tyrosine kinase domain. The same author (Takahashi and Cooper, 1987) showed that this gene encoded a protein homologous to a tyrosine kinase, and reported the first sequence of a *RET* cDNA derived from the THP-1 human leukemia cell line (Takahashi et al., 1988). The sequence coded for a protein of 1114 amino acids (Takahashi et al., 1989).

Subsequently, it was reported that alternative polyadenylation and mRNA splicing could generate at least five distinct 3'-ends (Tahira et al., 1990). These isoforms were predicted to encode RET proteins with two distinct intracellular C-terminal ends. The second isoform encoded a smaller protein of 1072 amino acids. These two proteins, containing either 1072 or 1114 amino acids differ from each other in their 9 and 51 C-terminal amino acids respectively. Those sequences were completely unrelated, designated as the **short** or **RET-9** (9 amino acids) and the **long** or **RET-51** (51 amino acids) isoforms of the RET protein. Further analysis demonstrated a third *RET* transcript that encoded a protein with an alternative 43 amino acids C-terminal, also called the **middle isoform** or **RET-43** (Myers et al., 1995). The intracellular domain of RET contains 14 Tyr residues; RET-9 lacks two Tyr at the C-terminus.

The structure of the extracellular region of the RET exhibits four domains, each of about 110 residues, containing the consensus motif of the cadherin sequence (CLD) and a Ca^{2+}-binding site located between two domains (starting at amino acid position 272), which is required for RET binding to GDNF but not for GDNF binding to the GFRα-1. Ca^{2+}-binding helps to linearize and rigidify the structure and to promote dimerization of CLDs. This region also contains a cysteine–rich motif (Cys) located between amino acids 516 and 635, corresponding to nucleotide sequences of exons 8 to 11 (Anders et al., 2001).

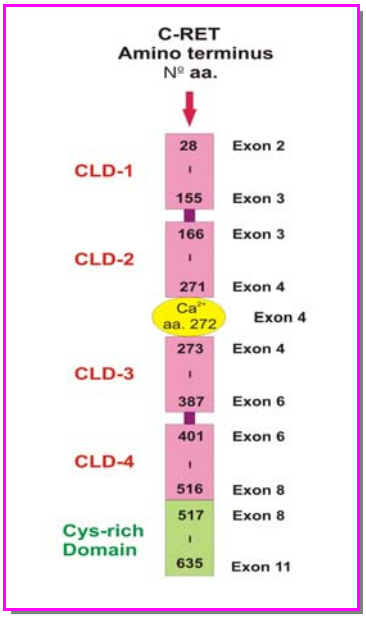

Figure 3: Scheme of the amino terminal and extracellular domain of the RET protein.

This scheme displays the relation between amino acid sequences and numbers of exons translated into the extracellular domain of the human RET protein. The amino terminal region of RET is depicted, including the four cadherin-like domains: CLD-1 to CLD-4, the Ca^{2+} binding site (starting at amino acid 272), and the cysteine-rich domain (Cys-rich). Exons encoding for each domain are numbered on the right side: CLD-1: amino acids 28 to 155 (exons 2 and 3). CLD-2: amino acids 166 to 271 (exons 3 and 4). CLD-3: amino acids 273 to 387 (exons 4 and 6). CLD-4: amino acids 401 to 516 (exons 6 and 8).

Overall, the RET protein contains an extracellular domain composed by a NH_2 region, including four CLD-1/4 domains and a Cys-rich motif; a transmembrane domain; and an intracellular domain formed by two tyrosine kinase domains, an inter-kinase domain, and the COOH-terminal region, as depicted in the next figure:

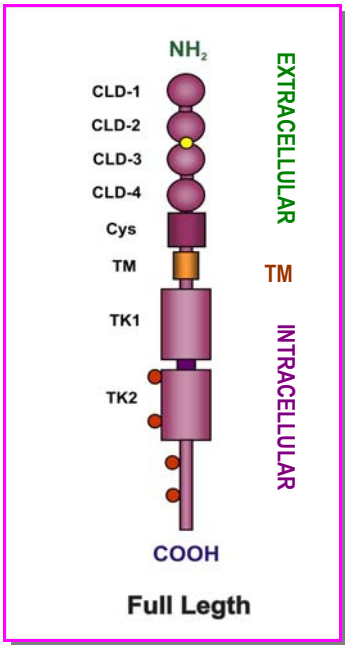

Figure 4: Scheme of the full length of the human RET protein representing the extracellular, the transmembrane and the intracellular domains.

The scheme shows from the upper part to the bottom: the amino terminal region **(NH_2)**, the Ca^{2+}-binding motif (yellow circle), four cadherin-like domains 1 to 4 (CLD-1, CLD-2, CLD-3, CLD-4), the cysteine rich region (Cys); the transmembrane domain (TM) and the intracellular part composed by the tyrosine kinase domains (TK_1 and TK_2) and the carboxyl terminus **(COOH)**. Red circles represent Tyr residues acting as docking sites for adaptor proteins (modified from Anders et al. 2001).

3.6.2. The RET gene

The human RET oncogene was mapped to chromosome 10q11.2 (Ishizaka et al., 1989). This gene contains 21 coding exons (Kwok et al., 1993; Myers et al., 1995). The first exon contains the translation start site and codes for most of the amino terminal signal sequence; the extracellular domain is encoded by the first 10 exons. A cadherin related sequence is located about 480 amino acids upstream of the transmembrane domain. Seven copies of a motif responsible for Ca^{2+} mediated homophilic binding are present within the extracellular domain. The transmembrane domain is encoded by a single exon (exon 11).
The cytoplasmic domain is encoded by the next 9 exons, which encode the two-tyrosine kinase domains and the C-terminus. The following scheme, Figure 5 shows the relation between exon structure and predicted domains of the RET protein, as well as the location of primers utilized for detecting spliced isoforms located at both ends of the gene, i.e. at the 5'-end and at the 3'-end regions.

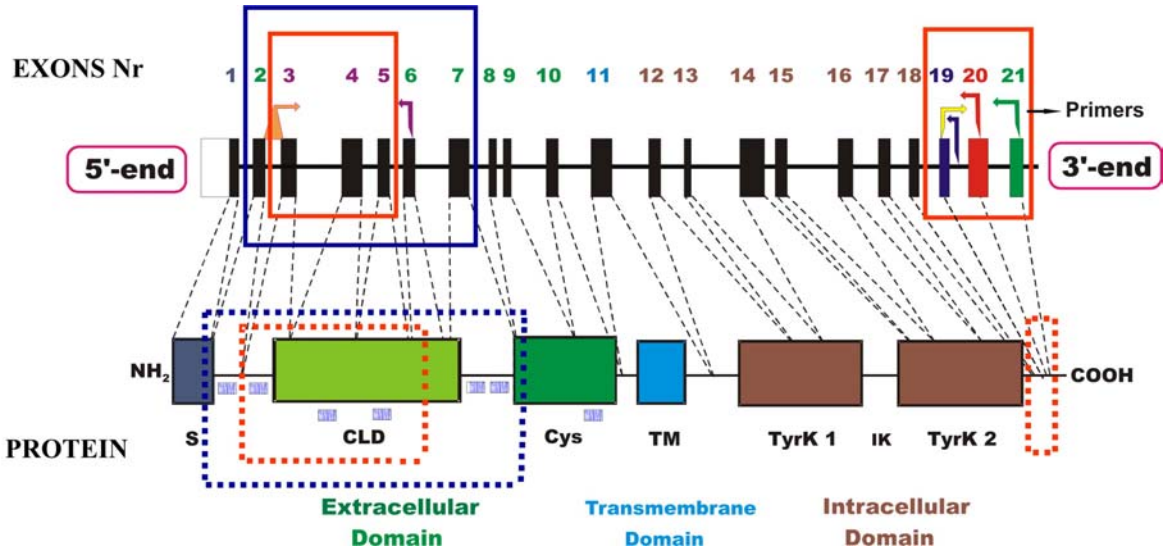

Figure 5: Correlation of the exon structure of the RET oncogene and the functional domains of the predicted protein. Solid black boxes indicate the exons. Dotted lines refer the exons to the corresponding domains found in the RET protein, which are represented as following: the amino terminal signal (NH_2) sequence (S), Ca^{2+} mediated binding motifs (hatched boxes), the cadherin like-domains (CLD), the cysteine rich region (Cys), the transmembrane domain (TM), the tyrosine kinase domains (TyrK 1 and TyrK 2), the inter-kinase domain (IK), and the COOH-terminal. Sites for alternative splicing **at the 5'-end region** are shown as exons inside of lined squares (red and blue). Primers used to amplify the isoforms hybridized in exons 2-3 (forward: orange arrow) and in exon 6 (purple arrow). Dotted squares represent altered sites in the

protein after splicing. Differential splicing **at the 3'-end region** results in transcripts encoding three isoforms that differ with respect to their C-terminal amino acid sequences. Head arrows to the left represent location of reverse primers for each isoform: blue arrow corresponds to the short isoform (RET-9) in intron 19; red arrow represents the long isoform (RET-51) in exon 20; green arrow shows the middle isoform (RET-43) located in exon 21. Arrow to the right (yellow) represents the forward primer. (Taken and modified from Kwok et al., 1993 and Myers et al., 1995).

3.6.2.1. RET splicing isoforms of the human gene

Extensive splice variants in the mRNA regions encoding the extracellular domain and the carboxyl terminal part of the RET protein provide high diversity, variation in the half life and in nuclear localization, and are predicted to affect the ligand-interacting properties or downstream signaling of the protein, respectively.

Alternative splicing of the primary transcript occurs at the 5'- or at the 3'-end regions; splice sites located at the 5'-end region encode RET proteins exhibiting differences at the amino-terminus (NH_2) and in the extracellular domain, due to having a truncated extracellular ligand-binding domain.

The splice variants at the 3'-end region of mRNA encode at least three different carboxyl terminal amino acid sequences, and therefore differences in the intracellular domain.

The *RET* exons 8 – 18, encoding the cysteine–rich, the transmembrane, and the major tyrosine kinase domains seem not to be subjected to alternative splicing. The transcriptional and post-transcriptional mechanisms of *RET* mRNA processing may contribute to the differential expression of RET protein in some carcinomas compared to non-neoplastic tissues (Carson and Walter, 1998; Fluge et al., 2001).

The 5'-end coding region of the RET gene:

Three alternatively splice isoforms due to exon skipping in the 5'-end region of the RET gene, that encodes the extracellular domain of the RET protein were described. Skipping occurs with the combination of exon 2 to exon 4, 5 or 6 (Lorenzo et al., 1995; Ivanchuk et al. 1997):

Full length mRNA (FL): exon 2 linked to exon 3

3-RET mRNA: exon 3 spliced out

3,4-RET mRNA: exons 3 and 4 spliced out

3,4,5-RET mRNA: exons 3, 4 and 5 spliced out

The FL mRNA is expressed three times more abundantly than the 3- and 3,4-RET mRNA isoforms in fetal human brain and kidney (Lorenzo et al., 1995).

3,4,5-RET mRNA isoform is the least abundantly expressed, only 10% of the amount of the full length transcript. All four *RET* mRNA isoforms are expressed in thyroid cells (from MTC) and in SHSY-5Y neuroblastoma cells. However, they are not tumor-specific, because they are also expressed in normal human adult tissues, such as thyroid, adrenal gland, kidney and brain.

3- and 3,4,5-RET mRNA isoforms maintain the published open reading frame and are predicted to encode RET proteins with deletions in the extracellular domain within the putative ligand-binding domain; they differ from FL in their ability to interact with the ligands since the cadherin domains are partially or completely removed. Relative to the published open reading frame (ORF), the 3- and 3,4,5- mRNA isoforms maintain the ORF and encode proteins, lacking aa. 113 to 209 and 113 to 354, respectively, Figure 6.

However, 3,4-mRNA does not maintain the published ORF. In this message, exon 5 is translated in another frame that has a stop codon within exon 5, at nucleotide 1204. The predicted protein contains the published exon 2 and 3 ORF plus 63 amino acids from the alternate frame of exon 5 at the C-terminus. This protein terminates before the TM domain, and would encode a soluble form of RET (next figure).

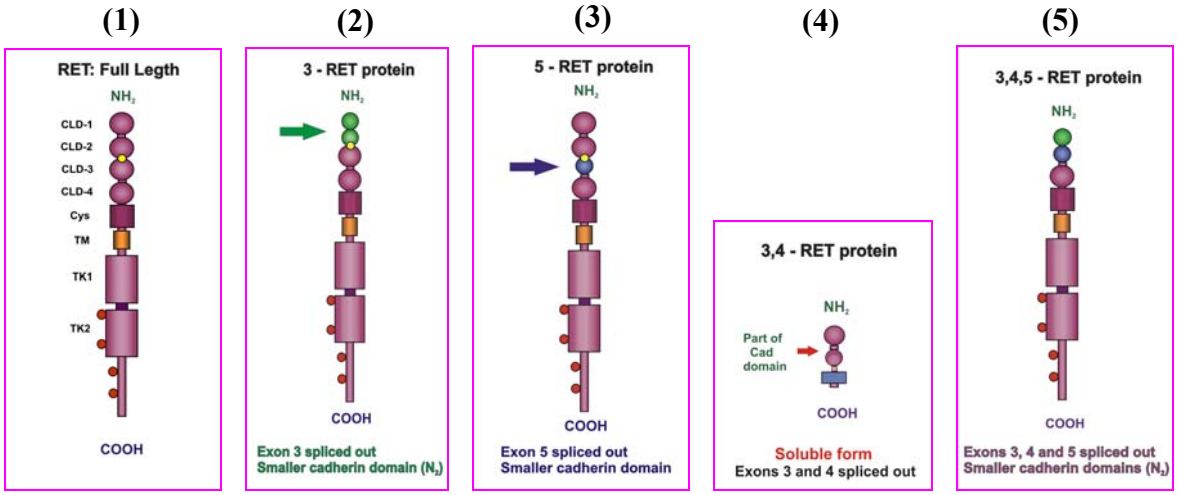

Figure 6: Putative proteins encoded by the RET mRNA isoforms located at the 5'-end region. (1) Full length RET protein. **(2)** 3-RET: exon 3 spliced out. **(3)** 5-RET: exon 5 spliced out. **(4)** 3,4-RET: exons 3 and 4 spliced out or soluble isoform. **(5)** 3,4,5-RET: exons 3, 4 and 5 spliced out. NH_2*:* amino terminus. COOH*:* carboxyl terminus. CLD-1 *to 4:* cadherin-like domains. Cys: cysteine-rich domain. TM*:* transmembrane

domain. TK1 and TK2*:* intracellular tyrosine kinase domains. The predicted proteins do not differ in the COOH terminus (modified from Lorenzo et al. 1995 and Ivanchuk et al., 1997).

Another variant, lacking exon 5 (Figure 6 (3)) has not been described; however in this work it was detected in some human immune cells by RT-PCR. This isoform would encode a protein with a smaller CLD-3 domain (see Results).

Recently, another publication describing the expression of alternative splicing isoforms of *RET* in normal thyroid tissue and in papillary carcinoma reported new variants at the 5'-end region of the gene. Four *RET* splicing events were found in this region. The open reading frames were all in-frame with the RET tyrosine kinase domain (Fluge et al., 2001). In the region encoding the Cys-rich, transmembrane, and Tyr kinase domains no alternative splicing has been detected.
The splice variants located between exons 1 and 8 are the following:
Ret 1-8 mRNA: exons 2, 3, 4, 5, 6 and 7 are spliced out
Ret 2-8 mRNA: exons 3, 4, 5, 6 and 7 are spliced out
Ret 3-8 mRNA: exons 4, 5, 6, and 7 are spliced out

The 3' end coding region of the RET gene:
The RET gene may encode 10 different 3'-termini producing three coding variants and four polyadenylation sites (Tahira et al., 1990; Myers et al., 1995; Ivanchuck et al., 1998).
RET-9 or **short isoform** is generated when exon 19 continues directly downstream with nine further codons, which lie within intron 19.
RET-51 or **long isoform** is expressed when exon 19 is spliced directly to exon 20, encoding 51 absolutely different amino acids at the COOH.
RET-43 or **middle isoform** occurs when exon 19 splices directly to exon 21. Exon 19 is followed by additional 43 codons downstream before a stop codon is reached.

The genomic organization of the 3'-end region of the human RET gene is represented:

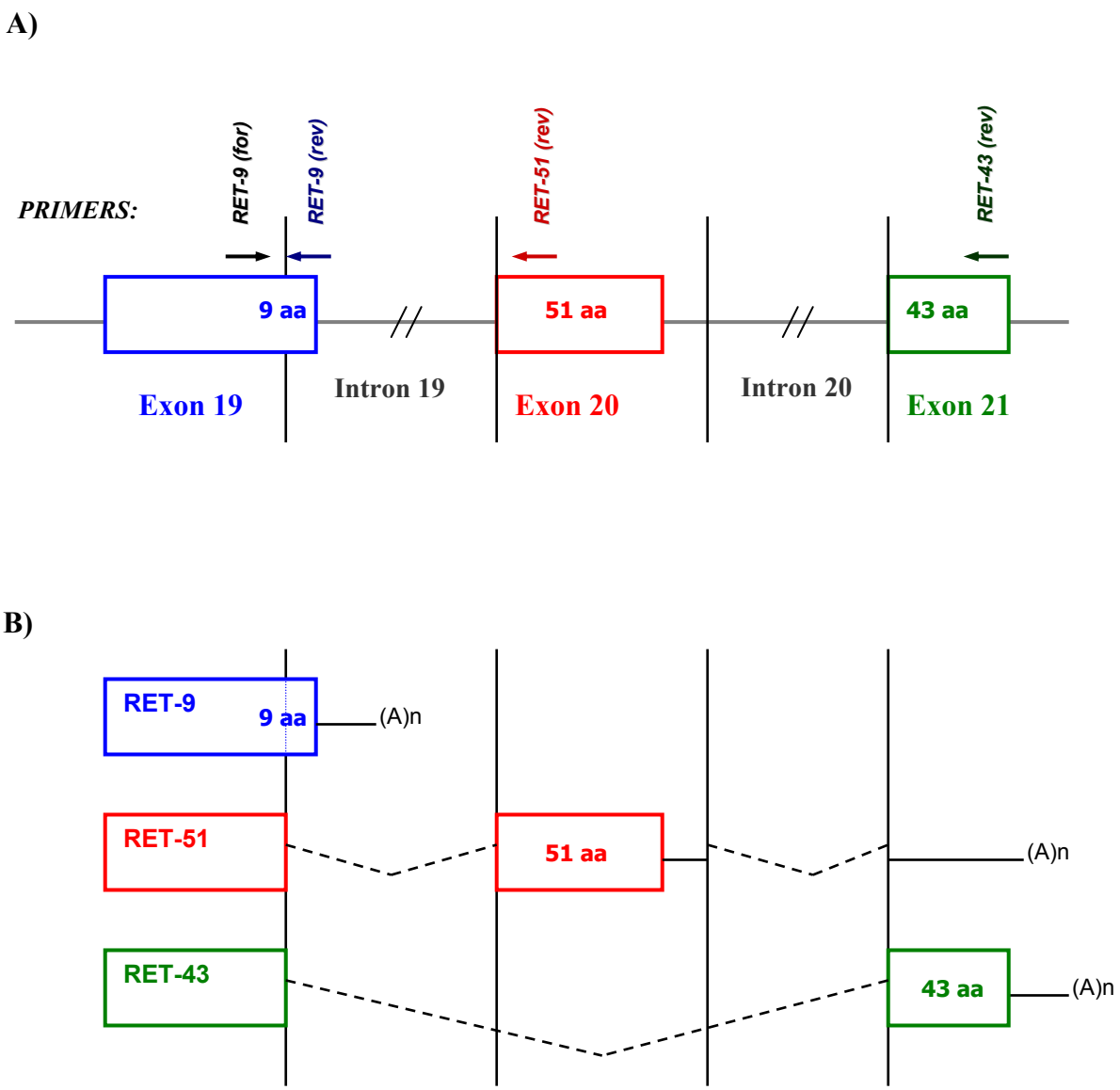

Figure 7: A) Genomic organization of the 3'-end region of *RET* showing intron and exon arrangement. Primers used in this study and their orientations are indicated by arrows. Boxes indicate coding sequences: RET–9 (short isoform), RET–51 (long isoform) and RET–43 (middle isoform), while lines represent untranslated regions. They differ in their amino acid composition, and length at the carboxyl terminus. **B)** Schematic representation of transcripts analyzed (taken from Ivanchuk et al., 1998).

Next scheme shows the nucleotide sequence of the isoforms located at 3'-end of *RET*:

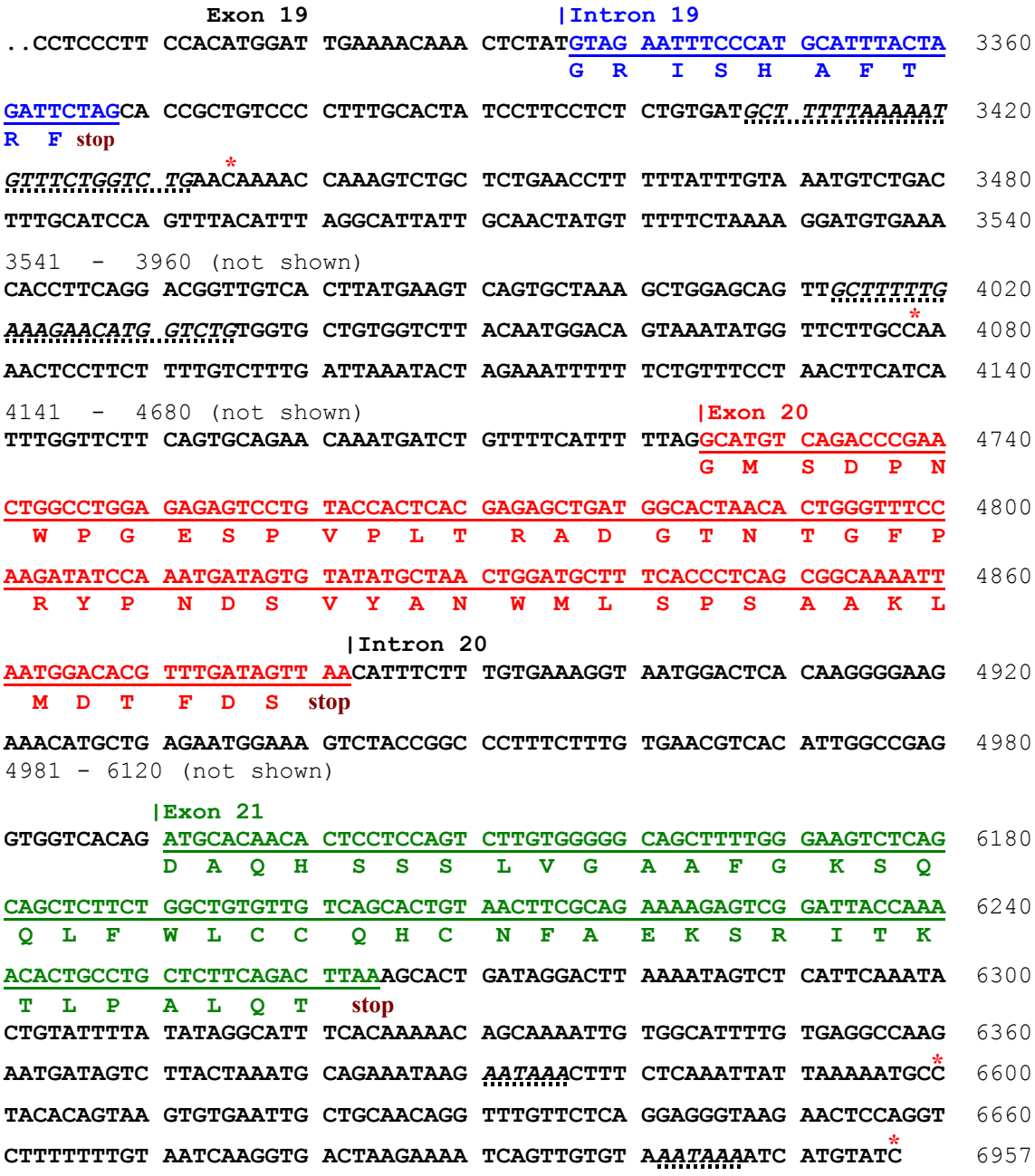

Figure 8: Sequence of the *RET* 3'-end terminus. The sequence begins at the 3'-end of exon 19 at bp 3337 according to Takahashi et al. (1988, 1989). Base position numbering after exon 19 through to the final 3' polyadenylation site includes all UTR and coding sequences and therefore does not agree with Takahashi. Coding sequences are underlined and colored and amino acids are shown below. Sequences related with polyadelylation are dotted-underlined and italicized. Polyadenylation sites are indicated by an asterisk (*) above the nucleotide preceding the poly A sequence. Stop codons are indicated. Nucleotide sequences from each isoform are marked with letters of different colors: RET-9 in blue, RET-51 in red and RET-43 in green (from Myers et al., 1995).

3.6.2.2. Functional differences between proteins encoded by the three isoforms located at the 3'-end region of *c-RET* gene:

Differences between the aforementioned isoforms have not yet been well defined and only few studies have demonstrated some specific characteristics in developing kidneys and in the ENS. RET-9 and RET-51 are necessary for specific temporal and spatial RET functions. The long isoform, RET-51, is essential for normal RET function, since the last two additional Tyr are implicated in autophosphorylation of RET and are docking sites for adaptor proteins. RET-9 and RET-43 do not encode these Tyr residues, suggesting differences in regulation or interactions. RET-43 is expressed in normal fetal and adult kidney, as well as in a neuroblastoma cell line.

RET-51 may contribute to cell differentiation and shaping of mature kidney because it only appears 8.5 weeks after onset of gestation rather than during the induction of this tissue. On the other hand, RET-9 and RET-43 expression in kidneys are higher from 7 through 24 weeks of gestation (Myers et al., 1995; Ivanchuck et al., 1998).

Mono-isoformic mouse strains showed that only signaling by RET-9, in the absence of RET-51, is sufficient for normal embryonic development and post-natal life. In contrast, signaling by RET-51, in the absence of RET-9, resulted in developmental defects of the excretory system and ENS. *RET* isoforms have distinct properties, thus RET-51 is important during embryogenesis, whereas RET-9 is necessary and sufficient for normal development of ENS and the excretory system (de Graaff et al., 2001).

As mentioned, RET-51 contains two additional Tyr residues (Tyr1092 and Tyr1096), Tyr1096 forms a docking site for the adaptor protein Grb2 and activates the PI_3-K and the MAP-K signaling pathways (Besset et al., 2000). The differential actions of RET-9 and RET-51 could be due to their specific C-terminal ends. The two isoforms diverge in sequence one amino acid after Tyr1062, a residue essential for binding of the adaptor protein Shc and the assembly of signaling complexes. Because amino acid flanking Tyr-residues can determine the efficiency of active complex formation and intracellular signaling, it is possible that in RET-51, Tyr1062 is a less efficient docking site for binding to Shc (Lorenzo et al., 1997; Ishiguro et al., 1999).

RET-9-specific amino acids at the C-terminus that are absent in RET-51 may have signaling properties that have to be delineated. Differential signaling by both isoforms could result from the segregation of RET-9 and RET-51 in distinct membrane sub-

domains, influencing their interactions with downstream components, receptors or ligands (de Graaff et al., 2001).

RET-51 but not RET-9 becomes phosphorylated upon binding by NGF. Probably, because both isoforms might be localized differently and NGF-dependent RET activation occurs specifically in sub-cellular compartments (Weiss et al., 1997). Recruitment of RET by NGF could be part of an antagonistic interaction between NGF and GFLs, which would allow NGF to gain control over GFL-mediated signaling by regulating the functional properties of RET (Tsui-Pierchala et al., 2002).

3.6.3. *c-RET* re-arrangements

Diverse mutations of the *c-RET* gene cause different human genetic diseases (Takahashi, 2001) due to the oncogenic potential of *RET*.

a) Activating mutations of c-RET gene are found in sporadic human thyroid carcinomas, such as papillary thyroid carcinoma (PTC) and in familiar medullar thyroid carcinoma (familiar MTC, 25% of all cases), in multiple endocrine neoplasia type 2 syndrome (MEN-2) and in sporadic phaeochromocytoma (Eng et al., 1994). A MEN-2 syndrome consists of three clinical varieties: MEN-2A, MEN-2B and familial MTC, all characterized by MTC and the variations depend on the presence of phaeochromocytoma, parathyroid hyperplasia or developmental abnormalities, affecting lineages of neural crest ectoderm (Santoro et al., 1990; Mulligan et al., 1994). Most of the MTCs express *RET*, and its ligands GDNF and GFRα-1, as well as NTN and GFRα-2, and binds preferentially to tumor cells adjacent to the stroma rather than normal thyroid tissues, suggesting that this complex is an important step in MTC development (Frisk et al., 2000).

In 25% of PTCs, the 3' tyrosine kinase domain of RET is fused to the 5'-terminal region of other genes inducing dimerisation and tyrosine activity (Grieco et al., 1990).

a.1) Mutations in the extracellular cysteine-rich domain of RET have been detected in MEN-2A leading to the formation of constitutively active RET homodimers (Romeo et al., 1994).

a.2) Mutations in the intracellular parts of c-RET found in MEN-2B produce a mutant *RET* kinase with changed substrate specificity, but this activity can be modulated by GFLs. The expression of MEN-2B in human neuroblastomas alters cell adhesion *in vitro*, enhances metastatic behavior *in vivo,* and activates the JNK pathway (Marshall et al.,

1997). A 2-point mutation in TyrK-1 has been described and induces FMTC. A 1-point mutation in the TyrK-2 domain causes MEN-2B (Airaksinen et al., 1999).

b) Inactivating mutations of RET cause Hirschsprung disease (HRSD), characterized by the absence of intramural ganglion cells in the hindgut, which results in aganglionic megacolon (Eng et al., 1997; Santoro et al., 1999; Takahashi, 2001).

b.1) HRSD is associated with other mutations of *RET* such as heterozygous deletions, frame-shifts, non-sense, and missense mutations, which are scattered throughout the whole gene (Romeo et al., 1994; Sakai et al., 2000) and some of them induce apoptosis (Bordeaux et al., 2000).

b.2) A mutation of tyrosine 905 to phenylalanine *(Y905F)* impairs the kinase activity and abolishes the transforming activity of RET-MEN2-A.

3.6.4. *RET* knock-out mice

RET$^{-/-}$ mice died soon after birth due to kidney agenesis and absence of enteric nervous system below the stomach. They did not display gross defects in the brain.

RET$^{-/-}$ embryos lacked 100% of sympathetic superior ganglion neurons, and had a reduced number of a subpopulation of other sensory neurons (Schuchart et al., 1994).

The hematopoietic system was not analyzed in these animals.

3.6.5. Expression and distribution

In the CNS, RET was detected in the cerebellum, forebrain, olfactory bulb, sub-thalamic nucleus, hippocampus and other limbic structures (Nosrat et al., 1997; Trupp et al., 1997). RET was higher expressed in neurons compared to astrocytes (Remy et al., 2001).

RET was strongly expressed in the spinal cord and was restricted to axons in normal and in avulsed DRG (Bär et al., 1998). Also, it was present in noradrenergic neurons (SCG) providing sympathetic innervation for the neck and cranial organs.

In embryonic kidneys *RET* was expressed along the nephric duct and in the newly formed uretheric bud (Pachnis et al., 1993), but became restricted to the growing tips of the bud as branching morphogenesis progressed (Tang et al., 1998).

Outside of the CNS, RET was found in the spleen, thymus, lymph nodes, salivary gland, and in the adrenal medulla (Belluardo et al., 1999). It was present in normal thyroid gland

(Forander et al., 2001), and was mostly restricted to the neural crest-derived C cells (Bunone et al., 2000), as well as several other neural crest-derived cell lines.
RET protein was found in the ganglia of human normal colon (Martucciello et al., 1995).
In the testis, RET, as well as GFRα-1 and GFRα-2, were distributed in overlapping patterns (Widenfalk et al., 2000).
All four isoforms encoded by alternative splicing at the 5'-end of the gene were expressed in adult thyroid, adrenal, kidney and brain tissues (Lorenzo et al., 1995).

3.6.6. Signaling

The *c-RET oncogene* encodes a receptor tyrosine kinase that functions as a signaling molecule of the multicomponent receptor system for all members of the GFLs (Durbec et al., 1996; Airaksinen and Saarma, 2002). Receptor tyrosine kinases (RTKs) are transmembrane proteins mediating cell-cell signaling. The intracellular domain is activated by ligand interaction with the extracellular domain, inducing its dimerisation and autophosphorylation leading to the activation of intracellular signal pathways with phosphorylation of cytoplasmic substrates (Schlessinger, 2000; Grimm et al., 2001).
Upon ligand binding, RET forms dimers and becomes phosphorylated at specific cytoplasmic tyrosine residues. Tyr autophosphorylation is required for the catalytic activity of RET and for downstream signaling, activated by all members of the GFLs. In addition, Ca^{2+} ions are necessary for the complex receptor formation of RET, indicating the importance of the CLD present in the extracellular domain (Nozaki et al., 1998).
GDNF/NTN-dependent RET activation triggers various intracellular signaling pathways via the phosphorylation of Tyr905, Tyr1015, Tyr1062 and Tyr1096 (Coulpier et al., 2002), which are docking sites for the adaptor proteins Grb7/Grb10 (Asai et al., 1996), phospholipase-Cγ (PLCγ) (Borello et al., 1996), Shc/ENIGMA (Arighi et al., 1997), DOK4/5 and Grb2 (Liu et al., 1996; Xing et al., 1998). Tyr1062 in the COOH terminus is the binding site of at least 5 different docking proteins: Shc, DOK4/5 (down-stream of Tyr kinase 4/5), FRS2 (fibroblast growth factor receptor substrate 2), IRS1/2 (insulin receptor substrate 1/2) and Enigma, which is phosphorylation-independent.
RET also activates Ras-MAPK (Worby et al., 1996), PI_3K (Van Weering et al., 1998), and JNK (Xing et al., 1998).

GDNF and NTN could trigger PLCγ-dependent Ca^{2+} release changing the intracellular free Ca^{2+} concentration that activates signal transduction cascades, such as those that regulate gene expression (Airaksinen et al., 1999).

Stimulation of RET *in cis* or *in trans* by GDNF in a complex with GPI-anchored or soluble GFRα-1, respectively, triggers different signaling pathways inside and outside the rafts (Figure 9), although both types of stimulation activates different RET Tyr phosphorylation sites with indistinguishable kinetics (Coulpier et al., 2002).

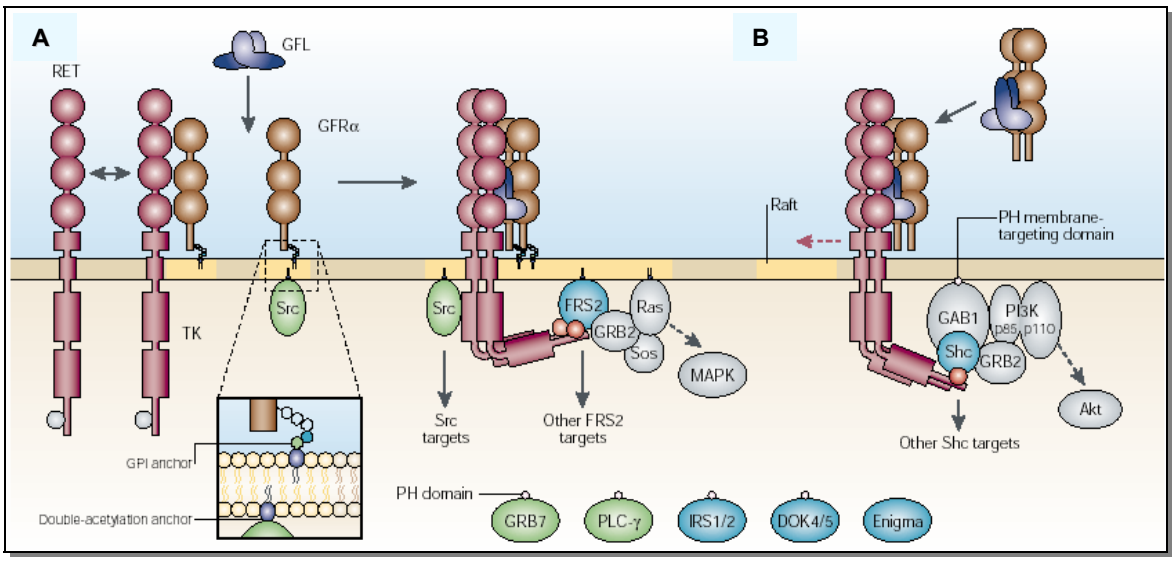

Figure 9: Intracellular RET-binding proteins and downstream signaling pathways activated by GDNF family ligands. Distinct GFLs inside and outside of lipid rafts showing different intracellular RET-binding proteins (blue) and activated downstream signaling pathways (gray) when RET tyrosine kinase (TK) is stimulated. **A) <u>in rafts</u>** (yellow) by GFL in a complex with GFRα *in cis*; or **B) <u>outside rafts</u>** by a soluble GFL-GFRα complex *in trans*. Docking proteins: FRS2, DOK4/5, IRS1/2, GAB1, GAB2-associated binding protein 1; GRB (growth factor receptor-bound protein), MAPK, PH (plextrin homology), PI3K, and PLC (from Airaksinen and Saarma, 2002).

In the absence of ligand, most GPI-anchored GFRα molecules are in lipid rafts; some are weakly bound to RET, while most RET is outside the rafts. GFLs may induce GFRα dimerisation. The enhanced affinity of the GFL-GFRα complex to RET attracts RET to the rafts and promotes its dimerisation. RET stimulation *in trans* by GFL bound to soluble GFRα outside the rafts activates signaling pathways that are mediated by soluble adaptors such as Shc recruiting RET to lipid rafts and triggering raft-specific signaling.

3.6.7. Physiological functions of RET

RET display a major role as growth and survival factor, as well as regulator of migration, differentiation and proliferation of neural crest cells. For example, RET was necessary for migrating neuroblasts that colonize the colon (Martucciello et al., 1995), migration of RET and GDNF-expressing neurons into the developing gut endoderm, to generate the enteric neurons of the intestinal tract; as well as being a survival factor for a variety of central and peripheral neurons (Schuchart et al., 1994),

In the embryonic kidney, RET-expressing uretheric bud epithelial cells grew towards the metanephric mesenchyme, which expressed GDNF. These epithelial cells were able to migrate towards a localized source of GDNF, indicating chemoattraction at the cellular level. For this reason, RET played an important role in the induction and development of the metanephric kidney (Pachnis et al., 1993), and also regulated uretheric bud outgrowth and branching (Tang et al., 1998).

A reciprocal signaling loop between the uretheric bud epithelium and the stromal mesenchyme was dependent on RET and vitamin A. Vitamin A-dependent signaling molecules secreted by stromal cells might control *RET* expression in the uretheric bud, subsequently uretheric bud signals dependent on RET controlled stromal cell patterning (Batourina et al., 2001).

Activated RET pathways promoted dysplasic cells to become metastatic and were then able to invade surrounding tissue, probably due to cytoskeletal and focal adhesion rearrangements and lamellipodia formation. These migrating cells were attracted to localized sources of GDNF, as in some neuroblastoma tumors (Marshall et al., 1997).

Hematopoiesis is a regulated process in which a small population of self-renewing basic progenitors generates an offspring of differentiated end cells with specific activities (Morrison et al., 1995). This process is controlled by several growth factors and cytokines, some of them exerting their functions through the binding to high-affinity RTKs, which are differentially expressed on many hematopoietic cells (Ehrhard et al., 1993a; Galli et al., 1994; Small et al., 1994). A putative role of RET in the regulation of hematopoietic cells was suggested by the presence of *RET* transcripts and protein in lympho-hematopoietic tissues of mice and rats, including fetal liver, thymus, spleen, and lymph nodes (Avantaggiato et al., 1994; Tahira et al., 1988); it was also present in two myeloid leukemia cell lines of human origin (HL-60 and THP-1) (Takahashi and Cooper, 1987;

Takahashi et al., 1989; Takahashi et al., 1991). Levels of *RET* and GFRα-1 mRNA were analyzed in purified normal and malignant cells of myeloid and lymphoid lineages mirroring various stages of differentiation, and in the BM microenvironment (Gattei et al., 1997). The results showed low levels of *RET* mRNA in early $CD34^+$ hematopoietic progenitors that increased with maturation along the myelomonocytic lineage, being up-regulated in circulating neutrophils and in resting or activated monocytes from peripheral blood. Findings in human myelomonocytic cell lines were consistent with the pattern found in normal cells, since a progressive increase of *RET* mRNA was present in cells representing early to late stages of granulocytic and monocytic differentiation. *RET* expression was maturation-associated in human myelopoiesis, suggesting a possible role in the regulation of intermediate and mature myelomonocytic cells. However, purified normal T cells from human peripheral blood, tonsil and thymus did not express *RET* mRNA, even after cellular activation.

In human normal and malignant B cells on different stages of maturation, *RET* mRNA was sporadically detected in SIg^+B cell tumors. These results were in agreement with results obtained from mouse B cells. *RET* was only expressed at early stages of B cell differentiation, being down-regulated after the expression of surface immunoglobulins.

Accessory cells of the BM microenvironment provided a physiologic source of GFRα-1 for RET-expressing hematopoietic cells as seen with human BM aspirate (Gattei et al., 1997) and mouse tissue (Nakayama et al., 1999). Human BM stromal cells, BM fibroblasts and other stromal cells did not express RET but expressed GFRα-1. Thus, GDNF may induce terminal differentiation of monocytic leukemia cells, because of enhanced maturation of monocyte/macrophage precursors from normal BM $CD34^+$cells in the presence of soluble GFRα-1 (Gattei et al., 1997 and 1999). The last reports also showed a higher RET expression in blood from patients with monocytic acute myeloid leukemia (AML). A statistically significant association was found between the amount of RET and the expression of surface molecules: β_2 integrins, ICAM-1/CD54, CD56, CD4 and CD14, were commonly expressed at high levels by blasts cells of monocytic AMLs. An inverse correlation between RET and $CD34^+$ on blasts of the stem cells was observed, which is usually lacking in monocytic leukemia (Gattei et al., 1999).

The association of elevated levels of RET with AMLs of monocytic phenotype, that were associated with cell infiltration of gingiva, skin, central nervous system, kidney and other

extra-haemopoietic sites and the presence on blast cells of several adhesion molecules, could indicate that cells characterized by a prominent migratory capacity, such as neural crest cells, embryonic cells in developing nervous tissues and kidneys, monocytes, neutrophils and dermatotropic T cells expressed high levels of RET. Accordingly, RET-mediated intracellular signaling in non-hemopoietic cells resulted in modifications of cell adhesive properties, cell scattering and increased metastatic potential, in agreement with the notion that signal transduction through RTK synergized with integrin-mediated changes in cell adhesion and migration (Miyamoto et al., 1996).

Since GDNF was highly expressed within the CNS, spinal cord, skin and other organs infiltrated by monocytic AML, probably RET-GDNF interactions may favor leukemia cell migration through these tissues. The stromal and endothelial components of these organs may represent the source of receptors GFRα and ligands available for interaction with RET-expressing blasts in AML, as well as with tissue granulocytes and monocytes during inflammatory and wound healing processes (Gattei et al., 1999).

A similar study was performed in monocytes obtained from peripheral blood and in leukemia cell lines (Nakayama et al., 1999). *RET* was highly expressed in intermediate mature myeloid cells and was down-regulated during terminal maturation. Hemopoietic cells from mouse BM expressed only RET among the genes examined (GDNF, NTN, GFRα-1 and GFRα-2), whereas bone marrow adherent cells (BMAC) or stromal cells expressed GFRα-1, GFRα-2 and GDNF but not RET. These results demonstrated that promyelocytes and myelocytes highly expressed RET rather than mature neutrophils and monocytes, although transcripts were also detected in mature cells. In addition, RET expression decreased during differentiation of HL-60 and THP-1 cells *in vitro*, suggesting that c-RET might play a role at an intermediate stage of myelomonocytic maturation rather than at its terminal stage.

BM hemopoietic cells (macrophages) expressed only RET, whereas BMAC expressed GFRα-1 and GFRα-2. As previously reported (Treanor et al., 1995; Jing et al., 1996; Klein et al., 1997; Nozaki et al., 1998), soluble GFRα was able to mediate GDNF or NTN signaling in cells that expressed RET but not GFRα. According to these results, both groups (Gattei et al., 1997 and 1999; Nakayama et al., 1999) have speculated that GFRα-1 on the cell surface of BM stromal cells might function like soluble GFRα receptor.

During development the survival of almost all sympathetic neurons in SCG depended on NGF and its receptor TrkA. GFLs (except PSP) also can act on SCG neurons. In addition to the GFLs dependent route, RET may be activated by NGF signaling via a novel indirect mechanism, which contributed to the post-natal maturation of SCG neurons. The mechanisms linking NGF/TrkA to RET activation remain unclear. This finding leads to the conclusion that growth factors and their receptors interact to form a net of trophic signaling routes that guide the development of SCG neurons, thus RTKs could be sensitive to ligand-dependent and ligand-independent mechanisms (Weiss et al., 1997).

The functions of neurotrophic factors from different families provided evidence for a hierarchy of TrkA and RET interactions in the SCG, showing that GDNF could antagonize the growth promoting effects of NGF on sensory neurons (Linnarsson et al., 2001). It was also reported that NGF activated RET (Tsui-Pierchala et al., 2002) *in vitro* and *in vivo* in rodent SCG neurons, by a mechanism independent of GFLs and GFRα receptors. NGF-dependent RET phosphorylation regulated soma size and metabolism but not survival of maturing post-natal sympathetic neurons (Dechant, 2002).

3.6.8. RET under pathological conditions

The higher expression of the RET gene was detected mainly in neuroblastomas (tumors of neuroectodermal origin) among the tumors from the neural crest cells (Ikeda et al., 1990), as well as in phaeochromocytoma and in medullar thyroid carcinomas.

Some human leukemia cells also expressed high levels of RET, i.e., HL-60 and THP-1 (Takahashi et al., 1991).

The expression of oncogenic re-arranged versions of *c-RET* in PTC derived from thyroid follicular cells was demonstrated, as well as the presence of *RET* transcripts in some follicular thyroid carcinoma lymph node metastases. RET could be active in thyroid follicular cells (Bunone et al., 2000).

After transient forebrain ischemia, *RET* mRNA expression was induced in the hippocampus, mainly 12 hours after artery occlusion. Its expression was reduced by local GDNF-pretreatment, suggesting that GDNF could modulate *RET* expression, and also some signaling pathways that contribute to brain injury induced by ischemia (Arvidsson et al., 2001; Miyazaki et al., 2002).

3.7. GDNF FAMILY RECEPTORS-α

3.7.1. General characteristics

The GFRα family of proteins is composed of a highly conserved group of co-receptors required for the binding of the GFLs and the subsequent activation of RET transmembrane receptor. GFRα proteins are linked to the plasma membrane through a cluster of small amino acids, namely glycosyl phosphatidylinositol (GPI) anchor (Brodbeck et al., 1998; Ferguson et al., 1999), and they are located within lipid rafts, which are structures resistant to cold detergent lyses (Muniz and Riezman, 2000; Ilangumaran et al., 2000). Structurally GFRαs possess three globular cysteine-rich domains (D1, D2, D3), except for GFRα-4 which has only two (Lindahl et al., 2000). GFLs bind to the second domain of GFRα receptors that is also crucial for RET binding (Scott and Ibanez, 2001).

The four GFRα genes are similar in structure and organization of exons. They share 30–45% amino acid identities and have similar arrangements of conserved Cys residues.

The cleavage by an unknown phospholipase or protease produces soluble forms, which are able to capture the ligand from the extracellular environment for subsequent assembly into a functional receptor complex on the cell membranes carrying the appropriate signaling subunits (Paratcha et al., 2001). In addition, GFRαs can negatively modulate levels of RET phosphorylation in the absence of ligand; thus, GFR-α receptors could increase the signal-to-noise ratio in response to the ligands (Ibanez, 1998).

"GFRα-X" is used for GDNF Family Receptor Alpha-X, where "X" denotes an Arabic numeral to be assigned based on the date of publication of the receptor. The term "alpha" served to clarify that these molecules are part of a multicomponent receptor complex (Nomenclature Committee, 1997).

All GFRα members retain the signal sequence that is required for GPI-anchoring and is found in the final coding exon of each gene (Vanhorne et al., 2001).

GFRα receptors can mediate activation of RET when expressed on the cell surface (activation *in cis*), or when presented in soluble form, immobilized on the cell matrix or in neighboring cells (activation *in trans).* GFRαs are often expressed in the absence of RET (i.e., in Schwann cells, or several areas of adult brain) suggesting that RET is not always required for signaling, or they may interact with RET in soluble forms.

3.8. GFRα-1

3.8.1. Description and characteristics

GFRα-1 is the surface receptor component of the GDNF/GFRα-1/RET signaling complex. It is a glycolipid-linked extracellular protein attached to the cell membrane by a GPI-linkage, without having an intracellular signaling domain. Its structure contains 30 Cys residues with similar spacing and arrangement to other members of this family. GFRα-1 contains 465 aa with a signal peptide at the amino terminus, with 20–23 hydrophobic aa at the carboxyl-terminus and 3 glycosylation sites (Treanor et al., 1995; Jing et al., 1996; Sanicola et al., 1997; Eng et al., 1998).

In the human GFRα-1 gene, exon 1 and the largest parts of exons 2 and 11 are not translated. The translation start site is located 247 nucleotides downstream the start of the second exon.

Two isoforms of GFRα-1 have been described in murine and in human tissues. The shorter variant has a deletion of 15 bp, which is contained within the entire exon 5. Both isoforms are able to bind GDNF and activate RET with high affinity and specificity (Eng et al., 1994; Sanicola et al., 1997; Angrist et al., 1998).

3.8.2. GFRα-1 knock-out mice

GFRα-1 deficient mice displayed deficits in the kidneys, the ENS, the spinal cord and in sensory neurons. They had complete bilateral renal and urethral deficits.

The neural crest-derived enteric neurons belonging to the myenteric and submucosal plexi were absent in the intestine and colon of these mice, similar to $GDNF^{-/-}$ and $RET^{-/-}$ mice.

$GFR\alpha\text{-}1^{-/-}$ mice exhibited small losses of lumbar spinal (24%) and trigeminal nucleus MN (22%), but not of facial MN. They did not show a reduction in the density of DA projections in the striatum and had normal noradrenergic neurons in the locus coeruleus.

Minimal or no losses of neurons were observed in a number of peripheral ganglia, which were severely affected in both c-RET and $GDNF^{-/-}$ mice, suggesting that while physiological interactions exist between GFRα-1 and GDNF in renal and in ENS development, significant cross talk between GDNF and other GFRα must also occur in peripheral ganglia (Enomoto et al., 1998). Adrenal glands, gonads, remaining abdominal and thoracic tissues appear to be normal (Calacano et al., 1998).

3.8.3. Signaling

GDNF bound specifically and with high affinity to GFRα-1 mediating activation of RET. Cells expressing GFRα-1 on the surface treated with GDNF rapidly stimulated RET autophosphorylation in a dose- and time–dependent manner. RET was also activated by treatment with GDNF and soluble GFRα-1 in cells lacking GFRα-1, because GFRα-1 does not need to be anchored to the cell membrane in order to interact with RET (Jing et al., 1996). GFRα-1 had some affinity for RET in the absence of ligand, suggesting that pre-formed complexes of GFRα/RET were also present on the cell surface.

The GDNF dose required to trigger a biological effect varies widely among different cell types, suggesting the existence of both high and low affinity GDNF receptors.

Modes of action of GFRα-1 in the activation of c-RET molecules *in trans:*

- Released and soluble GFRα-1 molecules can bind GDNF in the extracellular space and present it *in trans* to RET expressing cells located at a distance providing a trophic signal with excellent spatial resolution.
- Released GFRα-1 can be immobilized to the extracellular matrix by passive adsorption and present GDNF.
- GPI-anchored GFRα-1 molecules on standby cells can bind GDNF and present it *in trans* to RET receptor on adjacent cells by cell-cell contact (Paratcha et al., 2001).

3.8.4. Expression and physiological functions

GFRα-1 mRNA was present in defined brain areas: in midbrain DA neurons (SN and ventral tegmental areas), olfactory tubercle, hippocampus (Nosrat et al., 1997), cortex (occipital lobe), medial geniculate, caudate nucleus and the habenula (Trupp et al., 1996; Sanicola et al., 1997), and in rat-cultured microglia (Honda et al., 1999).

Schwann cells expressed GFRα-1 but not RET (Treanor et al., 1995).

In peripheral embryonic rat tissues, GFRα-1 expression showed high levels in fetal intestine and kidneys (Sanicola et al., 1997). In the rat thyroid tissue, GFRα-1 expression was widespread. In contrast, RET was expressed in a subpopulation of cells in the follicular epithelium and in the interfollicular spaces (Belluardo et al., 1999).

GFRα-1 protein was found on the membrane of capillary endothelial cells. GDNF activated the brain-blood barrier function of these cells in the presence of cAMP. Since

GDNF was secreted from astrocytes sheathing capillary endothelial cells in the brain cortex, GDNF/GFRα-1 may enhance the function of the tight junctions of the brain blood barrier and could also support neuronal survival (Igarashi et al., 1999).

GDNF activated by GFRα-1 and RET in corneal epithelial cells induced phosphorylation of Ras and FAK, followed by activation of MAPK to initiate gene transcription, and FAK-dependent phosphorylation of paxillin to initiate cell migration (You et al., 2001).

Immature adrenal medullar cells expressed GFRα-1 mRNA that increased upon GDNF treatment, promoting transformation of chromaffin cells into a neuronal-like phenotype (Forander et al., 2001).

3.8.5. GFRα-1 under pathological conditions

GFRα-1 and GDNF were expressed in human gliomas *in vivo*. However, it is unknown whether human astroglioma can produce GDNF and its receptors during the process of malignant transformation (Wiesenhofer et al., 2000).

GFRα-1 mRNA expression was elevated to variable levels in peripheral nerve biopsies from patients with various inflammatory neuropathies when compared to control subjects (Yamamoto et al., 1998). The increased levels of expression correlated well to the extent of axonal degeneration. The infiltration of T cells and macrophages is one of the important factors in the process of nerve injury and repair, especially in vasculitic and inflammatory neuropathies. Macrophage invasion into the nerve fascicles occurred in acute stages of axonal degeneration (Kiefer et al., 1998). The GFRα-1 mRNA expression was proportionally elevated to the extent of macrophage invasion as well as to the extent of axonal degeneration, suggesting that cytokines or other factors secreted by the macrophages and T cells may enhance the GFRα-1 expression.

As reported before, GDNF and GFRα-1 mRNAs, but not *RET* were up-regulated in Schwann cells of damaged nerves after axotomy. Nerve sprouting was induced and guided by processes that extended from Schwann cells to denervated muscles.

Schwann cells produced GFRα-1 that captured and concentrated GDNF in a cell-anchored GDNF/GFRα-1 complex that acted as a guide to attract re-growing motor axons extended from MN expressing RET to muscle cells. GDNF and GFRα-1 expressed by Schwann

cells of injured adult peripheral nerves probably play a role in nerve regeneration (Trupp et al., 1997; Naveilhan et al., 1998).

GFRα-1 and *RET* mRNA levels in MN were up-regulated following muscle contusion. This rapid and prominent up regulation may be important for regeneration of intramuscular motor nerves damaged by muscle contusion (Kami et al., 1999).

GFRα-1 and RET played a role in the regulation of GDNF signaling pathways in response to electroconvulsive seizures (ECS), because after acute and chronic ECS, levels of GFRα-1 mRNA in the dentate gyrus were increased. This in turn elevated GDNF expression, which could have beneficial effects on neuronal function/survival after seizures (Chen et al., 2001).

GFRα-1 was expressed in all bile duct carcinoma samples, indicating that carcinogenesis leads to aberrant expression of GFRα-1 (Iwahashi et al., 2002).

3.9. GFRα-2

3.9.1. Description and characteristics

GFRα-2 is the preferred surface receptor for the ligand NTN (Baloh et al., 1997; Buj-Bello et al., 1997; Sanicola et al., 1997).

Structural features essential for GFRα-1 function have been preserved in GFRα-2: **a)** a signal peptide for secretion at the N-terminus; **b)** three potential N-glycosylation sites located in similar positions; **c)** 30 conserved cysteine residues, and **d)** a stretch of 17 hydrophobic aa at the C-terminus preceded by a group of three small amino acids indicative of a typical cleavage-binding site for a GPI linkage. The protein contains 464 aa, having a molecular weight of 52 kDa and 47% identity to GFRα-1 (Wang et al., 1998).

3.9.2. The GFRα-2 gene

Using the human GFRα-1 sequence to search for homologues with the BLAST and BLASTN algorithms, the GFRα-2 gene was identified (Wang et al., 1998). The complete reading frame was encoded by nine exons (1526 bp) which were all translated (Baloh et al., 1997).

The nucleotide positions, as well as the splice isoforms have been described in mice (Wong et al., 1998) and in humans (Vanhorne et al., 2001; Wong et al., 2002). **GFRα-2a** corresponds to the full length mRNA. **GFRα-2b** lacks exon 2 (315 bp) and the deduced amino acid sequence is identical to GFRα-2 full length except for a 105 amino acid deletion at the N-terminus. The signal peptide cleavage site in GFRα-2b is located 20 amino acids downstream from the initiation of translation. **GFRα-2c** lacks exon 3 (84 bp). GFRα-2b and GFRα-2c have a deletion of eight Cys residues and a single glycosylation site at the N-terminus.

Another isoform described in human tissues (Vanhorne et al., 2001) resulting from the lack of exons 2 and 3 (399 bp) is the **Exon 1-4 mRNA** splice variant. The transcript encodes a protein of 331 amino acids that would not contain the N-terminal Cys-rich domain, lacking three N-terminal α helices of the protein and at least one N-glycosylation site. The deleted protein region is not critical for binding of NTN and RET to GFRα-2, and does not determine the specificity of interactions, ligand binding or signaling capabilities of GFRα and GDNF family ligands (Scott and Ibanez, 2001).

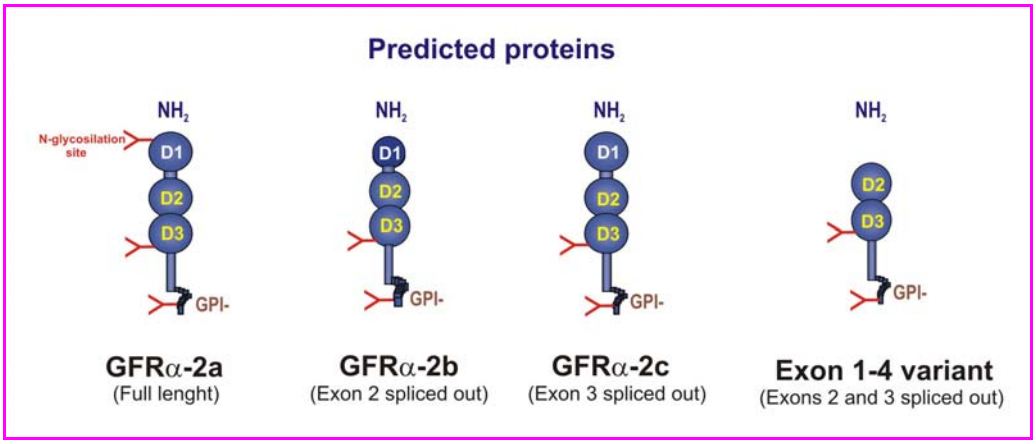

Figure 10: Predicted proteins encoded by the alternative splice isoforms of the GFRα-2 gene. GFRα-2a (F.L) has three globular domains. The difference between GFRα-2a and GFRα-2c is that the latter lacks a single glycosylation site at the N-terminus. GFRα-2b has a deletion of 105 amino acids at NH_2 terminus and therefore also lacks the glycosylation site. Exon 1-4 variant does not contain the first Cys-rich domain, because a total of 331 aa are not translated (modified from Airaksinen et al., 1999 and Vanhorne et al., 2001).

The first globular Cys-rich domain (D1) was not necessary for ligand specificity. Ligand-independent interaction with RET resides in the central domain of GFRαs (D2) within a distinct and smaller region required for ligand binding (Scott and Ibanez, 2001).

3.9.3. GFRα-2 knock-out mice

GFRα-2$^{-/-}$ mice are viable and fertile, but display dramatic growth retardation. Organs, which normally express high levels of GFRα-2, appear normal in morphology. However, the neuronal deficits led to dry eyes due to a reduction in tear secretion and increase blinking rate. In the gut, there was a decrease in the frequency, intensity, and synchrony of the gut contractile activity. These animals share a similar eye phenotype and deficits in the enteric and parasympathetic nervous system as NTN$^{-/-}$ mice, indicating a functional interaction between NTN and GFRα-2 *in vivo*. The cholinergic innervation of the lachrymal and salivary glands, as well as the small bowel was almost absent. They displayed deficits in fiber density of substantia P-positive neurons of the small intestine (Rossi et al., 1999).

3.9.4. Signaling

GFRα-2 was able to bind NTN with high affinity and GDNF with lower affinity *in vitro* (Cik et al., 2000), and both complexes signal through RET tyrosine phosphorylation (Baloh et al., 1997; Sanicola et al., 1997). GFRα-2 was unable to signal in the absence of RET (Pezeshki et al., 2001).

The signaling pathways activated after the ligand-receptor complex is formed were described in the section about RET signaling (3.6.6).

3.9.5. Expression and physiological functions

Within the brain (mouse, rat and human), the highest levels of GFRα-2 mRNA were found throughout the cerebral cortex, olfactory bulb, amygdaloid nuclei, superior/inferior colliculus, cerebellum and thalamus. Moderate levels were found in the hypothalamus and in the pre-optic area (Sanicola et al., 1997; Wang et al., 1998).

In mouse organs, GFRα-2 mRNA was present in developing sensory organs, in the gut myenteric intestinal plexus and in the gonads, being required for growth and proliferation

of neural crest cells. GFRα-2 was also expressed in the penile neurons in the major pelvic ganglia (Laurikainen et al., 2000).

In mouse (Widenfalk et al., 1997) and in rat tissues (Wang et al., 1998) GFRα-2 mRNA was expressed in the brain, spleen, placenta (Sanicola et al., 1997) and lungs (Naveilhan et al., 1998). Moderate to low levels were detected in kidneys, thymus, stomach and small intestine. GFRα-2 mRNA was not detectable in skeletal muscles or liver.

GFRα-2 also played a critical role in the parasympathetic innervations of the lachrymal and salivary glands through cholinergic neurons.

Astrocytes from rat glial cells expressed high amounts of GFRα-1 and GFRα-2 mRNA. Expression of GFLs and their receptors was not restricted to neurons and may be implicated in oligodendrocyte development (Remy et al., 2001). Enriched mature oligodendrocytes also expressed *RET*, GFRα-1 and GFRα-2 mRNA (Strelau and Unsicker, 1999).

3.9.6. GFRα-2 under pathological conditions

Cortical GFRα-2 mRNA transiently increased in the post-ischemic phase of local ischemic insults, as well as GFRα-1 and *RET* mRNAs, indicating that changes of GFL receptors could enhance neuroprotective and neuroregenerative responses, due to both endogenous and exogenous GFLs (Arvidsson et al., 2001).

Levels of GFRα-2 mRNA and GFRα-1, but not GDNF, were elevated after acute and chronic ECS implying that the regulation of the GFRαs may mediate adaptive responses of the GDNF system to acute and chronic stimulation (Chen et al., 2001). Epileptogenesis, in the hippocampal kindling model, was suppressed in GFRα-$2^{-/-}$ mice, thus providing evidence that GFRα-2 signaling was involved in mechanisms regulating the development and persistence of kindling epilepsy (Nanobashvili et al., 2000).

GFRα-2 polymorphism variants occurred naturally and did not contribute to the HRSD phenotype (Vanhorne et al., 2001).

Table 1 shows the distribution of GFLs and receptors in the nervous system and in peripheral organs.

Tissue	GDNF	GDNF	NTN	NTN	RET	RET	GFRα1	GFRα1	GFRα2	GFRα2
	Embryo	Adult	Embryo	Adult	Embryo	Adult	Embryo	Adult	Embryo	Adult
Olfactory bulb	++	+	_	_		++			++	+++
Cingulate cortex				_						++
Cortex cerebri	+	+	_	_	_	_	+	+	++	+++
Striatum	++	+	_	_	_	_	+	+	_	_
Septum				_						++
Dentate gyrus			_	_		+			+	++
DA neurons SN	-	-	++	_	+++	+++	+++	+++	_	_
Pituitary gland			++	++					++	+
Pineal gland				+						
Amygdale		+		_		+		+	+	++
Thalamus	++	+	_	_	++	+	++	++	+	++
Reticular thalamic N				_					+	++
Zona incerta				_					+++	+++
Hypothalamus	+		_	_	+	+	++		++	++
Cerebellum	++	+	_	_	+ / ++	++	+++	++	++	+
Brainstem	++	-	_	_	++	++	++	++	++	++
Trigeminal ganglia	_	+	_	+	+++	+++	++	+++	++	+++
Spinal cord, gray m.	+	+ post. H	_	_	+++	++	+++	++	++	+
Dorsal root ganglia	++	- / +	_	_	+++	+++	+++	+++	+++	+++
Autonomic ganglia	_		_		+++		+		++	
Peripheral nerve		+	_					+++		
Skeletal muscle	_	++	_	+	_	_	+	_	_	_
Inner ear			++						+	
Olfactory mucosa			++						++	
Skin	_		+++	++	_	_	_	_	+	_
Salivary glands			++						+	++
Lung		- / +	+	++		_		_	+	++
Myocardium	+	_	+	_	_	_	+	_	+	_
Heart vessels				_						_
Intestine	++	_	++	+++	++	++	++	_	+	_
Kidney	+++	_	++	+	+++	_	+++	+	_	_
Adrenal glands	+	_	_	++	_	_	_	+++	_	- / +
Thyroid	_	_			+	+	+	++		
Testis	+++	+	++	+++	_	_	_	+++	_	+++
Oviduct / Ovary		- / +++		- / +++		- / +		- / -		- / -
Thymus	_	_	+	+	- / +	_	_	_	_	++
Liver	_	- / +	++	+	_	- / +	++	+	+	_
Spleen		+			+	+			++	+++

Table 1: This table describes the localization of GDNF, NTN, RET, GFRα-1 and GFRα-2 in mouse, rat and human nervous system and in several peripheral tissues. The mRNA or protein expression usually changes from the development through the adult life (Suter-Crazzolara and Unsicker, 1994; Nosrat et al., 1996; Nosrat et al., 1997; Sanicola et al., 1997; Widenfalk et al., 1997; Naveilhan et al., 1998; Wang et al., 1998; Belluardo et al., 1999; Golden et al., 1999).

3.10. MYOBLASTS

Part of this work involved studying the expression of GDNF, NTN and their receptors on human myoblasts in culture. These experiments were carried out in collaboration with Dr. G. Chevrel.

At sites destined to form striated muscles, mononuclear, mesenchymal-like cells with precise phenotypic markers accumulate, permitting the discrimination of muscles from other, and non-muscle precursors.

Myoblasts are defined as post-mitotic, spindle shaped, mononuclear cells capable of synthesizing contractile proteins and capable of fusion with other myoblasts. They are the immediate descendents of presumptive myoblasts, which can neither fuse nor synthesize muscle-specific gene products. Subsequent to myoblast cell fusion, long, cylindrical, multinucleated or syncytial cells are formed, termed ***myotubes***. These cells exhibit central nucleation and peripherally disposed myofibrils, which confers a tube-like appearance. Alongside these initial, or primary, myotubes are longitudinally oriented myoblasts, which subsequently fuse to form secondary myotubes. Initially, the primary myotubes and their associated myoblasts and secondary myotubes are coupled by gap junctions and share a common basal lamina. As the muscle mature, secondary myotubes acquire their own basal lamina and become independent fibers. Primary and secondary myoblasts may synthesize different isoforms of myosin and have different developmental requirements for innervation.

Once the myonuclei shift from a central to a subsarcolemmal position, the muscle cells are termed ***myofibers*** to distinguish them developmentally from the more embryonic myotubes. The appearance of central nucleation within otherwise normal adult muscle is a sign of muscle regeneration within a tissue.

At some point, the presumptive myoblasts aggregate and cease migration. The cells enter a prolonged G1 period of the mitotic cell cycle and initiate the transcription of genes characteristic of the terminally differentiated muscle cells. If unfused, such cells are termed myoblasts; upon cytoplasmic fusion, they are termed myotubes. The migrated presumptive myoblasts express many of the cytoskeletal and contractile proteins characteristic of other non-muscle mesodermal cell types.

It is accepted that the contractile muscle fiber is a terminally differentiated cell type. In vertebrates, muscle regeneration in response to trauma or injury is affected by a reverse

cell population of satellite-undifferentiated stem cells, which are closely aligned along the fiber between the basal lamina and the sarcolema. The satellite cells proliferate and populate the laminar sheath of the degenerating fiber, and recapitulate the process of fusion and differentiation observed in embryonic muscles. The irreversibility of the differentiated end state of the muscle fibers may reflect the structural limitations imposed by its prospective function (Engel AG in Myology, 1986).

Previous studies have reported that GDNF was expressed in skeletal muscles as a target-derived neurotrophic factor. However, the action of GDNF on normal or pathological muscles of humans is unknown.

RT-PCR analyses showed that normal muscles expressed mostly truncated GDNF mRNA; on the contrary, muscles from polymyositis (PM) and Duchenne type muscular dystrophy (DMD) expressed the full length form (Li et al., 1995; Suzuki et al., 1998). The expression pattern of GDNF mRNA isoforms in amyotrophic lateral sclerosis was also different from controls (Yamamoto et al., 1998). On the other hand, the GFRα-1 mRNA expression did not change significantly in diseased muscles and *RET* mRNA was detected neither patients nor in control subjects.

The expression of GDNF and its receptors has not been studied in human myoblasts in culture. In light of the possible role of GDNF in normal and pathological conditions in muscles, we were interested in studying the expression and regulation of this factor in myoblasts under inflammatory stimuli.

4 OBJECTIVES

There is evidence that neurotrophins (NGF, NT-3, NT-4/5, and BDNF) exert functions in both the nervous and immune system.

The aim of this study was to understand the expression and functions of the GDNF family ligands and their receptors on immune and hematopoietic cells, since few reports have been published about this issue.

Most publications have given attention to RET receptor, and among them some have reported the presence of *RET* mRNA and protein in the lympho-hematopoietic tissues, such as fetal liver, thymus, spleen and lymph nodes (Avantaggiato et al., 1994; Tsuzuki et al., 1995), in human leukemia cell lines (Tahira et al., 1990; Takahashi et al., 1991), and in B and T cell leukemia/lymphomas and myelomonocytic cells (Gattei et al., 1997; Nakayama et al., 1999). RET may be a functional regulator of hematopoietic cells.

In addition, transcripts of GFRα-1, GFRα-2 and GFRα-3 were found neither in leukemia cell lines expressing RET nor in normal human peripheral blood cells. BM hemopoietic cells expressed only RET whereas bone marrow adherent cells (BMAC) or stromal cells expressed GFRα-1, GFRα-2 and GDNF.

Moreover, GFLs is a new family of trophic factors that are structurally related to the TGF-β superfamily, which is a prominent family of cytokines.

The complex distribution patterns of GDNF, RET and GFRα-1 and the relation of these patterns to those of NTN and GFRα-2 suggest that the GFLs and their receptors are required for both, the developing and adult organism, within and outside the nervous system. These relationships may be analogous to those for the neurotrophins and their receptors, as they also exert important functions in the IS and in the NS.

Therefore, we decided to investigate possible interactions between the nervous and the immune system mediated by members of the GDNF family ligands, GDNF, NTN and PSP, and their receptors: GFRα-1, GFRα-2 and RET.

To address this issue, the expression of these molecules was studied at the mRNA and at the protein level in sub-types of peripheral blood mononuclear cells: $CD4^+$ and $CD8^+$-T lymphocytes, $CD19^+$B lymphocytes and $CD14^+$ monocytes. Afterwards, to establish the potential functions of GDNF and NTN on immune cells, several functional experiments were also performed in this study.

5 MATERIALS AND METHODS

5.1. BUFFERS and REAGENTS

Phosphate buffered saline (1xPBS)

9.1 mM Na_2HPO_4 (Dibasic sodium phosphate)
1.7 mM NaH_2PO_4 (Monobasic sodium phosphate)
150 mM NaCl. Adjust pH to 7.4 with NaOH (Sodium hydroxide pellets)

Wash buffer (Western blot): PBS + 0.05% Tween-20 (polyoxyethylene-sorbitane monolaurate)

PFA – 4%

Paraformaldehyde 4% (w/v) in PBS, pH: 7.3
Dissolve PFA in water with a drop of NaOH, add PBS after complete dissolution

Tris buffered saline (1xTBS)

10 mM Tris-HCl, pH: 8.0
150 mM NaCl. Add distilled H_2O to 1 liter

Carbonate coating buffer

0.025 M sodium bicarbonate
0.025 M sodium carbonate, pH = 8.2

Lysis Buffer: RIPA Buffer

1xPBS
1% Nonidet P-40
0.5% Sodium deoxycholate
0.1% SDS
Add proteases and phosphatases inhibitors at time of use from, as follows:

- PMSF [10 mg/ml] in isopropanol: add at 10 µl/ml RIPA
- Aprotinin: add at 30 µl/ml RIPA
- Leupeptine: add at 30 µl/ml RIPA
- Sodium orthovanadate 100 mM, add at 10 µl/ml RIPA

MOPS - SDS Running Buffer (20x)

MOPS (3-(N-morpholino) propane sulfonic acid)	104.6 g
Tris Base	60.6 g
10% SDS	100 g
EDTA	3 g
Ultra pure water	to 500 ml; pH = 7.7

MES - SDS Running Buffer (20x)

MES (2-(N-morpholino) ethane sulfonic acid)	97.6 g
Tris Base	60.6 g
10% SDS	100 g
EDTA	3 g
Ultra pure water	to 500 ml; pH=7.3

Loading Buffer: LDS (4x)

Tris Base	0.682 g	EDTA	0.006 g
Tris HCL	0.666 g	Serva Blue G250	0.0075 g
Sucrose	4 g	Phenol Red	0.0025 g
SDS	0.8 g	Ultra pure Water	to 10 ml

Transfer buffer (20x)

60 ml H_2O
10 ml MeOH
10 ml 20x transfer buffer

Molecular weight marker

Rainbow Color Marker *(Amersham®)*: 250 kDa, 160 kDa, 105 kDa, 75 kDa, 50 kDa, 35 kDa, 20 kDa, and 15 kDa.

FACS buffer (staining buffer)

Dulbecco's PBS
1% heat-inactivated FCS
0.1% (w/v) sodium azide. Adjust buffer pH to 7.4 – 7.6

Fixation Buffer

Dulbecco's PBS
4% (w/v) paraformaldehyde
Add the paraformaldehyde to PBS
Adjust buffer pH to 7.4-7.6. Store at 4°C, protected from light

Permeabilization Buffer

Dulbecco's PBS
1% heat-inactivated FCS
0.1% (w/v) sodium azide
0.1% (w/v) saponin (*Sigma®*). Adjust buffer pH to 7.4 - 7.6

Propidium Iodide

[1 mg/ml] + PBS

5.2. CELL PREPARATIONS

All experiments were performed using two different cells preparations: human cell lines used as positive or negative controls (5.2.1), and freshly isolated human peripheral blood mononuclear cells (PBMCs), from which different cell types were obtained (5.2.2).

PBMCs were separated into $CD4^+$ and $CD8^+$-T lymphocytes (Ly), $CD19^+$-B lymphocytes and $CD14^+$-monocytes using different methods described in the following sections. Immune cells were used either non-activated or activated with specific mitogens, antibodies or cytokines, depending on the cell type and on the experiments.

The purity of the isolated cell types was >95% as determined by fluorescence-activated cell sorter scan (FACS) analysis (Becton-Dickinson FACSCalibur).

Supernatants (SN) were removed at different time intervals after stimulation and analyzed for protein concentrations. Cell subtypes were used at different time points to prepare mRNA, total protein lysate or to perform FACS experiments, proliferation assays, etc.

5.2.1. Cell line cultures

Under sterile conditions, different human cell lines were cultured in $75cm^2$ Falcon flasks, with 5%-10% fetal calf serum (FCS) *(Gibco®)*, either in RPMI *(Gibco®)* or in DMEM medium + penicillin (50-100 U/ml)/streptomycin (50-100 µg/ml), and were grown in 37°C incubators (95% humidity, 5% CO_2) (Current protocols of Immunology, 2001).

When adherent cells reached approximately 80% of confluence, cells were washed in PBS, then detached with trypsine, and split into two flasks.

5.2.2.1. Cell types:

3T3- fibroblasts transfected with rat-GDNF (from Dr. A. Fluegel, Max-Planck-Institute for Neurobiology, Germany)

3T3- fibroblast transfected with rat-NGF (from Dr. A. Fluegel)

293 cells (primary human embryonic kidney cells transformed with sheared human adenovirus type 5 DNA, epithelial morphology)

HeLa cells (human, cervix, epithelial adenocarcinoma)

HL-60 cells (human, leukemia, intermediate myeloid promyelocytic cell type)

Jurkat cells (human, leukemia, T cell type)

K-562 cells (human, leukemia, early myelo-erytroblasts cell type)

Myoblasts (human normal fetus, from Dr. Lochmüller, Genzentrum, Munich and Ludwig-Maximilians-University, Munich)

SHSY-5Y cells (human neuroblastoma cell line)

TE671 cells (human rabdomyosarcoma cell line)

TGW cells (human neuroblastoma cell line, given by Dr. M. Takahashi, Tokyo University, Japan)

5.2.2. Isolation of peripheral blood mononuclear cells from fresh blood

Peripheral blood mononuclear cells (PBMCs) were isolated from either fresh blood or from Buffy coat using the method of Bøyum: density centrifugation on Lymphoprep®, which is a mixture of sodium metrizoate and polysaccharide. The polysaccharide in this solution causes the erythrocytes to aggregate and settle to the bottom of the tube along with granulocytes. The density of the sodium metrizoate (1077 g/l) is such that lymphocytes, monocytes and platelets remain at the interface between the plasma and Lymphoprep® layers. This separation of cellular components is enhanced by low speed centrifugation, at room temperature (RT).

5.2.2.1. Gradient method using Lymphoprep®:

Ficoll-Hypaque density gradient centrifugation

Human fresh blood (collected in a 9 ml Sarstedt EDTA tube) diluted with an equal volume of PBS or 10 ml Buffy coat + 25 ml PBS were carefully layered on top of 15 ml of Lymphoprep® in a 50 ml Falcon tube. Red blood cells were centrifuged through the Lymphoprep® cushion at 1,600 rpm, for 20 min, at RT. PBMCs were concentrated in a white ring. The fluid above the PBMCs was discarded and PBMCs transferred to a new 50 ml Falcon tube. From then on, the cells were kept on ice or at 4°C. PBMCs were washed with PBS once, 10 min, 1,200 rpm, at 4 °C, and the pellet was resuspend in 10 ml of sterile RPMI 1640 + 5% FCS + antibiotics. Cells were counted and plated either at $2x10^5$ cells/100 µl medium/well in a 96 well plate or at $2x10^6$ cells/ml medium/well in a 24 well plate.

5.2.3. Isolation and activation of sub-types of immune cells from PBMCs

Immunomagnetic cell isolation using Ab-coated-beads is a reliable method for positive selection of immune cells, such as: $CD4^+$ and $CD8^+$-T lymphocytes, $CD14^+$ cells (monocytes) and $CD19^+$ cells (B Ly). Dynabeads® are uniform, magnetizable polystyrene beads coated with a primary mAb specific for a single membrane antigen that is predominantly expressed on the each subset of human immune cells. During a short incubation period, only positive cells (for each CD molecule) bind to Dynabeads® and subsequently, the rosetted cells can be isolated and washed by using a magnet.

Negative selection also can be used to separate cell sub-types. Each kit contains a highly optimized Antibody Mix and Depletion Dynabeads® to deplete all kinds of cells, except the ones that are needed. Selected cells remain free of both, surface Ab and beads.

5.2.3.1. Isolation of T Lymphocytes

T lymphocytes are divided into two classes. One class differentiates into cells that activate other cells such as B cells and macrophages through the secretion of cytokines; these cells are $CD4^+$-T cells (helper/inducer lymphocytes). The second class is the $CD8^+$-T cells (cytotoxic lymphocytes) that among other functions kill cells infected with viruses. Lymphocytes are small, with few cytoplasmic organelles and much of the nuclear chromatin inactive. They have no activity until they encounter an antigen, necessary to trigger their proliferation and functional differentiation.

a) <u>Positive isolation of $CD4^+$-T lymphocytes</u> *(Dynal®)*

- 10 ml Buffy Coat or 30-40 ml fresh blood were used to isolate PBMCs, as described in *"Gradient method using Lymphoprep®"*
- $CD4^+$-T cells were isolated with the magnetic beads selection method according to manufacturer′s instructions (catalogue # 111.05)
- During the next day, Dynabeads® were detached from the selected $CD4^+$-T cells in culture. The content of the wells was collected into a new tube and washed 3 times, placing the tube on magnet. SN containing $CD4^+$-T cells was kept, beads discarded
- Isolated cells were cultured at $2x10^5$ $CD4^+$-T cells/100 μl RPMI/5%FCS medium. They were activated after 6 hr in culture.

b) Positive isolation of $CD8^+$-T lymphocytes *(Dynal®)*

- Followed the same procedure as described in 5.1.2.1, changing amount and type of magnetic coated-beads anti-$CD8^+$ (catalogue # 111.07)
- The purity of the selected sub-sets obtained using this method was higher than 93%, confirmed by FACS analysis using mAbs (*see "Purity of cells"*).

c) T cells blasts from PBMCs

PBMCs incubated with ConA for a long period induces strong and rapid T cell proliferation. After four days in culture, monocytes and B cells die and more than 95% of the cell population are activated T cell blasts.

- To obtain activated T cell blasts ($CD3^+$-T cells) 200,000 PBMCs/100µl medium were treated with ConA and incubated for at least 96 hr, at 37°C
- IL-2 was added in order to keep T cell blasts proliferating.

d) Non-activated T cells from whole blood

Activation with ConA leads to morphologic and phenotypic changes in T cells. To obtain non-activated, resting T cells from whole blood, a direct isolation RosetteSep® procedure was used. This technique uses bi-functional Abs that are bound in bi-specific Ab complexes, which are directed against cell surface Ag on human hemopoietic cells (CD16, CD19, CD36, CD56) and glyphorin A on red blood cells. The cross-linked cells (granulocytes, monocytes, B cells and NK cells) precipitate with the erythrocytes, leaving the T cells in the low-density band of the gradient procedure:

- Peripheral blood should be diluted in PBS. Mixed well
- Added 50µl of RosetteSep Ab cocktail/ml of whole blood, incubated at RT
- Protocol was same as for *"Isolation of PBMCs from fresh blood"*.

e) T cell activation

PBMCs can be differentially activated depending on the mitogen or cytokine added to the culture. In this manner, it is possible to activate a selected group of cells, which will proliferate, differentiate and regulate expression of some molecules (cytokines, CD molecules). To activate 200,000 PBMC/100 µl medium/well:

1. **Polyclonal activation with Lectins** (polyvalent carbohydrate-binding proteins):
   1.1. ConA *(Sigma®)*: final concentration [10 µg/ml]
   1.2. PHA *(Sigma®)*: final concentration [10 µg/ml]

1.3. PMA + Ionomycine *(Sigma®)*

PMA: final concentration [3 ng/ml]

Ionomycine: final concentration [300 ng/ml]

2. **Mouse anti-human CD3 Ab** *(DAKO®)*: final concentration [1 μg/ml]
3. **Interleukine-2** (IL-2) *(Promocell®)*: final concentration [100 U/ml]

5.2.3.2. Isolation of B Lymphocytes

B-lymphocytes bear diverse receptors on their surface that allows them to recognize different antigens. These receptors are diverse in their antigen specificity, but an individual lymphocyte is equipped with receptors that will recognize only one particular Ag.

a) Positive isolation of $CD19^+$ B cells *(Dynal®)*

- Use the same procedure described in 5.1.2.1, changing the amount and type of magnetic beads for anti-$CD19^+$ coated beads (Catalogue # 111.03)
- On the next day, collected and discarded detached magnetic beads, as described
- Cultured isolated cells: 200,000 cells/100 μl RPMI/5% FCS medium
- Activated them after 6 hr resting in culture.

b) Negative isolation of $CD19^+$ B cells *(Dynal®)*

- PBMCs were isolated as described in Gradient method
- $CD19^+$ B lymphocytes were isolated according to manufacturer′s instructions, in which "1 Test" means $10x10^6$ PBMCs
- For 1 test: added 20 μl of Blocking Reagent and 20 μl Ab-Mix
- Cultured $2x10^5$ cells in 100 μl RPMI/5%FCS in a 96 wells/plate, at 37°C
- Activated B cells next day

c) B cell activation

1. **SAC** (Staphylococcus Aurous Cowan 1 antigen) *(Calbiochem®)*
   Dilution: 1:7,500
2. **mαh CD40** *(Pharmingen®)* + **gαh IgM** *(Jackson Imm.®)*
   final concentration [10 μg/ml] + final concentration [10 μg/ml]
3. **PWM** (Pokeweed mitogen) *(Sigma®)*: final concentration [5 μg/ml]

5.2.3.3. Isolation of monocytes

Macrophages are one of the two types of phagocyte in the immune system and they are distributed widely in body tissues, being part of an innate immunity. They are the mature form of monocytes, which circulate in the blood and differentiate continuously into macrophages upon migration into the tissues (Janeway, 1999).

a) Positive isolation of monocytes *(Dynal®)*

- PBMCs were isolated as described in 5.1.2.1
- $CD14^+$ cells were isolated with the magnetic beads selection method according to manufacturer′s instructions (catalogue # 111.11)
- Beads were engulfed by monocytes. It was not necessary to discard them
- Cultured monocytes: $2x10^6$ cells in 1 ml RPMI/10%FCS, at 37°C, 5% CO_2
- They were activated next day

b) Monocyte negative isolation *(Dynal®)*

- Isolated PBMCs, as described before
- $CD14^+$ monocytes were isolated according to the manufacturer's instructions, in which "1 Test" means $10x10^6$ PBMCs. It yielded ~ 1-2 x 10^6 monocytes
- Added Blocking Reagent (human γ-globulin to block monocyte Fc receptors) and Antibody Mix mixed and incubated for 10 min, at 2-8°C
- Added washed Depletion Dynabeads® to PBMCs, incubated 15 min, at 4°C with gentle rotation
- Cultured $2x10^6$ cells in 1 ml RPMI/10%FCS in a 24 wells/plate, at 37°C, 5% CO_2. Cells were activated the following day

c) Monocyte activation

Both isolation procedures described above yielded activated monocytes, either through the binding of coated beads to CD14 molecule (LPS receptor) in the case of positively isolated cells, or through the activation of Fc receptors in the negative isolation procedure. After 24 hr in culture, they are resting cells again and can be activated.

1. **LPS (055-B5)** (Lipopolysaccharides from E. coli) *(Sigma®)*:
   final concentration [300 ng/ml]
2. **IFN-γ** (Interferon-gamma) *(Roche®)*: final concentration [100 U/ml]
3. **TNF-α** (Tumor Necrosis Factor-α) *(Roche®)*: final concentration [50-100 U/ml]

4. **GM-CSF** (Granulocyte–Macrophage Colony Stimulating Factor) (*R&D®)*:
   Final concentration [250 ng/ml]

5.2.3.4. Human fetal myoblasts:

Normal human fetal myoblasts were cultured in DMEM + 15% containing 50 µg/ml fetuin, 1 ng/ml basic fibroblasts factor, 10 ng/ml epidermal growth factor, 10 µg/ml insulin, 0.4 µg/ml dexamethasone, 50 ng/ml amphotericin B and 50 µg/ml gentamicin. Adherent myoblasts were detached from the culture flask with Versene *(Gibco® BRL)*. Myoblasts cultures contained more than 95 % $CD56^+$ cells as determined by fluorescence-activated cell sorter scan (FACS) analysis.

a) ***Myoblasts activation:***

1. ***IFN-γ** (Interferon-gamma)* (Roche®)
2. **IL-1β** (Interleukine-1β) *(Sigma®)*

5.2.4. Purity of selected sub-sets

Because each isolated sub-type of immune cells expresses at least one specific CD molecule on its surface, it was possible to do FACS analysis using a fluorochrome-conjugated antibody specific for each cell surface antigen.

Extracellular staining determined the purity of selected sub-sets in each experiment, using directly labeled mouse mAbs against human CD4, CD8, CD14 and CD19 molecules. The analysis were performed 24 or 48 hours after selection of $CD4^+$ and $CD8^+$-T cells, B cells and monocytes, both resting and activated. Directly labeled mouse isotype controls matching with the Ab's isotype were always included.

The extracellular staining was performed either using two labeled Abs at the same time (each labeled with different fluorochromes) or separated Abs, i.e., mαhCD4-PE with mαhCD8-FITC and corresponding isotype IgG_1-PE and IgG_1-FITC.

In order to analyze only viable cell populations, Propidium Iodide *(Sigma®)* or Via Probe *(B-D®)* were used to identify and discard dead cells.

FACS protocols are described in Section 5.8 (FACS analysis).

5.2.4.1. Antibodies and Ig controls

(a) <u>Isotype controls</u>:

Mouse IgG_1-FITC labeled *(PharMingen®)*

Mouse IgG_1-PE labeled *(B&D®)*

Mouse IgG_{2a}-FITC labeled *(Dako®)*

(b) <u>Anti-human CD antibodies</u>:

Mouse IgG_1-α-human CD3-FITC labeled *(B&D®)*

Mouse IgG_1-α-human CD4-FITC labeled *(Biosource®)*

Mouse IgG_1-α-human CD4-PE labeled *(PharMingen®)*

Mouse IgG_1-α-human CD8-FITC labeled *(ImmunoTech®)*

Mouse IgG_{2a}-α-human CD14-FITC labeled *(PharMingen®)*

Mouse IgG_1-α-human CD14-PE labeled *(B&D®)*

Mouse IgG_1-α-human CD20-PE labeled *(PharMingen®)*

Samples were analyzed on a FACSCalibur *(B&D ®)* using CellQuest software.

5.3. PROLIFERATION ASSAYS

Proliferation assays measure the incorporation of radioactively labeled thymidine (^{3}H methyl-thymidine) into the DNA of proliferating cells after mitogen activity.

Only proliferating cells take up methyl-thymidine from the culture medium. After some days in culture, labeled cells were harvested onto a glass fiber filters that bind DNA. The radioactivity bound to the filter was measured for one minute in a β-Counter.

5.3.1. Protocol

- On day zero, PBMCs or any of the sub-sets were plated in 96 well plates, 200,000-cells/well 200 µl medium and stimulated with an activator, mitogen or antigen
- On different time-points (24, 48, 72 and 96 hr) cells were labeled by adding 20 µl (14800 Bq) of ^{3}H-thymidine (37 MBq/ml, 1:50 dilution) to the medium

- After 18 hr of labeling, cells were harvested onto a filter. Proliferating cells were measured by [^{3}H] thymidine incorporation in a gas scintillation counter for one minute (Matrix 9600 Direct beta Counter, Packard)
- All tests were performed in triplicate

5.3.2. Human myoblast proliferation

For the measurement of myoblasts proliferation, cells were plated into flat-bottomed microwells at 5,000 cells/well and incubated with cytokines during 48 hr.

To activate human myoblasts, 100 pg/ml of IL-1β or 100 U/ml of IFN-γ were used.

After cytokine induction, myoblasts were washed and detached with Versene. Myoblasts proliferation was also measured by [^{3}H] thymidine incorporation.

5.4. ENZIME LINKED IMMUNOSORBENT ASSAY (ELISA)

ELISA was employed to measure concentrations of cytokines or other soluble proteins (neurotrophic factors). Ags removed from the solution by capture Abs. A biotinylated 2nd Ab recognizing a different epitope of the same antigen was used to detect bound Ags. Bound 2nd Ab-biotin was quantified through a color reaction catalyzed by Avidin-HRP.

5.4.1. ELISA – GDNF

(GDNF E_{max}™ ImmunoAssay System. Promega®)

- Plates were coated with 100 µl/well of α-GDNF coating Ab, 10 µl diluted in carbonate coating buffer. Wells were sealed and incubated ON, at 4°C
- Contents were flicked out of the wells and the plate tapped upside down 3 times
- Wells were blocked adding 200 µl/well of Block & Sample buffer (B&S buffer), incubated at RT, for 1 hr, without shaking; then the plate was rinsed
- The standard curve was prepared performing serial dilutions, using human rec-GDNF. The standard curve is linear between 15.6 and 1,000 pg/ml of hr-GDNF
- Added 100 µl of the test samples/well, in triplicates and in serial dilutions. Incubated for 6 hours, at RT, with shaking
- Washed 5 times with PBS+0.05% Tween-20 (PBS-T)

- Incubated plate with 100 µl of anti-human GDNF pAb diluted in B&S buffer, O.N, at 4°C, without shaking. Next day, washed as above.
- Added 100 µl of anti-chicken IgY, HRP-conjugate diluted in B&S buffer. Incubated 2 hr, shaking, at RT. Washed as above
- Prepared the enzyme substrate by combining the same amount of TMB solution and peroxidase substrate and added 100 µl/well. Incubated at RT, for 15 min
- The reaction was stopped by adding 100 µl of 1M phosphoric acid to the wells. The blue coloration changed to yellow upon acidification
- The absorbance was recorded at 450 nm on a plate reader within one hour of stopping the reaction

Some samples were treated with acid (HCl, 1N) for 15 min in order to separate the ligand (GDNF) from its receptors, thus the specific epitope could be detected by the capture mAb (Okragly and Haak-Frendscho, 1997).

5.4.2. ELISA - TNF-α

(PharMingen®)

- Samples were the following: PBMCs ($2x10^6$ cells/ml) were seeded in a 24 well-plate, activated either with LPS+IFN-γ or with ConA, and cultured during different time points; then cells were incubated 24 hr or longer with of GDNF or NTN (100 ng/ml). SN were collected, spun down and stored at -20 °C until the assay was performed. Samples were tested in triplicates and with two serial dilutions
- Coated wells with 100 µl/well of capture Ab: mouse anti-human TNF-α in coating buffer. Sealed plate and incubated ON, at 4°C
- Aspirated content of wells and washed 3 times with PBS-T
- Wells were blocked adding PBS+10% FCS, 200 µl/well. Incubated at RT, 1 hr
- Standard curve and samples were prepared in assay diluent
- Added 100 µl of diluted samples/well. Sealed the plate, incubated 2 hr, at RT
- After washing, added 100 µl/well of biotinylated mouse anti-human TNF-α mAb + avidin-HRP conjugate in PBS+10% FCS, and incubated 1 hr, at RT
- Added 100 µl/well of substrate solution (TMB and hydrogen peroxide). Incubated maximal 30 min, at RT, in the dark
- Aspirated and washed the contents

- Stopped the reaction by adding 100 µl/well of 1 M H_3PO_4
- Read absorbance at 450 nm within 30 min of stopping reaction.

5.4.3. ELISA - IL-10

(PharMingen®)

- The procedure is similar to ELISA-TNF-α, antibodies are different.
- Capture Ab: mouse anti-human IL-10, diluted in coating buffer
- Detection Abs: biotinylated-mouse α-human IL-10 + avidin-horseradish peroxidase conjugate.

5.5. WESTERN BLOTTING

Proteins have a net positive or negative charge that reflects the mixture of charged amino acids they contain. If an electric field is applied to a solution containing a protein molecule, the protein will migrate at a rate that depends on its net charge and on its size and shape; this technique is called electrophoresis. Sodium dodecyl sulfate (SDS) polyacrylamide-gel electrophoresis (SDS-PAGE) uses a highly cross-linked gel of polyacrylamide as the inert matrix through which the proteins migrate. Proteins are released from their associations with other proteins or lipids and are soluble in the negatively charged detergent solution. In addition, a reducing agent (β-mercaptoethanol) is added to break any S-S linkages in the proteins so that all polypeptides in multi-subunit molecules can be analyzed separately. As a result, a mixture of proteins is fractionated into a series of protein bands with the same size, arranged in order of molecular weight (Molecular biology of the cell, 1999).

General Protocol: Once the gel is ready, separated proteins were transferred to a nitrocellulose membrane, which was then incubated with a primary Ab. To avoid unspecific binding, the membrane was blocked by incubation in 10% milk powder in PBS-T, ON, at 4°C. The first Ab was incubated for 1 hr, at RT, on a shaker and then, washed with PBS-T. When the Ab bound to the membrane, a secondary-HRP-linked Ab (diluted in skim milk+PBS-T) in combination with chemiluminescence was used to detect it. Chemiluminescence was visualized by exposing the membrane to a Kodak film.

5.5.1. Cell lysates

Cells were spun down to discard medium and debris, and then washed in PBS. They were pelleted and lysed in RIPA buffer, passed through a needle several times and incubated on ice for 30 min. Cell nuclei were eliminated by centrifugation 14,000 rpm, at 4°C, for 20 min. Total protein lysates were kept in small aliquots at -20 °C.

5.5.1.1. Protein concentration determination:

a) Lowry method: Tyr residues of the soluble protein react with Folin-Ciocalteu reagent to form a protein-dye complex with a maximal absorption at 600 nm. The assay was performed according to manufacturer's instructions *(Sigma®)* with different dilutions of protein. A calibration curve was established using bovine serum albumin (BSA) and concentration of the test sample was calculated from the absorption value.

b) Bradford method: The Coomassie brilliant blue G250 forms a protein/dye complex with arginine residues of proteins, with a maximal absorption at 595 nm. 1-10 µl of the protein lysate were incubated with 1 ml Bradford reagent (1/5 from the stock solution), 10-30 min, at RT. A calibration curve was established using BSA and the sample concentration was calculated from the absorption value. The method can be used for final concentrations of 1-10 µg/ml, and it is faster than method **a)**.

5.5.2. Polyacrylamid-Gel electrophoresis (PAGE)

5.5.2.1. Precast NuPAGE® Bis-Tris gels:

The NuPAGE® Bis-Tris System *(Novex®)* is based upon a Bis-Tris-HCl buffered polyacrylamide gel (gel matrix) available in different concentrations. Gels were used in conjunction with the recommended NuPAGE® denaturing SDS running buffers. Protein samples were loaded in 4xLDS buffer and gels were run for different times at 200 V, depending on which buffer was used. Separated proteins were transferred from the gel to a nitrocellulose membrane: *Semidry Western transfer method* (NuPAGE® Booklet, 1999).

5.5.2.2. Semidry Western transfer protocol:

- After wetting the surface of the gel with transfer buffer and position the pre-soaked transfer nitrocellulose membrane on the gel, all air bubbles were removed
- Placed the 3 pre-soaked anode filter papers on top of the membrane

- Placed the gel-membrane assembly in the same sequence, so that the gel was closest to the cathode plate. Pressed the anode onto the top and applied constant current.

5.5.3. Antibodies used in Western blot

5.5.3.1. Western blot: GDNF monoclonal Ab:

Monoclonal antibody against human GDNF (R&D Systems®)

- Loaded protein lysate inside the wells of a 4-12% Bis-Tris gel
- Running in 1xMES buffer: 200 V, 35 min
- Transferred proteins to a nitrocellulose membrane: 50 mA, 50 V, 90 min
- Blocked O.N, 4°C, 10% skim milk powder in PBS-T
- Washed 3 times with PBS-T
- 1° Ab: mAb-αhuman GDNF+2% skim milk in PBS-T, incubated for 2 hr, at RT
- Washed 3 times
- 2° Ab: Goatαmouse-HRP+2% skim milk in PBS-T, incubated for 30 min, at RT
- Washed 3 times. Developed with ECL *(Amersham®).*

5.5.3.2. Western blot: GDNF polyclonal Ab:

Polyclonal antibody against human GDNF-biotinylated (R&D Systems®)

- Same procedure as described above, changing antibodies
- 1° Ab: Goatαhuman GDNF-biotin+2% skim milk PBS-T, incubated for 2hr, at RT
- Washed 3 times with PBS-T
- 2° Ab: STP-HRP+2% skim milk powder in PBS-T, incubated for 45 min, at RT
- Washed 3 times. Developed with ECL.

5.5.3.3. Western blot: RET - short isoform:

Ret (SC-19) (Sta. Cruz Biotechnology®)

- Loaded protein lysates on 4–12% Bis-Tris gel
- Running in 1xMOPS: 200 V, 55 min
- 10 min gel pre-incubation in 0.02 % SDS in 2x transfer buffer
- Transfered proteins to nitrocellulose membrane: 100 mA, 50 V, 90 min
- Blocked 2 hr, at RT, with 10% skim milk in PBS-T. Washed 3 times
- 1° Ab: RabbitαRET pAb + 5% milk in PBS-T, incubated ON, 4°C, shaking

- Washed 3 times with PBS-T
- 2° Ab: Goatαrabbit-biotin + 2% skim milk in PBS-T, 50 min, at RT
- Washed 3 times with PBS-T
- 3° Ab: STP-HRP + 0.5% milk powder in PBS-T, incubated for 40 min, at RT
- Washed 3 times. Developed with ECL.

5.5.3.4. Western blot: RET - long isoform:

Ret (SC-20) (Sta. Cruz Biotechnology®)

- Molecular weight: 2 bands of 170 and 150 kDa can be detected, but also other bands of 100 and 120 kDa could be seen, corresponding to non-glycosylated forms.
- The six first steps were similar to those described for the short isoform of c-RET
- 1° Ab: GoatαRET pAb + 5% skim milk in PBS-T, incubated ON, at 4°C, shaking
- Washed 3 times with PBS-T
- 2° Ab: Rabbitαgoat-biotin+2% skim milk in PBS-T, incubated for 30 min, at RT
- Washed 3 times
- 3° Ab: STP-HRP + 0.5% skim milk in PBS-T, incubated for 40 min, at RT, shaking
- Washed 3 times with PBS-T. Developed with ECL.

5.6. IMMUNOFLUORESCENCE

5.6.1. Staining for adherent cells

- HeLa cells were grown in a slide-chamber in RPMI + 10% FCS, at 37°C, 5% CO_2, until they were 80% confluent
- Medium was removed and the plastic chamber was taken off
- After washing with 1xPBS, slides were incubated 10 min, in 4% PFA in PBS
- Staining with primary antibody was performed as following:
    - Incubated mouse-anti human NTN (IgG_{2b}), dilution 1:100, ON, at 4°C
    - Isotype control: mouse IgG_{2b}, equal concentration, ON, at 4°C
- Washed 3 times with 1xPBS
- Stained with secondary Ab: goat-αmouse IgG-Cy3, 2 hr, at RT. Washed 3 times
- Slides were dried at RT and then examined using fluorescence microscopy.

5.6.2. Staining for cells in suspension

- 100 µl of cells in suspension (PBMCs) were taken and placed on to glass slides in the cytospin device, then spun down at 600 rpm, 5 min, at RT
- Slides were dried and fixed with cold acetone, 10 min, at RT
- Incubated with first Ab and isotype IgG as described above
- Next day, incubated with secondary-labeled Ab, 2 hr, at RT, then washed with PBS
- Added mouse serum, concentration (1:100), 1 hr, at RT, to block unspecific binding or cross-reaction with the first antibody
- Washed slides with PBS
- Added anti-CD-FITC labeled antibodies, 45 min, at RT. Washed slides with PBS
- DAPI staining was added to show nuclei in blue
- Slides were dried and then examined using fluorescence microscopy.

5.7. FACS ANALYSIS

Fluorescence Assisted Cell Sorting/counting is a method used to assess the surface presentation of Ags. In a FACS instrument, cells are passed through a thin cuvette; at concentrations such that only one cell passes at a time. Using a laser a single excitation wavelength (488 nm) is utilized to illuminate cells; the forward scattered light (FSC) is a measure of the size of the cells. Light scattered perpendicular to the laser direction (side scatter, SSC) indicates the cell granularity. Fluorescent dyes bound to the cells through Ag-specific Abs are excited to emit light at specific wavelengths, i.e., FITC (fluorescein isothiocyanate), R-PE (R-phychoerythrin), Cy-Chrome, PrCP.

Cells can be counted; percentages of cell populations fitting certain criteria (gates) can be calculated, as well as changes in the expression of surface Ags under different conditions.

When two or more staining are used on the same sample, compensation is necessary.

Reagents that block Fc receptors may be useful for reducing non-specific staining.

5.7.1. Extracellular Immunostaining

5.7.1.1. Protocol

- Transfer 1–2x10^5 cells/well (96 conic bottom well plate, *NUNC®*)
- Spin down at 1,200 rpm, 5 min, at 4°C. Discard SN
- Wash the cells twice, adding 200 µl FACS staining buffer to each well, resuspend and spin down at 1,200 rpm, 5 min, at 4°C. Discard SN
- Incubation with first Ab diluted in 100 µl FACS staining, 30 min, at 4°C
- Spin down at 1,200 rpm, 5 min, at 4°C. Discard SN and wash cells twice
- If the first Ab is not fluorochrome-labeled, a secondary-labeled Ab (anti-first primary Ab) is used to stain the cells indirectly. Incubate secondary Ab as above
- Cells can be double stained using Abs labeled with different fluorochromes
- Add Via-Probe (*B-D®*) 10 µl, incubate 10 min, at 4°C and spin down
- Resuspend the pellet in 200-300µl of PBS
- Analyze samples during the next 2 hours. Fluorescence, as well as FSC and SSC are determined for at least 10,000 cells in a Becton Dickinson FACSCalibur.

5.7.1.2. Antibodies used for extracellular FACS

(a) GFRα-1:

1° Ab: Mouse anti human-GDNFR-α mAb (non-labeled) *(Transduction Lab.®)*

2° Ab: Goat anti mouse-FITC *(DAKO®)*

(b) GFRα-2:

1° Ab: Goat anti human-GFRα-2 pAb (non-labeled)

2° Ab: Donkey anti goat-PE *(Jackson Immunores®)*

(c) HLA-DR:

Mouse anti human-HLA-DR-PE *(Transduction Laboratories®)*

(d) Anti-CD molecules:

Mouse anti human-CD25-FITC *(PharMingen®)*

Mouse anti human-CD38-FITC *(ImmunoTech®)*

Mouse anti human-CD69-FITC *(PharMingen®)*

Mouse anti human-CD86-PE *(Serotec®)*

Isotype controls were described in Section 5.1.4 *"Purity of selected sub-sets"*.

5.7.2. Intracellular Immunostaining

5.7.2.1. Protocol

- Incubate cells with Monensin *(Sigma®)* (2 μM final conc.), for 3 hr, at 37°C
- Next three following steps are similar as described in *FACS Extracellular Staining*
- Cell fixation: with 4% PFA in PBS, 20 min, at 4°C, in the dark
- Spin down at 1,200 rpm, 5 min, at 4°C. Discard SN
- Wash 2x with permeabilization buffer, adding 200 μl/well, pipetting, spin down
- Incubation with first Ab in 100 μl permeabilization buffer, for 30 min, at 4°C
- Wash twice. Add labeled secondary Ab and incubate in the dark
- Wash twice, and add 200 μl PBS to analyze the samples
- Isotypes controls should be included

5.7.2.2. Antibodies used for Intracellular FACS

(a) GDNF (mAb):

1° Ab: Mouse anti human-GDNF mAb (non-labeled) *(R-D Systems®)*

2° Ab: Goat anti mouse-FITC *(DAKO®)*

(b) GDNF (pAb):

1° Ab: Goat anti human-GDNF biotinylated pAb *(R-D Systems®)*

2° Ab: Streptavidine-PE *(DAKO®)*

(c) RET:

1° Ab: Rabbit anti human RET pAb *(Sta. Cruz Biotech.®)*

2° Ab: Goat anti rabbit-Cy3 *(Jackson Immunoresearch®)*

(d) IL-4:

Mouse anti human-IL-4-PE mAb *(PharMingen®)*

(e) IFN-γ:

Mouse anti human-IFN-γ-PE mAb *(PharMingen®)*

(f) TNF-α:

Mouse anti human-TNF-α-FITC mAb *(B&D®)*

5.8. RT-PCR

The polymerase chain reaction (PCR) allows single-stranded cDNA to be amplified one billion-fold, if part of its nucleotide sequence is known. This sequence is used to design two synthetic DNA oligonucleotides, one complementary to each strand of the DNA double helix and residing on opposite sites of the region to be amplified. They serve as primers for *in vitro* DNA synthesis, which is catalyzed by a DNA polymerase.

Each reaction cycle requires a brief heat treatment to separate the two complementary DNA strands. A subsequent cooling of the DNA in the presence of primers allows them to hybridize to complementary sequences. The annealed mixture is incubated with DNA polymerase and the four-dNTP. When the procedure is repeated, the newly synthesized fragments in turn serve as templates, and after a few cycles the predominant product is a single DNA fragment.

5.8.1. RNA extraction

5.8.1.1. RNAzol method

- To prepare RNA from 1 to $10x10^6$ cells, washed cells in PBS and spun down
- Dissolved the pellet in 1 ml RNAzol, and centrifuged 10 min, 14,000 rpm, at 4°C
- Transferred the SN and added $CHCl_3$ (1/10 of SN volume)
- Centrifuged at 14,000 rpm, 20 min, at 4°C
- Put SN in a new tube and added same volume of Isopropanol (2-propanol)
- Kept 30 min, at -20°C, then centrifuged 10 min, 14,000 rpm, at 4°C
- Washed the pellet with 1 ml of ethanol-75%. Vortex
- Centrifuged 10 min, at 14,000 rpm. Dried pellet by air
- Added 34 µl DEPC water to solve the RNA
- Measured RNA concentration and digest genomic DNA with DNAse enzyme

5.8.1.2. Qiagen method

RNA extraction was performed following the manufacture's protocol. After total RNA was isolated, the genomic DNA contamination is higher using this method as compared with others. It is necessary to digest contaminating DNA with DNAse.

5.8.1.3. DNA digestion

One unit of RQ1 RNAse-Free DNAse is defined as the amount required to completely degrading 1 μg of λDNA, at 37°C, in 50 μl of a buffer containing: 40mM Tris-HCl, 10mM NaCl, 6mM $MgCl_2$ and 10mM $CaCl_2$. The **protocol** used was the following:

- 10 μl RNA (1-5 μg)
- 12 μl distillated water
- 6 μl 5x transcription buffer *(Promega®)*
- 2 μl RQ1 RNAse-free DNAse *(Promega®)*
- Heat at 37°C, for 60 min
- Use the "Clean-up RNA Protocol" from Rneasy-mini handbook *(Qiagen®)* following the manufacturer's instructions
- Measure amount of total RNA and continue with the ***cDNA synthesis***

5.8.1.4. RNA concentration

RNA concentration was determined by measuring the absorption at 260 nm and at 280 nm. A280 can be used as a measure of impurity of RNA (A280/A260 should be approx. 1.7).

5.8.2. First-strand cDNA synthesis

A DNA copy (cDNA) of a mRNA molecule can be produced by the enzyme reverse transcriptase, which is an unusual DNA polymerase that synthesizes a DNA chain from RNA template; forming a DNA/RNA hybrid helix. Treating the DNA/RNA hybrid with alkali degrades the RNA strand into nucleotides. The enzyme requires a small oligo-(dT) primer, which is annealed with the long poly-A tail at the 3'-end of most mRNAs. In this way, the single-stranded cDNA can be copied into double-stranded cDNA molecules.

5.8.2.1. Protocol:

- 1 μl Oligo$(dT)_{12\text{-}18}$ (500 μg/ml)
- Total RNA (from 1 ng to 5 μg)
- 1 μl dNTP mix (10mM each dATP, dGTP, dCTP and dTTP, at neutral pH)
- Sterile, distilled water to 12 μl
- Heat mixture to 65°C for 5 min and quickly chill on ice.

- Collect the contents of the tube by brief centrifugation and add:
  - 4 µl 5x first-strand buffer (250mM tris-HCl, pH 8.3; 375mM KCl; 15mM $MgCl_2$)
  - 2 µl 0.1 M DTT
  - Mix contents of the tube gently and incubate at 42°C, for 2 min
  - Add 1 µl (200 U) of SuperScript™II Rnase reverse transcriptase (*Gibco BRL®*)
  - Incubate 50 min, at 42°C.
  - Inactivate the reaction by heating to 70°C for 15 min

5.8.3. RT-PCR reaction

To prepare a ***final reaction volume of 50 µl:***

- 5 µl 10x PCR Buffer (200mM Tris-HCl, pH 8.4, 500mM KCl)
- 1.5 µl of 50 µM $MgCl_2$
- 1 µl of 10 µM dNTP mix
- 1 µl primer 1: forward (10 µM) and 1 µl primer 2: reverse (10 µM)
- 0.25 µl Taq DNA polymerase (5 U/µl)
- 2 µl cDNA (from first-strand reaction)
- 38 µl distilled water.

Perform 25 to 40 cycles of PCR. Annealing and extension conditions are primer and template dependent.

5.8.3.1. Agarose gel electrophoresis

PCR products were analyzed on 1.7% agarose gels. Agarose was boiled in TAE buffer, then 20 µl of diluted ethidium bromide were added and the gel was cast. The solidified gel was inside the running chamber that was filled with 1xTAE. PCR products were mixed with 6x loading buffer and loaded into the wells. Gels were run at 80 V, 40 min. Amplified PCR products were visualized by UV light (302 nm) and photographs were taken.

5.8.3.2. DNA purification

To remove contaminants (agarose, buffers) and primers from DNA, PCR products were purified using QIAGEN PCR purification kit (*Qiagen®*) according to the manufacturer′s instructions.

5.8.3.3. PCR-product sequencing

Sequencing of PCR products (purified DNA) were performed by Toplab, Martinsried.

5.9. PRIMER SEQUENCES

5.9.1. β-Actin

Human housekeeping gene used as internal control.

5.9.1.1. Actin $_{EM}$

Forward primer: 5'-CGG GAA ATC GTG CGT GAC AT-3' (bp 689-708)

Reverse primer: 5'-GAA CTT TGG GGG ATG CTC GC-3' (bp 1381-1400)

PCR product: 729 base pairs

5.9.2. GDNF

5.9.2.1. GDNF - A

Forward primer: 5'-TTC GCG CTG AGC AGT GAC-3' (Exon 2, bp 133-150)

Reverse primer: 5'-TAC ATC CAC ACC TTT TAG CGG-3' (Exon 3, bp 611-632)

PCR product: 498 base pairs

5.9.2.2. GDNF - B

Using GDNF-B primers, the spliced isoform and the FL of GDNF can be amplified.

Forward primer: 5'-ATG AAG TTA TGG GAT GTC GT-3' (Exon 2, bp 9-29)

Reverse primer: 5'-TCA GAT ACA TCC ACA CCT TT-3' (Exon 3, bp 510-530)

PCR product: 521 base pairs (FL) and 460 base pairs (short isoform) (Hishiki et al., 1998)

5.9.3. NEURTURIN

5.9.3.1. NTN - 2

Forward primer: 5'-CCT CAG TGC TCT GCA GCT C-3' (Exon 1, bp 29-47)

Reverse primer: 5'-TCG TGC ACC GTG TGG TAG-3' (Exon 2, bp 546-563)

PCR product: 535 base pairs

5.9.4. PERSEPHIN

5.9.4.1. PSP - 1

Forward primer: 5'-CTG GGC TCT CTG CTG CTC-3' (Exon 1, bp 22-39)

Reverse primer: 5'-CAT CAC CGA CGT GGC CTT-3' (Exon 2, bp 384-401)

PCR product: 389 base pairs

5.9.4.2. PSP - C

Forward primer: 5'-TCT CTG CTG CTC CTG TCC CTG CA-3' (Exon 1, bp 28-50)

Reverse primer: 5'-CGC ACC CAG CAT GGC CTG-3' (Exon 2, bp 304-321)

PCR product: 294 base pairs

5.9.5. RET

Multiple isoforms of the c-RET proto-oncogene can be amplified at the 5'-end or at the 3'-end regions of the mRNA sequence. The 5'-end region encodes for the NH_2 segment and the extracellular domain of the protein; the 3'-end region encodes for the COOH and the intracellular domain (see Figure 5).

5.9.5.1. RET (ex6)

Primers located between exons 2-3 and exon 6 used to amplify isoforms at the 5'-end.

Forward primer: 5'-TGT CCG CAA CCG CGG CTT TC-3' (Exon 2-3, bp 262-281)

Reverse primer: 5'-CTG ACC GGC AGC ACC GAC ACG TT-3' (Exon 6, bp 1327-1351)

PCR product: 873 base pairs (full length)

5.9.5.2. RET - 9-b

To detect the short isoform, RET-9 (Myers et al., 1995; Ivanchuck et al., 1998):

Forward primer: 5'-AAA CCC CTA TCC TGG GAT TCC T-3' (Exon 19, bp 2996-3017)

Reverse primer: 5'-ATC ACA GAG AGG AAG GAT AGT-3' (Intron 19, bp 3326-3337)

PCR product: 446 base pairs

5.9.5.3. RET - 51-b

To detect the long isoform, RET-51 (Myers et al., 1995; Ivanchuck et al., 1998).

Forward primer: 5'-AAA CCC CTA TCC TGG GAT TCC T- 3' (Exon 19, bp 2996-3017)

Reverse primer: 5'-TCA GCT CTC GTG AGT GGT-3' (Exon 20, bp 4762-4779)

PCR product: 430 base pairs

5.9.5.4. RET-43

To detect the middle isoforms, RET-43 (Ivanchuck et al., 1998).

Forward primer: 5'-AAA CCC CTA TCC TGG GAT TCC T- 3' (Exon 19, bp 2996-3017)

Reverse primer: 5'-GGG GTA CCT ATC AGT GCT TTA AGT CTG- 3' (Exon 21, bp 6256-6282)

PCR product: 354 base pairs

5.9.5.5. RET 9 – 18

To amplify other probable isoforms located upstream of exon 19 (Fluge et al., 2001)

Forward primer: 5'-ACT TCT CCA CCT GCT CTC C- 3' (Exon 9, bp 1592-1610)

Reverse primer: 5'-GCT GAT GTC GCG AAA CAC C- 3' (Exon 18, bp 2909-2927)

PCR product: 1335 base pairs.

5.9.6. GFRα-1

5.9.6.1. Rec-Alpha1(2)

Forward primer: 5'-ATG TTC CTG GCG ACC CTG T- 3' (Exon 1, bp 1-18)

Reverse primer: 5'-CTG GTA CAT GCT CCA GTA-3' (Exon 2, bp 324-307)

PCR product: 325 base pairs (Eng et al., 1998).

5.9.6.2. ALPHA-1

To amplify the splice isoform that lacks exon 5 (15 bp) (Hishiki et al., 1998):

Forward primer: 5'-TAC CAA CTG CCA GCC AGA GT- 3' (Exon 4, bp 777-796)

Reverse primer: 5'-GGT AGT GGC AGT GGT GGT CTG TA- 3' (Exon 7, bp 1086-1064)

PCR product: 310 base pairs.

5.9.7. GFRα-2

Three variants due to exon skipping have been described. They are generated when either exon 2 or exon 3 are spliced out, or when exons 2 + 3 are lacking (Wong et al., 1998).

5.9.7.1. GFRa2

Forward primer: 5'-CGT CCT CTT CTT CTT TCT AG-3' (Exon 1, bp 20-40)

Reverse primer: 5'-TGG TAA TTG TCC GCA GGG CA-3' (Exon 5, bp 850-870)

PCR products:

851 bp: Full Length (GFRα-2a)

537 bp: exon 2 spliced out (GFRα-2b)

453 bp: exon 2 and exon 3 spliced out (Exon 1-4 mRNA)

5.10. STATISTICAL ANALYSIS

Data are represented as the mean (or average) of at least three values (n=3 or n=6), which correspond to each bar in the graphics. Always "**n**" was indicated in the figure legend. Error bars represent standard error of the mean (SEM), calculated as following:

$$SEM = \frac{SD}{/n}$$

SD: standard deviation

The *Student`s t-test* was used as a test of significance for cytokine production (ELISA for TNF-α and IL-10) and proliferation assays, because independent values from two sample groups with normal distribution was compared.

6 RESULTS

6.1. PURITY OF CELLS

The purity of each sub-set of immune cells was assessed by FACS analysis using specific directly labeled-mouse mAb against human CD4, CD8, CD14 and CD20 surface molecules. Analyses were performed 24 or 48 hours after immunomagnetic selection.

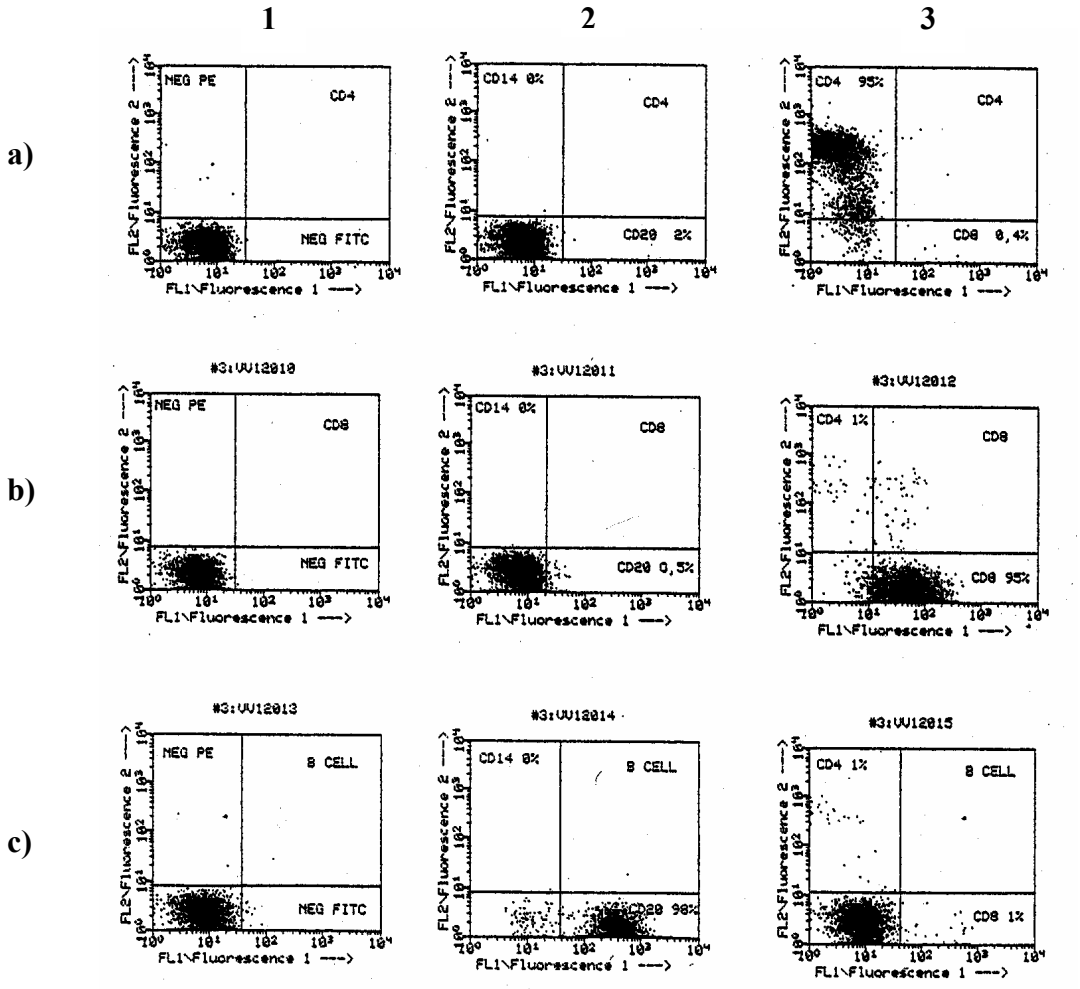

Figure 11: FACS analysis to assess the purity of cells after separation: $CD4^+$ and $CD8^+$-T lymphocytes, B lymphocytes. Positively isolated cells were incubated O.N and labeled after removed the beads. The purity of each sub-type was assessed by double staining with two different fluorochrome Abs. Each row of dot-blots represents each cell type, starting from the left side: a) $CD4^+$-T cells, b) $CD8^+$-T cells and, c) B lymphocytes. Each column represents the α-CD Ab: Column 1: isotype control: Neg-PE/Neg-FITC. Column 2: α-CD14-PE/α-CD20-FITC. Column 3: α-CD4-PE/α-CD8-FITC.The percentage of $CD4^+$ and $CD8^+$-T cells was 95% for both cell types. 98% was the purity for B cells. (Monocytes are not shown).

6.2. PROLIFERATION ASSAYS

Total PBMCs or a sub-set of immune cells were activated with different mitogens and cultured at $2x10^5$ cells/well in a 96-round bottom plate, in triplicates for each activator. Cells were labeled with ^{3}H-thymidine at different times points, and harvested after 18-hours of incubation. When cells are not well activated, they did not uptake ^{3}H-thymidine; and were discarded. Next graphic shows one example of lymphocytes proliferation:

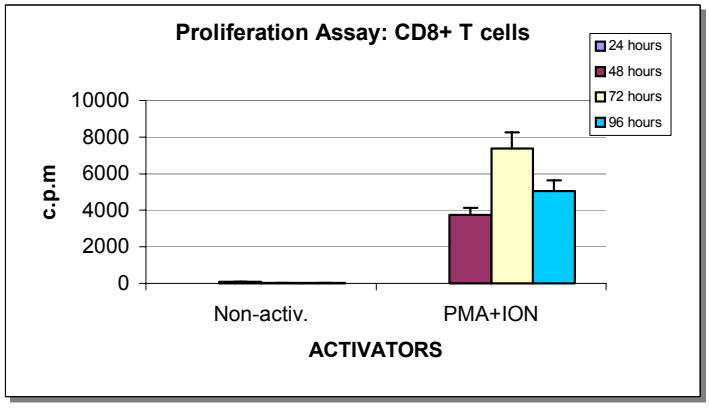

Figure 12: CD8$^+$-T cell proliferated after 24, 48, 72 and 96 hr of activation with PMA+Ionomycine. CD8$^+$-T lymphocytes were positively selected using immunomagnetic beads. ^{3}H-incorporation is expressed in counts per minute (c.p.m). Each bar represents the mean of three values, n=3, + Error bar= SEM (standard error of the mean).

This graphic Figure 13represents proliferation of PBMCs after different activators:

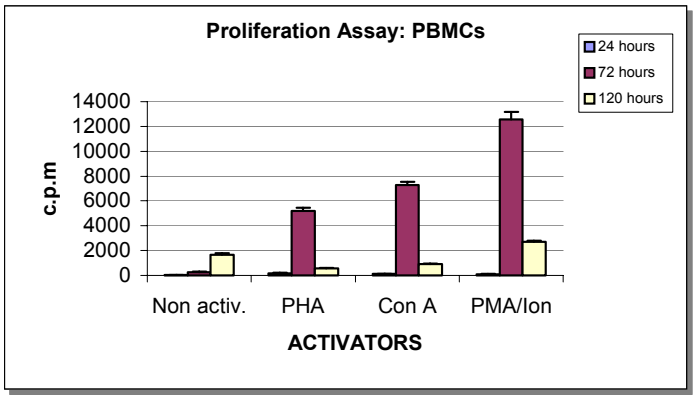

Figure 13: Representative proliferation assay of non-activated and activated PBMCs. Cells were either untreated or treated with PHA, ConA or PMA+Ion. ^{3}H-incorporation was measured after 24, 72 and 120 hr in culture. The best stimulation was observed after 72 hr. Representative results, mean of n=3, + SEM.

6.3. GDNF EXPRESSION

6.3.1. RT-PCR: GDNF

Two sets of primers were utilized to amplify GDNF transcripts from immune cells (both intron-spanning primers): **GDNF-A primers:** forward: 5'-TTC GCG CTG AGC AGT GAC-3' (exon 2, bp 133-150); reverse: 5'-TAC ATC CAC ACC TTT TAG CGG-3' (exon 3, bp 611-632), that amplify only the large isoform (Woodbury et al., 1998). **GDNF-B primers:** forward: 5'-ATG AAG TTA TGG GAT GTC GT 3' (exon 2, bp 9-29); reverse: 5'-TCA GAT ACA TCC ACA CCT TT-3' (exon 3: bp 510-530), which detect both isoforms (Hishiki et al., 1998).

Non-activated and activated PBMCs (either with PHA, ConA, LPS+IFN-γ or PMA+Ion), non-activated and activated $CD4^+$-T cells, $CD8^+$-T cells, B cells, and monocytes did not express GDNF mRNA. A few representative samples are shown in Figure 14.

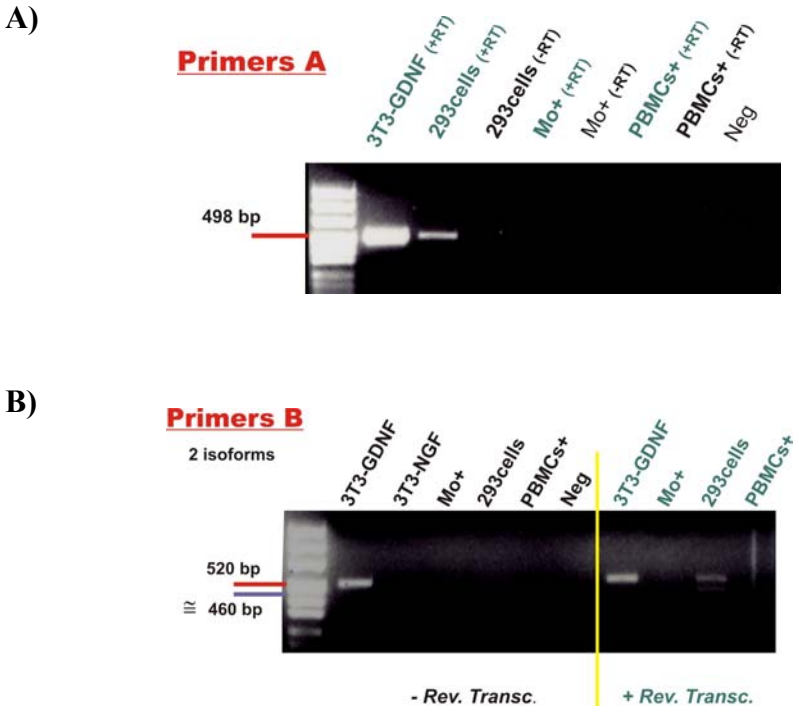

Figure 14: **Immune cells did not express GDNF.** A) RT-PCR using primers-A. Amplifications were observed neither in activated PBMCs (PBMCs+) nor in monocytes (Mo+). B) RT-PCR using GDNF-B primers, which detect both spliced isoforms Any of the immune cells studied expressed GDNF. PCR products: 521 base pairs: large isoform; 460 base pairs: short isoform (lacking 78 bp). 293 cells expressed both, full and truncated isoforms. (+RT): plus reverse transcriptase. (-RT): without reverse transcriptase.

RT-PCR using β-actin primers, as house keeping gene was performed with all cDNAs to test their quality.

Prior to the cDNA synthesis, total amount of RNA was divided into a two tubes, only one of them was incubated in the presence of the reverse transcriptase enzyme (+RT), the other part was incubated in its absence (-RT), to avoid the inclusion of samples containing genomic DNA.

6.3.2. ELISA-GDNF

6.3.2.1. ELISA: GDNF in immune cells

GDNF protein was not detected in the supernatant from cultured immune cells, even after activation with different mitogens and at different stimulation times, using ELISA detection kit for GDNF and following the manufacture's instructions. The acidic treatment was performed in some samples to separate bound GDNF from its receptors. In Table 2 treated and non-treated samples are indicated.

Cells were isolated from 24 different Buffy-coats. Different sub-types of immune cells were separated as described. T lymphocytes (both, $CD4^+$ and $CD8^+$-T lymphocytes), B lymphocytes, and monocytes were obtained and activated with diverse mitogens or activators, depending on the cell type. After different time-points (12, 24, 48, 72, 96 or 120 hours) in culture, supernatants were collected; spun down and stored at -20°C until the assay was performed. Samples were collected from the wells in triplicates.

As positive control, human recombinant GDNF (also for the standard curve) and supernatant from 3T3-GDNF transfected fibroblasts were used. 15p

As a negative control, supernatant from NGF-transfected fibroblasts was tested.

In a few SN of immune cells, the amount of GDNF detected was very low, close to the limit of detection.

Buffy Coat	*Cell sub-type*	*Activation*	*Results*	*Acidic treatment*
1	Mo	(-), LPS	Negative	Non-treated
2	CD4, CD8, Bcells, Mo	(-), PHA, LPS	Negative	Acidic
3	CD4, CD8, Bcells	(-), ConA	Limit of detection	Acidic
4	CD4, CD8, Bcells, Mo	(-), PHA, LPS	Negative	Non-treated
5	CD8	(-), PMA/Ion	Limit of detection	Non-treated
6	CD4, CD8, Mo	(-), PHA, LPS	Negative	Non-treated
7	B cells	(-), PWM	Negative	Non-treated
8	Mono	(-), LPS	Limit of detection	Acidic
9	CD4, B cells	(-), PHA	Negative	Non-treated
10	B cells	(-), PWM	Limit of detection	Non-treated
11	PBL, Bcells, Mo	(-), ConA, LPS	Negative	Non-treated
12	PBMC; B cells	(-), PHA, PWM	Negative	Non-treated
13	PBMC, B cells	(-), PHA, PWM	Negative	Non-treated
14	Mo	(-), LPS	Negative	Non-treated
15	Mo	(-), LPS	Negative	Non-treated
16	B cells, Mo	(-), α-IgM, LPS	Negative	Non-treated
17	Mo	(-), LPS	Negative	Non-treated
18	Mo	(-), LPS	Negative	Non-treated
19	PBMC, Mo	(-), PMA/Ion, LPS	Negative	Acidic
20	PBMC, Mo	(-), PMA/Ion, LPS	Limit of detection	Acidic
21	PBMC, Mo	(-), ConA, LPS	Negative	Acidic
22	PBMC, Mo	(-), ConA, LPS	Limit of detection	Acidic
23	PBMC, Bcells, Mo	(-), ConA, LPS	Negative	Acidic
24	CD4, CD8, Bcells, Mo	(-), ConA, PHA, LPS	Negative	Acidic

Table 2: **Summary of results obtained from different GDNF-ELISA.** Supernatants taken from sub-types of immune cells isolated from 24 different Buffy-coats. Samples in triplicates were stimulated for up to 120 hours. After collection, supernatants were stored at -20°C until the assay was performed. As positive control, human recombinant GDNF and supernatant from 3T3-GDNF transfected fibroblasts were used. In a few samples, the amount of GDNF detected was very low, close to the limit of detection (15 pg/ml), those values cannot be taken as positive results.

6.3.2.2. ELISA: GDNF in human sera

Sera from healthy donors (HD), multiple sclerosis patients (MS) and COP-treated (CopT) MS patients were also tested in the GDNF-ELISA.

In most of the samples, 17 out of 22 sera, GDNF was detected at different concentrations, ranging from 15 to 230 pg/ml. Thirteen samples, including the negatives, were treated with HCl (1 N), before GDNF was measured. In all negative samples, GDNF was detected; see Figure 15.

A.

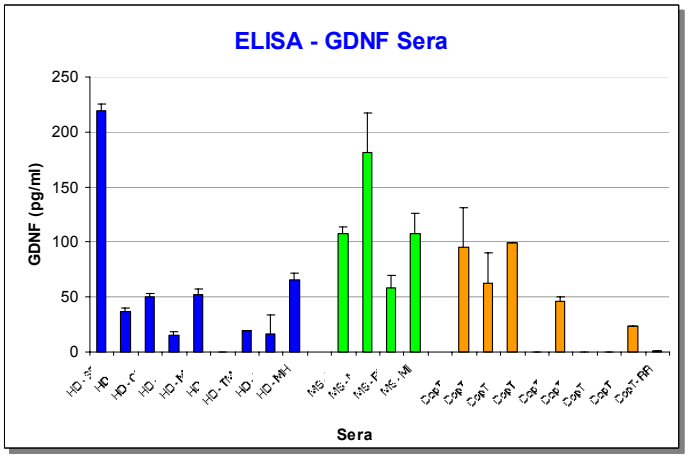

B.

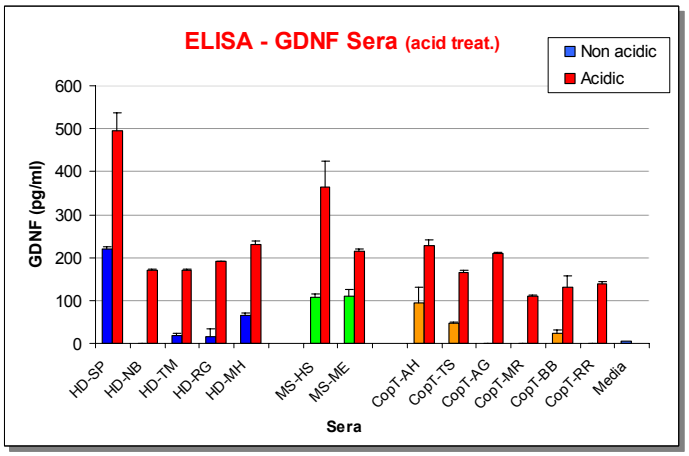

Figure 15: Concentration of GDNF protein (pg/ml) in sera from healthy donors (HD), multiple sclerosis patients (MS) and Cop-treated MS patients (CopT) detected by ELISA. **15-A)** In 4 out of 22 samples, GDNF was undetectable. Each sample was tested in triplicates, with 2 serial dilutions. Each value represents the mean of n=6 wells, + SEM. **15-B)** Some samples shown in Fig. 15-A were treated with 1 N HCl for 15 min (red bars). ELISA was performed afterwards and it was possible to detect GDNF protein in

all samples, even in those, which were negative. The amount of protein detectable in acidic-treated samples (red bars) was always higher than in non-treated ones. Each bar represents the mean of n=6, + SEM on each bar.

6.3.3. Western blot-GDNF

In order to identify GDNF protein in the studied immune cells, Western blot was performed using 2 different antibodies, a monoclonal antibody (Ab) and a biotinylated polyclonal antibody from the rabbit (pAb) against human GDNF.

Immunoprecipitation was also performed using pAb on total cell lysate with Protein G sepharose beads and mAb-anti GDNF was used for detection.

As shown in the following Western blots GDNF was not present in any of the immune cells tested.

6.3.3.1. Western blot: pAb anti-GDNF

pAb was used to perform Western blot using total lysate from human separated immune cells under different conditions. The secondary antibody was a donkey anti-rabbit-HRP. Human recombinant GDNF homodimer was loaded as positive control and has a molecular weight of 30 kDa, which was detected in this blot.

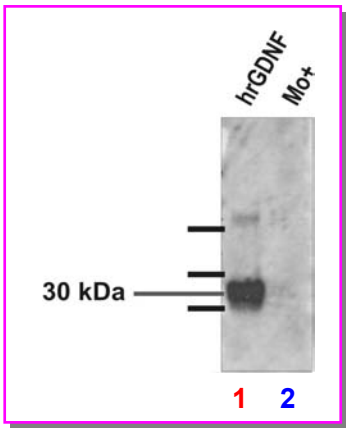

Figure 16: GDNF protein was not present in immune cells by Western blot. Using as primary antibody a biotinylated pAb α-human GDNF and as secondary antibody a donkey anti-rabbit-HRP, the Western blot was performed. Human recombinant GDNF = hrGDNF (10 ng/lane) was used as positive control (lane 1) and LPS-activated monocyte lysate is shown as immune cell (100 µg of protein lysate/lane) (lane 2).

As shown in Figure 16 no GDNF polypeptide was found in 100 µg of monocyte lysate, although 10 ng of hrGDNF gave a very strong signal. Other protein lysates from T and B cells, both un-stimulated and stimulated were tested with pAb as well; however GDNF protein could not be detectable (data not shown).

6.3.3.2. Western blot: mAb anti-GDNF

A monoclonal Ab, mouse against human GDNF, was used in Western blot.
All sub-types of immune cells, both, non-activated and activated for 72 hours, were included in different blots; however, none of the lysates was stained with the mAb.

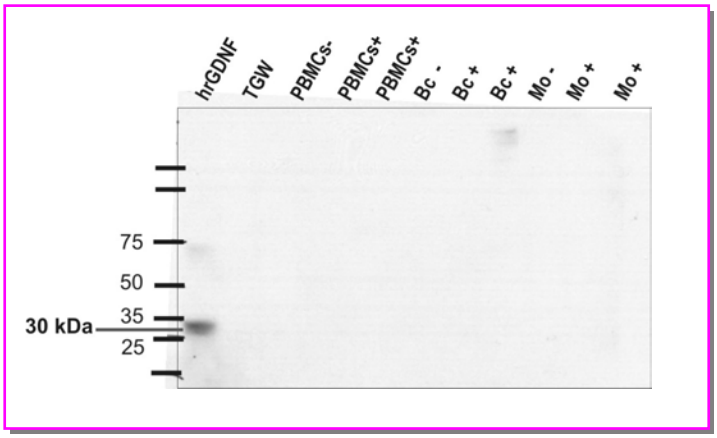

Figure 17: GDNF protein was not found in the immune cells by Western blotting using a mouse anti-human GDNF monoclonal antibody. The amount of protein lysate of each immune cell was ~50 µg/lane. The secondary antibody was a goat anti-mouse-HRP. The reaction was detected with ECL detection kit. As positive control: *hrGDNF* (10 ng/lane) showing a unique band approx. at 30 kDa. *TGW:* neuroblastoma cell line; *PBMCs-:* non-activated peripheral blood mononuclear cells; *PBMCs+:* PHA-activated PBMCs; *Bc -:* resting B cells; *Bc+:* SAC-activated B cells; *Mo–:* non-activated monocytes; *Mo+:* LPS-activated monocytes.

Also immunoprecipitation did not provide evidence that GDNF is expressed or can be induced in lymphocytes and monocytes (data not shown). These experiments performed in order to immunodetect GDNF protein (either by GDNF – ELISA or by Western blotting) were in agreement with the RT-PCR experiments, in which GDNF was not expressed at mRNA level in any human immune cells studied. Immunofluorescence and FACS analysis (intracellular staining) were also performed using mAb and pAb; however, the results were always negative for immune cells (data not shown).

6.4. NEURTURIN EXPRESSION

In contrast to the findings obtained for GDNF, the ligand Neurturin (NTN) was detected in both resting and activated human peripheral blood mononuclear cells as shown below.
At the mRNA level, NTN expression was demonstrated using RT-PCR. At the protein level, NTN was detected by Western blot and by immunofluorescence.

6.4.1. RT-PCR: NTN

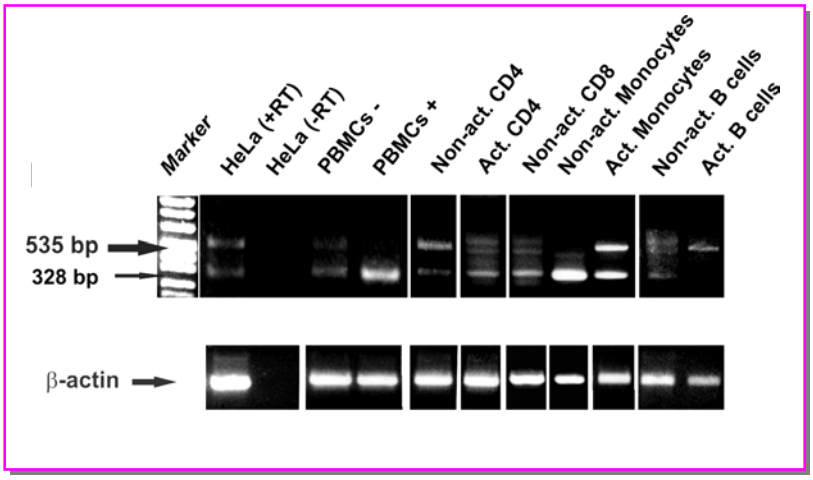

Figure 18: mRNA expression of NTN was studied in all immune sub-sets by RT-PCR. Cells were stimulated for 24 hrs. PCR was performed with the NTN primer pair binding to sequences encoded by exon 1 and exon 2. The large product could correspond to the full length mRNA (535 bp), the short fragment is 330 bp. As positive control: *HeLa cell line*. Next lanes: *PBMCs-:* non-activated peripheral blood mononuclear cells; *PBMCs+:* ConA-activated PBMCs; *CD4-:* non-activated $CD4^+$-T cells; *CD4+:* PHA-activated $CD4^+$-T cells; *CD8-:* non-activated $CD8^+$-T cells; *CD8+:* PHA-activated $CD8^+$-T cells; *Bc-:* resting B cells; *Bc+:* SAC-activated B cells; *Mo–:* non-activated monocytes; *Mo+:* LPS-activated monocytes. To control the cDNA quality a PCR for β-actin mRNA was also performed.

In the reactions two different PCR fragments were obtained using primers spanning exons 1 and 2. The large product corresponds to the full length mRNA (535 bp), the short one (330 bp) could be a new splice variant, in which 207 bp were lacking. No alternative splicing has been described for the human NTN gene; therefore the shorter fragment was sequenced. The 207 bp missing in the smaller PCR product (exactly 328 bp) corresponded

to a region consisting of 80 % GC and cannot be explained by alternative splicing. For this reason, the possibility that this amplification would be an artifact was tested changing diverse conditions to the PCR reaction to allow faithful amplification of GC-rich templates.

The addition of DMSO (5% final concentration) to the PCR master mix resulted only in the fragment of 535 bp. As the second band at 328 bp was not detected anymore, the 328-bp product must be an artifact.

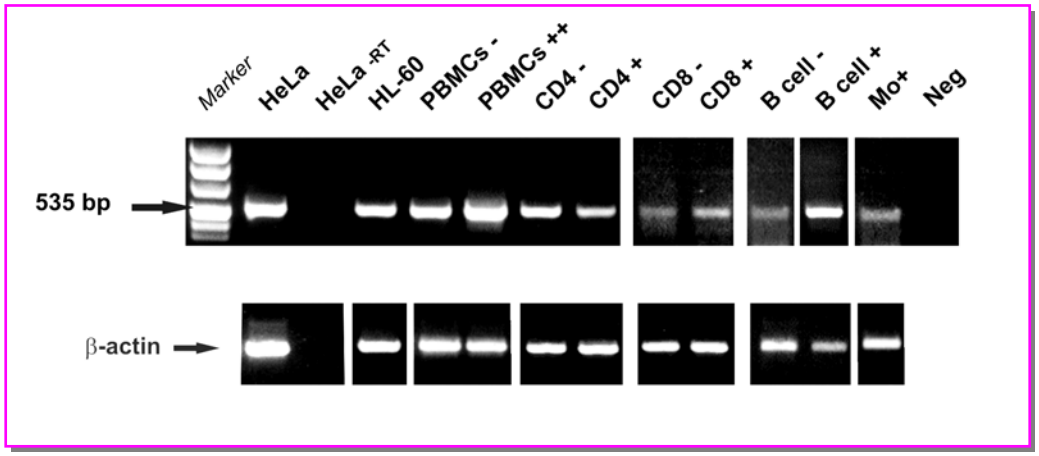

Figure 19: mRNA expression of NTN in immune cells after addition of DMSO to the PCR reaction. See legend to Figure 18. *HeLa* and *HL-60:* as positive controls. *PBMCs++:* LPS+IFN-γ activated PBMC. The PCR contained 5% DMSO.

PCR products from non-activated $CD4^+$-T lymphocytes and from LPS+IFN-γ-activated-PBMCs (PBMCs++) were sequenced and they showed 100% homology to the human NTN mRNA.

Resting and activated lymphocytes (all subpopulations) and monocytes express NTN mRNA.

6.4.2. Western blotting - NTN

Western blot analyses using a polyclonal antibody against human NTN was used to immuno-detect NTN in the various human immune cells.

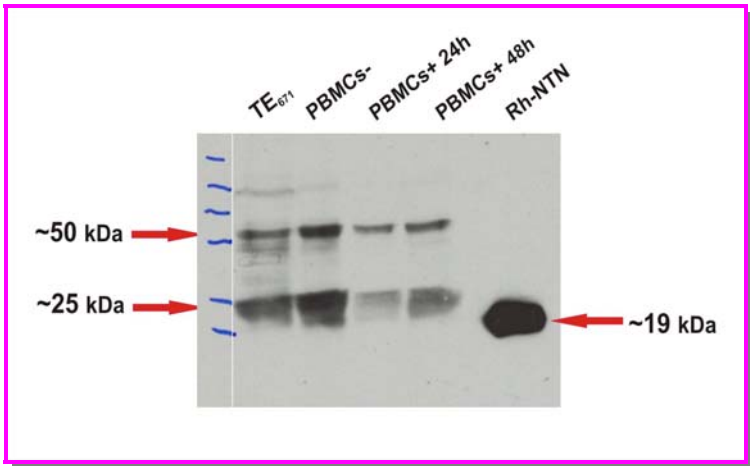

Figure 20: Detection of NTN in immune cells by Western blot. Protein was detected in 50 µg lysate of non-activated and PHA-activated PBMCs after 24 and 48 hour of activation. The positive control was 1 µg/lane human recombinant NTN (hr-NTN) ~ 19 kDa, which is not glycosylated. A band around 25 kDa is shown, corresponding to a monomer of NTN. The second band of 50 kDa size could correspond to dimers. The gel was run under non-reducing conditions. First Ab, a goat anti-human NTN polyclonal antibody (Sta. Cruz Biotechnology®) was used; the secondary Ab was a donkey anti-goat-biotin, and then a STP-HRP (Jackson Immunoresearch®) The enzymatic reaction of HRP was developed using ECL kit. *TE_{671}:* rabdomyosarcoma cell line. *PBMCs-:* non-activated peripheral blood mononuclear cells. *PBMCs+ 24 h:* PHA-activated PBMCs during 24 hours. *PBMCs+ 48 h:* PHA-activated PBMCs during 48 hours. The molecular marker was unstained and is drawn.

In the cell analyzed two proteins of about 25 kDa and 50 kDa were detected. Differences in the band sizes are due to the fact that NTN is secreted as a glycosylated dimer (around 50 kDa), for that reason the molecular weight of the monomer is higher than the recombinant protein, which is a non-glycosylated.

6.4.3. Immunofluorescence - NTN

Neurturin protein was also demonstrated by immunofluorescence staining intracellular NTN in human immune cells.

The following fluorescence micrographs show the positive control cell line (HeLa cells, see also Figure 19) and non-activated and activated PBMCs using diverse activators.

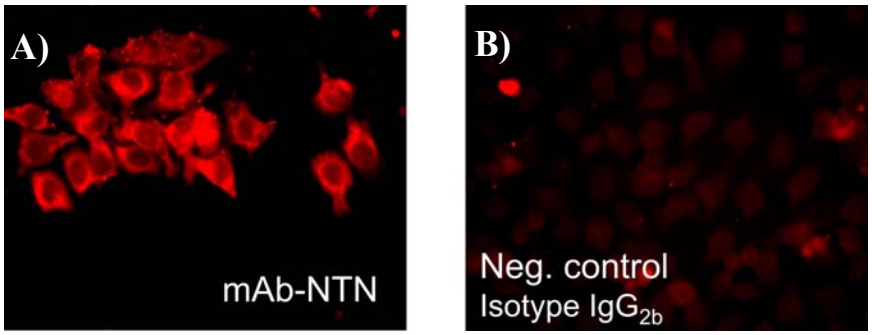

Figure 21: Neurturin is present in the cytoplasm of HeLa cells. Permeabilized HeLa cells were stained with the first Ab mouse anti-human NTN (mouse IgG_{2b}) in **A)**, or with the isotype control mouse IgG_{2b} in **B)** and the secondary Ab goat anti mouse IgG-Cy3 labeled. Cells were grown in slide-chambers until they were 80% confluent, then fixed with paraformaldehyde and incubated O.N. with primary Abs. Magnification 40x.

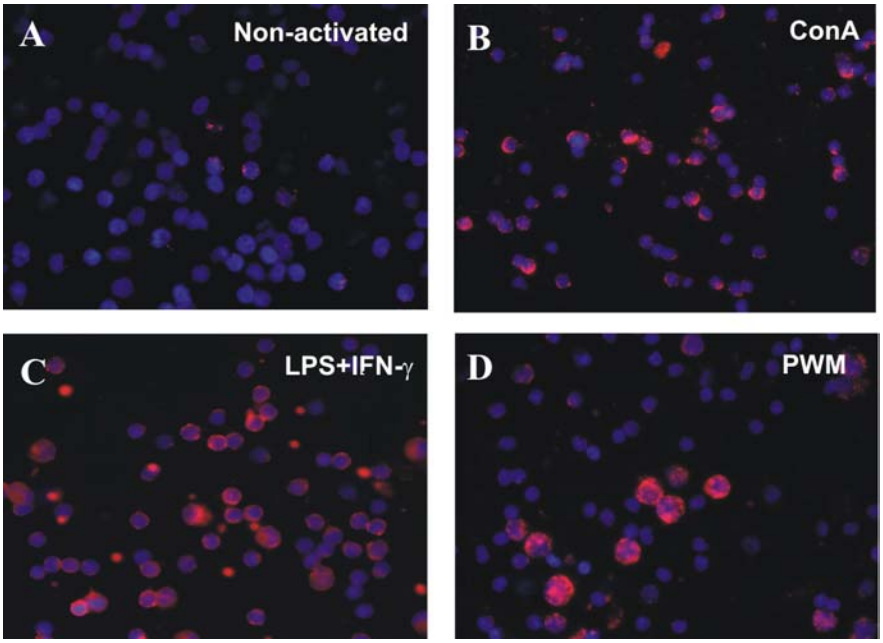

Figure 22: NTN is present in PBMCs. Non-activated and activated PBMCs were fixed and the same Abs were used to stain intracellular NTN as described above. **A)** Few non-activated PBMCs stained weakly for NTN, showing lower amounts inside their cytoplasm (red cells). **B)** 72 hrs ConA-activated PBMCs (T cell

activation) showed that most of the cells were positively stained. **C)** In LPS+IFN-γ-activated PBMCs most of the cells stained for NTN, some cells showed a higher amount of NTN. **D)** PWM-activated PBMCs showed fewer cells but strongly positive in comparison with the others. Nuclei are shown in blue after DAPI staining.

In non-stimulated PBMCs only few mononuclear cells stained positive for cytoplasmic NTN. All activations significantly increased the NTN-staining. Stimulation with ConA (mainly T cells) and LPS+IFN-γ (mostly monocytes and less lymphocytes) induced similar numbers of NTN^+ cells, whereas PWM (B cells) stimulated fewer cells which very strongly NTN positive.

To define clearly the NTN positive cells after the various stimuli, non-activated and activated PBMCs were stained for intracellular NTN, and additionally, double stained with a second directly labeled mAb to mark CD surface molecules, which are specific for each immune cell type. Thus, cells expressing NTN can be phenotypically characterized due to the present CD molecules. Examples are shown in the next pictures (Figure 24, 26 and 27).

To be sure that no cross-reactivity with a second labeled mouse anti-CD antibody could occur a control staining was performed with IgG_{2a}-FITC. As shown in the next figure (Figure 23) no cross-reactivity between the consecutively applied mice mAbs was found (anti-NTN and anti CDs antibodies).

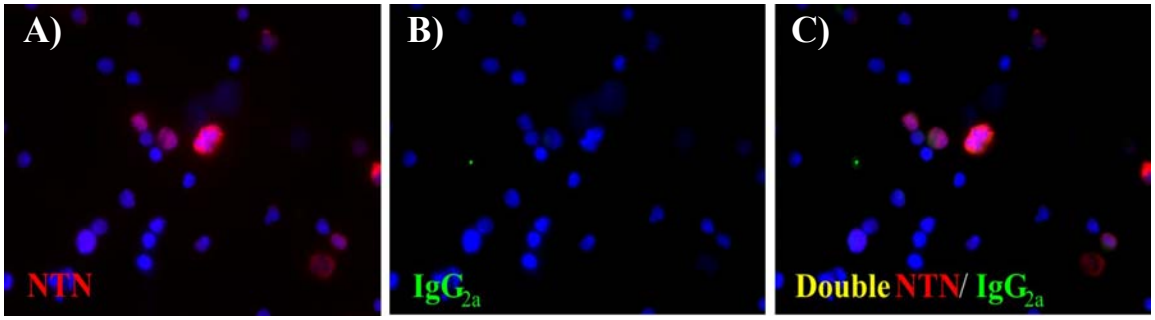

Figure 23: Cross-reactivity was not observed in this double immunostaining control. ConA-activated PBMCs were intracellularly stained with mAb against NTN (A) or IgG_{2a} (B) + gαm-Cy3. After this step the slides were incubated one hour with mouse serum (1:100), and then IgG_{2a}-FITC was added. **A)** Cy3 staining. **B)** FITC staining. **C)** Cy3 + FITC staining. Nuclei are stained in blue with DAPI (40x).

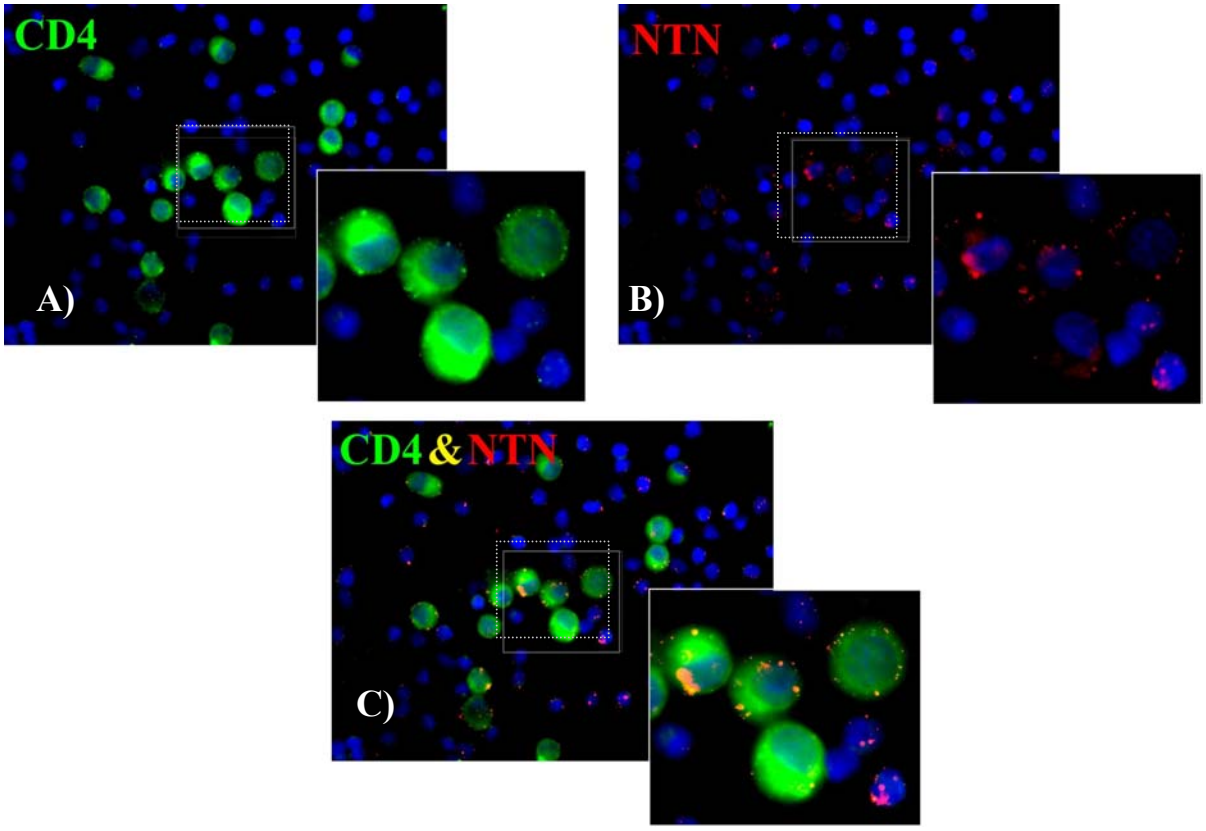

Figure 24: Double staining: CD4/FITC ($CD4^+$-T lymphocytes) and NTN/Cy3 in non-activated PBMCs. Non-activated PBMCs were double stained with mAb against NTN, indirectly labeled with goat α-mouse-Cy3 (intracellular staining), and then with a mouse anti-human α-CD4-FITC. Pictures were taken for both fluorescences (**A** and **B**) and then an overlaid in **C)**, in order to detect whether double stained cells were present. Nuclei are stained in blue with DAPI. Magnification of big micrographs was 40x. Small pictures: 100x.

Many non-activated PBMCs were $CD4^+$ T cells as shown by their surface green staining. But only few PBMCs stained weakly for NTN (Figure 24). Pictures overlaid showed that some resting PBMCs expressed both molecules: NTN and CD4. NTN seems to be accumulated in small patches (spots), as it was seen previously in Figure 22.

Another example of NTN expression in $CD8^+$ T cells of LPS+IFN-γ-activated PBMCs is given in Figure 25. Few $CD8^+$-T lymphocytes were stained double positive for intracellular

Neurturin and for surface CD8 molecule. The majority of the activated $CD8^+$ T cells are NTN negative.

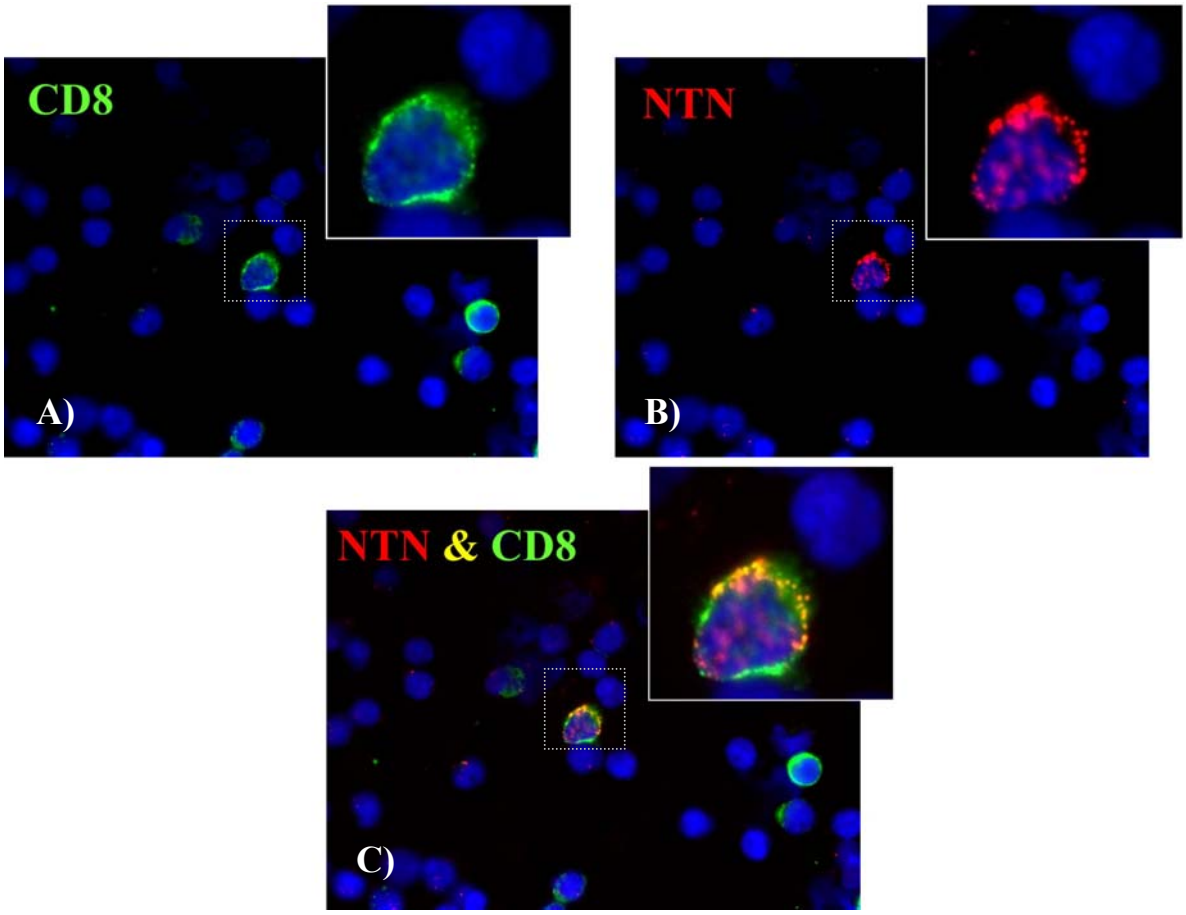

Figure 25: Double staining: CD8/FITC ($CD8^+$-T lymphocytes) and NTN/Cy3 in LPS-IFN-γ-activated PBMCs. **A)** Photograph taken to see only green fluorescence, meaning CD8/FITC positive cells. Some cells were positively stained for $CD8^+$-T cells on this preparation (LPS+IFN-γ-activated PBMCs). **B)** Picture showing cells intracellularly stained with mAb anti-NTN (red colored cells). Fewer cells were NTN positive in this part of the slide. **C)** This picture shows the overlaid images from A) and B). Nuclei are stained in blue with DAPI.

Similarly monocytes and B lymphocytes were tested by intracellular staining for NTN expression. Both unstimulated monocytes and B cells express NTN protein in the cytoplasm in some cells (Figure 26 and Figure 27).

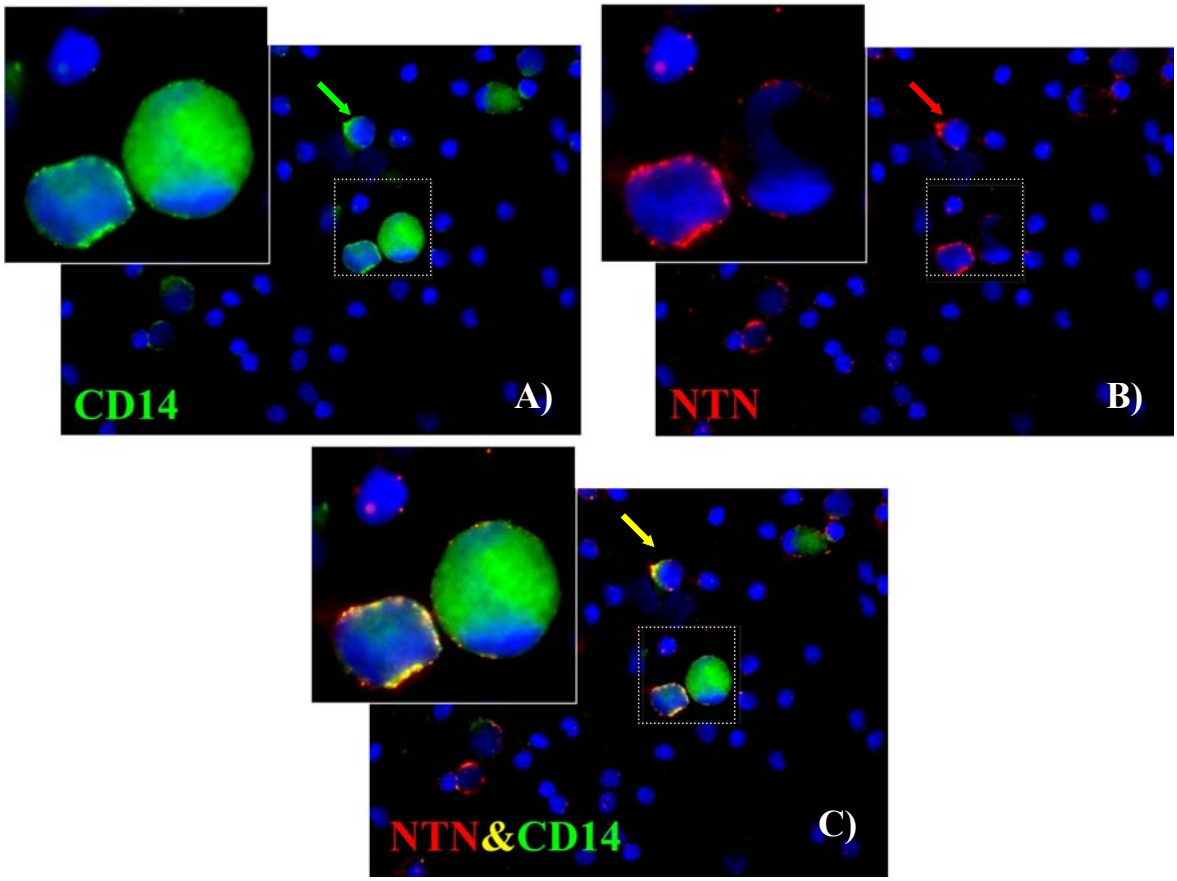

Figure 26: Double staining: CD14/FITC (monocytes) and NTN/Cy3 in non-activated PBMCs. Non-activated PBMCs were double stained as indicated. **A)** Cells stained with α-CD14-FITC Ab are monocytes (green cells). **B)** Few cells were weakly stained intracellularly with NTN (red cells), probably because they are resting cells. **C)** Overlaid images from A) and B). In the magnification, a representative example of two monocytes, only one expressing NTN is shown. In all pictures, arrows with different colors indicate another NTN^+ monocyte. Nuclei were stained in blue with DAPI.

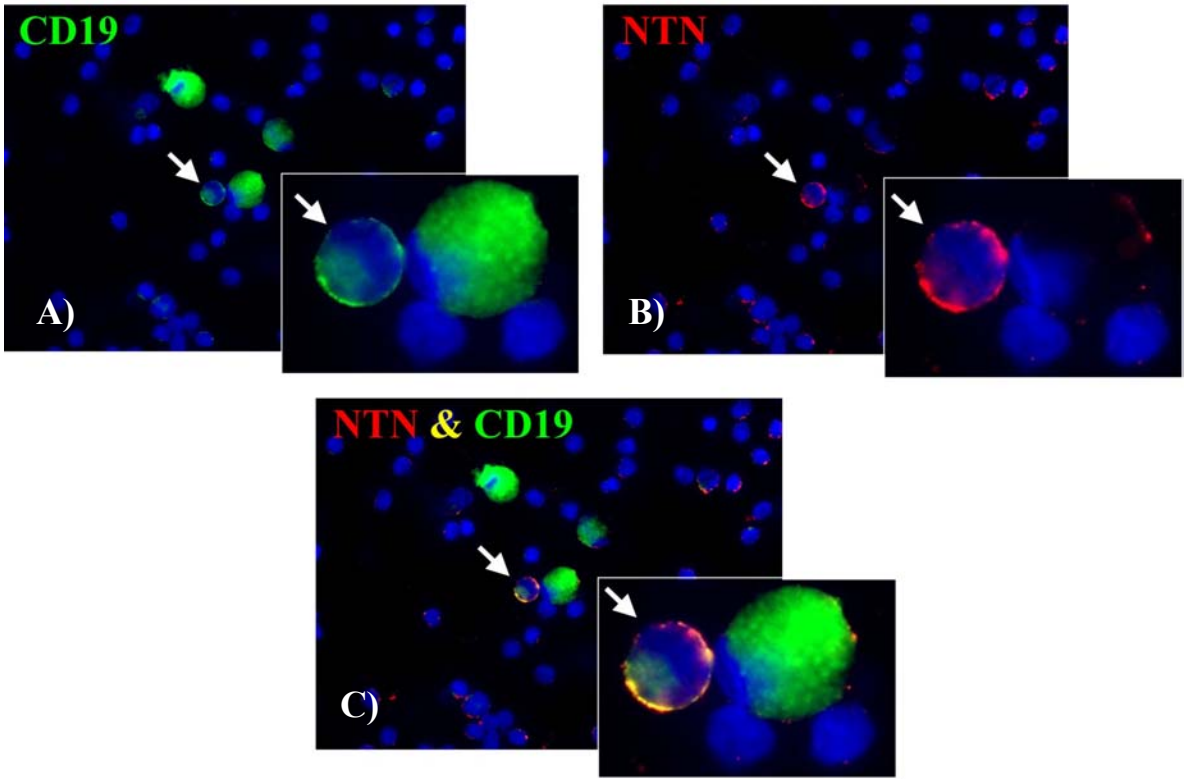

Figure 27: Double staining: CD19/FITC (B cells) and NTN/Cy3 in non-activated PBMCs. A) Resting PBMCs stained with α-CD19-FITC Ab identifying B cells (green cells, in low amounts). **B)** Few cells were stained intracellularly with NTN (red cells). **C)** Overlaid images A) and B) indicated in yellow the B cells expressing NTN. A pair of B cells is enlarged with only one cell expressing NTN. The nuclei are seen in blue (stained with DAPI).

6.5. PERSEPHIN EXPRESSION

6.5.1. RT-PCR: PSP

Similarly, Persephin mRNA was investigated by RT-PCR on the human immune cells. As the PSP gene also contains a rich-GC region, addition of DMSO to the PCR was useful to amplify the right product. Without DMSO a smaller band was amplified (approx. 88 bp) in all reactions. This product was eliminated after DMSO addition. The best results were obtained with 2% DMSO and 60°C of annealing temperature (Figure 28).

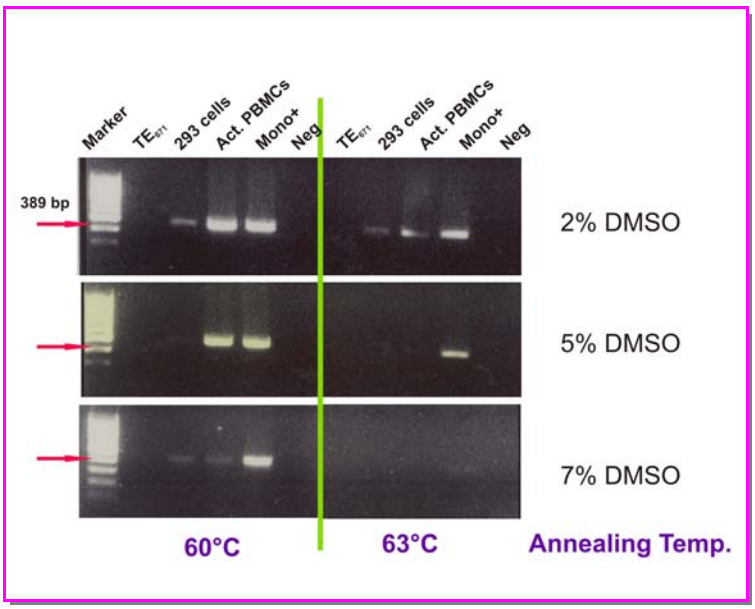

Figure 28: mRNA expression of PSP by human immune cells. Different concentrations of DMSO and two different annealing temperatures were tested in order to find the best amplification condition. These pictures show *TE_{671}:* as negative control. *293 cells:* as positive control (human embryonary kidney cells). *Act. PBMC:* ConA-activated PBMCs. *Mono+:* LPS-activated monocytes. *Neg:* no cDNA.

These preliminary results with the forward primer: exon 1, base pairs 22 - 39 and reverse primer: exon 2, base pairs 384 - 401 demonstrated that PSP mRNA is expressed in ConA-activated PMBCs and monocytes. Another set of primer pair: forward primer: exon 1 (base pairs 28 - 50) and reverse primer: exon 2 (base pairs 304 – 321) was also used for RT-PCR. The signals were not so clear, however, but the subsets of immune cells were also positive (data not shown).

6.6. *RET* EXPRESSION

The expression of the transmembrane receptor RET was assessed at the mRNA level using RT-PCR, and at the protein level performing Western blot using pAbs against the intracellular part of the protein, and with FACS analysis, using a mAb directed to the extracellular domain of RET (extracellular staining).

6.6.1. RT-PCR: *RET*

The *RET* mRNA is large and extensive alternative splicing. The isoforms have been reported for the exons encoding the extracellular portion and the intracellular enzymatic active domain respectively. mRNA expression of the *RET* transmembrane receptor tyrosine kinase was detected in all subsets of immune cells studied. Multiple splice isoforms were expressed, depending on the cell type and activation state. Specific sets of primers were used in this work to detect the alternatively splice variants of the RET gene by RT-PCR. These splice variants are located either at the 5'-end or at the 3'-end region.

6.6.1.1. Multiple splice variants at the 5'-end region of RET gene

An outline of the extracellular domain of the RET protein relative to the exon organization was presented in the introduction (see Figure 3). Most of the splice variants will encode proteins with deletions in the CLD-x, where the binding of ligand and the co-receptor GFRα take place, generating a truncated extracellular ligand-binding domain. The isoforms described in this region were found in fetal human brain and adult kidney (see Lorenzo et al., 1995). Exon 1 codes the initiator codon and 24 aa at the N-terminus, the signal sequence starts in exon 2 (aa 24 – 28).

6.6.1.1.1. RET (ex6) primers

First a primer pair (forward primer: exon 2 and 3 (base pairs 260 - 281) and reverse primer: exon 6 (base pairs 1327 - 1351)) was employed amplifying the full length (FL) RET cDNA (873 bp) and the alternative transcripts 5-RET lacking exon 5 (677 bp) and 3-RET missing exon 3 (585 bp).

The results for all different subpopulations, unstimulated or activated cells, is given in Figure 29 and will be explained individually.

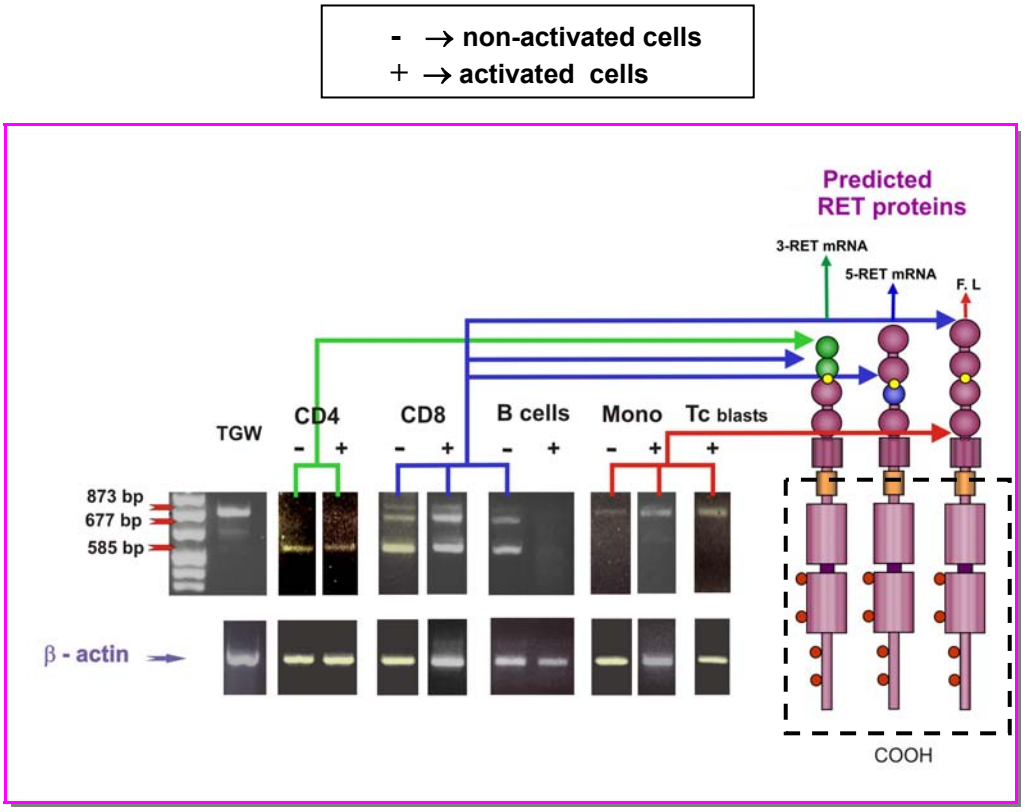

Figure 29: Multiple isoforms at the 5'-end region of *RET* were expressed by immune cells. RT-PCR showing cDNA from different sub-sets of immune cells, which amplified three isoforms of *RET* located at the 5'-end tail. First lane: pUC 8 marker. *TGW (neuroblastoma cell line):* positive control. *CD4-:* non-activated $CD4^+$-T cells. *CD4+:* PHA-activated $CD4^+$-T cells. *CD8-:* non-activated $CD8^+$-T cells. *CD8+:* PHA-activated $CD8^+$-T cells. *B cell-:* resting B cells. *B cell+:* SAC-activated B cells. *Mono-:* non-activated monocytes. *Mono+:* LPS-activated monocytes. *Tc blasts:* ConA-activated T cell blasts. cDNA were tested with β-actin primers as shown. Cell fractions were isolated by immunomagnetic selection and then activated with mitogens; total RNA was extracted using RNAzol method. 1 µg of total RNA was reverse-transcribed in a 20 µl reaction mix containing oligo-dT primers. 2 µl of cDNA were amplified using specific primers for *RET* located in exon2/3 (forward) and exon 6 (reverse). After 38 cycles of amplification, 15 µl of the amplified products were loaded on 1.7% agarose gel stained with ethidium bromide. The RET protein figures located at the right side represent predicted proteins encoded with deletions (small circles) in the extracellular domain, mainly in the cadherin-like domain (CLD). The protein portion encoded by the 3'-half of the transcript that was not analyzed with the primers is marked by the dotted line.

6.6.1.1.2. PCR products amplified in human immune cells:

*** Full length mRNA:** Exon 2 linked to exon 3 (873 base pairs) was detected in RNA of the control cell line TGW, in T cell blasts (ConA-activated T cells), unstimulated and activated $CD8^+$-T cells and monocytes and B $cells^+$, but only a very weak signal was seen

in non-activated B cells. In $CD4^+$-T cells, both non-activated and activated as well as in activated B cells no FL sequence was amplified (data from 3 different PCR reactions).
The PCR fragments from the full-length mRNA of activated PBMCs+ (data not shown) and activated monocytes were verified by sequencing and showed 99% identity to the published *RET* mRNA.
**** 5-RET mRNA:*** exon 5 is spliced out (exon 4 linked to exon 6). A PCR product of 677 bp was obtained for both non-activated and activated $CD8^+$-T cells, and non-activated B cells. This size could correspond to the isoform, which lacks exon 5. The predicted amino acid sequence would have a deletion in the CLD-3 (amino acids 273 to 387). This isoform has not been yet described.
**** 3-RET mRNA:*** exon 3 spliced out (exon 2 linked to exon 4). The third PCR product obtained was a band of 585 bp, corresponding to the isoform in which exon 3 is spliced out. A strong signal was observed in resting T and B cells, but not in monocytes. This variant encodes a protein lacking 68 amino acids in the CLD-1 (aa 28 to 156) and in CLD-2 (aa 166 to 272).
Surprisingly in contrast to stimulated T cells, in activated B cells no 5'-RET mRNA sequences were amplified, probably because exon 6, where the reverse primer was located, could be spliced out, since new isoforms at the 5'-end were published recently, some of them lacking exon 6 (Fluge et al., 2001).

Interestingly, $CD4^+$ and $CD8^+$-T cells expressed different *RET* isoforms, although they have the same origin; both are T lymphocytes. The main difference is that $CD8^+$-T cells expressed the full length, 3-RET mRNA and 5-RET mRNA; whereas $CD4^+$-T cells expressed only the shortest 3-RET mRNA. Experiments were performed at least four times for each cell type and activation (Figure 30).
In T cell blasts (PBMCs activated for 6 days with ConA) only the full length mRNA in this region was amplified. The results demonstrate differential regulation of alternative splicing in T cell subsets but not upon stimulation. In B cells and to a lower degree in monocytes activation influences the *RET* mRNA expression.

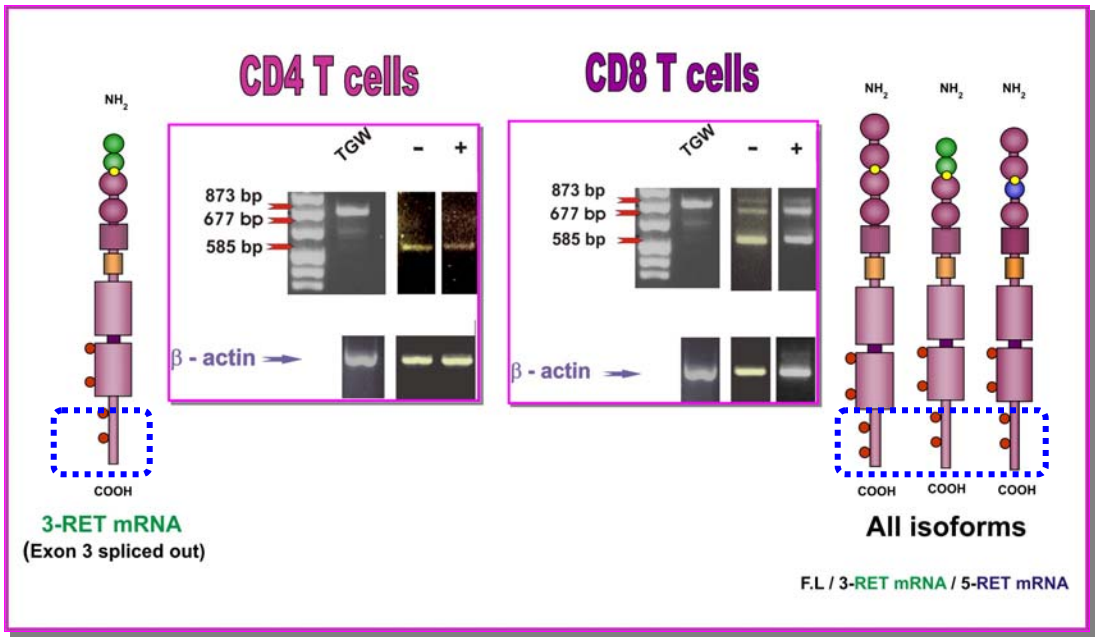

Figure 30: Comparison between the *RET* isoforms expressed by CD4$^+$ and CD8$^+$-T cells analyzing the 5'-end region. For details see Figure 30.

All RT-PCR reactions were performed at least three times with different PBMCs; always the same fragments were amplified. Results obtained by RT-PCR from different human immune cells and the isoforms expressed at the 5'-end region of *RET* mRNA are summarized in the following table:

ISOFORMS at 5' –end region of c-RET gene	CD4 -	CD4 +	CD8 -	CD8 +	T cell blasts	B cells -	B cells +	Monocytes-	Monocytes+
Full Length 873 bp	-	-	+	+	+	-	-	+	+
Exon 5 spliced out 677 bp	-	-	+	+	-	+	-	-	-
Exon 3 spliced out 585 bp	+	+	+	+	-	+	-	-	-

Table 3: Alternative spliced *RET* transcripts varying at the 5'-end expressed in different subtypes of human immune cells. + : c-RET mRNA expression. - : mRNA not detected. **CD4-**: resting CD4$^+$-T cells. **CD4+**: PHA-activated CD4$^+$-T cells. **CD8-**: resting CD8$^+$-T cells. **CD8+**: PHA-CD8$^+$-T cells. **T cell blasts**: ConA-activated PBMCs after 6 days in culture. **B cells-**: resting B cells. **B cells+**: SAC-activated B cells. **Monocytes-**: non-activated monocytes. **Monocytes+**: LPS-activated monocytes.

In summary:

- Resting and activated $CD4^+$-T cells expressed only the 3-RET mRNA isoform.
- Resting and activated $CD8^+$-T cells expressed the full length, the 3-RET mRNA and the 5-RET mRNA isoforms.
- Activated T cell blasts expressed only the full length RNA.
- Resting B cells expressed 3-RET mRNA and 5-RET mRNA isoforms, but not the full length mRNA. Activated B cells do not express RET mRNA in this region.
- Resting and activated monocytes express only the full length.

Additional possible alternatively spliced transcripts lacking more that 1 exon sequence were not observed: 3,4-RET mRNA and 3,4,5-RET mRNA were not detected in any of the immune cells studied. However, one splicing variant, which has not been described, was found. This PCR product of 677 base pairs of size could correspond to the skipping of exon 5. This novel splice variant was only detected in $CD8^+$-T cells and in resting B cells.

6.6.1.2. Multiple splice variants located at the 3'-end region of the RET gene

The 3'-end region codes for the intracellular domain of the RET protein. At least three spliced isoforms differing in the presence of intron 19 or the absence of exon 20 were described in human tissues: RET-9 or short isoform, RET-51 or long isoform and RET-43 or middle isoform (see Introduction, Figure 5). The encoded polypeptides differ in the length and in the sequence of the carboxyterminus.

Short isoform (RET-9) is generated when intron 19 is not removed. The ORF of exon 19 continues with nine further codons, which lie within intron 19.

Long isoform (RET-51) is expressed when exon 19 is spliced to exon 20, which encodes 51 amino acids at the carboxyl terminus in the protein.

Middle isoform (RET-43) occurs when exon 19 is spliced to exon 21. In this transcript, exon 21 codes for unique 43 amino acids.

6.6.1.2.1. RET-B primers

All 3'-end variants can be detected using a primer pair RET-B: forward primer: exon 16 (base pairs: 2701 - 2722) and reverse primer: exon 19 (base pairs: 3072 - 3102) with a PCR product of 402 bp (Figure 31).

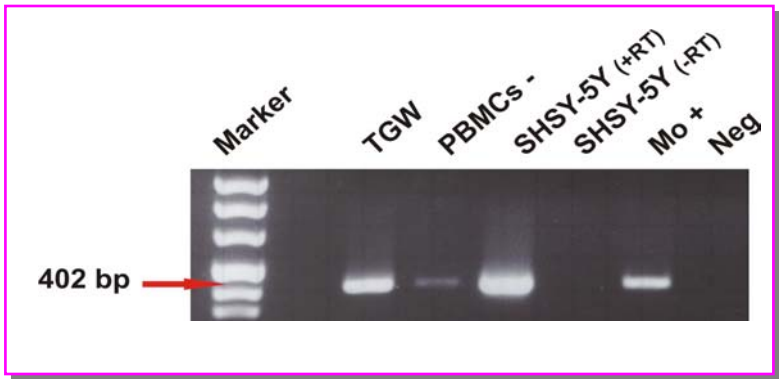

Figure 31: Expression of 3´-end *RET* with primers RET-B. *Marker:* pCU8; *TGW:* neuroblastoma cell line; *PBMCs-:* non-activated PBMCs; *SHSY-5Y (+RT):* neuroblastoma cell line (in the presence of reverse transcriptase); *SHSY-5Y (-RT):* neuroblastoma cell line (in the absence of reverse transcriptase); *Mo+:* LPS-activated monocytes; *Neg:* no DNA control.

A weak fragment of the expected size was detected in non-activated PBMCs; a stronger one in LPS-stimulated monocytes. Both PCR products from PBMCs and monocytes were sequenced and showed 99% identities to the human *RET* mRNA.

6.6.1.2.2. RET-9-b primers

Primers used to amplify specifically the **short isoform of *RET* (RET–9)** were: forward primer: exon 19 (base pairs: 2996 - 3017) and reverse primer: intron 19 (base pairs: 3326 - 3337) resulting in a PCR product of 446 bp.

These primers are specific for *RET*-cDNA with intron 19, because the reverse primer is located at the 5'-end of intron 19, which is not translated in any other isoform of *RET*.

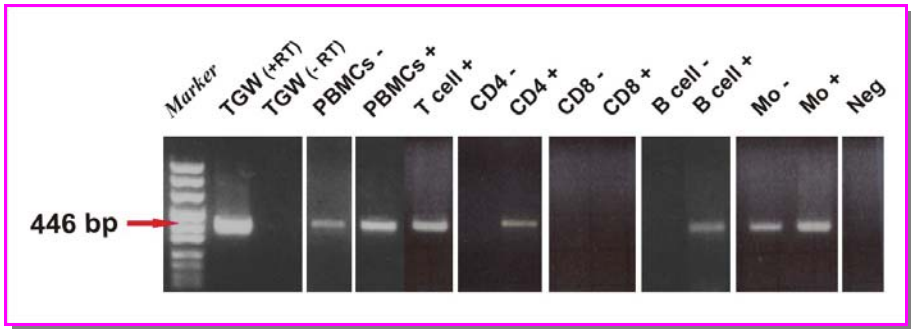

Figure 32: Several subtypes of immune cells expressed the short isoform of c-RET (RET-9), which encodes the short RET protein containing 9 unrelated amino acids at the C-terminus. *PBMCs-:* non-activated PBMCs; *Marker: pCU8; TGW (+RT):* as positive control, cDNA containing reverse transcriptase; *TGW (-RT):* cDNA without reverse transcriptase. *PBMCs-:* non-activated PBMCs; *PBMCs+:* LPS+IFN-γ-activated

PBMCs; *T cell+:* ConA-activated T cells blasts. *CD4 -:* resting $CD4^+$-T cells; *CD4 +:* PHA-activated $CD4^+$-T cells; *CD8 -:* resting $CD8^+$-T cells; *CD8 +:* PMA/Ion-activated $CD8^+$-T cells; *B cell -:* non-activated B cells; *B cell +:* SAC-activated B cells; *Mo-:* non-activated monocytes; *Mo+:* LPS-activated monocytes; *Neg:* no cDNA. β-actin transcripts for each cDNA were not included in this figure because they are shown in Figure 36, Figure 38, Figure 40, Figure 42, and Figure 44, in which RT-PCR results were separated depending on the cell type analyzed.

PCR products (446 bp) from activated PBMCs and TGW were sequenced and showed 100% identities to the *RET* mRNA short isoform.

Differential expression of RET-9 was observed in the subsets of immune cells analyzed. $CD8^+$-T cells did not have the short isoform. Otherwise, all activated cells expressed RET-9 (PBMCs+, B cell+, Mo+, T cell+). A RT-PCR product for the short isoform was also obtained with RNA of non-stimulated PBMCs and monocytes.

6.6.1.2.3. RET-51-b primers

The **long isoform of *RET* (RET–51)** was amplified using these pair of primers: forward primer: exon 19 (base pairs: 2996 - 3017) and reverse primer: exon 20 (base pairs: 4762 - 4779) resulting in a PCR product of 430 bp.

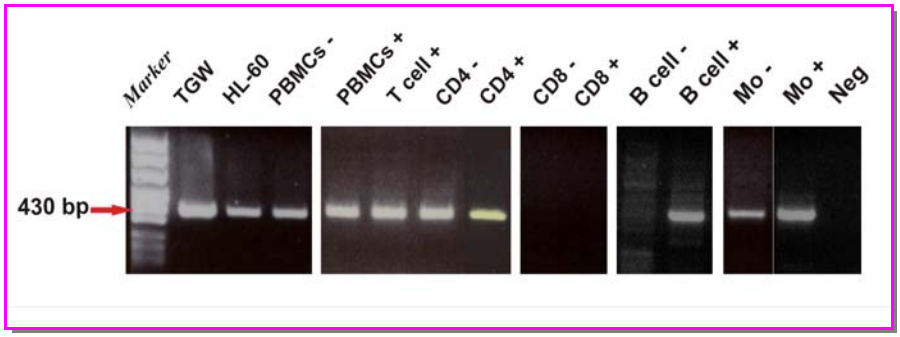

Figure 33: mRNA expression of the long isoform of *RET* (RET-51). *PBMCs-:* non-activated PBMCs; *PBMCs+:* LPS+IFN-γ-activated PBMCs; *T cell+:* ConA-activated T cells blasts. *CD4 -:* resting $CD4^+$-T cells; *CD4 +:* PHA-activated $CD4^+$-T cells; *CD8 -:* resting $CD8^+$-T cells; *CD8 +:* PHA-activated $CD8^+$-T cells; *B cell -:* non-activated B cells; *B cell +:* SAC-activated B cells; *Mo-:* non-activated monocytes; *Mo+:* LPS-activated monocytes; *Neg:* no cDNA. β-actin transcripts for each cDNA were not included in this figure because they are shown in Figure 36, Figure 38, Figure 40, Figure 42, and Figure 44, in which RT-PCR results were separated depending on the cell type analyzed.

PCR products of 430 bp obtained from the cDNA of activated PBMCs and activated monocytes were sequenced and showed 99% identity to the published *RET* sequence, corresponding to the RET-51 (long isoform).

Again, no cDNA fragment was isolated of unstimulated and activated $CD8^+$-T cells. Also resting B cells did not express the long isoform of *RET*. All the other sub-types of immune cells expressed the long isoform even without activation.

6.6.1.2.4. RET-43 primers

The **middle isoform of *RET* (RET-43)** is generated when exon 19 is spliced directly to exon 21, skipping exon 20 and was detected with the forward primer: exon 19 (base pairs: 2996 - 3017) and reverse primer: exon 21 (base pairs: 6256 - 6285) as PCR product of 354 bp.

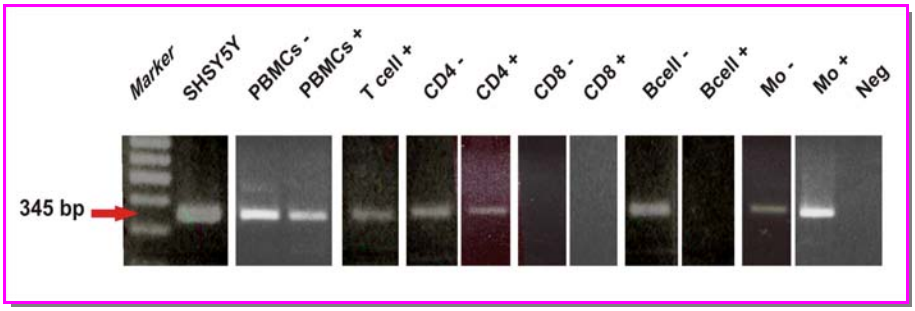

Figure 34: mRNA expression of the middle isoform RET-43 by RT-PCR in immune cells. PCR product of 354 bp was amplified from subsets of immune cells. *PBMCs-:* non-activated PBMCs; *PBMCs+:* LPS+IFN-γ-activated PBMCs; *T cell+:* ConA-activated T cells blasts. *CD4 -:* resting $CD4^+$-T cells; *CD4 +:* PHA-activated $CD4^+$-T cells; *CD8 -:* resting $CD8^+$-T cells; *CD8 +:* PHA-activated $CD8^+$-T cells; *B cell -:* non-activated B cells; *B cell +:* SAC-activated B cells; *Mo-:* non-activated monocytes; *Mo+:* LPS-activated monocytes; *Neg:* no cDNA control.

PCR products from non-activated PBMCs and activated monocytes were sequenced and showed 100% identity to the published *RET* sequence, corresponding to the RET-43 isoform (middle isoform).

Yet another picture was observed for the expression of the middle isoform in the immune cells. Again $CD8^+$-T cells were negative. In activated B cells this transcript was lost. All other cell types expressed this isoform.

Next table summarizes the results obtained by *RET*-RT-PCR at the 3'-end region of *RET* mRNA from different subsets of immune cells and the isoforms:

ISOFORMS at 3' –end region of c-RET gene	CD4 -	CD4 +	CD8 -	CD8 +	T cell blasts	B cells -	B cells +	Monocytes-	Monocytes+
RET – 9 SHORT ISOFORM	-	+	-	-	+	-	+	+	+
RET – 51 LONG ISOFORM	+	+	-	-	+	-	+	+	+
RET – 43 Exon 20 spliced out	+	+	-	-	+	+	-	+	+

Table 4: Spliced isoforms at the 3'-end of RET gene expressed in human immune cells. Results and PCR pictures were compiled from different PCR reactions, in which cDNAs from several donors were analyzed. + : *RET* mRNA expression. - : mRNA non-detected. **CD4-**: resting $CD4^+$-T cells. **CD4+**: PHA-activated $CD4^+$-T cells. **CD8-**: resting $CD8^+$-T cells. **CD8+**: PHA-activated $CD8^+$-T cells. **T cell blasts**: ConA activated PBMCs after 6 days in culture. **B cells-**: resting B cells. **B cells+**: SAC-activated B cells. **Monocytes-**: non-activated monocytes. **Monocytes+**: LPS-activated monocytes.

In summary:

- Resting $CD4^+$-T cells expressed RET-51 and RET-43 but not the short isoform RET-9. Activated $CD4^+$-T cells expressed all isoforms.
- Resting and activated $CD8^+$-T cells did not express any of these isoforms. Nevertheless, these cells expressed the isoforms located at the 5'-end.
- Activated T cell blasts expressed the three isoforms.
- Resting B cells expressed RET-43, but neither RET-9 nor RET-51. Activated B cells expressed both, RET-9 and RET-51 isoforms, but not the middle isoform RET-43.
- Resting and activated monocytes expressed the three isoforms.

As described above, RT-PCR reactions were performed using different set of primers (described in *Materials and Methods*) to detect all the spliced isoforms expressed from *RET*. To understand better the expression pattern of the *RET* isoforms at both, the 5'-end and 3'-end regions of the gene, a summary and schematic description for each cell type is presented below:

CD4$^+$-T CELLS:

At the 5'-end region of the RET gene coding for the extracellular domain of the mature RET protein only one isoform was detected, 3-RET lacking exon 3. No difference was observed in CD4$^+$ T cells activated with PHA (see Figure 29). The derived mature protein will have a truncated CLD-1 and CLD-2 domain. This deletion might interfere with the ligand binding properties of the RET receptor.

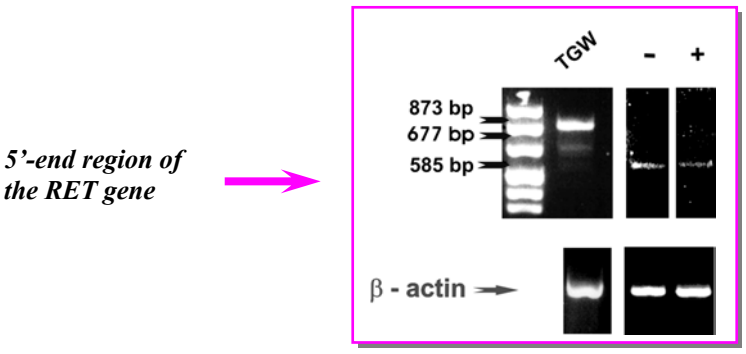

Figure 35: Both, non-activated and activated CD4$^+$-T cells expressed only one isoform of *RET* located at the 5'-end region of the gene. A product of 585 bp specific for a transcript lacking exon 3 is shown in both lanes. TGW: as positive control. (-) represents non-activated CD4$^+$-T cells; (+) represents PHA-activated CD4$^+$-T cells. PCR for β-actin as housekeeping gene using 28 cycles of amplification was always performed in all samples to test the cDNA quality.

Alternative transcripts were detected in CD4$^+$-T cells at the 3'-end region of the RET gene encoding the intracellular domain of the mature RET protein. The long and the middle isoform were synthesized in both non-activated and PHA-activated T lymphocytes, whereas the short transcript RET-9 is not present in non-stimulated CD4$^+$-T cells, but is induced by PHA stimulation.

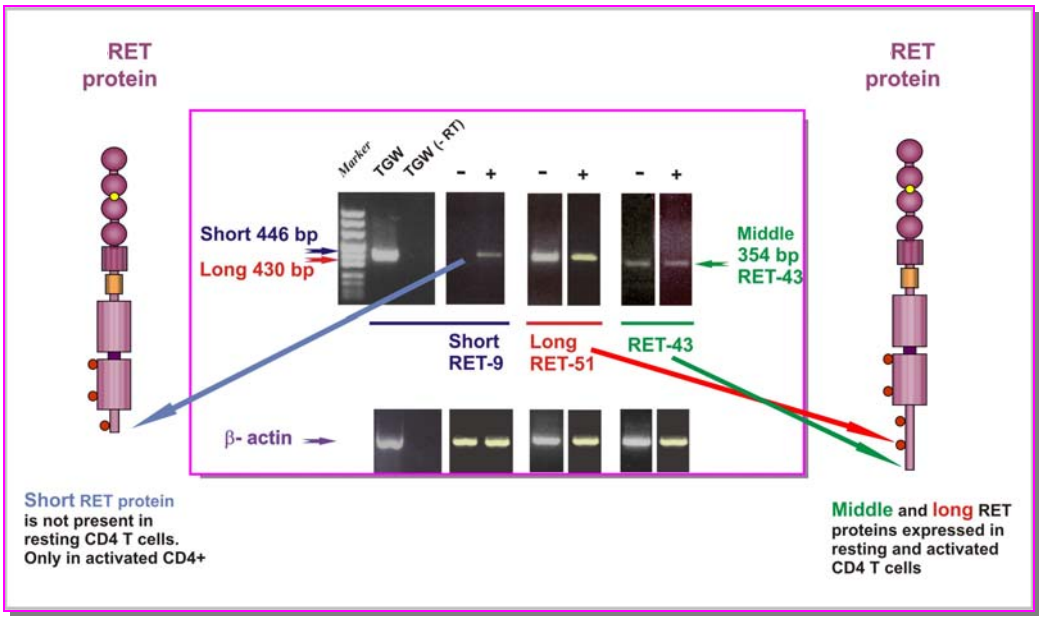

Figure 36: Summary of the splice isoforms of *RET* located at the 3'-end region of non-activated and activated CD4$^+$-T cells. Non-activated (-) and activated (+) CD4$^+$-T cells; cell line TGW as control. The quality of the cDNA was assessed by amplification of a β-actin cDNA fragment (below). The translated RET protein variants are shown on both sides. They differ in the carboxyl terminal sequence and the fourth tyrosine residue, which is only present in the middle and long RET proteins.

Upon PHA stimulation of CD4$^+$-T lymphocytes alternative splicing results in a *RET*-transcript encoding a carboxyl-terminal shortened RET receptor.

CD8$^+$-T CELLS

In contrast to CD4$^+$-T cells, all alternatively spliced transcripts at the 5'-end region of the RET gene were detected in CD8$^+$-T cells.

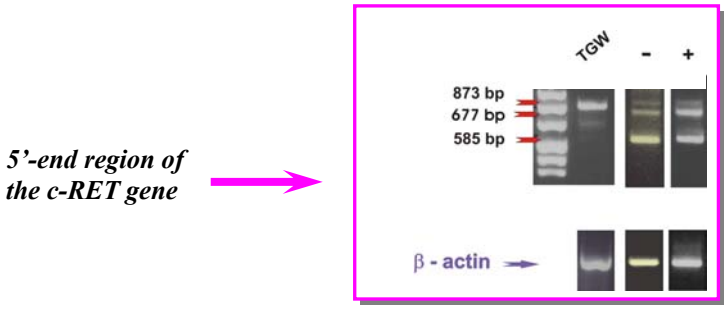

Figure 37: Both, non-activated and activated CD8$^+$-T cells expressed all isoforms of *RET* at the 5'-end. The full length of 873 bp, the product of 677 bp (5-RET mRNA) when exon 5 is spliced out and a product of

585 bp due to the absence of exon 3 (3-RET mRNA). TGW (human neuroblastoma cell line) is shown as positive control. (+): PHA-activation. β-actin for all cDNA was amplified and is shown below.

$CD8^+$-T lymphocytes (activated and non-activated cells) expressed the full length mRNA located at the 5'-end region of the gene, as well as the 3-RET mRNA and the 5-RET mRNA isoforms. The weakest signal in $CD8^+$-T cells was detected at 873 bp corresponding to the full length. It seems that the 5-end mRNA lacking exon 3 is the strongest expressed isoform in $CD8^+$-T lymphocytes, although the differences might also be explained by preferential amplification of the shortest fragment. No differences were seen after lymphocyte activation with PHA or PMA+Ionomycin (Data not shown).

Primers amplifying 3'-end cDNA fragments gave no results for $CD8^+$-T lymphocytes even after PHA activation. Surprisingly, although *RET*-transcripts were detected using primers for the 5'-end region of the gene and the cDNA quality was tested with β-actin primers, the RT-PCR for the 3'-end were negative. Presumably, *RET* mRNA expressed in resting or activated $CD8^+$-T cells lack either exon 19 or/and 20, 21. A simple explanation would be a premature termination of the *RET* transcript in $CD8^+$-T cells.

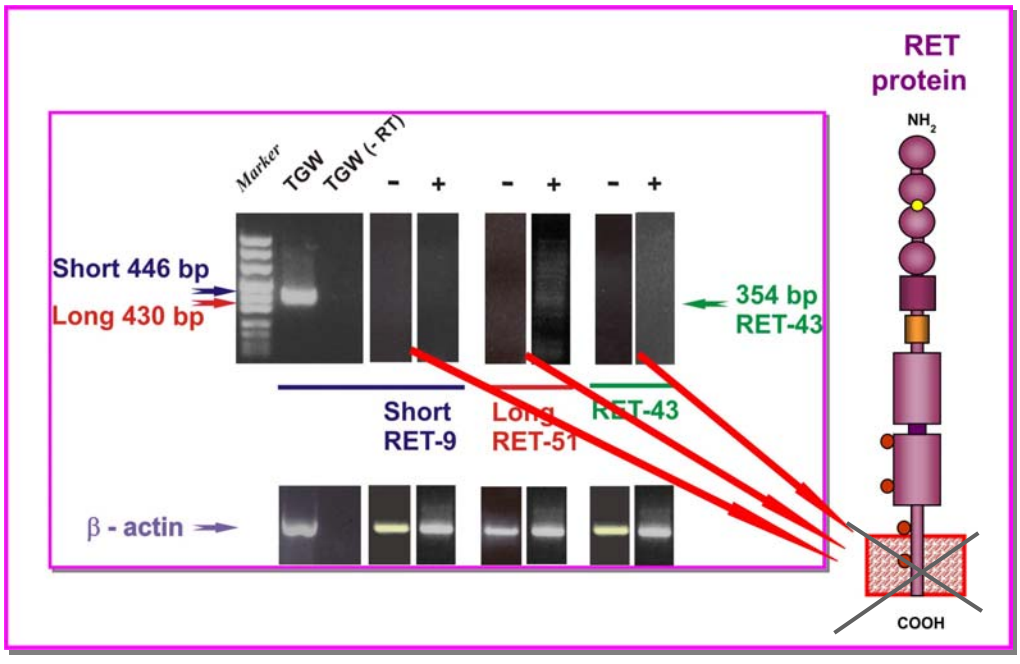

Figure 38: $CD8^+$-T cells did not express any of the three splice isoforms of *RET* located at the 3'-end. Three different RT-PCR reactions were performed in order to detect the spliced isoforms located in this region using as template cDNA from non-activated and PHA-activated $CD8^+$-T cells, and as forward primer a oligonucleotide binding to exon 19 sequence and different reverse primers annealing to sequences present

in intron 19, exon 20 and exon 21. None of the samples expressed any of the isoforms. β-actin amplifications are included to test the cDNA quality.

Other primer pairs were tested to find out the site where the intracellular domain stops in $CD8^+$-T cells (activated and non-activated cells). Primers pair was as follows: forward primer: exon 9 (base pairs: 1592 – 1610) and reverse primer: exon 18 (base pairs: 2909 – 2927). Results were not conclusive, and data not shown.

T CELL BLASTS:

Peripheral blood mononuclear cells were isolated from healthy donors and activated with ConA, cultured during 6 or 7 days. At that time almost 100% of the cells are activated $CD3^+$-T cells blasts (verified by FACS analysis; data not shown). These cells are a mixture of $CD4^+$ and $CD8^+$-T cells. RNA was prepared and analyzed by RT-PCR to detect alternative splice variants at both the 5'-end and the 3'-end region of *RET*.

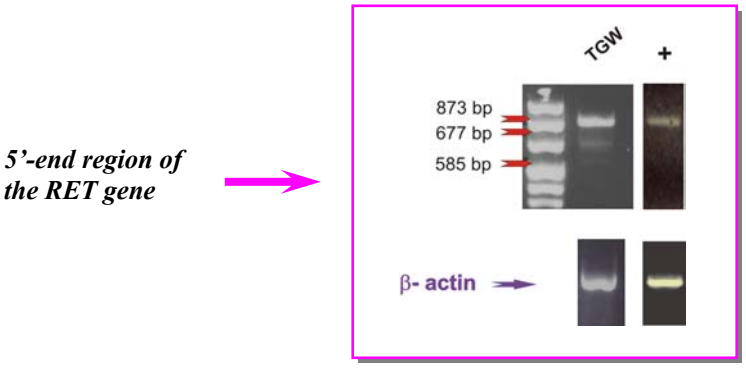

Figure 39: *RET* mRNA expression of the full length 5'-end mRNA in ConA activated T cell blasts. There is one signal at 873 bp corresponding to the full-length size. TGW: positive control. (+): activated T cell blasts after 7 days in culture with ConA.

ConA-activated T cells expressed only the full length of the *RET* transcript in the analyzed 5'-sequence. The expressed protein contains all four CLDs.

With regard to the intracellular domain, the T cell blasts should synthesize all three carboxy terminal receptor variants, as the RT-PCR analyses were positive for short RET-9, long RET-51 and middle RET-43 (see Figure 40).

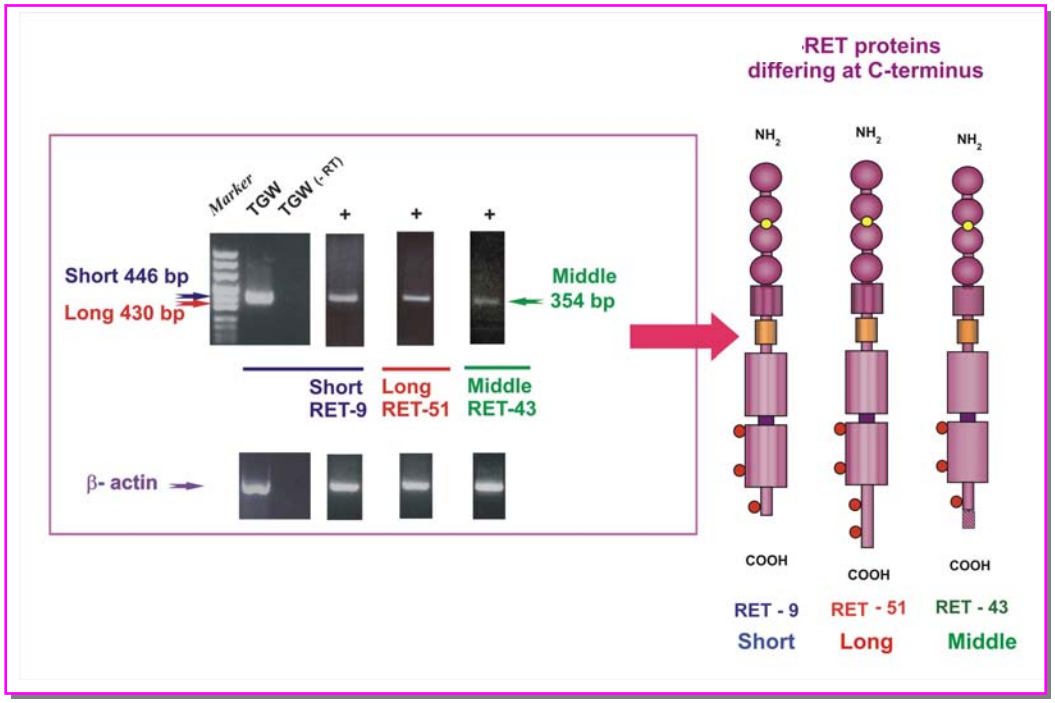

Figure 40: Activated T cell blasts after 7 days in culture with ConA expressed the three isoforms of *RET* located at the 3'-end of the gene. Predicted proteins encoded by the short (RET-9), long (RET-51) and middle (RET-43) isoforms are represented at the right side. (+) represents ConA-activated-T cells.

Although T cell blasts consist of activated $CD4^+$ and $CD8^+$-T lymphocytes, differences in the expressed *RET* splice variants were observed. Activated T cell blasts had the three isoforms located at the 3'-end region. These transcripts might be present in the $CD4^+$ fraction, as the $CD8^+$-T cells (activated and non-activated cells) were negative in the RT-PCR. T cell blasts in contrast to resting and PHA-activated $CD4^+$- and $CD8^+$-T cells only expressed the full length 5'-end *RET* mRNA sequence. The different isoform expression pattern observed in T cell blasts might be explained by the influence of cytokines induced in the population by the stimulation.

B CELLS:

In B cells the expression of the *RET* isoforms was found to be strongly regulated by activation. Resting B cells expressed the full length and the two shorter isoforms at the 5'-end, but only the middle sequence for the cytoplasmic domain. In contrast, SAC-activated B cells (and PWM-activated B cells, data not shown) did not contain any of these isoforms.

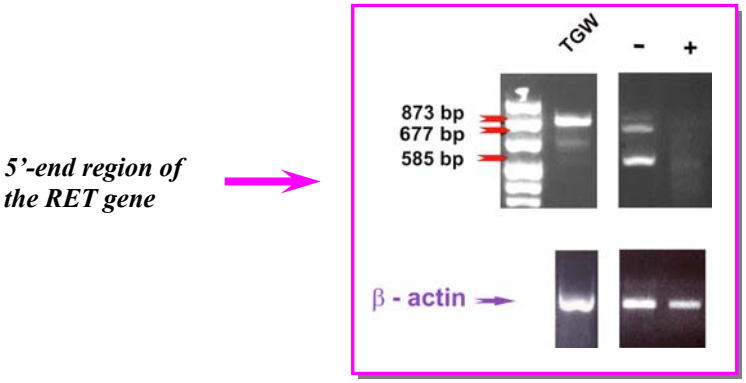

Figure 41: Multiple splice variants located at the 5'-end of *RET* were expressed in resting B cells. 5-RET mRNA (677 bp), 3-RET mRNA (585 bp) and very low expression of the full length (873 bp). In contrast, SAC-activated B cells did not express any of these *RET* isoforms.

As *RET* mRNA was detected in the RT-PCR with primers amplifying 3'-sequences, one explanation could be that the exon 6 is spliced out in B cells upon activation. Activation also changes the splicing pattern in the 3'-sequences, where either intron 19 is retained or intron 19 and exon 20 are removed.

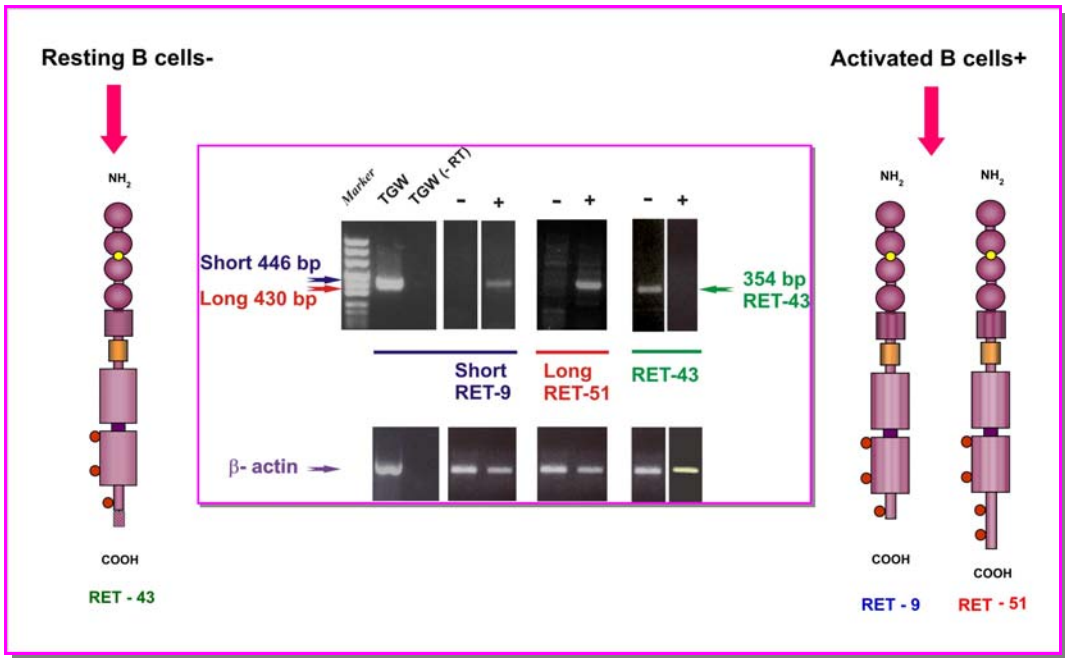

Figure 42: *RET* spliced isoforms located at the 3'-end region were differently expressed in non-activated and SAC-activated B cells. RT-PCR pictures show that activated B cells (+) expressed RET-9 and RET-51 but not RET-43. On the contrary, non-activated B cells (-) expressed only RET-43. The reactions were performed at least three times for each sample, from several donors. β-actin was amplified in 28 cycles to ensure the quality of the cDNAs and RNAs were tested for genomic contamination.

MONOCYTES:

Monocytes expressed *RET* constitutively and LPS activation had no effect on the expression pattern.

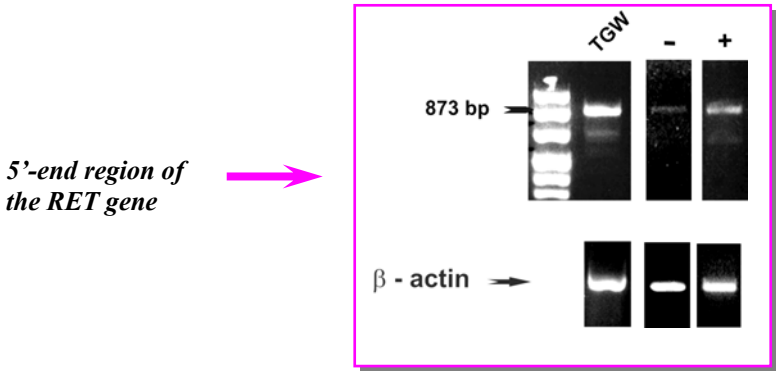

Figure 43: Both, non-activated (-) and LPS-activated monocytes (+) expressed only the full length at the 5'-end region of the RET gene by RT-PCR. Only a fragment for the full length 5'-end mRNA of 873 bp was amplified. β-actin is shown.

Non-activated (-) and activated (+) monocytes expressed only the full length *RET* mRNA at the 5'-end, whereas all splice isoforms were detected for the 3'-end.

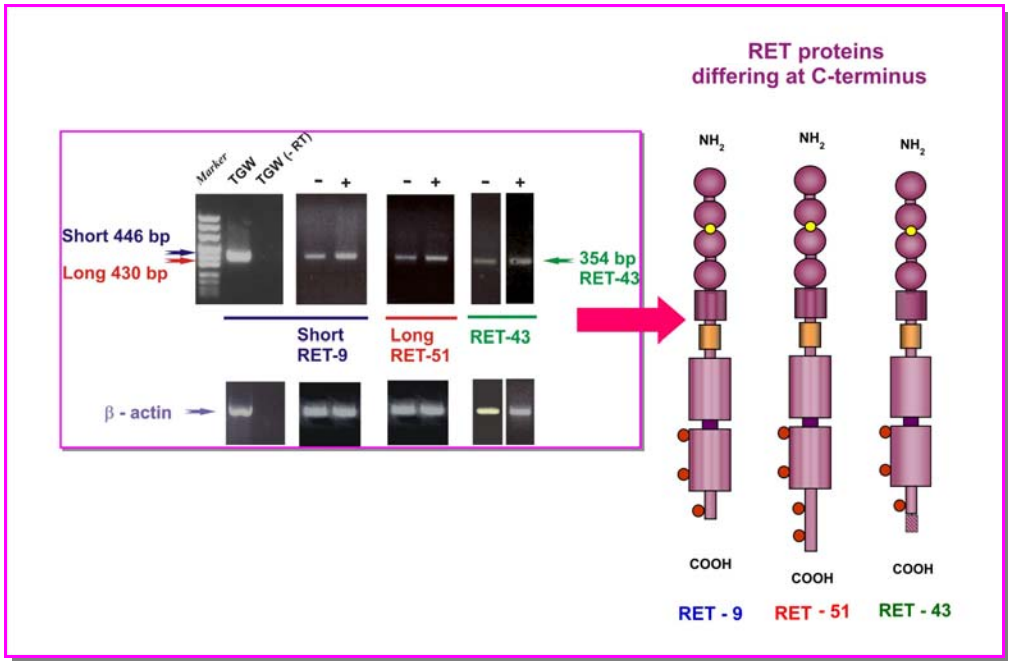

Figure 44: All spliced isoforms of *RET* at the 3'-end region were detected in non-activated and in activated monocytes by RT-PCR. RET-9 (short isoform: 446 base pairs), RET-51 (long isoform: 430 base pairs) and RET-43 (middle isoform: 354 base pairs) are shown. TGW as positive control for *RET*. β-actin is also shown.

Both, non-activated and activated monocytes express the normal extracellular RET protein that differ at the COOH-terminus.

6.6.2. Western blot - RET

At the protein level, the expression of RET receptor was assessed by Western blot and FACS analysis using mAb for extracellular staining.

6.6.2.1. Western blot – RET Short isoform

To detect the short isoform of RET (RET-9) Western blot using non-labeled rabbit anti-human RET directed against the short isoform of the intracellular domain (Sta. Cruz Biotechnology®) was performed. The secondary antibody was a goat anti-rabbit-biotin, and then streptavidine-horse peroxidase.

Several immune cells expressed the short isoform as 150-kDa polypeptide (Figure 45), with the exception of $CD8^+$-T lymphocytes, which did not express the short isoform mRNA (data from W.B. not shown).

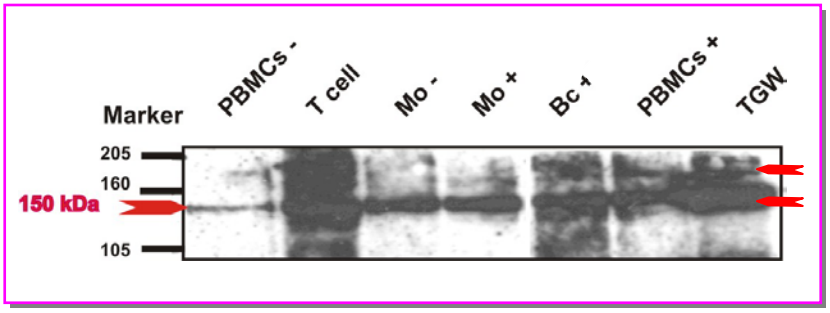

Figure 45: Detection of RET protein (short isoform) in human immune cells. Lysates from TGW neuroblastoma cell line (20 µg of protein/lane). From non-activated PBMCs (PBMCs-), ConA-activated T cell blasts (T cell), non-activated (Mo -) and LPS-activated monocytes (Mo +), SAC-activated B cells (Bc +) and LPS+IFN-γ-+αCD40-activated PBMCs (PBMCs+) were loaded approximately 80-100 µg/lane. Proteins were separated on 4-12% Bis-Tris gels and analyzed by Western blotting with anti-RET pAb that recognizes the intracellular domain of the short form of the protein.

Non-activated and activated PBMCs (LPS + IFN-γ + α-CD40), non-activated and LPS-activated monocytes, SAC-activated B cells; and ConA-activated T cell blasts showed a

strong band at 150 kDa and a weaker signal at 170 kDa. Unstimulated PBMCs had only little amounts of this RET protein. The highest level was found in T cell blasts and in the control cell line TGW.

6.6.2.2. Western blot – RET Long isoform

To detect the long carboxy-terminal isoform of RET (RET-51), Western blot using a goat pAb antibody against RET was performed. In immune cells, only the 150-kDa band was stained. With regard to the amount of RET polypeptides similar results were obtained as with the "RET-9"-specific antiserum.

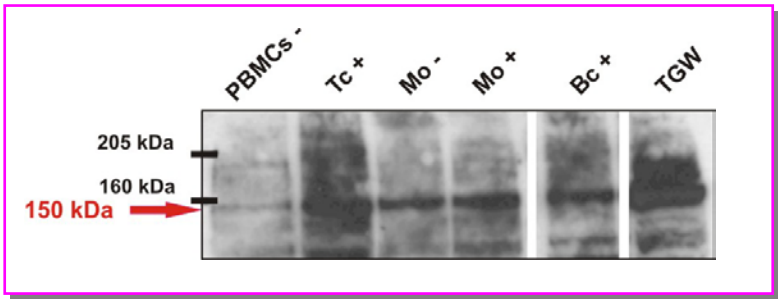

Figure 46: Detection of RET protein (long isoform) in several human immune cells. Lysates from TGW cells (20 µg of protein/lane), and from mononuclear cells: non-activated PBMCs (PBMCs-), activated T cell blasts (Tc +), non-activated (Mo -), activated monocytes (Mo +) and SAC-activated B cells (Bc +), approximately 100 µg/lane were separated on 4-12% Bis-tris gels, transferred to a nitrocellulose membrane, stained with anti-RET pAb that recognizes the long form of the protein and analyzed whit ECL kit. TGW cells showed two bands, 150 and 170 kDa RET proteins.

6.7. GFRα-1 EXPRESSION

The expression of the surface receptor GFRα-1 was studied at mRNA level using RT-PCR, and at the protein level using extracellular FACS staining and Western blot.

6.7.1. RT-PCR - GFRα-1

RT-PCR using specific primers for GFRα-1 was performed to analyze the message in immune cells. GFRα-1 mRNA expression was present in both $CD4^+$ and $CD8^+$-T lymphocytes, in B cells and monocytes.

In most of the cases, a weak signal was observed in different samples. The PCR reactions with cDNA from T and B cells had to be amplified for 38 or 40 cycles to obtain the signal indicating low transcript levels. When cDNA from monocytes was amplified, the PCR product was seen with a lower number of cycles.

To analyze GFRα-1 mRNA expression two different primer pairs were employed:

1) **Rec-Alpha1(2)** with the forward primer: Exon 1 (bp 1-18) and the reverse primer: Exon 2 (bp 307-324) resulting in a PCR product of 325 base pairs.

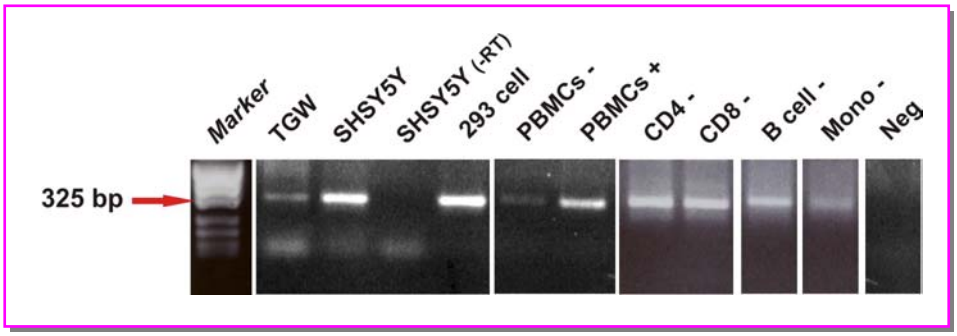

Figure 47: GFRα-1 mRNA expression was detected by RT-PCR in non-activated and in activated PBMCs. All reactions were performed at 40 cycles. As positive controls: *TGW* and *SHSY5Y* (with (+RT) and without (-) reverse transcriptase). *293 cells:* human embrionary kidney cell line. *PBMCs-:* non-activated peripheral blood mononuclear cells. *PBMCs+:* peripheral blood mononuclear cells activated with LPS, IFN-γ and α-CD40. *CD4-:* resting $CD4^+$-T cells. *CD8-:* resting $CD8^+$-T cells. *B cell-:* resting B cells. *Mono-:* non-activated monocytes.

Sequenced products were 99% identical to GFRα-1 mRNA in activated PBMCs and in SHSY-5Y. The mRNA expression of GFRα-1 is low in immune cells, for that reason the bands were visualized very weak on the gels. When the quality of cDNA was not good (i.e., no β-actin amplification was obtained after 30 cycles), signals from GFRα-1 PCR were not visible.

2) The primer pair ALPHA-1 with the forward primer: exon 5 (bp 777-796) and the reverse primer: exon 7 (bp 1064-1086) amplifying a fragment of PCR product of 310 base pairs.

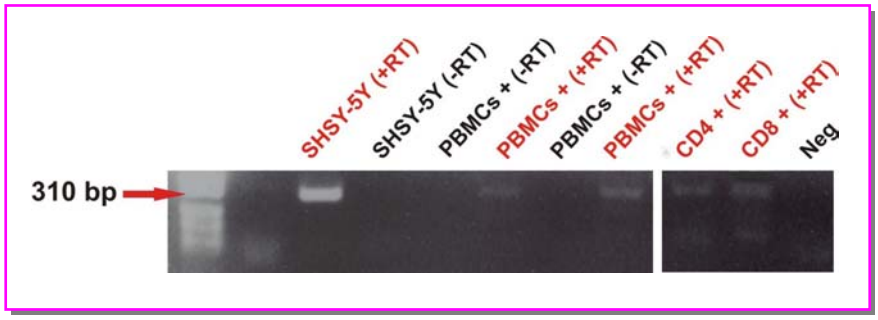

Figure 48: Amplification of GFRα-1 mRNA by immune cells using RT-PCR. This picture shows a very weak band at 310 base pairs in activated PBMCs, and in both, $CD4^+$ and $CD8^+$-T cells. cDNA from B cells was the weakest. SHSY-5Y: neuroblastoma cell line cDNA in the presence of reverse transcriptase, as positive control. (-RT): in the absence of reverse transcriptase.

As well as the reactions preformed with Rec-Alpha1 (2), the PCR products observed with these primer pairs were very weak. Also, the reactions were amplified 38 or 40 cycles to obtain the signal on immune cells. The positive control, SHSY-5Y, always showed higher expression.

PCR product from LPS-activated PBMCs was sequenced and the homology to the human GFRα-1 mRNA was 99%.

6.7.2. FACS-GFRα-1

FACS analysis using extracellular staining for GFRα-1 was performed to stain the surface receptor on immune cells. For this experiment living cells were carefully taken, then washed 2 times and incubated for 30 min with a primary, non-labeled monoclonal antibody, a mouse anti-human GFRα-1, which was posterior labeled with a secondary FITC-labeled goat anti-mouse pAb.

As positive control, TGW cell line was used. These cells expressed higher amounts of GFRα-1 mRNA, and therefore they should express also the protein in their surface.

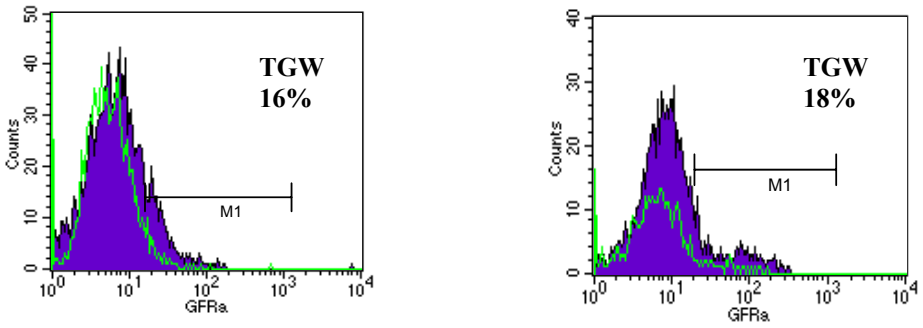

Figure 49: TGW cells are positive control for GFRα-1 protein detected by FACS. A percentage of TGW cells were positively stained with a mouse mAb against human GFRα-1 as non-labeled primary Ab, using as secondary Ab a goat-anti mouse-FITC labeled showed in FACS histograms. Green line represents the isotype control. Blue filled histograms show labeled cells with Ab against GFRα-1. First histogram showed 16% of positive cells, the second showed 18% of positive stained cells. Less than 20% of the TGW cells expressed GFRα-1 on the surface.

A negative cell line for GFRα-1 mRNA was found by RT-PCR, because they did not express GFRα-1 mRNA. These cells are the HL-60 cell line, which were stained with similar concentrations of mAb anti human-GFRα-1 for extracellular FACS. They did not stain their surface with GFRα-1 antibody:

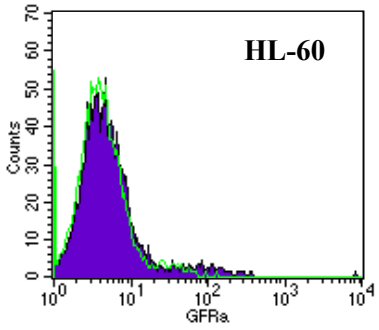

Figure 50: HL-60 cell line used as negative control for FACS analysis using a mAb α-GFRα-1, secondary labeled with gαm-FITC. Blue histogram represents cells stained with GFRα-1-FITC. Green line represents isotype control. No cells were positively stained with the Ab, meaning that they do not express GFRα-1 on their surface.

Fresh non-activated PBMCs were stained using the same protocol to determine whether they express GFRα-1 protein on the surface as it was found at mRNA level, Figure 47:
When fresh isolated and non-activated PBMCs were stained for GFRα-1, the lymphocytic population was not stained, only monocytic population; about 14% of the total amount of cells was stained positively for GFRα-1, this population corresponded to monocytes.

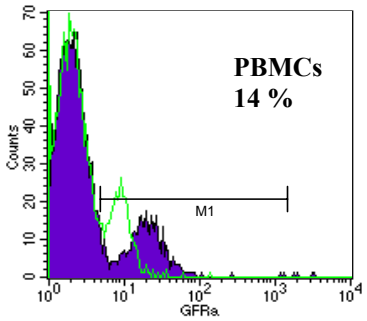

Figure 51: Fresh non-activated PBMCs expressed on their surface the receptor GFRα-1. Living cells were stained with mAb mouse against human GFRα-1, secondary labeled with goat anti-mouse-FITC. Most of the positively stained cells were located on the monocytic population. Almost non-lymphocytic cells were stained at day 1. Cells were treated with human Igs to block Fc receptors.

When non-activated PBMCs were cultured during 3 days without activation, a small population of lymphocytes was stained for GFRα-1 (~20%), as well as monocytes. Probably, after 3 days in culture, lymphocytes got a weak activation, which was enough to induce higher surface expression of GFRα-1 on their surface (data not shown).

After 72 hours of activation (LPS + IFN-γ), PBMCs were taken to perform flow cytometry, using a mAb against-human GFRα-1 and secondary labeled goat α-mouse-FITC. The extracellular staining showed that activated PBMCs expressed GFRα-1 on their surface; mainly positive cells were located on the monocytic population. A small sub-population of non-activated lymphocytes was also stained, next dot-plots (Figure 52).

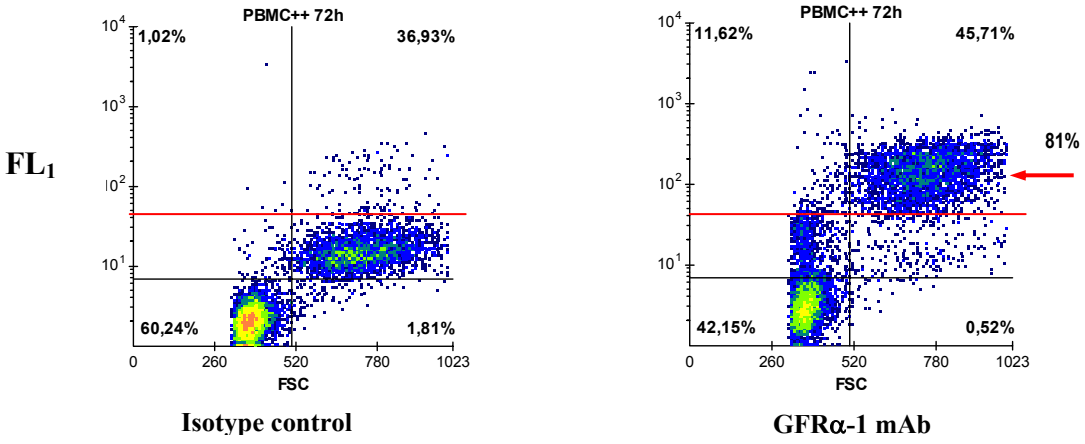

Figure 52: FACS analysis for GFRα-1 using extracellular staining on activated PBMCs. Dot-plot showing 72 hours activated PBMCs (with LPS and IFN-γ) and stained with mAb-GFRα-1 (non-labeled) and the secondary Ab goat anti mouse-FITC. Mainly monocytes were stained on the surface with GFRα-1 Ab.

A population of ~10% in the upper left quadrant was also stained. These were small cells with granularity similar to lymphocytes (SSC <10). The identity of this subset could be addressed by double staining for GFRα-1 and different CD antigens (not done).

The population of large cells (macrophages, upper right quadrant) also showed staining for GFRα-1, giving an increase of 15 folds between isotype and specific staining. To prove the identity of these cells, a double staining for CD14 and GFRα-1 could be performed.

Activated PBMCs were gated for lymphocytic (small size) and for monocytic (big size and high granularity) sub-populations. Then, the statistical analysis was better applied.

14 % of lymphocytic cells were positively stained for GFRα-1. 89% of monocytic cells were positive stained for GFRα-1 secondary labeled with FITC. A mixture of human Ig was added to the cells and incubated for 10 min, at 4°C, in order to block Fc receptors on monocytes, which can bind unspecific any antibody.

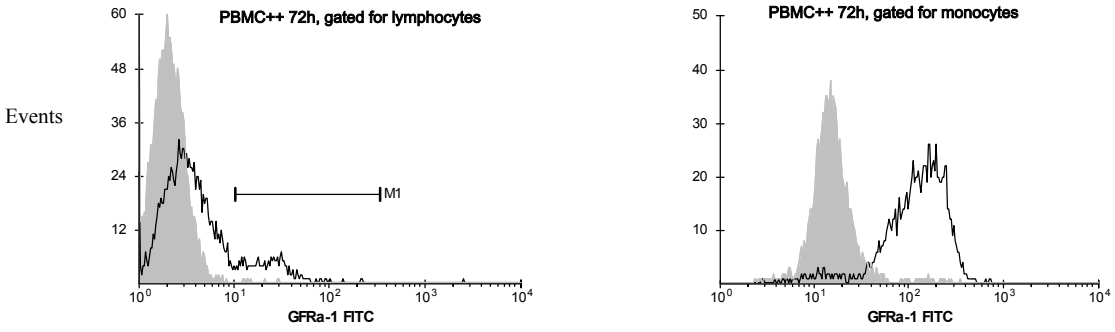

Figure 53: Histograms showing gated lymphocytes (on the left side) and gated monocytes (on the right side). PBMCs were 72 hours activated with LPS + IFN-γ; then were stained with GFRα-1 mAb, secondary labeled with FITC. Isotype control (mouse IgG_1) is represented in gray color. Ab-FITC is represented as a black line. Fluorescence-1 intensity was higher in monocytes (more than 10^2), approximately 80% of gated cells stained positive for this antibody.

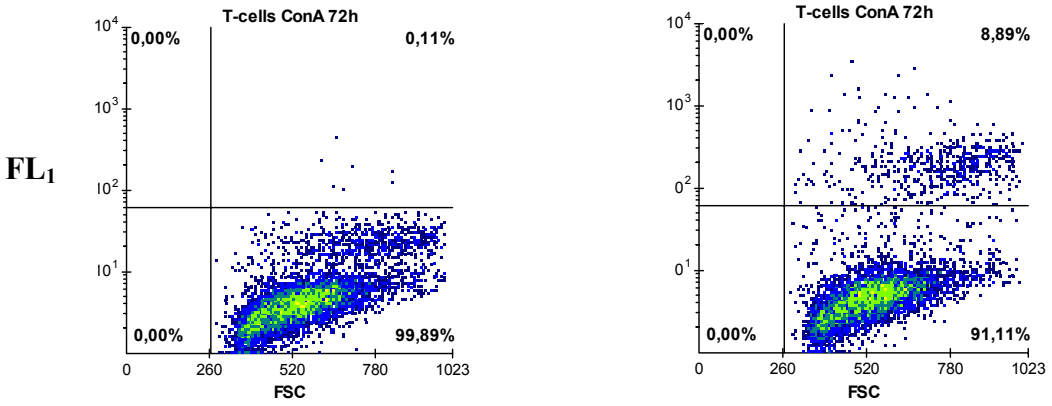

Figure 54: FACS analysis using extracellular staining for GFRα-1 surface receptor on ConA-activated PBMCs. Dot plots showing a population of ConA-activated T cell (72 hours in culture); approximately 9% of these cells expressed GFRα-1 on their surface.

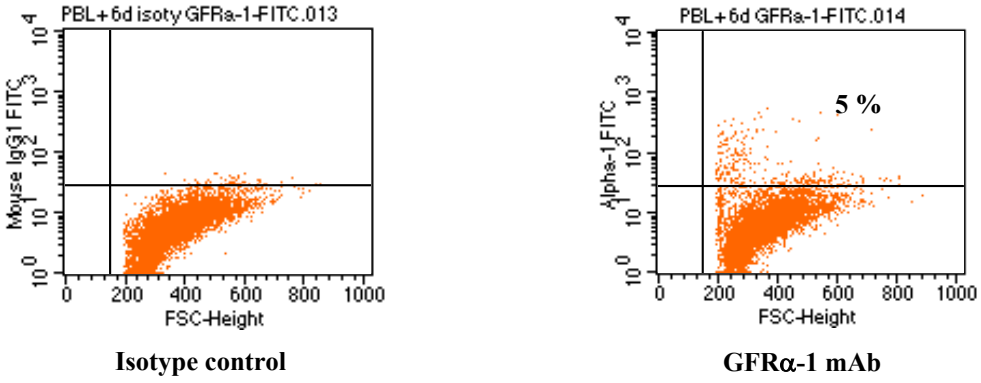

Figure 55: FACS analysis of T cell blasts after GFRα-1 surface staining. Dot-plots showing that after 6 days of ConA activation, a low percentage of T cells are positively stained with GFRα-1 mAb; the amount of positive cells was lower than 3 days before. Left dot plot represents the isotype control (mouse IgG_1). Right dot-plot shows the GFRα-1-FITC labeled stained activated T cell blast.

It seems that along ConA activation time, T cell blasts loose GFRα-1 from their surface. Probably, it is cleaved from the cell and liberated to the medium as soluble protein.

CULTURE CONDITIONS	Lymphocytic cells	Monocytic cells
Non-activated PBMCs	**- / +**	**+**
Activated PBMCs + ConA (24 hours)	**+**	**+**
Activated PBMCs + LPS, IFN-γ (72 hours)	**+**	**++**
ConA-activated T cells (5 days)	**-**	**/**
TGW (Positive control)	**+**	
HL-60 (Negative control)	**-**	
K562 (Negative control)	**-**	

Table 5: This table shows the summary of Flow Cytometry analysis using extracellular staining for GFRα-1 and blocking Fc receptors, which was done in groups of PBMCs, non-activated or activated with different mitogens.

These data suggest that the GFRα-1 receptor is mainly expressed on the surface of activated monocytes, and that a small sub-population of lymphocytes also expresses it. After 96 hours of ConA activation, those positive stained lymphocytic cells did not express the receptor anymore; however, mRNA transcripts from activated T cells were found in RT-PCR.

6.7.3. Western blot- GFRα-1

Western blot using the same monoclonal antibody against human GFRα-1 gave a positive and unique band at the expected size: between 55 – 60 kDa in all tested samples, even those, which were negative by RT-PCR, see Figure 57.

For that reason, the results obtained in these experiments cannot be taken as reliable.

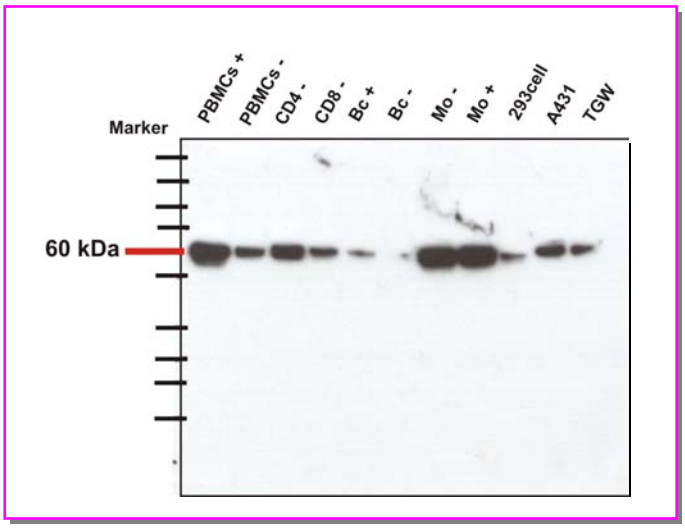

Figure 56: GFRα-1 protein expression in subtypes of peripheral mononuclear cells. Western blot was performed using a mouse mAb- anti human GFRα-1. The secondary antibody was a goat α-mouse-HRP. Different protein concentrations of each cell lysate were loaded/well (from 30 to 100 μg/lane). A unique band approx. at 60 kDa was seen on the stained nitrocellulose membrane. The detection system used was ECL. All immune cells and both positive controls (TGW and A431 cell lines) stained positively for GFRα-1.

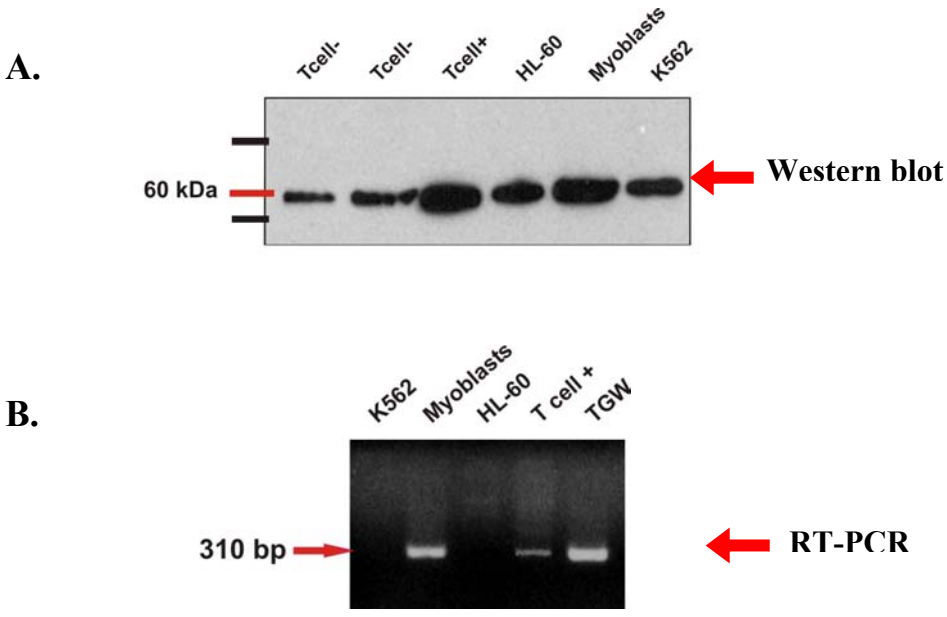

Figure 57: Western blot using mAb might give false positive results. Non-activated and ConA- activated T cells, and myoblasts stained positive for GFRα-1, but also the HL-60 and K562 cell lines, which were negative controls by RT-PCR, meaning that they did not express GFRα-1 mRNA. These experiments were performed four times, obtaining similar results.

A. Western blot performed with mAb against GFRα-1 showed a unique band at the right size: 60 kDa in all samples, even in the negative controls (K562 and HeLa cells).

B. Expression of GFRα-1 mRNA by RT-PCR in the TGW cell line (as positive control) and in the K562 and HeLa cells (as negative controls). Activated T cell blasts and myoblasts also expressed GFRα-1 mRNA.

Some monoclonal antibodies could give false positive signals, as shown in Figure 57, thereby, always the protein findings should be compared with mRNA results.

6.8. GFRα-2 EXPRESSION

GFRα-2 surface receptor for NTN was studied at the mRNA level using RT-PCR.
For protein detection, Western blot using two different antibodies were not useful for this approach (data not shown). On the contrary, FACS analysis using a goat α-human GFRα-2 pAb, secondary labeled with donkey anti-goat-PE was done in immune cells.

6.8.1. RT-PCR: GFRα-2

Pair of primers used to amplify GFRα-2 were as following; with them all spliced isoforms described can be amplified. Forward primer: Exon 1 (20 – 40 bp) and reverse primer: Exon 5 (853 – 872 bp).

PCR products*:*

851 bp: GFRα-2a (full length)

537 bp: GFRα-2b (exon 2 spliced out)

453 bp: Exon 1-4 mRNA (exon 2 and exon 3 spliced out)

280 bp: Unspecific

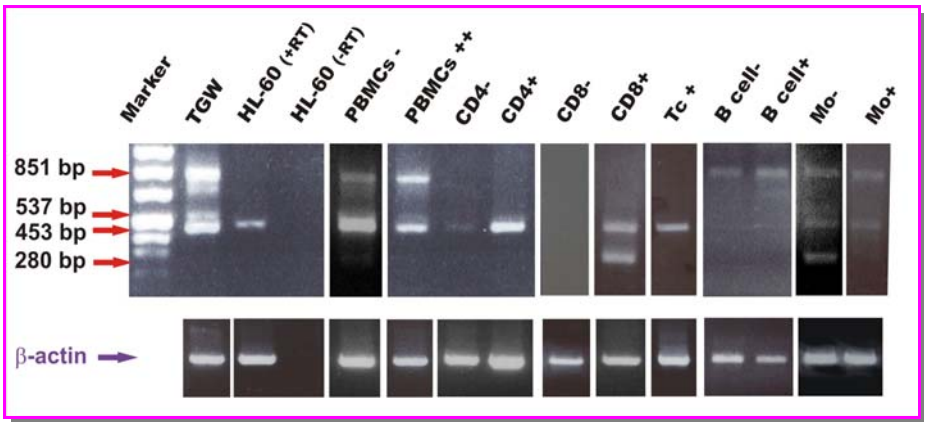

Figure 58: GFRα-2 mRNA expression by immune cells. RT-PCR was performed using primers spanning exons 1 to 5 that can detect all splice isoforms described. Sub-sets of immune cells amplified different isoforms. Non-activated $CD8^+$-T cells and B cells, both resting and activated, expressed low levels of GFRα-2. *TGW:* human neuroblastoma cell line, as positive control showing all isoforms. *HL-60* (+RT): human leukemia cell line, + reverse transcriptase. *PBMCs-:* resting PBMCs. *PBMCs++:* LPS+IFN-γ-activated PBMCs. *CD4-:* resting $CD4^+$-T cells. *CD4+:* ConA-activated $CD4^+$-T cells. *CD8-:* resting $CD8^+$-T cells. *CD8+:* PHA-activated $CD8^+$-T cells. *Tc+:* ConA-activated T cell blasts. *B cells-:* resting B cells. *B cells+:* PWM-activated B cells. *Mo-:* non-activated monocytes. *Mo+:* LPS-activated monocytes. β-actin for all samples is shown on the bottom.

The full length of GFRα-2 (GFRα-2a) was expressed in TGW, in non-activated and LPS-activated monocytes and in LPS+IFN-γ-activated PBMCs.

GFRα-2b isoform (537 bp) was amplified in low amounts by TGW, in activated PBMCs and in non-activated monocytes.

Exon 1-4 mRNA isoform (453 bp, lacking exons 2 and 3) was the most frequently expressed in all immune cells studied, as shown in Figure 58, it was present in activated and non-activated PBMCs, in activated and non-activated $CD4^+$-T cells, activated $CD8^+$-T cells, ConA-activated T cell blasts and in the positive control TGW. The expression of GFRα-2 in non-activated B cells was very low.

The PCR product of 851 bp from activated PBMCs was sequenced and showed 100% homology to the human GFRα-2 sequence.

6.8.2. FACS - GFRα-2

Protein levels of GFRα-2 were detected using extracellular staining for FACS analysis. As positive control, TGW cells were stained on the surface with GFRα-2 pAb, secondary labeled with a donkey anti-goat PE labeled Ab. Histogram is shown in Figure 58.

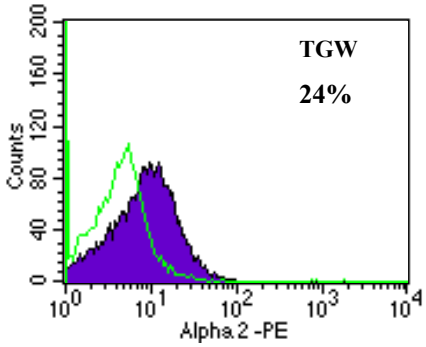

Figure 59: TGW cell line as positive control for GFRα-2 in FACS. TGW cell line stained positively for GFRα-2 using a pAb, secondary labelled with donkey-anti-goat-PE in extracellular staining and FACS. The histogram shows 24% of positive cells. Green line: isotype control. Blue: pAb α- GFRα-2.

Non-activated PBMCs were also stained with the same antibodies. In freshly isolated cells without activation approximately 9% of lymphocytes (Figure 60) and 8% of monocytes (Figure 61) expressed GFRα-2 on their surface by FACS analysis using extracellular staining:

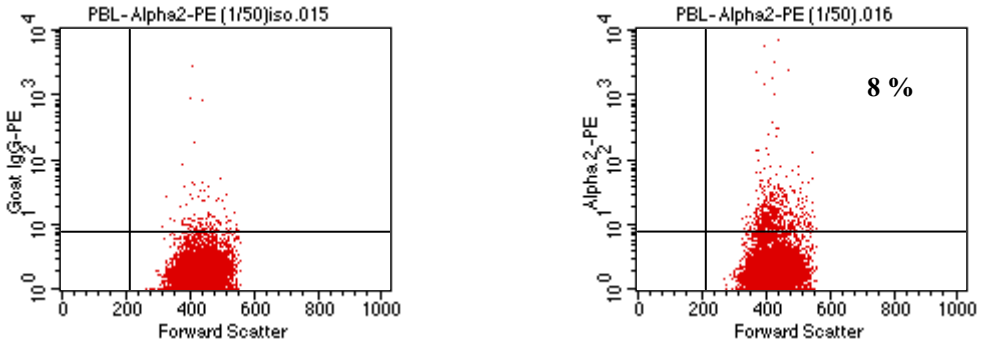

Isotype control **GFRα-2 - PE**

Figure 60: Fresh isolated PBMCs, gated for lymphocytes showed that 8% of cells were positively stained in their surface with GFRα-2 pAb. Non-activated PBMCs were isolated and stained with goat-anti human GFRα-2 pAb (1:50), secondary PE- labeled. Left dot-plot represents the isotype control (Goat IgG – PE). Right dot-plot shows gated lymphocytes stained with pAb GFRα-2 - PE labeled.

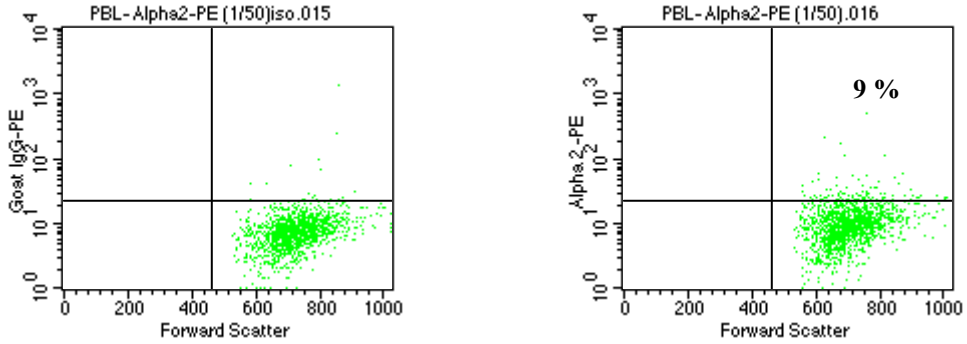

Isotype control **GFRα-2 - PE**

Figure 61: A percentage of the gated monocytes were stained positively for GFRα-2 with extracellular staining in FACS. Fresh isolated PBMCs from the above experiment were gated for monocytes showing that ~ 9% of monocytes expressed GFRα-2 on their surface. Non-activated PBMCs were stained in the same manner as described in Figure 60. Left dot-plot: isotype control (Goat IgG – PE). Right dot-plot: GFRα-2 – PE labeled cells.

Some experiments were done using double staining, means pAb anti-GFRα-2, secondary labeled with PE plus mAb anti-CD molecules, to know which sub-sets of immune cells express higher amounts of GFRα-2 (data not shown).

6.8.3. Indirect immunofluorescence – GFRα-2

Unstimulated and PWM-activated PBMCs were incubated during 1 hour, at 37°C, in the presence of mAb anti-NTN (1:100). Then, cells were washed in PBS, attached to glass slides (cytospin), fixed with paraformaldehyde and stained with a secondary Ab goat anti mouse-Cy3 labeled.

Positive cells are stained in red, showing that Neurturin is present or attached on the cell surface. The ligand NTN has to bind to the surface receptor GFRα-2 (located on the cellular membrane); otherwise it is free in the medium.

This method was an indirect way to show that the receptors are expressed on the surface and they are functional because they could bind the NTN, which is secreted either for the same cell or for neighboring cells.

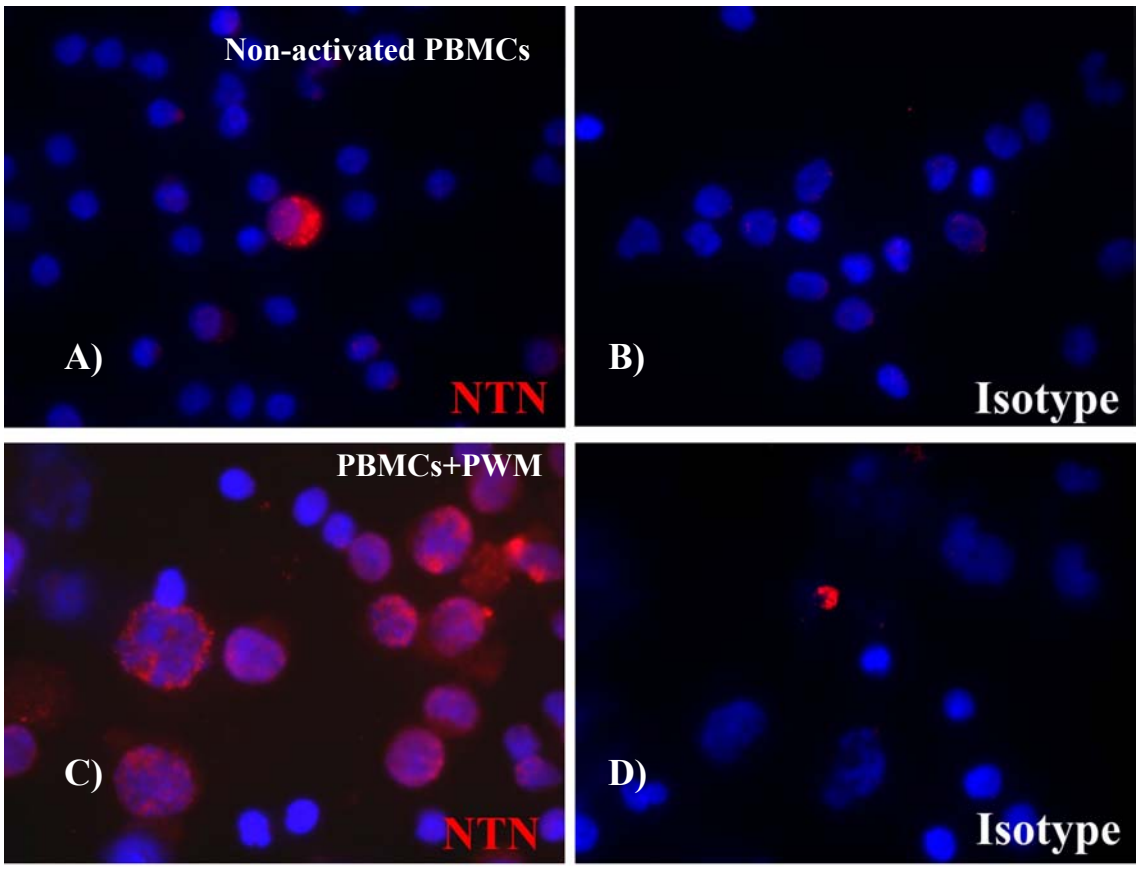

Figure 62: Surface staining of NTN on resting and PWM-activated PBMCs indicates the presence of the surface receptor GFRα-2. Non-activated and activated PBMCs were compared on their capacity to bind NTN, indicating indirectly the presence of the GFRα-2 coreceptor on their surface. This figure shows a big difference in the amount of positive stained cells after activation with pokeweed mitogen (PWM) in picture **C)**, when compared with resting cells in **A)**. After activation the majority of cells were stained in red (NTN+). Isotype controls are shown in **B)** and in **D).**

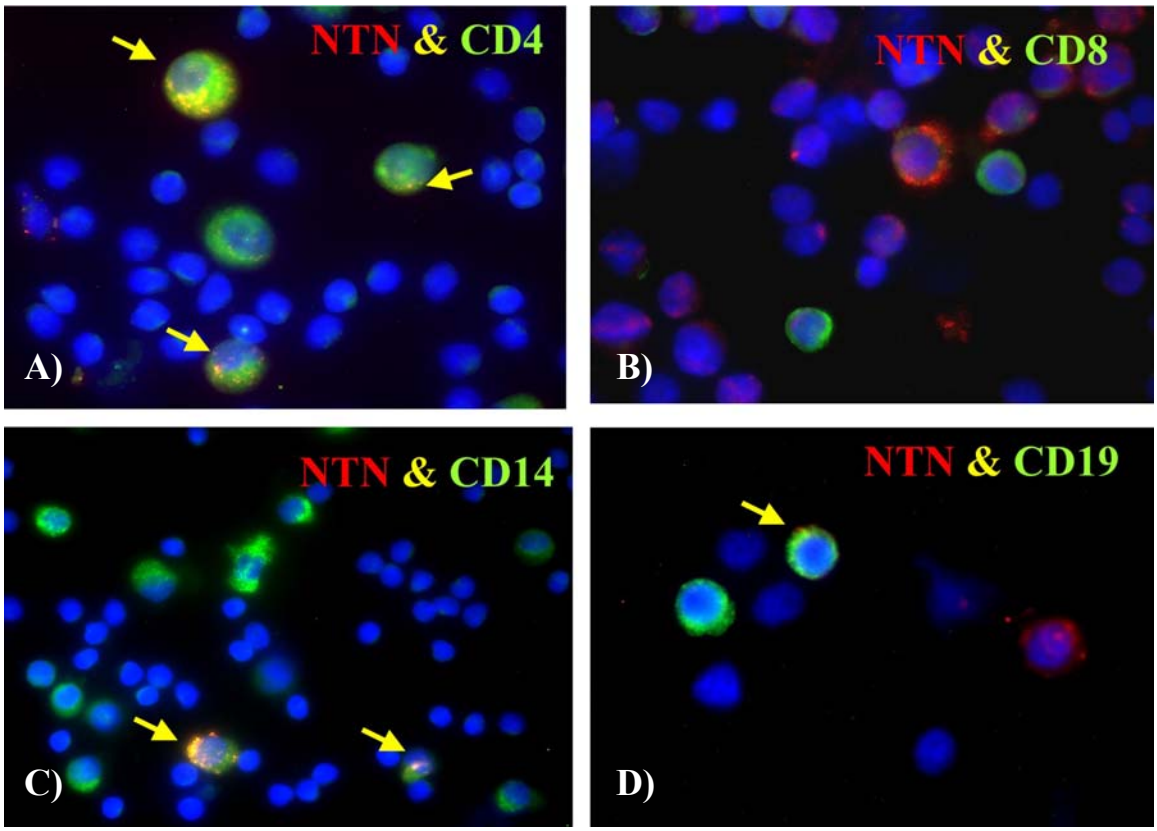

Figure 63: Double staining: anti-NTN/Cy3 and anti-CD/FITC antibodies on the surface of resting PBMCs to demonstrate the presence of the receptor GFRα-2, which binds with high affinity NTN. After to have incubated PBMCs with monoclonal antibody against human Neurturin, cells were fixed and stained with secondary Ab (goat anti-mouse-Cy3), then double stained using monoclonal and labeled antibodies against the surface molecules: CD4 **(A)**, CD8 **(B)**, CD14 **(C)** and CD19 **(D)**. Yellow regions from overlaid micrograph show the presence of both molecules on the surface of these cells (NTN + CD molecules), yellow arrows indicate them. Even that few cells were positively stained for NTN because they were non-activated PBMCs, a difference between each sub-type could be seen: $CD4^+$-T cells **(A)** and CD14 monocytes **(C)** stained stronger for surface NTN than $CD8^+$-T cells **(B)** and B cells **(D)**.

$CD4^+$-T and $CD14^+$ monocytes were the immune cells that stained stronger with anti-NTN Ab than CD19 (B cells), which expressed lower amounts of NTN. In contrast, in $CD8^+$-T lymphocytes the amount of NTN was very low, almost not seen in this picture

6.9. GDNF and RECEPTORS IN HUMAN MYOBLASTS

6.9.1. GDNF

GDNF was not expressed by human myoblasts, neither at the mRNA level nor at the protein level.

6.9.1.1. RT-PCR GDNF:

Same primers used to detect GDNF on immune cells were used to perform PCR reactions with myoblast's cDNA. Samples were prepared either with non-stimulated or with IL-1β or IFN-γ–stimulated cells. All reactions were negative, indicating that human myoblasts did not express GDNF mRNA (data not shown).

6.9.1.2. ELISA - GDNF

To measure GDNF protein, myoblasts were either non-treated or treated 48 hours with 100 pg/ml of IL-1β or 100 U/ml of IFN-γ. After 48 hours, the supernatants were analyzed using the same ELISA kit used for GDNF detection on immune cells supernatants.
We used as positive control NIH-3T3 cells transfected to produce GDNF.
Non-stimulated and stimulated myoblasts did not produce GDNF protein (data not shown).

6.9.1.3. Proliferation:

We did not find any effect on the induction of myoblasts proliferation after GDNF treatment using different GDNF concentrations (ranging from 0.1 to 500 ng/ml of human recombinant GDNF).

6.9.2. GFRα-1

6.9.2.1. RT-PCR GFRα-1:

Human myoblasts in culture expressed GFRα-1 mRNA, as shown in Figure 64. We used SHSY-5Y cells as positive control and HL-60 cell line as negative control.
Primers used to amplify GFRα-1 were already described for immune cells.

A PCR product of 324 bp was sequenced showing 100% homology to GFRα-1 mRNA.

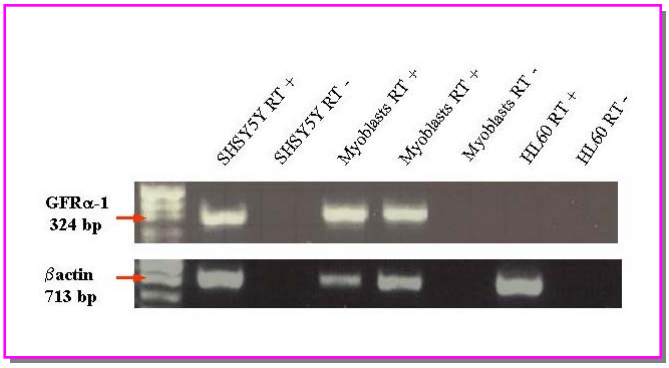

Figure 64: RT-PCR showing the mRNA expression of the GFRα-1 receptor in human myoblasts. Positive control: SHSY-5Y. Negative control: HL-60 cell line. Myoblasts expressed transcripts of GFRα-1. β-actin is shown to verify the cDNA quality. RT+: cDNA in the presence of reverse transcriptase. RT –: cDNA in the absence of reverse transcriptase.

6.9.3. RET

RET was also studied on human myoblasts. These cells expressed the long and the short isoform of *RET*.

6.9.3.1. RT-PCR RET:

c-RET large (430 bp) and short isoforms (446 bp) were expressed by SHSY-5Y cells used as positive control and also by myoblasts, as shown in the next picture:

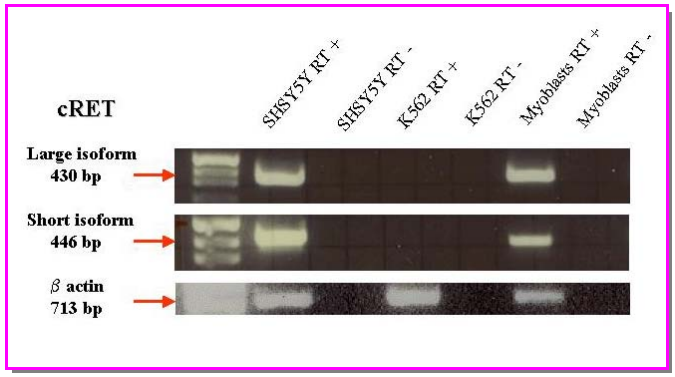

Figure 65: Human myoblasts expressed RET mRNA by RT-PCR. Both isoforms, long and short RET were detected. As positive control: SHSY-5Y; as negative control: K562 cells. All samples were prepared with (RT+) or without reverse transcriptase (RT-). β-actin was used as housekeeping gene.

6.9.3.2. Western Blotting - RET:

Western blot to stain RET protein in human myoblasts is shown in Figure 66. The Ab used was: as primary, a rabbit anti human RET pAb that detects the short isoform, and as secondary: a goat anti-rabbit biotinylated pAb; to catalyze the reaction, a streptavidine – HRP was used.

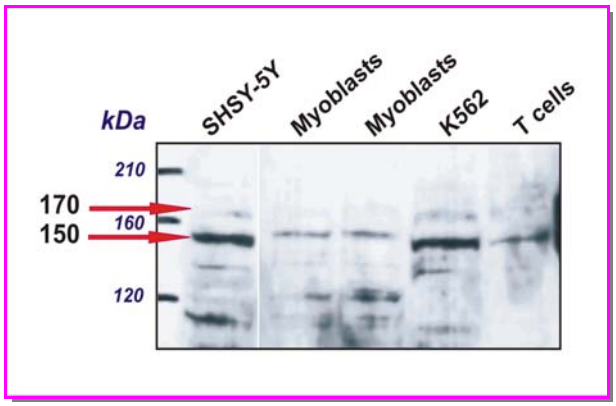

Figure 66: RET protein was also detected in myoblasts performing Western blotting. Two bands at 150 and 170 kDa were seen in the positive control SHSY-5Y; the upper band of 170 kDa is very weak. In myoblasts and in activated T cell blasts RET protein was also detected, but in lower amounts. The negative control K562 did not show signals at the right size.

6.10. FUNCTIONAL EXPERIMENTS

6.10.1. Proliferation Assays

^{3}H-Thymidine incorporation was assessed in order to find an effect of GDNF and NTN on the proliferation of immune cells. PBMCs or separated subtypes of cells were activated as it was described in Materials and Methods, then after 24, 48, 72, 96 and 120 hours of activation, GDNF or NTN was added to the wells. Immune cells were Thymidine-labeled at different time-points and were harvested 18 hours later. Samples were always were measured in triplicates. Different concentrations of GDNF and NTN were tested. Neither GDNF nor NTN had an effect on lymphocyte proliferation (data not shown).

6.10.2. ELISA-TNFα

TNF-α ELISA was performed using supernatants from non-activated PBMCs or PMBCs that had been stimulated with either LPS+IFN-γ to activate monocytes or with ConA to activate T cells.

Results obtained from these experiments indicated that the amount of TNF-α measured in the supernatant of 24 hours GDNF- or NTN-treated cells after some days in activation was significantly reduced in comparison with non-treated cells.

The strongest difference was detected when activated cells (either with ConA or with LPS + IFN-γ) were cultured during 5 or 6 days and then treated for 24 hours with GDNF or NTN. By contrast, if the cells were treated from day 0 with mitogens plus GDNF or NTN, no effect of GDNF or NTN on the TNF-α content of the supernatant obtained at day 4 was observed.

Results are shown in the following graphics, first ConA-activated PBMCs (T cell+ or activated T cell blasts) and then, LPS+IFN-γ-activated PBMCs (PBMCs++):

An example of 7 days ConA-activated PBMCs (activated T cell blasts) is shown in Figure 67, in which after 6 days in culture (ConA added at day 0) cells were treated for 24 hours with GDNF or NTN (100 ng/ml). SN were taken and afterwards measured, observing a significant difference between treated and non-treated samples ($p<0.005$ or **).

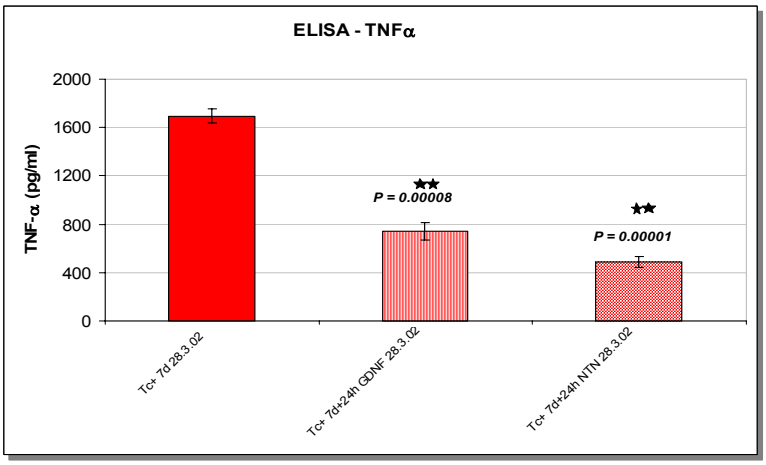

Figure 67: TNF-α ELISA was performed using supernatants from 6 days ConA-activated PBMCs and 24 hours treated with GDNF or NTN. A significant reduction in the TNF-α concentration (pg/ml) was found in 6 days ConA-activated-PBMCs and then treated 24 hours with either GDNF or NTN. Supernatants were taken at day 7. In this graphic Tc+: activated T cell blasts. Each bar represents the mean of triplicates, +/- SEM (standard error of the mean). Statistical analysis was calculated with the *Student's t- test*. ** : p< 0.005.

Similarly, a significant difference was observed when cells were activated at day 0 for 5 days with ConA and then 4 days treated with GDNF or NTN. In Figure 68 this difference is less evident than in the previous one:

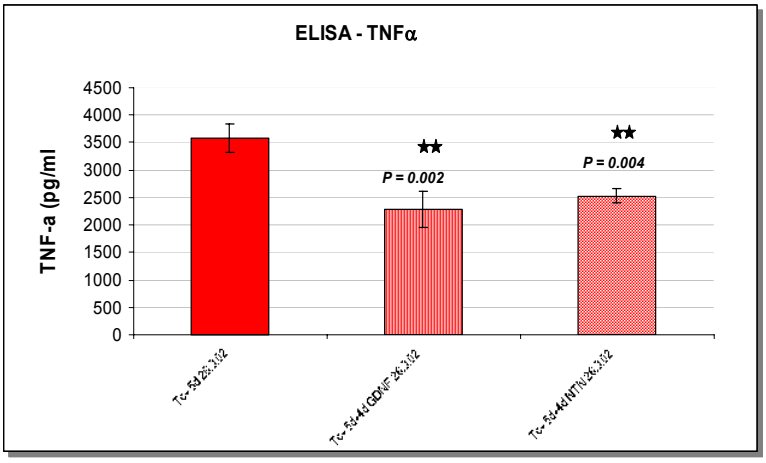

Figure 68: TNF-α ELISA was performed using supernatants from 5 days ConA-activated PBMCs, treated 4 days with GDNF or NTN. A significant reduction in the TNF-α concentration (pg/ml) was found in PBMCs activated during 5 days and treated 4 days with either GDNF or NTN (100 ng/ml). Tc+: ConA-activated T cell blasts: Each bar represents the mean of triplicates (n-3), +/- SEM. ** : p< 0.005. *p* was lower than in Figure 67.

When PBMCs were activated and treated with NTN or GDNF from the first day of culture and incubated during 4 or 5 days, no difference in the TNF-α concentration was observed between treated and non-treated samples, Figure 69 shows only NTN-treated and non-treated ConA-activated PBMCs:

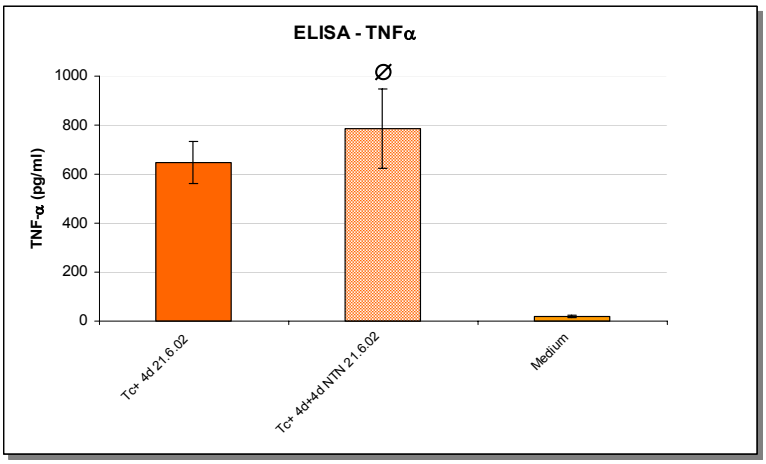

Figure 69: No differences were detected in TNF-α concentration when PBMCs were activated with ConA and treated with NTN from the first day and then cultured during 4 days. Each bar represents the mean of n=3, +/- SEM. Results were analyzed with the *Student's t-test.* ∅ : Non-statistically significant.

Examples of LPS+IFN-γ stimulated PBMCs in the absence or presence of GDNF and NTN are the following:

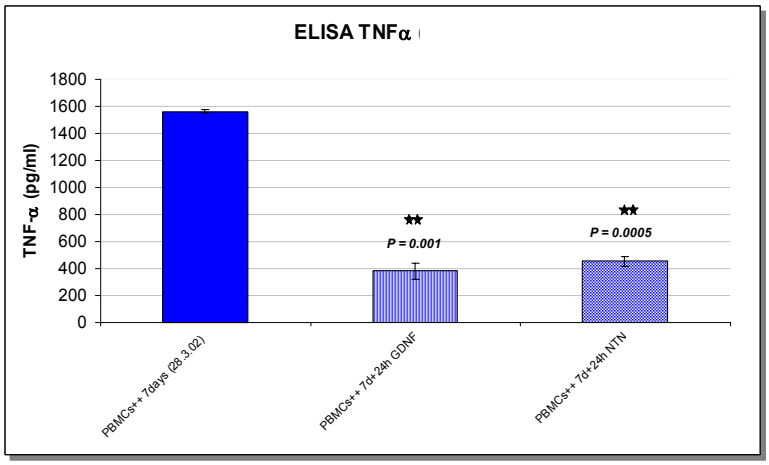

Figure 70: TNF-α ELISA was done using SN from LPS+IFN-γ-activated PBMCs (PBMCs++). A significant reduction in the TNF-α concentration was found when GDNF or NTN was added to activated PBMCs 6 days after activation with LPS+IFN-γ for 24 hours. Each bar represents the mean of triplicates, +/- SEM. Results were analyzed with the *Student's t- test.* ** : $p < 0.005$.

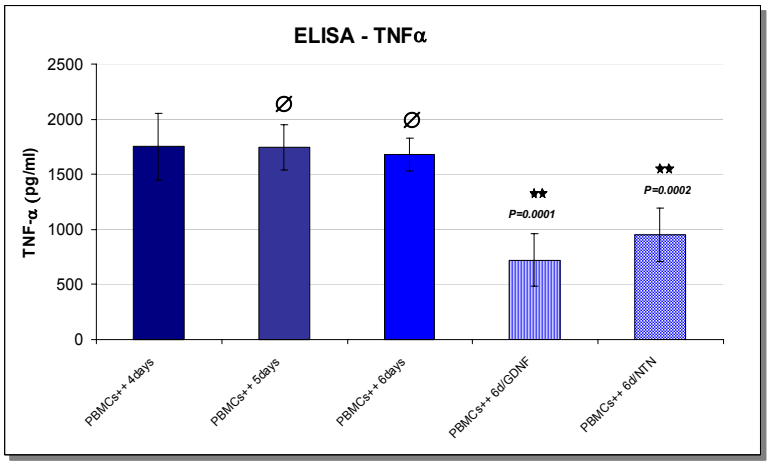

Figure 71: TNF-α ELISA performed with the supernatants from LPS+IFN-γ-activated PBMCs (PBMCs++). This graphic shows that the amount of TNF-α was similar after 4, 5 or 6 days in the medium of activated-PBMCs. In contrast, when LPS+IFN-γ-activated PBMCs were treated at day 5 with 100 ng/ml of either GDNF or NTN during 24 hours, a statistically significant reduction was seen in TNF-α concentration. ∅: not statistically significant. p< 0.005 or **

When PBMCs were cultured from day 0 in the presence of GDNF / NTN plus activators (LPS + IFN-γ) and kept in culture during 4 days, neither GDNF nor Neurturin had an effect on the TNF-α content Figure 72:

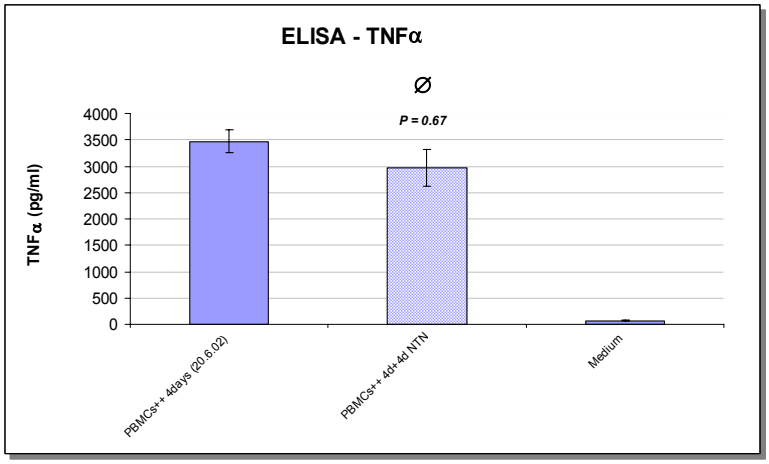

Figure 72: LPS+IFN-γ-activated PBMCs treated at the same time (day 0) with NTN and cultured during 4 days, no difference was found in the TNF-α production. *p*=0.67. ∅: Non-statistically significant (p> 0.05).

When a blocking Ab against GDNF was added to GDNF-treated and activated PBMCs, the amount of TNF-α was similar to the non-GDNF treated cells, indicating that the Ab (15 μg/ml) could block the effect of GDNF, see next figure:

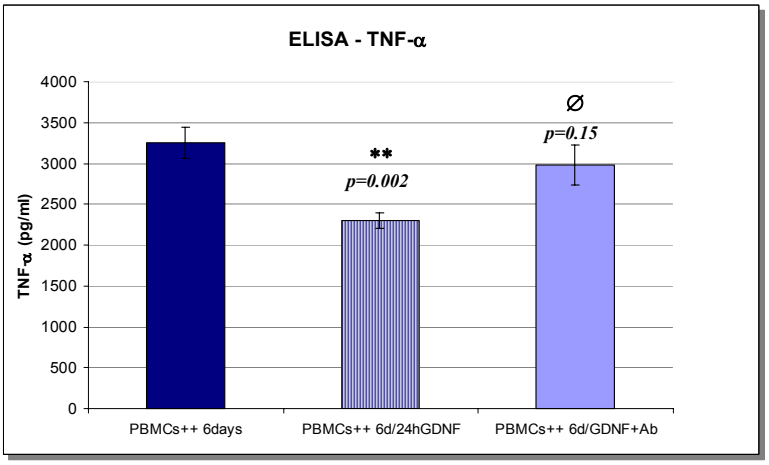

Figure 73: Blocking antibody was added to the GDNF-treated sample. After 5 days in culture with LPS+IFN-γ, activated PBMCs were 24 hours treated with GDNF (100 ng/ml), then supernatants were collected and TNF-α concentration was measured. There was a significant reduction in the soluble TNF-α from treated sample (second bar). $p<0.005$ (∗∗). After addition of GDNF plus 15 μg/ml of blocking antibody, the amount of TNF-α did not change ($p=0.15$). Each bar represents the mean of triplicates, +/- SEM. Results were analyzed with the *Student Test*. ∅: Not statistically significant ($p> 0.05$). Statistically significant ∗: $p<0.05$.

In order to understand whether the reduction of TNF-α concentration after treatment with GDNF or NTN was due to an increase in its consumption, an increase in the uptake, or due to a reduction of its production, the following experiment was performed: LPS+IFN-γ-activated PBMCs were cultured during 5 days, then cells were washed with PBS and cultured again with fresh medium in the presence or absence of 2,000 pg/ml of human recombinant TNF-α, as well as in the presence or in the absence of 100 ng/ml of GDNF. After 24 hours, supernatants were taken and TNF-α concentration was measured.

These data indicated that GDNF had the capacity of reducing TNF-α from the medium; see Figure 74:

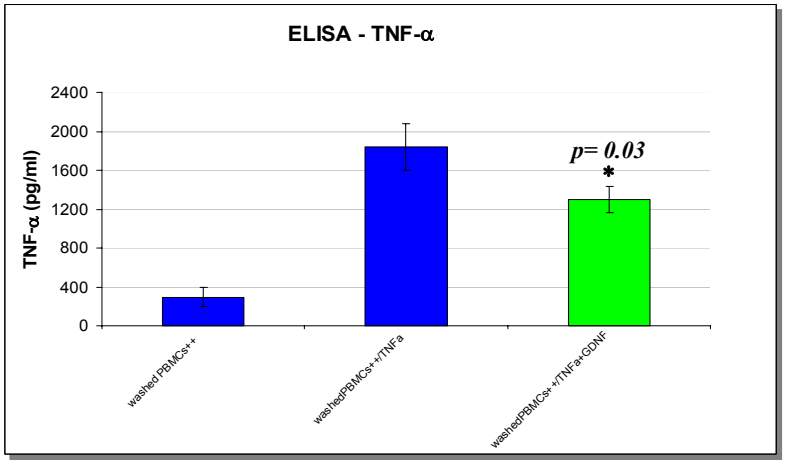

Figure 74: Increased uptake or consumption by LPS+IFN–γ-activated PBMCs? After 6 days in culture with LPS+IFN–γ, activated PBMCs were washed and 2,000 pg/ml of human recombinant TNF-α were added to the fresh medium in the presence (green bar) or in the absence (second blue bar) of GDNF (100 ng/ml), after 24 hours supernatants were collected and measured TNF-α concentration. GDNF treatment resulted in a statistically significant reduction in the soluble TNF-α. Each bar represents the mean of triplicates from two different wells. +/- SEM. ∗ : $p < 0.05$.

6.10.3. ELISA-IL-10

PBMC were stimulated with LPS+IFN-g or with ConA for 6 days and then GDNF or NTN was added at a concentration of 100 ng/ml. The supernatants were collected 24 h later and the IL-10 content was measured by ELISA. It seems that there was a slight reduction of the IL-10 concentration in the supernatants taken from GDNF or NTN-treated cells.
However, 3 out of 6 experiments did not show any difference (data not shown).

6.10.4. FACS for IL-4 and IFN-γ

FACS analysis using fluorochrome labeled-mAbs against IL-4 and IFN-γ was performed in order to find an effect of GDNF and NTN on the cytokine production of immune cells. Non-activated PBMCs, 24 hours and 72 hours LPS+IFN-γ-activated PBMCs were treated with either 100 ng/ml or 1 ng/ml of GDNF or NTN, during 2 or 24 hours. Cells were taken and processed as described in intracellular staining protocol, and analyzed by FACS.
All samples were tested in duplicates.

Treatment with GDNF or NTN did not change the percentage of cells stained with the anti IL-4 or anti-IFN-γ mAbs (data not shown).

6.10.5. FACS: Expression of surface molecules

The expression of surface molecules that are present in activated lymphocytes or in monocytes was measured by FACS analysis using the extracellular staining protocol (concentration of isotype controls and mAbs were described in *Materials and Methods*). Specificity of the labeled-Abs tested: HLA-DR, CD25, CD38, CD40, CD69 and CD86.
GDNF or NTN (100 ng/ml) was added to resting PBMC and to PBMC that had been activated with LPS+IFN-g or ConA. FACS analysis performed 24 h later showed that GDNF or NTN did not alter the expression of the above mentioned surface markers (data not shown).

7 DISCUSSION

Recent studies have demonstrated that the four members of the GDNF family ligands (GFLs) represent the ligands for RET tyrosine kinase receptor, although they do not bind RET with high affinity when a ligand binding component, the GFRα receptor, is not present (Treanor et al., 1995; Baloh et al., 1997; Trupp et al., 1998). GDNF and NTN play crucial roles in the survival and differentiation of various types of neurons, as well as in the development of kidneys and the enteric nervous system.

Few reports have been published about the expression of GFLs and their receptors in human immune and hematopoietic cells.

A putative role of RET in the functional regulation of hematopoietic cells was suggested by the presence of RET in lympho-hematopoietic tissues (fetal liver, thymus, spleen and lymph nodes) of mice and rats (Tahira et al., 1990; Avantaggiato et al., 1994; Tsuzuki et al., 1995), and in two human leukemia cell lines (Takahashi et al., 1985; Tahira et al., 1990; Takahashi et al., 1991). Subsequently, *RET* mRNA expression was shown in some myelomonocytic, B and T cell leukemia/lymphoma cell lines, although the expression levels appear to be higher in myelomonocytic leukemia cells than in T and B cell lines. *RET* mRNA expression increased at later stages of myelomonocytic maturation, suggesting that RET may be involved in terminal differentiation of these cells (Gattei et al., 1997).

Nevertheless, these results were in contrast with another study (Nakayama et al., 1999), where the findings suggested that RET may play a role at an intermediate stage of myelomonocytic maturation rather than at its terminal stages. This study showed that promyelocytes and myelocytes highly expressed *RET* in comparison to mature neutrophils and monocytes, although *RET* mRNA was also detected in these mature cells.

However, most of the RET positive leukemia/lymphoma cell lines examined did not express GFRα-1, GFRα-2 and GFRα-3, and neither GDNF nor NTN induced RET tyrosine-phosphorylation in these cells (Gattei et al., 1997; Nakayama et al., 1999).

Bone marrow (BM) hemopoietic cells expressed only *RET* whereas BM adherent cells (or stromal cells) expressed GFRα-1, GFRα-2 and GDNF. Soluble GFRα receptors are able to mediate GDNF or NTN signaling in cells that express *RET* but not GFRα. Therefore, it has

been speculated that GFRα on the surface of BM stromal cells functions like soluble GFRα. Thus, the interaction between BM and stromal cells may induce the formation of functional GDNF/RET receptors and may be involved in GDNF signaling and maturation of myelomonocytic cells in the BM microenvironment.

In addition, *RET* and GFRα-1 mRNAs were also studied in some purified human cell populations from healthy donors (Gattei et al., 1997). *RET* transcripts were amplified from $CD34^+$ hematopoietic progenitors taken from peripheral blood and cord blood; higher levels were found in circulating neutrophils and adherent $CD14^+$ monocyte/macrophages, being further increased upon GM-CSF stimulation. In contrast, circulating eosinophils and different T cell sub-sets from peripheral blood, thymus and tonsils did not express *RET*-specific mRNA. Cell lines of mature T cell phenotype displayed higher levels of *RET* mRNA than cell lines of post-thymic phenotype, whereas no *RET* transcripts were found in cell lines of the thymic phenotype.

Similarly, tonsil and peripheral blood $CD19^+$B cells did not express *RET* mRNA. Most tumor B-cell lines encompassing early pre-B to plasma cell differentiation stages were either negative or displayed low levels of RET mRNA. No *RET* expression was detected in cell lines derived from erythroid precursors.

As opposed to *RET*, transcripts specific for GFRα-1 were never found in any of the normal cell types analyzed. Expression of GFRα-1 was very infrequent, being confined to cell lines of myelomonocytic type, T cell and B cell phenotype.

Despite these few preliminary indications, which mostly concerned the expression of RET in human lymphohematopoietic cells, and human tumor cell lines, no further reports have been published, that examined the expression and/or functions of GDNF family ligands and GFRα receptors on immune-hematopoietic cells. This question was analyzed in this thesis.

7.1. EXPRESSION OF GDNF

The ligand GDNF was not detected in any of the immune cells studied.

Many attempts were made to search for GDNF in immune cells; however, GDNF was not found either at the mRNA (RT-PCR) or at the protein level (Western blot, immunoprecipitation, ELISA, intracellular staining and FACS).

The presence of all the receptors necessary for GDNF/NTN signaling on immune cells suggests that also the ligand would be expressed, as it was demonstrated for almost all neurotrophins (see Introduction). However, the GDNF family ligands are a different family of neurotrophic factors, having different functions on each cell type. In this work, receptors for GDNF and NTN were found on immune cells, nevertheless only the ligands NTN (mRNA and protein) and PSP (mRNA, preliminary data) were expressed but not GDNF.

On the other hand, GDNF protein was found in all human sera studied (after acidic treatment) and since immune cells are also circulating in the serum, receptors for GFLs on immune cells have probably some function after binding GDNF from the surrounding environment, such as endothelial cells or other tissues.

Our present data showing that immune cells do not express GDNF, excludes the possibility of a RET/GFRα-1 - GDNF autocrine loop. The presence of the GDNF receptors and the absence of ligand could suggest that functional c-RET activation in human mononuclear cells could be mediated by the ligand NTN instead of GDNF, since NTN is produced by blood mononuclear cells, and it is known that GFRα-1 is able to bind NTN in the absence of GDNF under certain conditions.

In addition, exogenous GDNF can be provided by different microenvironment cell types, for example, GDNF and GFRα-1 are produced by bone marrow stromal cells (Gattei et al., 1997; Gattei et al., 1999), by brain endothelial cells (Igarashi et al., 1999), by normal and damaged muscles, and by Schwann cells after nerve inflammation (Yamamoto et al., 1998).

7.2. EXPRESSION OF NEURTURIN

This is the first report demonstrating that NTN is expressed at mRNA and at protein levels in human immune cells. Some studies have reported that NTN was present in neonatal mouse blood and in spleen using Northern blot analysis (Creedon et al., 1997).

In this work, NTN mRNA expression was detected in all immune cells studied, as shown in Figure 19. It was found in PBMCs, activated and non-activated $CD4^+$ and $CD8^+$-T cells, activated B lymphocytes and monocytes expressed NTN mRNA.

NTN protein was detected by Western blot analysis using a polyclonal Ab against human NTN, thus confirming the presence of the protein in mononuclear cells, as shown in Figure 20.

Also, immunofluorescence using a mouse mAb against human NTN was performed to stain intracellular NTN in blood mononuclear cells. The Ab stained intracytoplasmic NTN present in non-activated PBMCs as well as in PBMCs activated with different mitogens, such as: ConA, LPS+IFN-γ, GM-CSF and PWM. It was possible with this method to demonstrate that the amount of NTN was up-regulated markedly after activation in comparison to resting states (See Figure 22).

7.3. EXPRESSION OF PERSEPHIN

Preliminary results from RT-PCR using intron-spanning primers showed that PSP mRNA is expressed by PBMCs and activated monocytes. Other sub-types of immune cells will be studied in the near future.

PSP protein expression will be also investigated.

7.4. EXPRESSION OF RET RECEPTOR

The transmembrane tyrosine kinase receptor RET, a component of the receptor-complex for GFLs was detected at the mRNA and protein level in T cells, B cells, and monocytes. The human RET gene contains at least 21 exons and generates several isoforms through alternative splicing at the 5'-end and at the 3'-end regions. The 5'-end region encodes the extracellular domain of the protein, and the 3'-end region encodes the intracellular domain. In this work, a detailed study about all mRNA variants, in each subtype of immune cells was performed using RT-PCR with specific primers that were able to amplify each isoform. Several already described isoforms of *RET* were detected in different patterns in each subtype of human immune cells.

At the 5'-end coding region of *RET* mRNA:

Three alternatively spliced isoforms due to exon skipping in the 5'-region of the RET gene have been described (Lorenzo et al., 1995).

Full length mRNA (FL): exon 2 linked to exon 3

3-RET mRNA: exon 3 spliced out

3,4-RET mRNA: exons 3 and 4 spliced out

3,4,5-RET mRNA: exons 3, 4 and 5 spliced out

The full length mRNA is expressed 3 times more abundantly than 3-RET and 3,4-RET mRNAs. The 3,4,5-RET mRNA isoform is the least abundantly expressed, only 10% of the amount of FL have been found in human fetal kidney (Lorenzo et al., 1995).

All of them have been expressed in a range of normal human adult tissues: thyroid, adrenal glands, kidneys and brain, none of them are tumor-specific variants.

3-RET and 3,4,5-RET mRNA isoforms adhere to the published open reading frame (ORF) and are predicted to encode RET proteins with deletions in the extracellular domain within the ligand-binding domain, because part or the entire cadherin domain is removed.

However, the 3,4-mRNA does not adhere to the published ORF, if this message is translated from the initiating ATG codon as published, exon 5 is translated in another frame that reaches a stop codon within exon 5 and the translated protein terminates before the transmembrane domain, encoding a soluble form of c-RET.

Recently, new isoforms with variations at the 5'-end of the gene were reported (Fluge et al., 2001):

Ret 1-8 mRNA: exons 2, 3, 4, 5, 6 and 7 are spliced out

Ret 2-8 mRNA: exons 3, 4, 5, 6 and 7 are spliced out

Ret 3-8 mRNA: exons 4, 5, 6, and 7 are spliced out

Ret 2-3 mRNA: exon 3 is spliced out (already described)

In the central *RET* mRNA region encoding the cysteine-rich, transmembrane, and the main tyrosine kinase domains no alternative splicing has been detected.

The results obtained in this work are the following:

- Resting and activated $CD4^+$-T cells expressed only the 3-RET mRNA isoform (exon 3 spliced out, PCR product: 585 base pairs).
- Resting and activated $CD8^+$-T cells expressed the full length (PCR product: 873 bp), and two isoforms: 3-RET mRNA (PCR product: 585 base pairs) and 5-RET mRNA (PCR product: 677 base pairs).
- Activated T cell blasts expressed only the full length mRNA.
- Resting B cells expressed 3-RET mRNA and 5-RET mRNA isoforms, but not the full length mRNA. Surprisingly, activated B cells did not express *RET* mRNAs that contained the extracellular domain of the mature RET protein.
- Resting and activated monocytes expressed only the full length.

It is important to emphasize the evident difference found between $CD4^+$, $CD8^+$ and activated T cell blasts, since all of them are T lymphocytes, but they expressed different *RET* isoforms. Blast cells expressed only the full length; in contrast, mature $CD4^+$ and $CD8^+$-T cells are able to express other isoforms, which, when translated, would give rise to a different extracellular domains, probably having the capacity to bind different ligands.

The second largest PCR product, the 5-RET mRNA isoforms (677 base pairs) could be a new splice variant, which has not been described. The size could correspond to an isoform lacking exon 5. The predicted amino acid sequence would lack 65 amino acids belonging to the cadherin-like domain-3 (CLD-3).

The third PCR product obtained was a band of 585 base pairs, corresponding to the isoform in which exon 3 is spliced out (3-RET mRNA). A high number of these transcripts were expressed in resting T and B cells, but not in monocytes. This isoform will encode a protein lacking 96 amino acids between CLD-1 (aa 28 to 156) and CLD-2 (aa 166 to 272) (Anders et al., 2001). The deleted part of the protein does not contain the Ca^{2+} binding site, which is necessary to linearize and rigidify the structure of the entire extracellular domain,

and also to promote dimerisation of cadherins, increasing their adhesivity, required for RET/GDNF interaction.

The functional consequences of deletions of each CLD are the following:

CLD-1 is important for the stabilization and folding of this domain due to the presence of hydrogen bonds and a hydrophobic core. Mutations that disrupt RET folding result in accumulation of a lower molecular mass isoforms, which is only partially glycosylated and does not reach the membrane but is retained in the endoplasmic reticulum, resulting in the accumulation of partially processed RET at the expense of the fully matured species. Deletion of CLD-1 would induce alterations in the ligand-binding and in receptor activation.

CLD-2 has three Cys residues that form disulfide-bridges. If it is deleted, it could affect the stability of the protein, because an unfolded domain would be generated.

CLD-3 interferes with the folding of this domain, after its disruption decreases the structural stability.

CLD-4 contains two disulfide bonds and they stabilize the folding of this domain.

The expression of spliced isoforms that vary at the 5'-end indicates that part of the extracellular domain of the RET protein is not encoded, therefore interfering with ligand interactions. The 3-RET mRNA (exon 3 spliced out) would encode a protein lacking 96 aa in the cadherin domain; probably, $CD8^{+}$-T and B lymphocytes would have differences in the ligand binding in comparison with monocytes and activated T cell blasts, which expressed the full length transcript (Anders et al., 2001).

Surprisingly, in activated B cells no PCR product that contained exons from the 5'-end region was amplified, probably because exon 6 (or exon 2), where the reverse (or forward) primer was located, can also be spliced out. After this part of the study was finished, a report describing three new isoforms at the 5'–end region of RET gene was published (Fluge et al., 2001): **Ret 1-8 mRNA, Ret 2-8 mRNA** and **Ret 3-8 mRNA**. These isoforms were expressed in human thyroid carcinoma and in normal thyroid tissue. This finding could explain why activated B cells did not express any product. For this reason, new primers were designed for exon 2 (forward) and exon 8 in order to detect these recently described isoforms.

3,4-RET mRNA and 3,4,5-RET mRNA variants, which have been detected in low amounts in some human tissues (Ivanchuck et al., 1998), were not expressed in any of the immune cells studied.

At the 3' end coding region of RET gene:

The RET gene may encode 10 different 3' termini reflecting three different coding variants and four polyadenylation sites (Tahira et al., 1990; Myers et al., 1995; Ivanchuck et al., 1998). This region encodes the intracellular domain and the COOH terminus of the RET protein. The isoforms are the following:

Short isoform (RET-9) is generated when exon 19 is not spliced to any other exon and continues directly downstream with nine further codons, which lie within intron 19. RET-9 will encode a protein having 9 unrelated amino acids at the C-terminus.

Long isoform (RET-51) is expressed when exon 19 is spliced directly to exon 20, encoding 51 completely different amino acids at the carboxyl terminus.

Middle isoform (RET-43) occurs when introns 19 and 20, in addition to exon 20 are absent, so that exon 19 is directly spliced to exon 21. In this transcript, exon 19 is followed by additional 43 codons downstream until a stop codon in exon 21 is reached. RET-43 encodes a completely different COOH sequence from the first two isoforms described.

The functional differences between these three isoforms at the C-terminus of RET proteins have not yet been well characterized, probably because it depends on the tissue and cell type studied, and on the developmental time when they have been investigated.

During development, RET-9 is essential for development of normal kidneys and normal ENS (de Graaff et al., 2001), and probably RET-51 is most important later to induce shaping and differentiation of cells (Ivanchuck et al., 1998).

Another difference is that the long RET-51 but not the shorter RET-9 isoform becomes phosphorylated upon stimulation of NGF. Probably, both isoforms may be localized differently and that NGF-dependent RET activation occurs specifically in subcellular compartments (Weiss et al., 1997).

RET-9 and RET-51 have different signaling properties *in vivo* and might define specific temporal and spatial requirements of RET functions, which are currently not well understood (Myers et al., 1995; de Graaff et al., 2001).

In this work, the 3'-end *RET* mRNA variants described are: the short (RET-9), long (RET-51) and middle isoform (RET-43) that were amplified by RT-PCR using several primer pairs. The identity of each amplified PCR product was confirmed by sequencing.

The results obtained for each cell type and activation state are the following:

- Resting $CD4^+$-T cells expressed RET-51 and RET-43 but not the short isoform RET-9. Activated $CD4^+$-T cells expressed all isoforms.
- Resting and activated $CD8^+$-T cells did not express any of the isoforms with variations at the 3'-end region. Nevertheless, these cells expressed three isoforms with variations at the 5'-end region.
- Activated T cell blasts expressed all three isoforms. This group of cells contains $CD4^+$ and $CD8^+$-T cell blasts.
- Resting B cells expressed RET-43, but neither RET-9 nor RET-51. Activated B cells expressed both, RET-9 and RET-51 isoforms, but not RET-43.
- Resting and activated monocytes expressed all three isoforms.

Based on these results, a surprising difference was detected between T lymphocytes, due to the fact that $CD8^+$-T cells (both, resting and activated cells) did not express any of the isoforms at the 5'-end, in contrast to activated T cells blasts and activated $CD4^+$-T cells, which expressed all of them. Probably, the functional responses of $CD4^+$ and $CD8^+$-T lymphocytes to GFLs and perhaps to other ligands could be completely different.

Summary of the *RET* splice isoforms for cell type:

$CD4^+$-T cells:

The 3-RET mRNA spliced isoform lacking exon 3 is expressed in both, non-activated and activated $CD4^+$-T cells, predicting a deletion in part of the cadherin motif (part of CLD-1 and part of CLD-2) located in the extracellular domain of the mature protein. Probably, it could interfere with the ligand-binding properties of this receptor (Anders et al., 2001).

From the 3'-end region that codes for the C-terminus, resting and activated $CD4^+$-T cells expressed the three isoforms, with the exception of RET-9 in non-activated $CD4^+$-T cells.

$CD8^+$-T cells:

Both, non-activated and activated $CD8^+$-T cells expressed the FL and two other isoforms that encode for the extracellular domain of the RET protein, indicating that $CD8^+$-T cells

are able to bind any of the GFLs because the extracellular domain is intact. Due to deletions in the CLD, these cells could confer additional ligand specificities.

In contrast, they do not express any of the 3 splice isoforms generated at the 3'-end region, which encodes for the intracellular domain (probably exons 19 to 21 are spliced out). Primers spanning exon 9–18 provided indeed evidence for transcription of the intracellular part of c-RET in $CD8^+$-T cells. Studies are on the way to characterize whether there are presumably novel splice variants in $CD8^+$-T lymphocytes.

B cells:

B cells did not express the full length version of *RET* from the 5'-end terminus; resting B cells expressed the isoforms lacking either exon 3 or exon 5.

Activated B cells did not express any transcript containing exons from the 5'-end. One explanation for this finding could be that exon 6 is not present. If exon 6 is spliced out, no PCR product could be amplified with the reverse primer used in this work, which was located in exon 6. Also, new primers will be tested on these samples.

At the COOH-terminus, non-activated B cells expressed only RET-43 (middle isoform); however, activated cells expressed both, the short RET-9 and the long RET-51 isoforms.

Monocytes:

Both, non-activated and activated monocytes translate the complete extracellular domain at the N-terminal because they expressed the FL mRNA. Monocytes can bind any of the GFLs through the RET receptor and GFRα. They did not express any alternative variant.

Monocytes are also able to generate three proteins that differ from each other at the C-terminus, probably having different functions, which until now have not been described.

In all RT-PCR reactions using as a template cDNA from human immune cells, RET was reliably detected after 35 cycles; this indicates that low levels of *RET* mRNA are present in immune cells, results that are in agreement with other reports, where RET was found in human normal monocytes (Gattei et al., 1997; Nakayama et al., 1999; Gattei et al., 1999) and in neutrophils (Nakayama et al., 1999), at lower levels when compared with myelocytic leukemia cells. Nevertheless, Gattei and colleagues could not detect *RET* mRNA in T or in B lymphocytes taken from normal human peripheral blood using RT-PCR with primers in exon 7 and 12. These primers amplify a 790 base pairs region spanning from the extracellular domain upstream of the cysteine-rich domain to the kinase domain downstream of the ATP binding site.

In this work, however, using different primers for both end regions, it was demonstrated that T and B cells transcribed *RET* and generated a spectrum of splice variants. Further studies have to be done to clarify whether splice variants lacking exon 7 and/or 12 can account for the negative results of Gattei (Gattei et al., 1997; Gattei et al., 1999).

$CD8^+$-T cells expressed very low levels of *RET* full length; the highest expressed isoforms were 3- and 5-RET mRNAs. If exons 6 or 7 are spliced out in these cells, the product probably could not be amplified with Gattei's primers because the length of the amplified region is too short to be detected.

In $CD4^+$-T cells only the variant 3-RET mRNA was detected with our primers (from exons 2-3 to exon 6): if other alternative splicing occurs, for example, if RET 3-8 mRNA is generated (exons 4, 5, 6 and 7 deleted), this isoform would not be amplified and therefore, similarly to Gattei et al., was not seen in these cells. But at the C-terminus, the three isoforms were present, indicating that *RET* mRNA was expressed in $CD4^+$-T cells but not the full length version. A similar explanation for B cells, in this work B cells did not express the FL mRNA, only resting B cells expressed two isoforms which stopped before exon 7. If exon 6 and 7 are spliced out our primers would not amplify it as was the case for other variants that were not detected by Gattei et al.

At the protein level, Western blotting was performed. RET antibodies used in W. B. stained almost all immune cells studied, with the exception of non-activated B cells and $CD8^+$-T lymphocytes, because they express only the RET-43 isoform, and the available antibodies (pAbs) are directed against the carboxy terminus of either the short (RET-9) or the long (RET-51) proteins, but not against the middle form (RET-43).

There was a notable difference in the signal obtained from neuroblastoma cells (TGW and SHSY-5Y) and from immune cells. Larger amounts of protein from immune cells had to be loaded (more than 100 μg/lane) in order to detect only a weak signal in comparison with neuroblastoma cells (20 μg/lane), shown in Figure 45 and Figure 46. This means that the amount of RET protein in immune cells is much lower than in neuroblastoma cell lines, which served as positive controls.

7.5. EXPRESSION OF GFRα-1 RECEPTOR

At the mRNA level, GFRα-1 transcripts were present in low amounts in all immune cells studied. The PCR products were seen only after 38–40 amplification cycles, indicating indirectly that the number of GFRα-1 mRNA transcripts is relatively low.

In agreement with our results, Yamamoto (Yamamoto et al., 1998) has reported that mRNA levels of GFRα-1 were elevated to variable extents (in addition to RET and GDNF) in various nerve biopsies from patients with peripheral neuropathies, and they found that there is a significant correlation between the extent of inflammatory cell invasion, such as T cells and macrophages infiltrates, and levels of GFRα-1 mRNA.

Honda et al. (Honda et al., 1999) have found GFRα-1 mRNA and protein in rat cultured microglia. GFRα-1 was able to phosphorylate RET in the presence of GDNF. Because microglia in the CNS is related to monocytes in the peripheral blood, it is probable that both cell types express similar receptors.

On the contrary, another publication (Gattei et al., 1997) did not find GFRα-1 mRNA expression in human peripheral T and B lymphocytes using RT-PCR. They used only 35 cycles for their RT-PCR reactions, which may not be sufficient to amplify low numbers of GFRα-1 transcripts.

One spliced isoform of this gene has been described, lacking 15 base pairs in exon 5. Even though the primers used were located in the appropriate region of the gene, this small difference between both isoforms would not have been detected on agarose gels. Nevertheless, no functional differences have been described between them.

At the protein level, the GFRα-1 receptor was detected using extracellular staining and FACS with a primary non-labeled mAb. The surfaces of small lymphocyte sub-populations of non-activated and activated PBMCs, mainly after LPS+IFN-γ activation were positively stained, and the strongest expression was seen in monocytes (activated and non-activated).

In ConA-activated PBMCs, a reduction in the percentage of GFRα-1 expressing cells over time was found. Nevertheless, a low mRNA expression in these cells was observed in different experiments.

The positively stained lymphocytic population expressing GFRα-1 on the surface (~ 10%) in Figure 52 disappeared after ConA stimulation (Figure 55). After 96 hours of ConA

activation, more than 95% of the PBMCs are activated T cell blasts ($CD3^+$-T cells). Since GFRα-1 is a GPI-linked receptor that can be cleaved from the cell surface by the action of the PI-PLC enzyme, the receptor may remain in a soluble form in the medium or may bind to the extracellular matrix or to the surface of neighboring cells, which happen to bind GFLs as well. This theory could explain why activated T cells are positive for GFRα-1 mRNA but not the receptor protein on the cell surface, as the receptor may rapidly be cleaved (Paratcha et al., 2001).

Because of this, it would be interesting to detect GFRα-1 protein in the supernatant of activated- and non-activated T cells in culture, e.g. with an ELISA for GFRα-1.

7.6. EXPRESSION OF GFRα-2 RECEPTOR

GFRα-2, the specific receptor for NTN, was studied **at the mRNA level** by RT-PCR.

In this work, amplification reactions were performed using primers spanning exons 1 to 5, which can detect all spliced isoforms described.

In our experiments, only the full length and two spliced variants were detected in immune cells. The following PCR products were obtained:

GFRα-2a: full length (PCR product: 851 base pairs)

GFRα-2b: exon 2 spliced out (PCR product: 537 base pairs). It has a deletion of 315 bp (entire exon 2), the deduced amino acid sequence is identical to GFRα-2a (full length) except for the 105 amino acid deleted at the N-terminus of the protein, that contains eight Cys residues and a single glycosylation site.

Exon 1-4 mRNA: exon 2 and exon 3 spliced out (PCR product: 453 base pairs) generating a deletion of 399 base pairs from the full length GFRα-2a. The resultant transcript is predicted to encode a protein of 331 amino acids that would not contain the N-terminal Cys-rich domain of the protein and one N-glycosylation site. The deleted protein region is not critical for binding of NTN and RET to GFRα-2 and does not determine the specificity of interactions of GFRα and GFLs (Scott and Ibanez, 2001).

The mammalian GFRα-4 completely lacks the corresponding Cys-rich domain (Masure et al., 1998), suggesting functional similarities between GFRα-4 and the shortened form of GFRα-2 (Exon 1-4 mRNA) (Lindahl et al., 2000; Scott and Ibanez, 2001).

The results obtained from immune cells are the following:

- The full length GFRα-2a (851 bp) was expressed in non-activated and in LPS-activated monocytes, as well as in LPS+IFN-γ-activated PBMCs.
- The GFRα-2b isoform (537 bp) was expressed at low levels in TGW cells, in activated PBMCs and in non-activated monocytes.
- The isoform Exon 1-4 mRNA (453 bp) was found in all immune cells studied. This isoform was expressed in activated and non-activated PBMCs, in activated and non-activated $CD4^+$-T cells, PHA-activated $CD8^+$-T cells, ConA-activated T cell blasts and in TGW. In non-activated B cells, the expression was very low, i.e. almost undetectable with 35 cycles of amplification.

Other reports (Wong et al., 1998; Wong et al., 2002) have shown that in mouse brain the most abundant isoform of GFRα-2 mRNA was the full length GFRα-2a, but probably the differences are due to the different tissues investigated. The authors detected GFRα-2 variants in human and murine whole brain tissue and found that the most prominent mRNA transcripts were the GFRα-2a full length and the least abundant isoforms detected was the Exon 1-4 mRNA variant, but this isoform is designated by them as GFRα-2c, because they did not find mRNA transcripts in which exon 3 is spliced out.

In this work, GFRα-2c is referred to as the spliced isoform lacking exon 3 (Vanhorne et al., 2001).

At the protein level, it was at first difficult to clearly demonstrate the presence of the GFRα-2 receptor by Western blot using two different pAbs against human GFRα-2. Subsequently, a goat anti-human GFRα-2 was used to stain the extracellular surface of fresh PBMCs, followed by FACS analysis. The results demonstrated that approx. 8% of lymphocytes and 9% of monocytes stained positively for GFRα-2 (see Figure 60 and Figure 61, respectively).

7.7. FUNCTIONAL EXPERIMENTS

To investigate whether GFLs receptors (GFRα-1, GFRα-2 and c-RET) are functional on human immune cells, several assays were performed in non-treated and GDNF- or NTN-treated cells. Most of them did not show any difference in proliferation assays, IL-4 and IFN-γ production and modulation of surface molecules (HLA-DR, CD40, CD69, and CD83).

On the contrary, GDNF and NTN did have an effect on the TNF-α concentration of supernatants from activated immune cells.

Supernatants from ConA activated T cell blasts and LPS+IFNγ-activated PBMCs cultured for 5 or 6 days, followed by treatment with GDNF or NTN (100 ng/ml) for 24 hours induced a significant reduction of the TNF-α concentration when compared with non-treated cells, as measured by ELISA. Whether the reduction of TNF-α after the treatment was due to an increase in its consumption, an increase in the uptake, or a reduction of production was addressed by the following experiment: to PBMCs, which had been activated for 5 days before being washed with fresh medium, a constant amount of human recombinant TNF-α (2,000 pg/ml) was added. Then, cells were incubated either in the presence or in the absence of GDNF or NTN for 24 hours. After this time, TNF-α levels were measured. The result was that GDNF and NTN were able to reduce the amount of TNF-α from the SN of treated samples, suggesting that an increase in the uptake or in the consumption, instead of a reduced production was caused by GDNF and NTN. Further experiments should be done to fully understand which mechanisms underlie this finding.

7.8. MYOBLASTS

In collaboration with Dr. G. Chevrel, we have examined the presence of GDNF, GFRα-1 and c-RET on human normal myoblasts in culture. We report that GDNF is not expressed by myoblasts contrary to its receptors GFRα-1 and RET. GDNF was not expressed by myoblasts even after stimulation by inflammatory cytokines such as interleukin-1β or interferon-γ. We did not find any effect of GDNF on the induction of the proliferation of

myoblasts. GDNF could be a factor implicated in muscle repair but its action on myoblasts is still unknown.

Results from RT-PCR analysis of myoblast cDNA showed the expression of GFRα-1, see Figure 64.

RET large and short isoforms were also expressed by human myoblasts, shown in Figure 65. The presence of RET protein in myoblasts was also confirmed by Western blot analysis, Figure 66.

No effect of GDNF was found on the proliferation of myoblasts (data not shown).

The classical concept suggests that GDNF is involved in the survival of the motoneurons, which have established contact with their target muscles. RT-PCR analyses have shown that GFRα−1 mRNA is expressed in the ventral horn of human spinal cord, but not in the skeletal muscles. In contrast, GDNF mRNA was detected in normal skeletal muscles, but not in the ventral horn, and its expression was up-regulated in regenerating muscle fibers (Suzuki et al., 1998) of two different muscle diseases, namely inflammatory PM and degenerative DMD.

In order to avoid contamination by other cells, we studied the expression of GDNF and its receptors, GFRα−1 and RET on normal human myoblasts. Indeed, the preparation of muscle tissue that is not contaminated by nerve and other cell types is difficult, and it cannot be excluded that cell types other than muscle cells, such as blood vessels or Schwann cells that also express GDNF. We found that GFRα-1 and *RET* are expressed on myoblasts but not GDNF. The presence of GDNF receptors indicates that human myoblasts may be a target for GDNF. The action of GDNF on myoblasts or muscles remains unclear. One possibility could be the induction of repair mechanisms in muscles after destruction or inflammation. Indeed, myoblasts derive from satellite cells of muscle tissue, which suggests their involvement in such repair processes.

8 CONCLUSIONS

While **GDNF**, the prototype of this family, was not expressed by any of the studied human immune cells, the related molecule **Neurturin** (**NTN**) was found to be expressed by T and B cells and monocytes as seen by RT-PCR, Western blot and immunofluorescence. NTN protein was up-regulated after cell activation.

Additionally, **Persephin** (**PSP**), another member of the GFLs was also detected at the mRNA level in activated PBMCs, activated monocytes and $CD4^+$-T lymphocytes (preliminary results).

RET, the transmembrane receptor was expressed in all human immune cells studied. Several alternatively spliced *RET* transcripts are frequently present in immune cells. Different cells expressed distinct isoforms:

- In T and B cells, the isoforms related the 3'-end region were regulated by activation.
- Various *RET* spliced variants may affect the ligand-interacting and / or downstream signaling properties of the receptor.
- Isoforms related to the 5'-end affects the ligand interaction sites in the extracellular domain of the predicted protein.
- $CD4^+$ and $CD8^+$-T lymphocytes showed distinct expression patterns of *RET* isoforms.
- A new isoform lacking exon 5 was detected (partial deletion of CDL-2 in the extracellular domain).
- Monocytes expressed only the full length mRNA indicating their responsiveness to all GFLs.

Immune cells also expressed the surface receptors **GFRα-1** and **GFRα-2** that preferentially bind NTN. The full length and one isoform of GFRα-2 were detected in different cell types by RT-PCR.

The most abundant isoform in T cells and monocytes lacked exons 2 and 3 (Exon 1-4 mRNA); the predicted protein lacks a region not critical for binding of NTN and interaction with RET. Additionally, GFRα-2 protein was detected on the surface of immune cells by FACS analysis (extracellular staining).

Functional finding: TNF-α was regulated in PBMCs by both GDNF and NTN, after activation by LPS+IFN-γ or by ConA. A reduced amount of TNF-α probably was due to an increased uptake or consumption rather than a reduced production.

All components of the GDNF and NTN receptor complex (GFRα-1, GFRα-2 and RET), but not the ligand GDNF, are expressed by immune cells, indicating that these cells are receptive for GDNF and NTN mediated signaling, specifically for GDNF family ligands supplied by neurons that may be involved in neuro-immune communication, as well as GFLs derived from peripheral blood mononuclear cells, such as NTN and PSP, and bone marrow stromal cells. We could speculate that immune cells may communicate via NTN and PSP with other cells in a paracrine fashion, or within a restricted immune cell microenvironment using an autocrine loop.It might be possible that the up-regulation or down-regulation of these receptors on immune cells is important in some pathological situations, in which both, nervous and immune systems are in close relation (i.e., CNS inflammation, neuromuscular autoimmune diseases: demyelinating neuropathies, Myasthenia gravis, polymyositis, etc.).

9 REFERENCES

Abe K, Hayashi T and Itoyama Y (1997a). Amelioration of brain edema by topical application of glial cell line-derived neurotrophic factor in reperfused rat brain. Neurosci. Lett. 231: 37-40.

Abe K and Hayashi T (1997b). Expression of the glial cell line-derived neurotrophic factor gene in rat brain after transient MCA occlusion. Brain Res. 776: 230-234.

Adams RD and Victor M (1993). Degenerative diseases of the nervous system. In Principles of Neurology (R. D. Adams, Ed.). McGraw-Hill, New York.

Airaksinen MS, Titievsky A and Saarma M (1999). GDNF family neurotrophic factor signaling: four masters, one servant? Mol. Cell. Neurosci. 13: 313-325.

Airaksinen MS and Saarma M (2002). The GDNF family: signaling, biological functions and therapeutic value. Nature Rev. Neurosci. 3: 383-394.

Alberts B, Bray D, Lewis J, Raff M, Roberts K and Watson JD (1997). Molecular biology of the cell. Third Edition. Garland Publishing, Inc.

Anders J, Kjar S and Ibanez CF (2001). Molecular modeling of the extracellular domain of the RET receptor tyrosine kinase reveals multiple cadherin-like domains and a calcium-binding site. J. Biol. Chem. 276: 35808-35817.

Arenas E, Trupp M, Akerud P and Ibáñez CF (1995). GDNF prevents degeneration and promotes the phenotype of brain noradrenergic in vivo. Neuron 15: 1465-1473.

Angrist M, Jing S, Bolk S, Bentley K, Nallasamy S, Halushka M, Fox G and Chakravarti A (1998). Human GFRa-1: cloning, mapping, genomic structure and evaluation as a candidate gene for Hirschsprung Disease susceptibility. Genomics 48: 354-362.

Arighi E, Alberti L, Torriti F, Ghizzoni S, Rizzetti M, Pelicci G, Piutti C, Pierotti M and Borrello M (1997). Identification of Shc docking site on Ret tyrosine kinase. Oncogene 14: 773-782.

Arvidsson A, Kokaia Z, Airaksinen MS, Saarma M and Lindvall O (2001). Stroke induces widespread changes of gene expression for glial cell line-derived neurotrophic factor family receptors in the adult rat brain. Neurosci. 106: 27-41.

Asai N, Murakami H, Iwashita T and Takahashi M (1996). A mutation at tyrosine 1062 in MEN2A-Ret and MEN2B-Ret impairs their transforming activity and association with shc adaptor proteins. J. Biol. Chem. 271: 17644-17649.

Avantaggiato V, Dathan NA, Grieco M, Fabien N, Lazzaro D, Fusco A, Simeone A and Santoro M (1994). Developmental expression of the RET proto-oncogene. Cell Growth Differ. 5: 305-311.

Baloh R H, Tansey MG, Lampe PA, Fahmer TJ, Enomoto H, Simburger KS, Leitner ML, Araki T, Johnson EM. Jr and Mildbrandt J (1996). Artemin, a novel member of the GDNF ligand family, supports peripheral and central neurons and signals through the GFRalpha3-RET receptor complex. Neuron 21: 1291-1302.

Baloh R. H, Tansey M. G, Golden J. P, Creedon D. J, Heuckeroth R. O, Keck C, L, Zimonjic D. B, Popescu N. C, Johnson E. M and Mildbrandt J (1997). TrnR2, a novel receptor that mediates neurturin and GDNF signaling through RET. Neuron 18: 793-802.

Barde YA. Help from within for damaged axons (1997). Nature 385: 391-393.

Batourina E, Gim S, Bello N, Shy M, Clagett M, Costantini F and Mendelsohn C (2001). Vitamin A controls epithelial/mesenchymal interactions through Ret expression. Nat. Genet. 27: 74-78.

Bär KJ, Saldanha J, Kennedy A, Facer P, Birch R, Carlstedt T and Anand P (1998). GDNF and its receptor component RET in injured human nerves and dorsal root ganglia. NeuroReport 9: 43-47.

Becher B, Prat A and Antel JP (2000). Brain-Immune connection: Immuno-regulatory properties of CNS-resident cells. Glia 29: 293-304.

Belluardo N, Mudo G, Caniglia G, Corsaro M, Cheng Q, Frasca F, Belfiore A and Condorelli DF (1999). Expression of neurotrophins, GDNF, and their receptors in rat thyroid tissue. Cell Tissue Res. 295: 467-475.

Benett GJ (1999). Does a neuroimmune interaction contribute to the genesis of painful peripheral neuropathies? Proc. Natl. Acad. Sci. USA. 96: 7737-7738.

Besser M and Wank R (1999). Clonally restricted production of the neurotrophins brain-derived neurotrophic factor and neurotrophin-3 mRNA by human immune cells and Th1/Th2-polarized expression of their receptors. J. Immunol. 162: 6303-6306.

Besset V, Scott RP and Ibanez CF (2000). Signaling complexes and protein-protein interactions involved in the activation of the Ras and phosphatidylinositol 3-kinase pathways by the c-Ret receptor tyrosine kinase. J. Biol. Chem. 275: 39159-39166.

Bjorklund A, Kirik D, Rosenblad C, Lundberg C and Mandel RJ (2000). Towards a neuroprotective gene therapy for Parkinson's disease: use of adenovirus, AAV and lentivirus vectors for gene transfer of GDNF to the nigrostriatal system in the rat Parkinson model. Brain Res. 886: 82-98.

Bordeaux MC, Forcet C, Granger L, Corset V, Bidaud C, Billaud M, Bredesen DE, Edery P and Mehlen P (2000). The RET proto-oncogene induces apoptosis: a novel mechanism for Hirschsprung disease. EMBO J. 19: 4056-4063.

Borello MG, Alberti L, Arighi E, Borganzone I, Battistini C, Bardeli A, Pasini B, Piutti C, Rizzetti MG, Mondellini P, Radice MT and Pierotti MA (1996). The full oncogenic activity of Ret/ptc2 depends on tyrosine 539, a docking site for phospholipase C. Mol. Cell. Biol. 16: 2151-2163.

Brodbeck U (1998). Signalling properties of glycosylphosphatidylinositols and their regulated release from membranes in the turnover of glycosylphosphatidylinositol-anchored proteins. Biol. Chem. 379: 1041-1044.

Buj-Bello A, Buchman VL, Horton A, Rosenthal A and Davies AM (1995). GDNF is an age-specific survival factor for sensory and autonomic neurons. Neuron 15: 821-828.

Buj-Bello A, Adu J, Pinon LG, Horton A, Thompson J, Rosenthal A, Chinchetru M, Buchman VL and Davies AM (1997). Neurturin responsiveness requires a GPI-linked receptor and the Ret receptor tyrosine kinase. Nature 387: 721-724.

Bunone G, Uggeri M, Mondellini P, Pierotti MA and Bongarzone I (2000). RET receptor expression in thyroid follicular epithelial cell-derived tumors. Cancer Res. 60: 2845-2849.

Burazin TC and Gundlach AL (1999). Localization of GDNF/Neurturin receptor (*c-ret*, GFRα-1 and α-2) mRNAs in post-natal rat brain: Differential regional and temporal expression in hippocampus, cortex and cerebellum. Mol. Brain Res. 73: 151-171.

Burgi B, Otten U, Ochensberger B, Rihs S, Ehrhard P, Ibanez C and Dahinden C (1996). Basophil priming by neurotrophic factors. Activation through the trk receptor. J. Immunol. 157: 5582-5588, 1996.

Calacano G, Farinas I, Wang LC, Hagler K, Forgie A, Moore M, Armanini M, Phillips H, Ryan AM, Reichardt LF, Hynes M, Davies A and Rosenthal A (1998). GFRalpha1 is an essential receptor component for GDNF in the developing nervous system and kidney. Neuron 21: 53-62, 1998.

Carson-Walter EB, Smith DP, Ponder BA, Baylin SB and Nelkin BD (1998). Post-transcriptional silencing of RET occurs, but is not required, during raf-1 mediated differentiation of medullary thyroid carcinoma cells. Oncogene 17: 367-376.

Cass WA (1996). GDNF selectively protects dopamine neurons over serotonin neurons against the neurotoxic effects of methamphetamine. J. Neurosci. 16: 8132-8139.

Chen AC, Eisch AJ, Sakai N, Takahashi M, Nestler EJ and Duman RS (2001). Regulation of GFRalpha-1 and GFRalpha-2 mRNAs in rat brain by electroconvulsive seizure. Synapse 39: 42-50.

Chevalier S, Praloran V, Smith C, MacGrogan D, Ip NY, Yancopoulos GD, Brachet P, Pouplard A and Gascan H (1994). Expression and functionality of the trkA proto-oncogene product/NGF receptor in undifferentiated hematopoietic cells. Blood 83: 1479-1485.

Cik M, Masure S, Lesage AS, Van Der Linden I, Van Gompel P, Pangalos MN, Gordon RD and Leysen JE (2000). Binding of GDNF and neurturin to human GDNF family receptor alpha 1 and 2. Influence of c-RET and cooperative interactions. J. Biol. Chem. 275: 27505-27512.

Coulpier M, Anders J and Ibañez C (2002). Coordinated activation of autophosphorylation sites in the RET receptor tyrosine kinase. J. Biol. Chem. 277: 1991-1999.

Creedon DJ, Tansey M, Baloh R, Osborne P, Lampe P, Fahrner T, Heuckeroth R, Milbrandt J and Johnson Jr. (1997). Neurturin shares receptors and signal transduction pathways with glial cell line-derived neurotrophic factor in sympathetic neurons. Proc. Natl. Acad. Sci. USA. 94: 7018-7023.

Current protocols in Immunology. (2001).

Dalton TP, Li Q, Bittel D, Liang L and Andrews GK (1996). Oxidative stress activates metal-responsive transcription factor-1 binding activity. Occupancy in vivo of metal response elements in thematallothionein-I gene promoter. J. Biol. Chem. 271: 26233-26241.

Date I, Aoi M, Tomita S and Ohmoto T (1998). GDNF administration induces recovery of the nigrostriatal dopaminergic system both in young and aged parkinsonian mice. NeuroRep. 9: 2365-2369.

Dechant G (2002). Chat in the trophic web: NGF activates Ret by inter-RTK signaling. Neuron 33: 156-158.

de Graaff E, Srinivas S, Kilkenny C, D'Agati V, Mankoo BS, Costantini F and Pachnis V (2001). Differential activities of the RET tyrosine kinase receptor isoforms during mammalian embryogenesis. Gen. Dev. 15: 2433-2444.

Durbec P, Marcos-Gutierrez CV, Kilkenny C, Grigoriou M, Suvanto P, Costantini F, Saarma M, et al. (1996). GDNF signaling through the Ret receptor tyrosine kinase. Nature 381: 789-793.

Ehrhard PB, Ganter U, Stalder A, Bauer J and Otten U (1993a). Expression of functional trk protooncogene in human monocytes. Proc. Natl. Acad. Sci. USA. 90: 5423-5427.

Ehrhard PB, Erb P, Graumann U and Otten U (1993b). Expression of nerve growth factor and nerve growth factor receptor tyrosine kinase Trk in activated CD4-positive T-cell clones. Proc. Natl. Acad. Sci. USA. 90: 10984-10988.

Ehrhard PB, Erb P, Graumann U, Schmutz B and Otten U (1994). Expression of functional trk tyrosine kinase receptors after T cell activation. J. Immunol. 152: 2705-2709.

Elkabes S, DiCicco Bloom EM and Black IB (1996). Brain microglia/macrophages express neurotrophins that selectively regulate microglial proliferation and function. J Neurosci. 16: 2508-2521.

Eng C, Smith DP, Mulligan LM, Nagai MA, Healey CS, Ponder MA, Gardner E, Scheumann GF, et al. (1994) Point mutation within the tyrosine kinase domain of the RET proto-oncogene in multiple endocrine neoplasia type 2B and related sporadic tumors. Hum. Mol. Genet. 3: 237-241.

Eng C and Mulligan LM (1997). Mutations of the RET proto-oncogene in the multiple endocrine neoplasia type 2 syndromes, related sporadic tumours, and Hirschsprung disease (Review). Hum. Mutat. 9: 97-109.

Eng C, Myers S, Kogon M, Sanicola M, Hession C, Cate R and Mulligan LM (1998). Genomics structure and chromosomal localisation of the human GDNFR-alpha gene. Oncogene 16: 597-601.

Engel AG and Banker BQ (1986). The anatomy, physiology, and biochemistry of muscle. *In Myology*. Vol. 1. McGraw-Hill, Inc. USA.

Enomoto H, Araki T, Jackman A, Heuckeroth RO, Johnson EM Jr. and Milbrandt J (1998). GFRalpha1-deficient mice have deficits in the enteric nervous system and kidneys. Neuron 21: 317-324.

Enomoto H, Heuckeroth R, Golden J, Johnson E and Milbrandt J (2000). Development of cranial parasympathetic ganglia require sequential actions of GDNF and neurturin. Development 127: 4877-4889.

Ferguson MA (1999). The structure, biosynthesis and functions of glycosyl-phosphatidylinositol anchors, and the contributions of trypanosome research. J. Cell. Sci. 112: 2799-2809.

Fluge O, Haugen D, Akslen L, Marstad A, Santoro M, Varhaug J and Lillehaug JR (2001). Expression and alternative splicing of c-ret RNA in papillary thyroid carcinomas. Oncogene 20: 885-892.

Forander P, Broberger C and Stromberg I (2001). Glial-cell-line-derived neurotrophic factor induces nerve fibre formation in primary cultures of adrenal chromaffin cells. Cell Tissue Res. 305: 43-51.

Franke B, Figiel M and Engele J (1998). CNS glia are targets for GDNF and neurturin. Histochem. Cell. Biol. 110: 595-601.

Frisk T, Farnebo F, Zedenius J, Grimelius L, Höög A, Wallin G and Larsson C (2000). Expression of RET and its ligand complexes, GDNF/GFRα-1 and NTN/GFRα-2, in medullary thyroid carcinomas. Eur. J. Endocrin. 142: 643-649.

Galli SJ, Zsebo KM and Geissler EN (1994). The kit ligand, stem cell factor (Review). Adv. Immunol. 55: 1-96.

Gash DM, Zhang Z, Cass WA, Ovadia A, Simmerman L, Russell D, Martin D, Collins FC, Hoffer BJ and Gerhardt GA (1995). Morphological and functional effects of intranigrally administered GDNF in normal rhesus monkeys. J. Comp. Neurol. 363: 345-358.

Gash DM, Zhang Z, Ovadia A, Cass WA, Yi A, Simmerman L, Russell D, Martin D, Lapchak PA, Collins FC, Hoffer BJ and Gerhardt GA (1996). Functional recovery in GDNF-treated Parkinsonian monkeys. Nature 380: 252-255.

Gattei V, Celetti A, Cerrato A, Degan M, De Iuliis A, Rossi F, Chiappetta G, Consales C, Improta S, Zagonel V, Aldinucci D, Agosti V, Santoro M, Vecchio G, Pinto A and Grieco M (1997). Expression of the RET receptor tyrosine kinase and GDNFR-alpha in normal and leukemic human hematopoietic cells and stromal cells of the bone marrow microenvironment. Blood 89: 2925-2937.

Gattei V, Degan M, Rossi FM, De Iuliis A, Mazzocco FT, Cesa E, Aldinucci D, Zagonel V and Pinto A (1999). The RET receptor tyrosine kinase, but not its specific ligand, GDNF, is preferentially expressed by acute leukaemias of monocytic phenotype and is up-regulated upon differentiation. Br. J. Haematol. 105: 225-240.

Golden JP, DeMaro JA, Osborne PA, Milbrandt J and Johnson EM Jr (1999). Expression of neurturin, GDNF, and GDNF family-receptor mRNA in the developing and mature mouse. Exp. Neurol. 158: 504-528.

Grieco M, Santoro M, Berlingieri MT, Melillo RM, Donghi R, Bongarzone I, Pierotti MA, Della Porta G, Fusco A and Vecchio G (1990). PTC is a novel rearranged form of the ret proto-oncogene is frequently detected in vivo in human thyroid papillary carcinomas. Cell 60: 557-563.

Grimm J, Sachs M, Britsch S, Di Cesare S, Schwartz-Romond T, Alitalo K and Birchmeier W (2001). Novel p62dok family members, dok-4 and dok-5, are substrates of the c-Ret receptor tyrosine kinase and mediate neuronal differentiation. J. Cell. Biol. 154: 345-354.

Grundstrom E, Lindholm D, Blennow K and Askmark H (2000). GDNF but not BDNF is increased in cerebrospinal fluid in amyotrophic lateral sclerosis. NeuroRep. 11: 1781-1783.

Corse AM, Coccia CF, Rothstein JD and Kuncl RW (1995). GDNF provides potent neuroprotection of motor neurons against chronic glutamate toxicity. Soc. Neurosci. Abs. 21: 544.

Grundstrom E, Askmark H, Lindeberg J, Nygren I, Ebendal T and Aquilonius SM (1999). Increased expression of glial cell line-derived neurotrophic factor mRNA in muscle biopsies from patients with amyotrophic lateral sclerosis. J. Neurol. Sci. 162: 169-173.

Hamilton JF, Morrison PF, Chen MY, Harvey-White J, Pernaute RS, Phillips H, Oldfield E and Bankiewicz KS (2001). Heparin coinfusion during convection-enhanced delivery (CED) increases the distribution of the glial-derived neurotrophic factor (GDNF) ligand family in rat striatum and enhances the pharmacological activity of neurturin. Exp. Neurol. 168: 155-161.

Hammarberg H, Piehl F, Cullheim S, Fjell J, Hokfelt T and Fried K (1996). GDNF mRNA in Schwann cells and DRG satellite cells after chronic sciatic nerve injury. NeuroRep. 7: 857-860.

Hashino E, Shero M, Junghans D, Rohrer H, Milbrandt J and Johnson EM Jr. (2001) GDNF and Neurturin are target-derived factors essential for cranial parasympathetic neuron development. Development 128: 3773-3782.

Heese K, Fiebich BL, Bauer J and Otten U (1998). NF-kappaB modulates lipopolysaccharide-induced microglial nerve growth factor expression. Glia 22: 401-407.

Hellmich HL, Kos L, Cho ES, Mahon KA and Zimmer A (1996). Embryonic expression of glial cell-line derived neurotrophic factor (GDNF) suggests multiple developmental roles in neural differentiation and epithelial-mesenchymal interactions. Mech Dev. 54: 95-105.

Henderson CE, Philips HS, Pollock RA, Davies AM, Lemeulle M, Armanini M, Simpson LC, Moffet B, Vandlen RA, Koliatsos VE and Rosenthal A (1994). GDNF: a potent survival factor for motoneurons present in peripheral nerve and muscle. Science 266: 1062-1064.

Heuckeroth RO, Kotzbauer P, Copeland NG, Gilbert DJ, Jenkins NA, Zimonjic DB, Popescu NC, Jhonson EM Jr. and Mildbrandt J (1997). Neurturin, a novel neurotrophic factor, is localized to mouse chromosome 17 and human chromosome 19p13.3. Genomics 44: 137-140.

Heuckeroth RO, Enomoto H, Grider J, Golden J, Jackman A, Molliver D, Bardgett M, Johnson E and Milbrandt J (1999). Gene targeting reveals a critical role for Neurturin in the development and maintenance of enteric, sensory, and parasympathetic neurons. Neuron 22: 253-263.

Hishiki T, Nimura Y, Isogai E, Kondo K, Ichimiya S, Nakamura Y, Ozaki T, Sakiyama S, Seki N, Takahashi H, Tanabe M and Nakagawara A (1998). Glial cell line-derived neurotrophic factor/neurturin-induced differentiation and its enhancement by retinoic acid in primary human neuroblastomas expressing c-Ret, GFR alpha-1, and GFR alpha-2. Cancer Res. 58: 2158-2165.

Ho A, Gore AC, Weickert CS and Blum M (1995). Glutamate regulation of GDNF gene expression in the striatum and primary striatal astrocytes. NeuroReport 6: 1454-1458.

Ho TW, Bristol LA, Coccia C, et al. (2000) TGFbeta trophic factors differentially modulate motor axon outgrowth and protection from excitotoxicity. Exp. Neurol. 161: 664-675.

Hohlfeld R, Kerschensteiner M, Stadelmann C, Lassmann H and Wekerle H (2000). The neuroprotective effect of inflammation: implications for the therapy of multiple sclerosis (Review). J. Neuroimmunol. 107: 161-166.

Honda S, Nakajima K, Nakamura Y, Imai Y and Kohsaka S (1999). Rat primary cultured microglia express glial cell line-derived neurotrophic factor receptors. Neurosci. Lett. 275: 203-206.

Horger BA, Nishimura MC, Aramanini MP, Wang L, Poulsen KT, Rosenblad C, Kirik D, Moffat B, Simmons L, Johnson Jr. E, Milbrandt J et al. (1998). Neurturin exerts potent actions on survival and function of midbrain dopaminergic neurons. J. Neurosci. 18: 4929-4937.

Houenou LJ, Oppenheim RW, Li L, Lo AC and Prevette D (1996). Regulation of spinal motoneuron survival by GDNF during development and following injury. Cell Tissue Res. 286: 219-223.

Hudson J, Granholm AC, Gerhardt GA, Henry MA, Hoffman A, Biddle P, Leela NS, Mackerlova L, Lile JD, Collins F and Hoffer BJ (1995). Glial-cell-line-derived neurotrophic factor augments midbrain dopaminergic circuits in vivo. Brain Res. Bull. 36: 425-432.

Ibáñez CF (1998). Emerging themes in structural biology of neurotrophic factors (Review). TINS 21: 438-444.

Igarashi Y, Utsumi H, Chiba H, Yamada-Sasamori Y, Tobioka H, Kamimura Y, Kokai Y, Mori M and Sawada N (1999). Glial cell line-derived neurotrophic factor induces barrier function of endothelial cells forming the blood-brain barrier. Biochem. Biophys. Res. Commun. 261: 108-112.

Ikeda I, Ishizaka Y, Tahira T, Suzuki T, Onda M, Sugimura T and Nagao M (1990). Specific expression of the ret proto-oncogene in human neuroblastoma cell lines. Oncogene 5: 1291-1296.

Ilangumaran S, He HT and Hoessli DC (2000). Microdomains in lymphocyte signalling: beyond GPI-anchored proteins. Immunol. Today. 21: 2-7.

Ishiguro Y, Iwashita T, Murakami H, Asai N, Iida K, Goto H, Hayakawa T and Takahashi M (1999). The role of amino acids surrounding tyrosine 1062 in ret in specific binding of the shc phosphotyrosine-binding domain. Endocrinology 140: 3992-3998.

Ishizaka Y, Itoh F, Tahira T, Ikeda I, Sugimura T, Tucker J, Fertitta A, Carrano AV and Nagao M (1989). Human ret proto-oncogene mapped to chromosome 10q11.2. Oncogene 4: 1519-1521.

Ivanchuck SM, Eng C, Cavenee WK and Mulligan LM (1997). The expression of RET and its multiple splice isoforms in developing human kidney. Oncogene 14: 1811-1818.

Ivanchuck SM, Myers SM and Mulligan LM (1998). Expression of RET 3' splicing variants during human kidney development. Oncogene 16: 991-996.

Iwahashi N, Nagasaka T, Tezel G, Iwashita T, Asai N, Murakumo Y, Kiuchi K, Sakata K, Nimura Y and Takahashi M (2002). Expression of glial cell line-derived neurotrophic factor correlates with perineural invasion of bile duct carcinoma. Cancer 94: 167-174.

Janeway Ch, Travers P, Walport M and Capra D (1999). Immunobiology: the immune system in health and disease. 4th Edition. Current Biology Publications, Churchill Livingstone, Garland Publishing.

Jaszai J, Farkas L, Galter D, Reuss B, Strelau J, Unsicker K and Krieglstein K (2000). GDNF-related factor persephin is widely distributed throughout the nervous system. J. Neurosci. Res. 53: 494-501.

Jing S, Wen D, Yu Y, Holst PL, Luo Y, Fang M, Tamir R, Antonio L, Hu Z, Cupples R, Louis JC, Hu S, Altrock BW and Fox GM (1996). GDNF-induced activation of the ret protein tyrosine kinase is mediated by GDNFR-alpha, a novel receptor for GDNF. Cell 85: 1113-1124.

Kami K, Morikawa Y, Kawai Y and Senba E (1999). Leukemia inhibitory factor, glial cell line-derived neurotrophic factor and their receptor expressions following muscle crush injury. Muscle Nerve 22: 1576-1586.

Kawamoto Y, Nakamura S, Matsuo A, Akiguchi I and Shibasaki H (2000a). Immunohistochemical localization of glial cell line-derived neurotrophic factor in the human central nervous system. Neurosci. 100: 701-712.

Kawamoto Y, Nakamura S, Matsuo A and Akiguchi I (2000b). Glial cell line-derived neurotrophic factor-like immunoreactivity in the cerebella of normal subjects and patients with multiple system atrophy. Act. Neuropath. 100: 131-137.

Kearns CM and Gash DM (1995). GDNF protects nigral dopamine neurons against 6-hydroxydopamine in vivo. Brain Res. 672: 101-111.

Keller-Peck CR, Feng G, Sanes JR, Yan Q, Lichtman JW and Snider WD (2001). Glial cell line-derived neurotrophic factor administration in postnatal life results in motor unit enlargement and continuous synaptic remodeling at the neuromuscular junction. J Neurosci. 21: 6136-6146.

Kerschensteiner M, Gallmeier E, Behrens L, Vargas V, Misgeld T, Klinkert W, Kolbeck R, Oropeza-Wekerle R, Stadelmann C, Lassmann H, Wekerle H and Hohlfeld R (1999). Activated human T cells, B cells and monocytes produce brain-derived neurotrophic factor in vitro and in inflammatory brain lesions: a neuroprotective role of inflammation? J. Exp. Med. 189: 865-870

Kerschensteiner M, Stadelmann C, Dechant G, Wekerle H and Hohlfeld R (2003). Neurotrophic cross-talk between the nervous and immune systems: implications for neurological diseases. Ann. Neurol. 53: 292-304.

Kiefer R, Kieseier BC, Bruck W, Hartung HP and Toyka KV (1998). Macrophage differentiation antigens in acute and chronic autoimmune polyneuropathies. Brain 121: 469-479.

Klein RD, Sherman D, Ho WH, Stone D, Bennett GL, Moffat B, Vandlen R, Simmons L, Gu Q, Hongo JA, Devaux B, Poulsen K, Armanini M, Nozaki C, Asai N, Goddard A, Phillips H, Henderson CE, Takahashi M and Rosenthal A (1997). A GPI-linked protein that interacts with Ret to form a candidate neurturin receptor. Nature 387: 717-721.

Kokaia Z, Airaksinen MS, Nanobashvili A, Larsson E, Kujamaki E, Lindvall O and Saarma M (1999). GDNF family ligands and receptors are differentially regulated after brain insults in the rat. Eur. J. Neurosci. 11: 1202-1216.

Kordower JH, Palfi S, Chen E, Ma S, Sendera T, Cochran J, Mufson EJ, Penn R, Goetz CG and Comella CD (1999). Clinicopathological findings following intraventricular Glial-Derived Neurotrophic Factor treatment in a patient with Parkinson's disease. Ann. Neurol. 46: 419-424.

Kotzbauer PT, Lampe PA, Heuckeroyh RO, Golden JP, Creedon DJ, Johnson EM and Mildbrandt J (1996). Neurturin, a relative of glial cell line-derived neurotrophic factor. Nature 384: 467-470.

Krieglstein K, Henheik P, Farkas L, Jaszai J, Galter D, Krohn K and Unsicker K (1998). Glial cell line-derived neurotrophic factor requires transforming growth factor-beta for exerting its full neurotrophic potential on peripheral and CNS neurons. J. Neurosci. 18: 9822-9834.

Kwok JB, Gardner E, Warner JP, Ponder BA and Mulligan LM (1993). Structural analysis of the human RET proto-oncogene using exon trapping. Oncogene 8: 2575-2582.

Lapchak PA, Jiao S, Collins F and Miller PJ (1997a). GDNF: Distribution and pharmacology in the rat following a bolus intraventricular injection. Brain Res. 747: 92-102.

Lapchak PA, Miller PJ, and Jiao S (1997b). Glial cell line-derived neurotrophic factor induces the dopaminergic and cholinergic phenotype and increases locomotor activity in aged Fisher 344 rats. Neurosci. 77: 745-752.

Lapchak PA, Gash DM, Collins F, Hilt D, Miller PJ and Araujo DM (1997c). Pharmacological activities of Glial Cell Line-Derived Neurotrophic Factor (GDNF): Preclinical development and application to the treatment of Parkinson's Disease (Review). Exp. Neurol. 145: 309-321.

Lapchak PA, Araujo DM, Hilt D, Jiao S, Collin F, Zhang Z and Gash DM (1998a). Topographical distribution of [125I]-glial cell line-derived neurotrophic factor in unlesioned and MPTP-lesioned rhesus monkey brain following a bolus intraventricular injection. Brain Res. 789: 9-22.

Lapchak PA (1998b). A preclinical development strategy designed to optimize the use of Glial cell line-Derived Neurotrophic Factor in the treatment of Parkinson's disease. Mov. Disor. 13: 49-54.

Laurenzi MA, Barbany G, Timmusk T, Lindgren JA and Persson H (1994). Expression of mRNA encoding neurotrophins and neurotrophin receptors in rat thymus, spleen tissue and immunocompetent cells. Regulation of neurotrophin-4 mRNA expression by mitogens and leukotriene B4. Eur. J. Biochem. 223: 733-741.

Laurikainen A, Hiltunen JO, Thomas-Crusells J, Vanhatalo S, Arumae U, Airaksinen MS, Klinge E and Saarma M (2000). Neurturin is a neurotrophic factor for penile parasympathetic neurons in adult rat. J. Neurobiol. 43: 198-205.

Lee R, Kermani P, Teng KK and Hempstead BL (2001). Regulation of cell survival by secreted proneurotrophins. Science 294: 1945-1948.

Leon A, Buriani A, Dal Toso R, Fabris M, Romanello S, Aloe L and Levi-Montalcini R (1994). Mast cells synthesize, store, and release nerve growth factor. Proc. Natl. Acad. Sci. USA. 91: 3739-3743.

Levi-Montalcini R (1987). The nerve growth factor 35 years later. Science 237: 1154-1162.

Lewin GR and Barde YA (1996). Physiology of the neurotrophins. Ann. Rev. Neurosci. 19: 289-317.

Li L, Wu W, Lin LF, Lei M, Oppenheim R and Houenou LJ (1995). Rescue of adult motoneurons from injury-induced cell death by GDNF. Proc. Natl. Acad. Sci. USA. 92: 9771-9775.

Lie DC and Weis J (1998). GDNF expression is increased in denervated human skeletal muscle. Neurosci. Lett. 250: 87-90.

Lin LF, Doherty DH, Lile JD, Bektesh S and Collins F (1993). GDNF: a glial cell line-derived neurotrophic factor for midbrain dopaminergic neurons. Science 260: 1130-1132.

Lindahl M, Timmusk T, Saarma M and Airaksinen MS (2000). Expression and alternative splicing of mouse GFRα4 suggest roles in endocrine cell development. Mol. Cell. Neurosci. 15: 522-533.

Lindahl M, Poteryaev D, Yu L, Arumae U, Timmusk T, Bongarzone I, Aiello A, Pierotti MA, Airaksinen MS and Saarma M (2001). Human glial cell line-derived neurotrophic factor receptor alpha 4 is the receptor for persephin and is predominantly expressed in normal and malignant thyroid medullary cells. J. Biol. Chem. 276: 9344-9351.

Linnarsson S, Mikaels A, Baudet and Ernfors P (2001). Activation by GDNF of a transcriptional program repressing neurite growth in dorsal root ganglia. Proc. Natl. Acad. Sci. USA.. 98: 14681-86.

Liu X, Vega Q, Decker R, Worby C and Dixon J (1996). Oncogenic RET receptors display different autophosphorylation sites and substrate binding specificities. J. Biol. Chem. 271: 5309-5312.

Lorenzo MJ, Eng C, Mulligan L, Stonehouse T, Ponder B and Smith D (1995). Multiple mRNA isoforms of the human RET proto-oncogene generated by alternate splicing. Oncogene 10: 1377-1383.

Lorenzo MJ, Gish GD, Houghton C, Stonehouse TJ, Pawson T, Ponder BA and Smith DP (1997). RET alternate splicing influences the interaction of activated RET with the SH2 and PTB domains of Shc, and the SH2 domain of Grb2. Oncogene 14: 763-771.

Maier SF, Watkins LR and Fleshner R (1994). Psychoneuroimmunology. The interface between behavior, brain, and immunity (Review). Am. Psychol. 49: 1004-1007.

Maier SF and Watkins LR (1998). Cytokines for psychologists: implications of bidirectional immune-to-brain communication for understanding behavior, mood, and cognition (Review). Psychol. Rev. 105: 83-107.

Marshall GM, Peaston AE, Hocker JE, Smith SA, Hansford LM, Tobias V, Norris MD, Haber M, Smith DP, Lorenzo MJ, Ponder BA and Hancock JF (1997). Expression of multiple endocrine neoplasia 2B RET in neuroblastoma cells alters cell adhesion in vitro, enhances metastatic behavior in vivo, and activates Jun kinase. Cancer Res. 57: 5399-5405.

Martin D, Miller G, Rosendahl M and Russell DA (1995). Potent inhibitory effects of glial derived neurotrophic factor against kainic acid mediated seizures in the rat. Brain Res. 683: 172-178.

Martucciello G, Favre A, Takahashi M and Jasonni V (1995). Immunohistochemical localization of RET protein in Hirschsprung's disease. J. Pediatr. Surg. 30: 433-436.

Masure S, Geerts H, Cik M, Hoefnagel E, Van Den Kieboom G, Tuytelaars A, Harris S, Leysen J, Van Der Helm, Verhasselt P, Yon J and Gordon RD (1999). Enovin, a member of the glial cell-line-derived neurotrophic factor family with growth promoting activity on neuronal cells. Existence and tissue-specific expression of different splice variants. Eur. J. Biochem. 266: 892-902.

Masure S, Cik M, Hoefnagel E, Nosrat CA, et al. (2000). Mammalian GFRalpha-4, a divergent member of the GFRalpha family of coreceptors for glial cell line-derived neurotrophic factor

family ligands, is a receptor for the neurotrophic factor persephin. J. Biol. Chem. 275: 39427-39434.

Matheson CR, Carnahan J, Urich JL, Bocangel D, Zhang TJ and Yan Q (1997). Glial cell line-derived neurotrophic factor (GDNF) is a neurotrophic factor for sensory neurons: comparison with the effects of the neurotrophins. J. Neurobiol. 32: 22-32.

Matsuda H, Coughlin MD, Bienenstock J and Denburg JA (1988). Nerve growth factor promotes human hemopoietic colony growth and differentiation. Proc. Natl. Acad. Sci. USA. 85: 6508-6512.

Mazurek N, Weskamp G, Erne P and Otten U (1986). Nerve growth factor induces mast cell degranulation without changing intracellular calcium levels. FEBS Lett. 198: 315-320.

McDonald NQ and Hendrickson WA (1993). A structural superfamily of Growth Factors containing a Cysteine Knot Motif (Minireview). Cell 73: 421-424.

Meng X, Lindahl M, Hyvonen ME, Parvinen M, de Rooij DG, Hess MW, Raatikainen-Ahokas A, Sainio K, Rauvala H, Lakso M, Pichel J, Westphal H, Saarma M and Sariola H (2000). Regulation of cell fate decision of undifferentiated spermatogonia by GDNF. Science 287: 1489-1493.

Mildbrandt J, de Sauvage FJ, Fahmer TJ, Baloh RH, Leitner ML, Tansey MG, Lampe PA, Heuckeroth RO, Kotzbauer PT, Simburger KS et al. (1998). Persephin, a novel nerotrophic factor related to GDNF and neurturin. Neuron 20: 245-253.

Miyamoto S, Teramoto H, Gutkind JS and Yamada KM (1996). Integrins can collaborate with growth factors for phosphorylation of receptor tyrosine kinases and MAP kinase activation: roles of integrin aggregation and occupancy of receptors. J. Cell. Biol. 135: 1633-1642.

Miyazaki H, Okuma Y, Fujii Y, Nagashima K and Nomura Y (1999). Glial cell line-derived neurotrophic factor protects against delayed neuronal death after transient forebrain ischemia in rats. Neurosci. 89: 643-647.

Miyazaki H, Nagashima K, Okuma Y and Nomura Y (2002). Expression of Ret receptor tyrosine kinase after transient forebrain ischemia is modulated by glial cell line-derived neurotrophic factor in rat hippocampus. Neurosci. Lett. 318: 1-4.

Moalem G, Leibowitz R, Mor F, Cohen I and Schwartz M (1999). Autoimmune T cells protect neurons from secondary degeneration after central nervous system axotomy. Nat. Med. 5: 49-55.

Moalem G, Gdalyahu A, Shani Y, Otten U, Lazarovici P, Cohen IR and Schwartz M (2000). Production of neurotrophins by activated T cells: implications for neuroprotective autoimmunity. J. Autoimmunity 15: 331-345.

Molliver D, Wright D, Leitner ML, Parsadanian AS, Doster K, Wen D, Yan Q and Snider WD (1997). IB4-binding DRG neurons switch from NGF to GDNF dependence in early post-natal life. Neuron 19: 849-861.

Moore MW, Klein RD, Farinas I, Sauer H, Armanini M, Phillips H, Reichardt LF, Ryan AM, Carver-Moore K and Rosenthal A (1996). Renal and neuronal abnormalities in mice lacking GDNF. Nature 382: 76-79.

Moretto G, Walker DG, Lanteri P, Taioli F, Zaffagnini S, Xu RY and Rizzuto N (1996). Expression and regulation of glial-cell-line-derived neurotrophic factor (GDNF) mRNA in human astrocytes in vitro. Cell Tissue Res. 286: 257-262.

Morrison SJ, Uchida N and Weissman IL (1995). The biology of hematopoietic stem cells (Review). Ann. Rev. Cell. Dev. Biol. 11: 35-71.

Mount HT, Dean DO, Alberch J, Dreyfus CF and Black IB (1995). Glial cell line-derived neurotrophic factor promotes the survival and morphologic differentiation of Purkinje cells. Proc. Natl. Acad. Sci. USA. 92: 9092-9096.

Mulligan LM, Eng C, Healey CS, Clayton D, Kwok JB, Gardner E, Ponder MA, Frilling A, Jackson CE, Lehnert H, et al. (1994). Specific mutations of the RET proto-oncogene are related to disease phenotype in MEN 2A and FMTC. Nat. Genet. 6: 70-74.

Muniz M and Reizman H (2000). Intracellular transport of GPI-anchored proteins. EMBO J. 19: 10-15.
Myers SM, Eng C, Ponder BA and Mulligan L (1989). Characterization of RET proto-oncogene 3' splicing variants and polyadenylation sites: a novel C-terminus for RET. Oncogene 4: 2039-2045.

Nakayama S, Iida K, Tsuzuki T, Iwashita T, Murakami H, Iwata Y, Ichihara M, Ito S, Kawai K, Asai M, Kurokawa K and Takahashi M (1999). Implication of expression of GDNF/Ret signaling components in differentiation of bone marrow haemopoietic cells. Brit. J. Haematol. 105: 50-57.

Nanobashvili A, Airaksinen MS, Kokaia M, Rossi J, Asztely F, Olofsdotter K, Mohapel P, Saarma M, Lindvall O and Kokaia Z (2000). Development and persistence of kindling epilepsy are impaired in mice lacking glial cell line-derived neurotrophic factor family receptor alpha 2. Proc. Natl. Acad. Sci. USA. 97: 12312-12317.

Naveilhan P, Baudet C, Mikaels A, Shen L, Westphal H and Ernforns P (1998). Expression and regulation of GFRα-3, a glial cell line-derived neurotrophic factor family receptor. Proc. Natl. Acad. Sci. USA. 95: 1295-1300.

Nguyen QT, Parsadanian AS, Snider WD and Lichtman JW (1998). Hyperinnervation of neuromuscular junctions caused by GDNF overexpression in muscle. Science 279: 1725-1729.

Nomenclature of GPI-linked receptors for the GDNF ligand family. GFR(alpha) Nomenclature Committee (1997). Neuron 19: 485.

Nosrat CA, Tomac A, Lindqvist E, Lindskog S, Humpel C, Stromberg I, Ebendal T, Hoffer BJ and Olson L (1996). Cellular expression of GDNF mRNA suggests multiple functions inside and outside the nervous system. Cell Tissue Res. 286: 191-207.

Nosrat CA, Tomac A, Hoffer BJ and Olson L (1997). Cellular and developmental patterns of expression of Ret and glial cell line-derived neurotrophic factor receptor alpha mRNAs. Exp. Brain. Res. 115: 410-422.

Nozaki C, Asai N, Murakami H, Iwashita T, Iwata Y, Klein R, Rosenthal A and Takahashi M (1998). Calcium-dependent Ret activation by GDNF and Neurturin. Oncogene 16: 293-299.

NuPAGE™ Electrophoresis System (1999). Instruction Booklet. Novex™.

Okragly AJ and Haak-Frendscho M (1997). An acid-treatment method for the enhanced detection of GDNF in biological samples. Exp. Neurol. 145: 592-596.

Oppenheim RW, Houenou LJ, Johnson JE, Lin LF, Li L, Lo AC, Newsome AL, Prevette DM and Wang S (1995). Developing motor neurons rescued from programmed and axotomy-induced cell death by GDNF. Nature 363: 344-346.

Otten U, Ehrhard P and Peck R (1989). Nerve growth factor induces growth and differentiation of human B lymphocytes. Proc. Natl. Acad. Sci. USA. 86: 10059-10063.

Pachnis V, Mankoo B and Costantini F (1993). Expression of the c-ret proto-oncogene during mouse embryogenesis. Development 119: 1005-1017.

Paratcha G, Ledda F, Baars L, Coulpier M, Besset V, Anders J, Scott R and Ibanez CF (2001). Released GFRalpha1 potentiates downstream signaling, neuronal survival, and differentiation via a novel mechanism of recruitment of c-Ret to lipid rafts. Neuron 29: 171-184.

Pezeshki G, Franke B and Engele J (2001). Evidence for a ligand-specific signaling through GFRalpha-1, but not GFRalpha-2, in the absence of Ret. J. Neurosci. Res. 66: 390-395.

Pichel JG, Shen L, Sheng HZ, Granholm AC, et al. (1996). Defects in enteric innervation and kidney development in mice lacking GDNF. Nature 382: 73-76.

Ramer MS, Priestley JV and McMahon SB (2000). Functional regeneration of sensory axons into the adult spinal cord. Nature 403: 312-316.

Rapalino O, Lazarov-Spiegler O, Agranov E, Velan GJ, Yoles E, Fraidakis M, Solomon A, Gepstein R, Katz A, Belkin M, Hadani M and Schwartz M (1998). Implantation of stimulated homologous macrophages results in partial recovery of paraplegic rats. Nature Med. 4: 814-821.

Remy S, Naveilhan P, Brachet P and Neveu I (2001). Differential regulation of GDNF, neurturin, and their receptors in primary cultures of rat glial cells. J. Neurosci. Res. 64: 242-251.

Romeo G, Ronchetto P, Luo Y, Barone V, Seri M, Ceccherini I, Pasini B, Bocciardi R, Lerone M, Kaariainen H, et al. (1994). Point mutations affecting the tyrosine kinase domain of the RET proto-oncogene in Hirschsprung's disease. Nature 367: 377-378.

Rosenblad C, Gronborg M, Hansen C, Blom N, Meyer M, Johansen J, Dago L, Lundberg C, Trono D and Johansen TE (2000a). In vivo protection of nigral dopamine neurons by lentiviral gene transfer of the novel GDNF-family member neublastin/artemin. Mol. Cell. Neurosci. 15: 199-214.

Rosenblad C, Kirik D and Björklund A (2000b). Sequential administration of GDNF into substantia nigra and striatum promotes dopamine neuron survival and axonal sprouting but not striatal reinnervation or functional recovery in the partial 6-OHDA lesion model. Exp. Neurol. 161: 503-516.

Rossi J, Luuko K, Poteryaev D, Laurikainen A, Sun Y, Laakso T, Eerikaeinen S, Arumae U, Saarma M and Airaksinen MS (1999). Retarded growth and deficits in the enteric and parasympathetic nervous system in mice lacking GFRα2, a functional neurturin receptor. Neuron 22: 243-252.

Saarma M (2000). GDNF- a stranger in the TGF-β superfamily? Eur. J. Biochem. 267: 6968-6971.

Saarma M (2001). GDNF recruits the signaling crew into lipid rafts (Review). Trends Neurosci. 24: 427-429.

Sainio K, Suvanto P, Davies J, Wartiovaara J, Wartiovaara K, Saarma M, Arumae U, Meng X, Lindahl M, Pachnis V and Sariola H (1997). Glial-cell-line-derived neurotrophic factor is required for bud initiation from ureteric epithelium. Development 124: 4077-4087.

Sakai T, Nirasawa Y, Itoh Y and Wakizaka A (2000). Japanese patients with sporadic Hirschsprung: mutation analysis of the receptor tyrosine kinase proto-oncogene, endothelin-B receptor, endothelin-3, glial cell line-derived neurotrophic factor and neurturin genes: a comparison with similar studies. Eur. J. Pediatr. 159: 160-167.

Sanchez MP, Silos-Santiago I, Frisen J, He B, Lira SA and Barbacid M (1996). Renal agenesis and the absence of enteric neurons in mice lacking GDNF. Nature 382: 70-73.

Sanicola M, Hession C, Worley D, Carmillo P, Ehrenfels C, Walus L, Robinson S, Jaworski G, Wei H, Tizard R, Whitty A, Pepinsky RB and Cate RL (1997). Glial cell line-derived neurotrophic factor-dependent RET activation can be mediated by two different cell-surface accessory proteins. Proc. Natl. Acad. Sci. USA. 94: 6238-6243.

Santambrogio L, Benedetti M, Chao MV, Muzaffar R, Kullig K, Gabellini N and Hochwald G (1994). Nerve growth factor production by lymphocytes. J. Immunol. 153: 4488-4495.

Santoro M, Rosati R, Grieco M, Berlingieri MT, D'Amato GL, de Franciscis V and Fusco A (1990). The ret proto-oncogene is consistently expressed in human pheochromocytomas and thyroid medullary carcinomas. Oncogene 5: 1595-1598.

Santoro M, Melillo RM, Carlomagno F, Visconti R, De Vita G, Salvatore G, Fusco A and Vecchio G (1999). Different mutations of the RET gene cause different human tumoral diseases (Review). Biochimie 81: 397-402.

Sauer H, Rosenblad C and Bjorklund A (1995). Glial cell line-derived neurotrophic factor but not transforming growth factor β3 prevents delayed degeneration of nigral neurons following striatal 6-hydroxydopamine lesions. Proc. Natl. Acad. Sci. USA. 92: 8935-8939.

Sawai H, Clarke DB, Kittlerova P, Bray GM and Aguayo AJ (1996). Brain-derived neurotrophic factor and neurotrophin-4/5 stimulate growth of axonal branches from regenerating retinal ganglion cells. J. Neurosci. 16: 3887-3894.

Scharr DG, Sieber BA, Dreyfus CF and Black I (1993). Regional and cell-specific expression of GDNF in rat brain. Exp. Neurol. 124: 368-371.

Schlessinger J (2000). Cell signaling by Receptor Tyrosine Kinases (Review). Cell 103: 211-225.

Schuchart A, D'Agati V, Larsson L, Constantini F and Pachnis V (1994). Defects in the kidney and enteric nervous system of mice lacking the tyrosine kinase receptor RET. Nature 367: 380-383.

Schwartz M, Moalem G, Leibowitz-Amit R and Cohen IR (1999). Innate and adaptive immune responses can be beneficial for CNS repair. TINS 22: 295-299.

Scott RP and Ibanez CF (2001). Determinants of ligand binding specificity in the GDNF family receptor alphas (GFRs). J. Biol. Chem. 276: 1450-1458.

Semkova I and Krieglstein J (1999). Neuroprotection mediated via neurotrophic factors and induction of neurotrophic factors. Brain Res. Rev. 30: 176-188.

Sendtner M, Holtman B, Kolbeck R, Thoenen H and Barde YA (1992). Brain-derived neurotrophic factor prevents the death of motoneurons in newborn rats after nerve section. Nature 360: 757-760.

Shu X and Mendell L (1999). Neurotrophins and hyperalgesia. Proc. Nat. Acad. Sci. USA. 96: 7693-7696.

Shultz CW, Kimber T and Martin D (1996). Intrastriatal injections of GDNF attenuates the effects of 6-hydroxydopamine. NeuroRep. 7: 627-631.

Small D, Levenstein M, Kim E, Carow C, Amin S, Rockwell P, Witte L, Burrow C, Ratajczak MZ, Gewirtz AM, et al. (1994). STK-1, the human homolog of Flk-2/Flt-3 is selectively expressed in CD34+ human bone marrow cells and is involved in the proliferation of early progenitor/stem cells. Proc. Natl. Acad. Sci. USA. 91: 459-463.

Snider WD and Wright DE (1996). Neurotrophins cause a new sensation. Neuron 16: 229-232.

Snider WD and McMahon SB (1998). Tackling pain at the source: new ideas about nociceptors (Minireview). Neuron 20: 629-632.

Solomon A, Aloe L, Pe'er J, Frucht Pery J, Bonini S and Levi-Schaffer F (1998). Nerve growth factor is preformed in and activates human peripheral blood eosinophils. J. Allergy Clin. Immunol. 102: 454-460.

Springer JE, Seeburger JL, He J, Gabrea A, Blankenhorn EP and Bergman LW (1995). cDNA sequence and differential mRNA regulation of two forms of glial cell line-derived neurotrophic factor in Schwann cells and rat skeletal muscle. Exp. Neurol. 131: 47-52.

Stadelmann C, Kerschensteiner M, Misgeld T, Bruck W, Hohlfeld R and Lassmann H (2002). BDNF and gp145trkB in multiple sclerosis brain lesions: neuroprotective interactions between immune and neuronal cells? Brain 125: 75-85.

Strelau J and Unsicker K (1999). GDNF family members and their receptors: expression and functions in two oligodendroglial cell lines representing distinct stages of oligodendroglial development. Glia 26: 291-301.

Stromberg I, Bjorklund L, Johansson M, Tomac A, Collins F, Olson L, Hoffer BJ and Humpel C (1993). Glial cell line-derived neurotrophic factor is expressed in the developing but not adult striatum and stimulates developing dopamine neurons in vivo. Exp. Neurol. 124: 401-412.

Suter-Crazzolara C and Unsicker K (1994). GDNF is expressed in two forms in many tissues outside the CNS. NeuroRep. 5: 2486-2488.

Suzuki H, Hase A, Miyata Y, Arahata K and Akazawa Ch (1998a). Prominent expression of glial cell line-derived neurotrophic factor in human skeletal muscle. J. Comp. Neurol. 402: 303-312.

Suzuki H, Hase A, Kim BY, Miyata Y, Nonaka I, Arahata K and Akazawa C (1998b). Up-regulation of glial cell line-derived neurotrophic factor (GDNF) expression in regenerating muscle fibers in neuromuscular diseases. Neurosci. Lett. 257: 165-167.

Tahira T, Ishizaka Y, Sugimura T and Nagao M (1988). Expression of proto-ret mRNA in embryonic and adult rat tissues. Biochem. Biophys. Res. Commun. 153: 1290-1295.

Tahira T, Ishizaka Y, Itoh F, Sugimura T and Nagao M (1990). Characterization of ret proto-oncogene mRNAs encoding two isoforms of the protein product in a human neuroblastoma cell line. Oncogene 5: 97-102.

Takahashi M, Rity J and Cooper GM (1985). Activation of a novel human transforming gene, *ret*, by DNA rearrangement. Cell 42: 581-588.

Takahashi M and Cooper GM (1987). Ret transforming gene encodes a fusion protein homologous to tyrosine kinases. Mol. Cell. Biol. 7: 1378-1385.

Takahashi M, Buma Y, Iwamoto T, Inaguma Y, Ikeda H and Hiai H (1988). Cloning and expression of the ret proto-oncogene encoding a tyrosine kinase with two potential transmembrane domains. Oncogene 3: 571-578.

Takahashi M, Buma Y and Hiai H (1989). Isolation of ret proto-oncogene cDNA with an amino-terminal signal sequence. Oncogene 4: 805-806.

Takahashi M, Buma Y and Taniguchi M (1991). Identification of the ret proto-oncogene products in neuroblastoma and leukemia cells. Oncogene 6: 297-301.

Takahashi M, Vandlen R, Henderson CE and Rosenthal A (1996). Characterization of a multicomponent receptor for GDNF. Nature 382: 80-83.

Takahashi M (2001). The GDNF/RET signaling pathway and human diseases (Review). Cytok. Growth. Fact. Rev. 12: 361-373.

Tang MJ, Worley D, Sanicola M and Dressler GR (1998). The RET-glial cell-derived neurotrophic factor (GDNF) pathway stimulates migration and chemoattraction of epithelial cells. J. Cell. Biol. 142: 1337-1345.

Thoenen H (1995). Neurotrophins and neuronal plasticity. Science 270: 593-598.

Thorpe LW and Perez Polo JR (1987). The influence of nerve growth factor on the in vitro proliferative response of rat spleen lymphocytes. J. Neurosci. Res. 18: 134-139.

Tolbert DL, Bradley MW, Tolod EG, Torres-Aleman I and Clark BR (2001). Chronic intraventricular infusion of Glial Cell Line-Derived Neurotrophic Factor (GDNF) rescues some cerebellar Purkinje cells from heredodegeneration. Exp. Neurol. 170: 375-379.

Tomac A, Lindqvist E, Lin LF, Ogren SO, Young D, Hoffer BJ and Olson L (1995a). Protection and repair of nigrostriatal dopaminergic neurons by GDNF in vivo. Nature 373: 335-339.

Tomac A, Widenfalk J, Lin LF, Kohno T, Ebendal T, Hoffer BJ and Olson L (1995b). Retrograde axonal transport of GDNF in the adult nigrostriatal system suggests a trophic role in the adult. Proc. Natl. Acad. Sci. USA. 92: 8274-8278.

Tomac AC, Agulnick AD, Haughey N, Chang CF, Zhang Y, Backman C, Morales M, Mattson MP, Wang Y, Westphal H and Hoffer BJ (2002). Effects of cerebral ischemia in mice deficient in Persephin. Proc. Natl. Acad. Sci. USA. 99: 9521-9526.

Torcia M, Bracci Laudiero L, Lucibello M, Nencioni L, Labardi D, Rubartelli A, Cozzolino F, Aloe L and Garaci E (1996). Nerve growth factor is an autocrine survival factor for memory B lymphocytes. Cell 85: 345-356.

Treanor JJ, Goodman L, de Sauvage F, Stone DM, Poulsen KT, Beck CD, Gray C, Armanini MP, Pollock RA, Hefti F, Phillips HS, Goddard A, Moore MW, Buj-Bello A, Davies AM, Asai N, Trupp M, Arenas E, Fainzilber M, Nilsson AS, Sieber BA, Grigoriou M, Kilkenny C, Salazar-Grueso E, Pachnis V and Arumae U (1996). Functional receptor for GDNF encoded by the c-RET proto-oncogene. Nature 381: 785-789.

Trupp M, Ryden M, Jornvall H, Funakoshi H, Timmusk T, Arenas E and Ibanez CF (1995). Peripheral expression and biological activities of GDNF, a new neurotrophic factor for avian and mammalian peripheral neurons. J. Cell. Biol. 130: 137-148.

Trupp M, Belluardo N, Funakoshi H and Ibanez CF (1997). Complementary and overlapping expression of GDNF, c-RET proto-oncogene, and GDNF receptor-alpha indicates multiple mechanisms of trophic actions in the adult rat CNS. J. Neurosci. 17: 3554-3567.

Trupp M, Raynoschek C, Belluardo N and Ibanez CF (1998). Multiple GPI-anchored receptors control GDNF-dependent and independent activation of the c-RET receptor tyrosine kinase. Mol. Cell. Neurosci. 11: 47-63.

Trupp M, Scott R, Whittemore SR and Ibanez CF (1999). Ret-dependent and -independent mechanisms of glial cell line-derived neurotrophic factor signaling in neuronal cells. J. Biol. Chem. 274: 20885-20894.

Tseng JL, Bruhn SL, Zurn AD and Aebischer P (1998). Neurturin protects dopaminergic neurons following medial forebrain bundle axotomy. NeuroRep. 9: 1817-1822.

Tsui-Pierchala BA, Milbrandt J and Johnson EM Jr. (2002) NGF utilizes c-Ret via a novel GFL-independent, inter-RTK signaling mechanism to maintain the trophic status of mature sympathetic neurons. Neuron 33: 261-273.

Tsuzuki T, Takahashi M, Asai N, Iwashita T, Matsuyama M and Asai J (1995). Spatial and temporal expression of the ret proto-oncogene product in embryonic, infant and adult rat tissues. Oncogene 10: 191-198.

Unsicker K (1996). GDNF: a cytokine at the interface of TGF-βs and neurotrophins (Minireview). Cell 286: 175-178.

Urbano AG, Suarez-Penaranda JM, Dieguez C and Alvarez CV (2000). GDNF and RET-gene expression in anterior pituitary-cell types. Endocrinology 141: 1893-1896.

Vanhorne JB, Gimm O, Myers SM, Kaushik A, von Deimling A, Eng C and Mulligan LM (2001). Cloning and characterization of the human GFRα2 locus and investigation of the gene in Hirschsprung disease. Hum. Genet. 108: 409-415.

Van Weering DH, de Rooij J, Marte B, Downward J, Bos JL and Burgering BM (1998). Protein kinase B activation and lamellipodium formation are independent phosphoinositide 3-kinase-mediated events differentially regulated by endogenous Ras. Mol. Cell. Biol. 18: 1802-1811.

Verity AN, Wyatt TL, Lee W, Hajos B, Baecker PA, Eglen RM and Johnson RM (1999). Differential regulation of glial cell line-derived neurotrophic factor (GDNF) expression in human neuroblastoma and glioblastoma cell lines. J. Neurosci. Res. 55: 187-197.

Wang Y, Lin SZ, Chiou AL, Williams L and Hoffer BJ (1997). Glial cell line-derived neurotrophic factor protects against ischemia-induced injury in the cerebral cortex. J. Neurosci. 17: 4341-4348.

Wang C, Jiang H, Hsu T, Dugich M, Feng L, Zhang M and Lu B (1998). Cloning and characterisation of glial cell line-derived neurotrophic factor receptor-B: A novel receptor for members of Glial cell line-Derived Neurotrophic Factor Family of neurotrophic factors. Neurosci. 83: 7-14.

Wasserman R, Li Y and Hardy R (1995). Differential expression of the blk and ret tyrosine kinases during B lineage development is dependent on Ig rearrangement. J. Immunol. 155: 644-651.

Watkins LR and Maier SF (1999). Implications of immune-to-brain communication for sickness and pain. Proc. Natl. Acad. Sci. USA. 96: 7710-7713.

Weiss FU, Daub H and Ullrich A (1997). Novel mechanisms of RTK signal generation (Review). Curr. Opin. Genet. Dev. 7: 80-86.

Widenfalk J, Nosrat C, Tomac A, Westphal H, Hoffer B and Olson L (1997). Neurturin and glial cell line-derived neurotrophic factor receptor-b (GDNF-b), novel proteins related to GDNF and GDNF-α with specific cellular patterns of expression suggesting roles in the developing and adult nervous system and in peripheral organs. J. Neurosci. 17: 8506-8519.

Widenfalk J, Parvinen M, Lindqvist E and Olson L (2000). Neurturin, RET, GFRalpha-1 and GFRalpha-2, but not GFRalpha-3 mRNA are expressed in mice gonads. Cell Tissue Res. 299: 409-415.

Wiesenhofer B, Stockhammer G, Kostron H, Maier H, Hinterhuber H and Humpel C (2000). Glial cell line-derived neurotrophic factor (GDNF) and its receptor (GFR-alpha 1) are strongly expressed in human gliomas. Acta Neuropathol. 99: 131-137.

Woodbury D, Schaar DG, Ramakrishnan L and Black IB (1998). Novel structure of the human GDNF gene. Brain Res. 803: 95-104.

Worby CA, Vega QC, Zhao Y, Chao HH, Seasholtz AF and Dixon JE (1996). Glial cell line-derived neurotrophic factor signals through the RET receptor and activates mitogen-activated protein kinase. J. Biol. Chem. 271: 23619-23622.

Wong YW and Too HP (1998). Identification of mammalian GFRα-2 splice isoforms. NeuroRep. 9: 3767-3773.

Wong YW, Sia GM and Too HP (2002). Quantification of mouse glial cell-line derived neurotrophic factor family receptor alpha 2 alternatively spliced isoforms by real time detection PCR using SYBR Green I. Neurosci. Lett. 320: 141-145.

Wright DE and Snider WD (1996). Focal expression of glial cell line-derived neurotrophic factor in developing mouse limb bud. Cell Tissue Res. 286: 209-217.

Xing S, Furminger TL, Tong Q and Jhiang SM (1998). Signal transduction pathways activated by RET oncoproteins in PC12 pheochromocytoma cells. J. Biol. Chem. 273: 4909-4914.

Yamamoto M, Mitsuma N, Ito Y, Hattori N, Nagamatsu M, Li M, Mitsuma T and Sobue G (1998). Expression of glial cell line-derived neurotrophic factor and GDNFR-α mRNAs in human peripheral neuropathies. Brain Res. 809: 175-181.

Yan Q, Matheson C and Lopez OT (1995). In vivo neurotrophic effects of GDNF on neonatal and adult facial motor neurons. Nature 373: 341-344.

You L, Ebner S and Kruse FE (2001). Glial cell-derived neurotrophic factor-induced migration and signal transduction in corneal epithelial cells. Invest. Ophthalmol. Vis. Sci. 42: 2496-2504.

Zwick M, Teng L, Mu X, Springer JE and Davis BM (2001). Overexpression of GDNF induces and maintains hyperinnervation of muscle fibers and multiple end-plate formation. Exp. Neurol. 171: 342-350.

10 APPENDICES

10.1. ABBREVIATIONS

aa	amino acid
Ab	Antibody
Ag	Antigen
ALL	Acute Lymphoid Leukemia
AML	Acute Myeloid Leukemia
ART	Artemin
BM	Bone Marrow
BMAC	Bone Marrow Adherent Cells
bp	base pairs
BSA	Bovine Serum Albumin
CLD-1/4	Cadherin Like Domain-1 to 4
c-RET	RET transmembrane receptor
CNS	Central Nervous System
ConA	Concanavalin A
Cys	Cysteine
DA	DopAmine
DAPI	DiAmino-2-PhenylIndole
DMEM	Dulbecco's Modified Eagle Medium
DMSO	DiMethylSulfOxide
DRG	Dorsal Root Ganglia
DTT	DiThioThreitol
ECS	ElectroConvulsive Seizures
EDTA	EthylenDiaminTetrAcetate
ELISA	Enzyme Linked ImmunoSorbent Assay
ELISPOT	ELISA SPOT assay
ENS	Enteric Nervous System
FACS	Fluorescence Assisted Cell Sorting
FCS	Fetal Calf Serum
FITC	Fluoresceine IsoThioCyanate
F.L	Full Length mRNA
FL1	Fluorescence 1
FSC	Forward SCatter
GDNF	Glial cell line–Derived Neurotrophic Factor
GFLs	GDNF Family Ligands
GFRα	GDNF Family of Receptors alpha
GFRα-1	GDNF Receptor α-1
GFRα-2	GDNF Receptor α-2
GM-CSF	Granulocyte-Macrophage Colony-Stimulating Factor
GPI	Glycosyl-PhosphatidylInositol
HL-60	Promyelocytic leukemia cell line
HRP	HorseRadish Peroxidase
HRSD	Hirschsprung Disease
IFN-γ	Interferon-γ
Ig	Immunoglobulin
IL-1	Interleukin-1
IL-2	Interleukin-2
IL-10	Interleukin-10

kb	kilo base
kDa	kilo Daltons
LPS	LipoPolySaccharide
mAb	monoclonal Antibody
MAP-K	Mitogen-Activated Protein Kinase
MES	2-(N-Morpholino) Ethane Sulfonic acid
MN	MotoNeurons
MOPS	3-(N-Morpholino) Propane Sulfonic acid
MPTP	1-Methyl-4-Phenyl-1,2,3,6-TetrahydroPyridine
NGF	Nerve Growth Factor
NT	NeuroTrophins
NTN	NeurTuriN
O.N	Over-Night
pAb	polyclonal Antibody
PBMC	Peripheral Blood Mononuclear Cells
PBS	Phosphate Buffered Saline
PCR	Polymerase Chain Reaction
PD	Parkinson's Disease
PE	PhycoErythrin
PFA	ParaFormAldehyde
PHA	PhytoHemAgglutinin (from Phaseolus vulgaris red kidney bean)
PI_3-K	Phosphatidyl-Inositol 3-Kinase
PI-PLC	Phosphatidyl-Inositol PhosphoLipase C
PWM	PokeWeed Mitogen
PMA	Phorbol 12-Myristate 13-Acetate
PMSF	PhenylMethylSulfonyl Fluoride
PSP	Persephin
PTC	Papillary Thyroid Carcinoma
PTK	Protein Tyrosine Kinase
PVDF	PolyVinylDeneFluoride
RET-9	RET short isoform
RET-43	RET middle isoform
RET-51	RET long isoform
rpm	rounds per minute
RT	Room Temperature
RT-PCR	Reverse Transcriptase - PCR
RTK	Receptor Tyrosine Kinase
SAC	Staphylococcus Aurous Cowan A
SCG	Superior Cervical Ganglia
SDS	Sodium-DodecylSulfate
SEM	Standard Error of the Mean
SHSY-5Y	human neuroblastoma cell line
SN	SuperNatant
SSC	Side SCatters
TBS	Tris Buffered Saline
TGF-β	Transforming Growth Factor-beta
TGW	human neuroblastoma cell line
THP-1	human monocytic leukemia cell line
TMB	3,3',5,5'-TetraMethylBenzidine
TNF-α	Tumor Necrosis Factor-alpha
Tyr	Tyrosine

10.2. CURRICULUM VITAE

Family name: Vargas-Leal
First name: Vivian R. E
Date of birth: 16 April 1965
Place of birth: Santiago, Chile
Nationality: Venezuelan
Gender: Female

Post-graduate studies:

1998 - 2003	*PhD student (Biology Faculty – LMU, München)* Max-Planck-Institute for Neurobiology, Martinsried, Germany Department of Neuroimmunology Supervisor: Prof. Dr. Edgar Meinl
12/1996-12/1997	*Specialty in Applied Neurophysiology: "Electromyography and neuromuscular diseases"* University Hospital of Caracas. Faculty of Medicine. Department of Neurology. Central University of Venezuela
12/1993-12/1996	*Specialty in Neurology* University Hospital of Caracas. Faculty of Medicine. Department of Neurology. Central University of Venezuela
9/1991-12/1993	*Magister Scientiarum in Biology: Physiology and Biophysics.* Instituto Venezolano de Investigaciones Cientificas (IVIC), Venezuela. Center for Biophysics and Biochemistry. Lab. Structural Biology

University career:

04/1989	Medical Doctor of the Central University of Venezuela.
08/1982-04/1989	Medical studies: "Medico – Cirujano general" Central University of Venezuela, Caracas

Medical Jobs:

8/1991-12/1993	Psychiatric Center of Caracas, Venezuela Internship in Medicine: medical care of psychiatric patients
01/1990-09/1991	Department of Internal Medicine, General Hospital "R. Baquero G.", Caracas, Venezuela. Internship in Internal Medicine
01/1989-12/1989	"Monte-Piedad Maternal Children's Center", Caracas, Venezuela Internship in Medicine: Prevention and primary attention

Scientific publications:

1. Fernandez M, **Vargas V**, Montagnani S, Cotua M, Ogando V and Layrisse Z (2004). HLA class II and class I Polymorphism in Venezuelan patients with Myasthenia gravis. *Human Immunology 65: 54-59.*

2. **Vargas Leal V**, Cotua M, Borges I, Vonasek E, Vargas R, Cespedes G and Mateu L (2003). Structural characteristics of sural nerve myelin from patients with chronic inflammatory demyelinating polyneuropathy: an X-ray diffraction study. Rev. *Neurol. 36(7): 614-619.*

3. Farina C, **Vargas V,** Heydari N, Kumpfel T, Meinl E and Hohlfeld R (2002). Treatment with glatiramer acetate induces specific IgG_4 antibodies in multiple sclerosis patients. *J. Neuroimmunol. 123(1-2): 188-192.*

4. **Vargas V,** Vargas R, Marquez G, Vonasek E, Mateu L, Luzzati V and Borges J (2000). Malnutrition and myelin structure: an X-ray scattering study of rat sciatic and optic nerves. *Eur. Biophys. J. 29(7): 481-486.*

5. **Vargas V,** Kerschensteiner M and Hohlfeld R (1999). GDNF and GDNF-receptor expression in human immune cells. *Immunobiology 200(3-5): 700.*

6. Kerschensteiner M, Gallmeier E, Behrens L, **Vargas Leal V**, et al. (1999). Activated human T cells, B cells and monocytes produce Brain-derived Neurotrophic Factor in vitro and in inflammatory brain lesions: A neuroprotective role of inflammation? *J. Exp. Med. 189: 865–870.*

7. **Vargas V,** Vargas R, Mateu L and Luzzati V (1997). The effects of undernutrition on the physical organization of rat sciatic myelin sheaths: an X-ray scattering study. *Ann. New York Acad. of Sci. 817: 368-371.*

8. Arevalo J, **Vargas V** and Elvir J. La Enfermedad de Creutzfeldt-Jakob (1993). [Review] *Rev. Med. Hond. 61: 59–62.*

9. Lynch NR, Hagel I, **Vargas V,** Rotundo A, Varela MC, Di Prisco MC and Hodgen AN (1993). Comparable seropositivity for ascariasis and toxocariasis in tropical slum children. *Parasitol. Res. 79(7): 547-550.*

10. Lynch NR, Hagel I, **Vargas V,** Perez M, Lopez RI, Garcia NM, Di Prisco MC and Arthur IH (1993). Effect of age and helminthic infection on IgE levels in slum children. *J. Invest. Allerg. & Clin. Immunol. 3(2): 96-99.*

Congress Assistance:

VIth International Congress of Neuroimmunology, Edinburgh, UK. September, 2001
Farina C, Vargas V, Heydari N, et al. *"S.C administration of Glatiramer Acetate to multiple sclerosis patients induces specific IgG4 antibodies".*

53rd Annual Meeting of the American Academy of Neurology, Philadelphia, USA. May-2001
Vargas V, Meinl E, Kerschensteiner M, and Hohlfeld R. *"Glial cell-Derived Neurotrophic Factor (GDNF) and GDNF-receptors expression in human immune cells".*

XXXth Annual Meeting Deutsche Gesellschaft für Immunologie, Hannover, Germany. Sept-1999
Vargas V, Kerschensteiner M and Hohlfeld R. *"GDNF and GDNF-receptor expression in human immune cells"*.

American Academy of Neurology, Toronto, Canada. April-1999
Kerschensteiner M, Staedelman C, **Vargas V,** et al. *"Inflammatory cells produce Brain-derived Neurotrophic Factor (BDNF) in Multiple Sclerosis brain lesions"*.

XVIth Venezuelan Congress of Psychiatry, Venezuela. October-1995
Torrealba E. and **Vargas V.** *"Progressive aphasia"*.

Les Stratégies Therapeutiques dans la Sclérose en Plaques, Les Rendez-vous de L'arsep, Paris, France. November-1994
Mateu L, Luzatti V, Vargas R, **Vargas V,** Vonasek E and Borgo M. *"Une technique nouvelle pour l'étude de la structure et des défauts structurels de la myéline des systémes central el periphérique"*.

IIth Iberoamerican Congress of Biophysics, Mexico. October-1993
Vargas V, Vonasek E. Vargas R and Mateu L. *"Cambios estructurales causados en la mielina por desnutrición. Estudio por difracción de rayos-X."*

IXth Latinoamerican Congress of Parasitology, Venezuela. November-1989
Vargas V and Campo-Aasen I. *"Prevalencia de protozoos y helmintos intestinales en pacientes de una zona marginal de Caracas"*.

Fellowships and Awards:

1998-2002	Fundacion Gran Mariscal de Ayacucho, fellowship for PhD studies (4 years)
1999	"P. Castro Foundation", Neurology Award: Venezuelan Society of Neurology
1994-1997	Member of the Research Promotion Program, CONICIT, Venezuela
1991-1993	Fundacion Gran Mariscal de Ayacucho, fellowship for MSc studies (2 years)